CANADIAN THESES ON MICROFICHE

I.S.B.N.

THESES CANADIENNES SUR MICROFICHE

National Library of Canada
Collections Development Branch

Canadian Theses on
Microfiche Service

Ottawa, Canada
K1A 0N4

Bibliothèque nationale du Canada
Direction du développement des collections

Service des thèses canadiennes
sur microfiche

NOTICE

The quality of this microfiche is heavily dependent upon the quality of the original thesis submitted for microfilming. Every effort has been made to ensure the highest quality of reproduction possible.

If pages are missing, contact the university which granted the degree.

Some pages may have indistinct print especially if the original pages were typed with a poor typewriter ribbon or if the university sent us a poor photocopy.

Previously copyrighted materials (journal articles, published tests, etc.) are not filmed.

Reproduction in full or in part of this film is governed by the Canadian Copyright Act, R.S.C. 1970, c. C-30. Please read the authorization forms which accompany this thesis.

THIS DISSERTATION
HAS BEEN MICROFILMED
EXACTLY AS RECEIVED

AVIS

La qualité de cette microfiche dépend grandement de la qualité de la thèse soumise au microfilmage. Nous avons tout fait pour assurer une qualité supérieure de reproduction.

S'il manque des pages, veuillez communiquer avec l'université qui a conféré le grade.

La qualité d'impression de certaines pages peut laisser à désirer, surtout si les pages originales ont été dactylographiées à l'aide d'un ruban usé ou si l'université nous a fait parvenir une photocopie de mauvaise qualité.

Les documents qui font déjà l'objet d'un droit d'auteur (articles de revue, examens publiés, etc.) ne sont pas microfilmés.

La reproduction, même partielle, de ce microfilm est soumise à la Loi canadienne sur le droit d'auteur, SRC 1970, c. C-30. Veuillez prendre connaissance des formules d'autorisation qui accompagnent cette thèse.

LA THÈSE A ÉTÉ
MICROFILMÉE TELLE QUE
NOUS L'AVONS REÇUE

NL-339 (r. 82/08)

Canada

THE EFFECTS OF CYCLOPROPANE RINGS, STEROLS AND ANTIBIOTICS ON THE STRUCTURE AND DYNAMICS OF PHOSPHOLIPID MEMBRANES. A DEUTERIUM SOLID STATE NUCLEAR MAGNETIC RESONANCE APPROACH

by

Erick Joël Dufourc

maître ès sciences et techniques

A thesis presented to the School of Graduate Studies, University of Ottawa, in partial fulfillment of the requirements for the degree of Doctor of Philosophy.

Ottawa, Ontario
June, 1983

© Erick Joël Dufourc, 1983

UNIVERSITÉ D'OTTAWA
UNIVERSITY OF OTTAWA

A Martine, ma compagne.

A ma famille.

Savoir ce n'est pas assez. On doit essayer de comprendre aussi.

André Brink
"Un turbulent silence".

Les généralisations philosophiques doivent être fondées sur des résultats scientifiques. Une fois formées et largement acceptées, elles influencent très souvent le développement ultérieur de la pensée scientifique en indiquant entre les nombreux procédés possibles, celui qu'il faut suivre.

Albert Einstein
et Léopold Infeld
"L'évolution des idées en Physique".

RÉSUMÉ

Le marquage spécifique au deutérium (^2H), par voie de synthèse organique, de molécules d'intérêt biologique telles que 1-2-dimyristoyl-sn-glycero-3-phosphocholine (DMPC), 1-palmitoyl-2-dihydrosterculoyl-sn-glycero-3-phosphocholine (PDSPC) et les deux isomères (α- et β-) du cholestérol a permis grâce à la résonance magnétique nucléaire (RMN) du deutérium de caractériser l'organisation et les propriétés dynamiques de telles molécules engagées dans des systèmes membranaires. L'ajout de perturbants tels que l'antibiotique polyénique Amphotéricine B à certaines des membranes modèles mentionées ci-dessus a été également étudié.

Les données spectrales de la RMN-^2H ont été analysées en termes de fluctuations angulaires (paramètre d'ordre S_α) des segments C-^2H et d'orientation (paramètre S_γ) de ces segments par rapport à l'axe du mouvement (la normale à la bicouche).

Il a été montré dans une première partie que le cyclopropane présent (en position 9'-10') sur l'une des chaînes d'acides gras de PDSPC modifie considérablement le profil d'ordre (S_α) en fonction du carbone marqué, comparativement à des systèmes lipidiques à chaînes saturées ou insaturées. En effet, le cyclopropane possède un paramètre d'ordre S_α supérieur d'environ 40% à la valeur de S_α pour des positions marquées antérieures au cycle (ex: S_α au niveau C5'). Parallèlement au calcul de l'ordre du cycle, l'orientation moyenne de ce dernier a été déterminée et montre que la liaison 9'-10' du cyclopropane est quasiment parallèle à la surface de la bicouche. Contrairement aux résultats de la chaîne sn-2, la chaîne palmitique (en position sn-1) offre un profil d'ordre-position semblable à celui que l'on rencontre dans des systèmes ayant les deux chaînes saturées. La transition de phase gel-cristal-liquide des membranes modèles de PDSPC, observée grâce aux modifications de forme des spectres de poudre du deutérium, se produit entre -10°C et -15°C. L'analyse des temps de relaxation, T_{1_Z}, du deutérium a apporté des conclusions semblables à celles obtenues grâce au paramètre d'ordre S_α. La variation de la vitesse de relaxation ($1/T_{1_Z}$) en fonction du carbone marqué montre une brusque discontinuité au niveau du cyclopropane, indiquant que les deutérons de ce dernier ont une vitesse de relaxation plus élevée que les positions antérieures ou postérieures au cycle. La chaîne sn-1 ne présente en aucune manière cette discontinuité et offre un plateau de vitesses de relaxation par T_{1_Z}, en fonction du carbone marqué,

semblable à celui observé à l'aide du paramètre d'ordre S_{α}. A la lumière de ces observations, il a été conclu que les variations d'amplitude ou de vitesse de mouvement des liaisons C-^{2}H étaient transmises à courte distance, et préférentiellement par l'intermédiaire de liaisons plutôt qu'à travers l'espace. La comparaison de systèmes à chaînes alkyles saturées (DPPC), insaturées (POPC) et contenant un groupe cyclopropane (PDSPC) a amené la classification suivante, selon une échelle où l'ordre local (S_{α}) et la vitesse de relaxation par T_{1z} augmentent:

$$\text{DPPC} < \text{POPC} < \text{PDSPC},$$

ceci à une même température par rapport à T_c (la température de la transition de phase gel cristal-liquide). Les résultats d'ordre local et de vitesse de relaxation du cyclopropane ont amené à identifier le cycle à une barrière régulant la propagation du mouvement et permettant ainsi à la membrane d'être très stable et cependant très "fluide" sur une large échelle de températures.

Dans une deuxième partie, l'interaction de molécules telles que DMPC et cholestérol, engagées en un système membranaire (en proportion molaires 7:3, respectivement), à été étudiée grâce aux réponses en RMN-^{2}H du lipide et du stérol, et ceci, à diverses profondeurs dans la bicouche. En utilisant un formalisme analogue à celui employé pour extraire l'ordre local et l'orientation moyenne du cyclopropane dans PDSPC il a été possible de calculer la position de l'axe du mouvement du stérol ainsi que le paramètre d'ordre S_{mol} (ou S_{α}) de ses quatre cycles. Il a été constaté que les fluctuations angulaires du β-cholestérol son quasi-indépendantes de la tempéreture alors que les segments lipidiques, au même niveau membranaire, sont beaucoup plus sensibles à un changement thermique du système. Deux cas sont à distinguer: en dessous de la température de transition de phase, T_c, du lipide pur (23°C) les fluctuations angulaires des segments lipidiques ont une amplitude plus faible que les fluctuations des quatre cycles du β-cholestérol, alors qu'au-dessus de T_c la situation est inversée. En comparant le profil d'ordre-température du lipide pur avec celui du lipide contenant β-cholestérol, il apparaît que la faible sensibilité thermique des fluctuations de β-cholestérol contrôle les variations angulaires des chaines alkyles du lipide: le stérol réduit S_{mol} du lipide en dessous de T_c et augmente ce dernier au-dessus de T_c. Le marquage du cholestérol sur la chaine terminale a permis de montrer que cette dernière possède un paramètre d'ordre S_{mol} quasi-identique à celui des quatre cycles. Les données de la RMN-^{2}H du lipide marqué en bout de chaine, cumulées à celles du cholestérol marqué en fin de chaine ont permis d'étendre l'effet d'ordre-désordre, tel que décrit plus haut, à toute la membrane lipidique. Il a égale-

ment été montré que l'isomère α- du cholestérol possède certaines des propriétés de contrôle de la flexibilité des segments lipidiques. Il est cependant moins efficace dans ce rôle que β-cholestérol: il induit en effet moins d'organisation sur DMPC que ne le fait l'isomère β- du cholestérol, au-dessus de T_c. De plus, le calcul de la position de l'axe du mouvement d'épicholestérol montre que ce dernier n'occupe pas une position verticale dans la membrane lipidique comme le fait β-cholestérol, mais offre plutôt une inclinaison marquée par rapport à la normale à la bicouche. Cette particularité a été invoquée comme étant l'une des raisons pour lesquelles α-cholestérol n'est pas présent dans les membranes naturelles. Il a également été observé que l'isomère α-, à l'inverse de l'isomère β-, change d'orientation moyenne par rapport à la normale à la bicouche lorsque l'on augmente la température. Le profil d'ordre-température du lipide en présence de cholestérol (α- ou β-) présente un changement de pente remarquable, autour de T_c (la température de transition de phase du lipide pur), ce qui indique que même dans des systèmes complexes, le lipide conserve une "mémoire" de sa transition de phase. Les temps de relaxation T_{1z} du β-cholestérol dans DMPC ont été interprétés en termes de mouvement lent et mouvement rapide. Bien que l'analyse requière de plus amples données expérimentales, il apparaît que le mouvement lent participe pour 65 à 84% dans la relaxation par T_{1z} du cholestérol.

La troisième partie de ce travail consistait à étudier l'effet d'un antibiotique polyénique, Amphotéricine B, sur une membrane modèle (DMPC) en présence ou absence de stérol. Cette étude a été réalisée en marquant au deutérium soit le lipide, soit le cholestérol(α - ou β-). Il apparaît que l'Amphotéricine B, lorsqu'employée sur une membrane contenant uniquement DMPC (dans un rapport 3:7, respectivemennt), accroît d'une manière générale l'organisation du lipide et forme un agrégat avec une certaine partie de DMPC. Cet agrégat dont les proportions molaires sont proches de 1:1, est quasi-insensible à des changements de température. Lorsque l'antibiotique est ajouté à DMPC, en présence de β-cholestérol, la composante spectrale représentant l' agrégat cité plus haut n'est plus observée. De plus les spectres du lipide ou du β-cholestérol ne sont pratiquement pas modifiés par l'ajout d'Amphotéricine B, exception faite des positions marquées au centre de la bicouche. Alors que l'addition d'antibiotique n'induit pas d'ordre sur DMPC ou sur β-cholestérol, il en induit sur le lipide ou le stérol du système α-cholestérol: DMPC. Il a également été observé que l'Amphotéricine B déplace la position du minimum observé pour les T_{1z} du β-cholestérol d'environ 5°C vers les températures plus élevées. Grâce à ces constatations, il a été proposé que le "complexe" Amphotéricine B:Cholestérol était plutôt dynamique que statique et que les stérols, de par leur caractère de "cylindre" rigide, constituaient l'infrastructure de tels complexes.

REMERCIEMENTS

Je voudrais tout d'abord exprimer ma profonde gratitude à Pierre Bothorel, Professeur à l'Université de Bordeaux I, pour son encouragement constant à l'obtention d'un Ph.D. outre-atlantique ainsi que pour l'intérêt qu'il a su susciter en moi pour la Biophysique Moléculaire.

Avant ma venue au Canada, j'ai eu le loisir de me familiariser avec le vocabulaire et les techniques de la Biologie Moléculaire grâce à la compétence et à l'enthousiasme de Jean Dufourcq, maître de recherches au CNRS; que ce dernier trouve ici mes sinceres remerciements.

Je n'oublierai pas les francophones du groupe de Biophysique Moléculaire du CNR canadien pour leur chaleureux soutien, et en particulier, Roxanne Deslauriers, éminente microbiologiste, dont l'enthousiasme envers la RMN du vivant communique une véritable dynamique au groupe.

Je voudrais enfin apporter mes remerciements à mon directeur de recherches, le Pr. Ian Smith, directeur du groupe de Biophysique Moléculaire du CNR. Durant les années de travail commun il a toujours utilisé la langue française autant pour débattre de mes résultats scientifiques que pour donner son avis sur les meilleurs vins de France, montrant par là même son éclectisme.

ACKNOWLEDGEMENTS

I wish to express my deep gratitude to my co-supervisor, Dr. Harold C. Jarrell, for his stimulative discussions and constant encouragements during the years I have worked with him. His patience seemed to be unbounded while teaching me the basis of organic synthesis.

I would like to thank Dr. R. Andrew Byrd whose home-built probe, software modifications and advice concerning operation of the spectrometers aided in the NMR studies; Dr. Mark A. Rance for his help when debugging programs on both computers and Mrs. Lise Bramall whose encyclopedic knowledge of the IBM/TSS system aided in the writing of computer programs.

I would also like to express my gratitude to all members of the Molecular Biophysics group, especially to my fellow graduate student Eric C. Kelusky who tried to improve my english by constant and patient discussions.

I am grateful to the NRC for allowing me to use the facilities through the Guest Worker program and to the WUSC for financial support.

The manuscript was expertly typed by Mrs. Yvonne Rowe.

TABLE OF CONTENTS

PART II. CYCLOPROPANE-CONTAINING LIPIDS

PART III. CHOLESTEROL IN MEMBRANE LIPIDS

PART IV. AMPHOTERICIN B AND MODEL MEMBRANES

PART V. CONCLUSIONS AND SUGGESTIONS

APPENDICES

LIST OF FIGURES

LIST OF TABLES

Pages

PART I

GENERALITIES

CHAPTER I.1

INTRODUCTION

I.1.1 The Membranes of Life

Black holes, quasars, pulsars and neutron stars are some of the astonishing remote celestial phenomena which force man to question himself about the origins of the Origin.

More intriguing is life.

If we can understand black holes, the origins of life still remain a subject of controversy. The concept of life, whatever definition one can give, is tightly related to the existence of a biological membrane: "... sans la membrane à perméabilité sélective, il n'y a pas de cellule viable" (Jacques Monod, 1975).

The most universal function of a membrane is to separate the inside from the outside, thus defining the cell or the cell organelle as an entity. The plasma membrane defines the living cell, the skin defines the man. However, the membrane has many other functions. It also provides a permeability barrier between the interior and the exterior of the cell, maintaining high gradients of chemical potential for entities such as Na^+, K^+ or Ca^{++}. The membrane can possess, intimately inserted in its structure, entities, such as enzymes, which are responsible for the transport of essential

compounds: amino acids, sugars and many other molecules. The membrane surface can act as an initial binding site for hormones and contain antigens which define the immunological properties of the cell.

Thus, the biological membrane appears to be the site where many physical-chemical reactions occur. However, these mechanisms of action are not always well characterized, and often, not understood at all. This poor state of knowledge arises essentially from the complexity of the membrane. The principal components of the membranes are lipids, proteins and carbohydrates. The major classes of membrane lipids are phospholipids such as the diacylphosphatidylcholines, neutral lipids such as the sterols and glycolipids such as monoglucosyldiglycerides. It seems that the biological activity of the membrane is intimately related to the concentration of these compounds, as well as to their spatial and/or temporal arrangement. Thus, the study of the structure and dynamics of the membranes could provide a potential tool in the understanding of various biological mechanisms.

I.1.2 The Membrane Morphology

An early overview of the structure and dynamics of the biological membrane was presented by Bothorel and Lussan (Bothorel & Lussan, 1968, 1970; Lussan & Bothorel, 1969a,b).

Their model (Figure I.1-1a) can be thought as a dynamic arrangement of lipids and proteins to form the membrane unit. This concept was further developed by Singer and Nicholson (Singer, et al., 1972) who pictured the biological membrane as a "fluid mosaic" (Figure I.1-1b). All these models for membranes were based on thermodynamical considerations of the relationships of the various membrane components.

The basic idea resides in the amphipathic properties of the membrane elements: membrane organization thus depending on both hydrophilic and hydrophobic interactions. A hydrophilic interaction may be defined as a thermodynamic preference for the ionic and polar groups to interact with water rather than with a non polar environment. In the same way, a hydrophobic interaction can be defined as the thermodynamic sequestering of non polar groups away from water (for example, the immiscibility of hydrocarbons and water).

Hydrogen bonding and electrostatic interactions may also contribute to the general membrane organization (for example, binding sites for hormones at the membrane surface). However, these interactions, though not negligible, are of secondary importance compared to the hydrophobic and hydrophilic interactions.

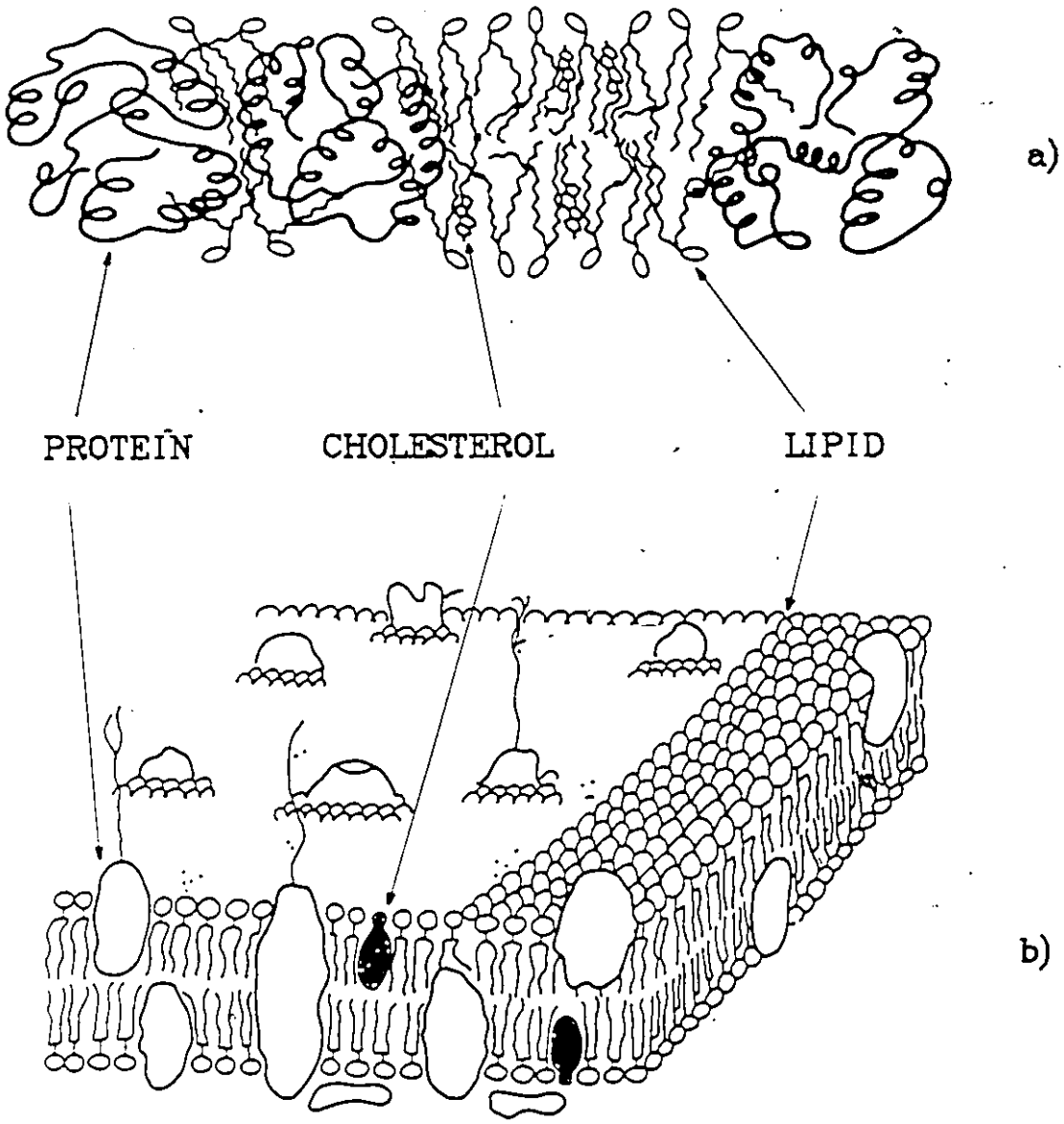

Fig. I1–1. Models for biological membranes.
a) The dynamic model, from Bothorel and Lussan (1968).
b) The "fluid mosaic" model, from Singer and Nicolson (1972).

The final consequence of these thermodynamic considerations is explicitly seen in Figures I.1-1a,b. The lipids, possessing a polar head and hydrophobic acyl chains are oriented such that the polar groups face the water and the fatty acyl chains face away from it: two layers - a bilayer - of such lipids are needed to maximize both hydrophobic and hydrophilic interactions. In these models, the proteins appear as large bodies located within the lipid bilayer and/or on its surface.

It is important at this stage to differentiate between proteins according to their location with respect to the lipid bilayer. One usually distinguishes peripheral from integral proteins. These two species are characterized by the biochemical treatment needed to extract them from the lipids: peripheral proteins will be easily extracted whereas integral proteins will require stronger chemical action. The first category can be extracted by mild treatments such as increase in ionic strength of the medium or addition of chelating agents; these proteins dissociate, molecularly intact, free from lipids and in the dissociated state they are soluble in neutral aqueous buffers. Peripheral proteins can be thus expected to stay in contact with the membrane by weak non-covalent interactions (possibly electrostatic - Dufourcq, et al., 1981) and therefore be located at the surface of the membrane. The other category, the integral proteins,

requires drastic treatment such as the use of organic solvents, detergents or protein denaturants to be dissociated from membranes. After isolation, they are usually not free from lipids and are not soluble (when completely free from lipids) in neutral aqueous buffers; they often form aggregates.

One sees from the above presentation that only the integral proteins will participate to the membrane structure. This will require that such proteins must be amphiphatic as are the lipids, that is, they must possess structural asymmetries such as one polar end and one non polar end or two polar tails separated by a non polar region when they span the membrane. The polar region will be constituted by ionic amino acid residues or covalently bound saccharide residues and will be in contact with the aqueous phase. Conversely, the non polar region will be composed of non polar amino acid residues and will be free from saccharides. It is thus clear that the only possible location for this water insoluble region is the hydrophobic membrane interior, that is, in contact with the lipid fatty acyl chains. Therefore, the structure of integral proteins depends strongly on the amino acid sequence within the membrane, and on its interaction with the surroundings. The final result being a protein conformation such that the free energy of the system is at a minimum.

As was mentioned before, the concentration of lipids versus that of proteins may vary in a way such that some membranes are almost completely constituted by lipids, whereas others show a very high protein content. It may be difficult to determine which of these elements is the matrix. To paraphrase Singer and Nicolson: "which component is the mortar, which the bricks?" A lipid matrix and a protein matrix may be expected to exhibit very different structural and functional properties; the question is thus of first importance. According to this discrimination, high lipid content membranes can be viewed as a two-dimensional liquid crystal-like phase (the lipid bilayer) with monomeric or aggregated integral proteins dispersed in it. The biological membrane can therefore be considered to be dynamic rather than static.

When one wishes to study such complex systems it is suitable to understand first the lipid matrix properties, and then observe their modification upon the addition of "perturbants" such as sterols, antibiotics (vide infra) or proteins.

I.1.3 The Model Membranes

The lipid matrix of natural membranes contains various classes of lipids among which the phospholipids (PL), whose

general structure is shown in Figure I.1-2a, are the most common. The fatty acyl chains, R_1 and R_2, may contain unsaturations, small rings or branched methyl groups, and have a length varying from 12 to 24 carbon atoms. Some common head groups, denoted as X, are shown in Figure I.1-2. Depending on the head group, the lipid can be zwitterionic or negatively charged, at physiological pH.

A mean of understanding the lipid matrix properties is to study model membranes, that is, aqueous mixtures of given phospholipids.

As shown in Figure I.1-2b, PL may adopt, when mixed with water, lamellar liquid crystalline phases. As has already been discussed, to account for the amphipathic properties of PL, these lamellar phases will be constituted by bilayers of lipids separated by a water layer. These phases are characterized, as are many other binary systems, by the concentration of the components and the temperature.

In the present work, two lipids will be studied as aqueous dispersions: 1-Palmitoyl-2-DihydroSterculoyl-sn-glycero-3-PhosphoCholine (PDSPC) and the 1,2-DiMyristoyl-sn-glycero-3-PhosphoCholine (DMPC).

It would be trivial to think that the properties of these models will mimic exactly those of the natural membranes. However, in some cases the structure and evolution of the living membranes may be mainly understood by analogy

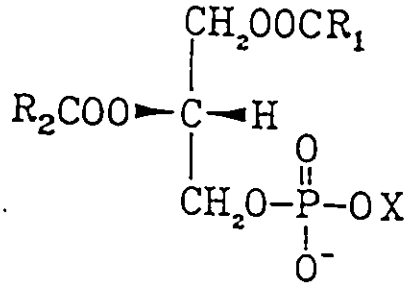

a)

X=$-CH_2CH(NH_2)COOH$
(Phosphatidyl Serine (PS))

X=$-CH_2CHOHCH_2OH$
(Phosphatidyl Glycerol (PG))

X=$-CH_2CH_2\overset{+}{N}(CH_3)_3$
(Phosphatidyl Choline (PC))

X=$-CH_2CH_2\overset{+}{N}H_3$
(Phosphatidyl Ethanolamine (PE))

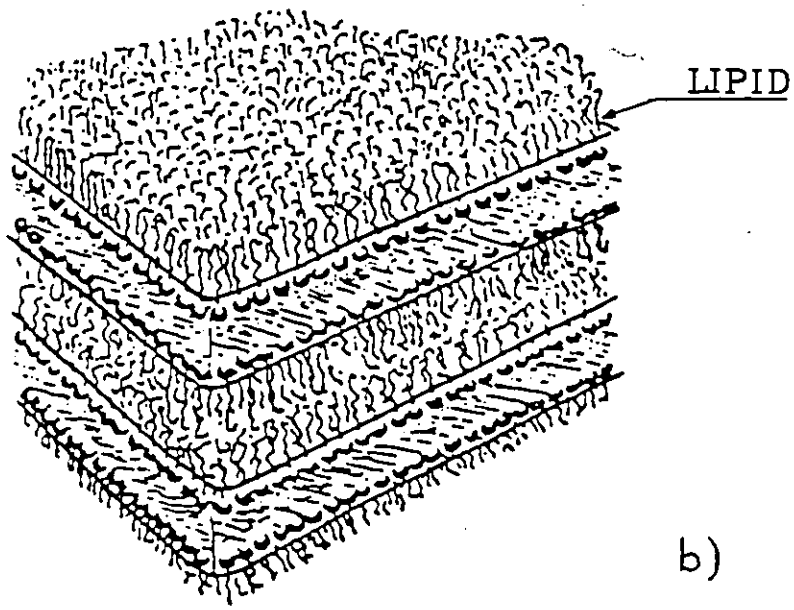

b)

Fig. I.1–2. The model membrane.
a) General phospholipid structure.
b) Lamellar liquid–crystalline phase.

with the model membrane systems. Their responses to perturbations may give some insight into the response of the biological medium.

I.1.4 Deuterium NMR in Biology

Model and natural membranes have been studied by a wide variety of techniques: differential scanning calorimetry (DSC), electron microscopy, x-ray and neutron diffraction, electron spin resonance (ESR), nuclear magnetic resonance (NMR), infra-red (IR), Raman and fluorescence spectroscopies. The aim of all of these physical methods is to characterize the organization and dynamics of membrane components. The lipid structures are liquid-crystalline, and therefore, the concept of orientational order (Saupe, 1964) within the bilayer can be extended to these systems. Among the techniques cited above, deuterium NMR (^{2}H-NMR) appears to be the most powerful for the estimation of such order. Indeed, by selective isotopic substitution of protons, the local order parameter, associated with the fluctuations in time of the C-^{2}H bond, may be directly measured from the solid state ^{2}H-NMR observables.

Chemical synthesis (see Chapter I.3) or biochemical incorporation may provide a means to place a deuterium probe, a reporter, almost anywhere in the molecule of interest.

The advantages of having such a probe and using such a technique (^{2}H-NMR) may be sketched as follows:

1. The position of the probe on the molecule is known.
2. Due to the low natural abundance of deuterium (0.016%) the ^{2}H-NMR signals will be only due to the incorporated deuterium.
3. Deuterium has a spin I=1, which means that under certain conditions there will be quadrupolar interactions (see Chapter I.2) between the electric quadrupolar moment of the nucleus and the surrounding electric fields. This coupling will yield a considerable amount of information about the microscopic environment of the probe. For instance, a spectral feature called the deuterium powder pattern is a proof that the lipid bearing the ^{2}H probe is in an anisotropic medium, for example, a lamellar liquid crystal.
4. The spin lattice relaxation of deuterium is totally dominated by the quadrupolar interaction (Abragam, 1961) which simplifies analysis of relaxation data.
5. The replacement of hydrogens by deuterons is not expected to perturb structure and dynamics of the molecule under study. The problem of perturbation by the probe is encountered, for instance, in fluorescence spectroscopy (when using external probes)

or ESR (the spin-label used here as a probe is usually a rather bulky group); the observables may be perturbed by the observer.

6. These two latter techniques which can also estimate order parameters are more sensitive than ^{2}H-NMR: a low amount of the perturbant probe may be used diminishing thus the perturbation. However, this low amount of probe can be suspected not to give a statistical description of the medium as does ^{2}H-NMR (Davis, 1983), thus turning the advantage into a drawback.

In order to terminate this paragraph, we refer the reader to very good reviews on the field of ^{2}H-NMR in biology, dealing in detail with its drawbacks and its advantages over the other physical techniques (Seelig, 1977; Smith, 1982; Davis, 1983).

I.1.5 Aims of the Research

As the title of this thesis suggests, the work described herein is an attempt to extract from the ^{2}H-NMR observables the ordering, that is, the amount of motion (fluctuations of C-^{2}H bonds), at several locations in the model membrane. This knowledge is hoped to provide answers to the following questions:

a) Why the cyclopropane-containing lipids (the ring being on the fatty acyl chains) is the final stage in the growth of some bacteria and protozoa? Does the cyclopropane ring stabilize the membrane of these organisms?

b) What is the role of cholesterol in biological membranes?

c) What happens to a membrane on addition of a polyene antibiotic such as Amphotericin B (Ampho B)?

d) Does the Ampho B complex with cholesterol to form a geometrical entity within the membrane, called a pore, allowing the leakage of the internal cell components and hence the death of the cell?

It would be ambitious to think that all of these striking questions can be answered by looking at model membranes using only the ^{2}H-NMR technique. Nevertheless, even if a complete answer cannot be given, it will be seen throughout this thesis that some pathways of understanding have been found. These beginnings of answers will lead to new hypotheses (see the end of the thesis) which have to be taken as all hypotheses: they have to be questioned.

The hope here is that some of these ideas about membrane behaviour will have been pointed in the right direction.

I.1.6 Thesis Outline

The thesis is split into five main parts. The first (Chapters I.1 to I.3) is a general introduction to ^{2}H-NMR in anisotropic systems. Chapter I.2 describes the theory of ^{2}H-NMR whereas Chapter I.3 shows "how to make it work", that is, the materials (chemical synthesis) and the methods (hardware and software). The second part (Chapters II.1 to II.3) reports and discusses the organization and the dynamics of cyclopropane-containing lipids as water-mixtures. The third part will describe the behaviour of sterol-containing membranes (Chapters III.1 to III.2) where the fourth will show what happens when one adds Ampho B to a membrane without sterol (Chapter IV.2) and with sterol (Chapters IV.3 to IV.4).

Although the different parts contain their own concluding chapters, a main conclusion will be drawn and some suggestions for future work given (Chapters V.1 and V.2).

REFERENCES TO CHAPTER I.1

Abragam, A. (1961), Principles of Nuclear Magnetism, Oxford University Press, London.

Bothorel, P. and Lussan, C. (1968), C.R. Acad. Sci. Ser. D, Paris, 266, 2492.

Bothorel, P. and Lussan, C. (1970), ibid., 271, 680.

Davis, J.H. (1983), Biochim. Biophys. Acta, 737, 117.

Dufourcq, J., Faucon, J.F., Maget-Dana, R., Pileni, M.P. and Hélène, C. (1981), Biochim. Biophys. Acta, 649, 67.

Lussan, C. and Bothorel, P. (1969a), C.R. Acad. Sci. Ser. D, Paris, 268, 1118.

Lussan, C. and Bothorel, P. (1969b), ibid., 269, 792.

Monod, J. (1970), Le Hasard et la Nécessité, Ed. du Seuil, Paris.

Saupe, A. (1964), Z. Naturforsch., 19a, 161.

Seelig, J. (1977), Quart. Rev. Biophys., 10, 353.

Singer, S.J. and Nicolson, G.L. (1972), Science, 175, 720.

Smith, I.C.P. (1982), Bull. Magn. Reson., 3, 120.

CHAPTER I.2

THE THEORY OF DEUTERIUM NUCLEAR MAGNETIC RESONANCE

I.2.1 Introduction

Entities possessing both an angular momentum and a magnetic dipole moment exhibit magnetic resonance properties. Such properties are found, for instance, on nuclei having a magnetic moment $\vec{\mu}$ and a spin angular momentum $\hbar\vec{I}$. The corresponding operators are linked by the relationship:

$$\mu = \gamma\hbar.I \qquad (I.2.1)$$

where γ is a scalar, the magnetogyric ratio, whose value is intrinsic to each nucleus and where $\hbar.I$ is defined such that the spin operator I is dimensionless. The nuclear spins within a sample may interact with magnetic, and with electric (for $I>\frac{1}{2}$) fields. The magnetic couplings can be external (applied magnetic fields) and therefore allow the detection of NMR signals or they can be internal (local fields within the sample) giving information on molecular motions. The electric interactions belong also to the internal coupling category.

The nuclei, by means of both internal and external couplings, can then be used as probes to study the dynamic behaviour of molecules in a given sample.

The best way to describe the couplings of the nuclear spins with their surroundings is to use the concept of the nuclear spin Hamiltonian, H, (Abragam, 1961). This spin Hamiltonian must be able to account for all the phenomenological coupling parameters, that is, describe the observables (spectra and relaxation) in a correct manner.

The complete spin Hamiltonian, for spin $I>\frac{1}{2}$, in an anisotropic environment, for example, a liquid crystal, may be written as:

$$H = H_0 + H_1 + H_Q + H_D \qquad \text{(I.2.2)}$$

where H_0 and H_1 represent the Hamiltonians describing the couplings of the magnetic dipole moment of a nucleus i, $\vec{\mu}_i$, with the externally applied static magnetic field $\vec{H}_0$ and the radio-frequency (rf) field $\vec{H}_1(t)$, respectively. H_D describes the internal dipolar couplings with other neighbouring spins. Nuclei with spin $I>\frac{1}{2}$ can experience quadrupolar interactions, represented by H_Q, between their quadrupolar moment and the internal electric field gradient (efg) at the nucleus site (see I.2.3).

In a large magnetic field, for instance H_0=7.03 Tesla, the Larmor frequency of the deuterium atom (I=1) is 46.063 MHz. The maximum quadrupolar splitting which can be observed for deuterium (^2H) in C-^2H bonds in anisotropic media is

around 250 kHz, therefore demonstrating that the quadrupolar interaction represents less than 0.5% of the Zeeman coupling. The quadrupolar interaction can thus be treated as a small perturbation of the Zeeman coupling. Moreover, the dipolar, H_D, interaction for these C-^{2}H segments yields a maximum dipolar splitting of about 4 kHz. It can then be seen that the dipolar coupling, though not theoretically negligible is much smaller than the quadrupolar term and, therefore, will be practically neglected. Since the present work deals with deuterium in biological membranes, H_Q will be more discussed than the other internal coupling. Prior to detailing the quadrupolar interaction, the couplings between the nucleus and the externally applied magnetic fields, $\vec{H}_0$ and $\vec{H}_1(t)$, will be briefly described.

I.2.2 The Nuclear Zeeman Coupling

The simplest NMR experiment consists of placing a sample containing resonant nuclei inside a magnet and applying a rf field $\vec{H}_1(t)$ in order to observe a signal. The interaction energy between the magnetic moment $\vec{\mu}$ and the magnetic field $\vec{H}$ can be represented in such a case by the Zeeman Hamiltonian, H_Z:

$$H_Z = - \mu.H = - \gamma\hbar.I.H \qquad (I.2.3)$$

$$= - \gamma\hbar . I . (H_0 + H_1(t))$$

where $\vec{H}_0$ and $\overrightarrow{H_1(t)}$ are the externally applied static field and time-dependent rf field, respectively. The following discussion will be limited to the "high field" approximation (Abragam, 1961; Slichter, 1980), that is, the case where the Zeeman interaction dominates the other couplings. In such a situation, the axis of quantization of the nuclear spins will be defined by $\vec{H}_0$ and the internal couplings treated as a perturbation of the Zeeman energy levels. As a general convention, the axis of quantization of the spins is often chosen as being the z-axis of the coordinate system bound to $\vec{H}_0$. Hence Equation (I.2.3) can be expressed as:

$$H_Z = - \omega_0 \hbar I_Z - \gamma\hbar I . H_1(t) \qquad \text{(I.2.4)}$$

where $\omega_0 = \gamma H_0$ is the Larmor precession frequency. The oscillating rf field $\overrightarrow{H_1(t)}$ is usually applied in a direction perpendicular to $\vec{H}_0$ such as the x-axis.

$$\overrightarrow{H_1(t)} = 2H_1 \cos(\omega t + \phi) . \vec{i} . \qquad \text{(I.2.5)}$$

In Equation (I.2.5), $2H_1$ is the amplitude of the rf field, ω the frequency, ϕ the relative phase of the applied radiation and $\vec{i}$ the unit vector of the x-direction. It can be

shown that this linearly polarized field is equivalent to the sum of two circularly polarized fields, one rotating in the sense of the Larmor frequency, the other in the opposite direction. It has also been shown that this later component has no effect in an NMR experiment (Carrington & McLachlan, 1967). $\overrightarrow{H_1}(t)$ can therefore be taken as:

$$\overrightarrow{H_1}(t) = H_1(\cos(\omega t+\phi)\vec{i} + \sin(\omega t+\phi)\vec{j}). \qquad (I.2.6)$$

The full Zeeman coupling is then represented by:

$$H_Z = - h\nu_0 I_z - h\nu_1(I_x\cos(\omega t+\phi) + I_y \sin(\omega t+\phi)) \qquad (I.2.7)$$

where $2\pi\nu_1 = \gamma H_1$ and I_k, (k=x,y,z) represents the spin along the k direction.

I.2.3 The Electric Quadrupolar Coupling

As has been demonstrated in (I.2.1) the quadrupolar interaction dominates both the spectral lineshapes and the relaxation phenomena. The magnitude of the ratio between H_Q and H_Z allows us to treat H_Q as a perturbation of H_Z. In what follows, it will be seen that the quadrupolar coupling may split the Zeeman resonance lines into several components. The number of these components and the magnitude of their

frequency separation will yield information about the efg at the nucleus site. The alterations of the Zeeman resonances can be useful in the study of solid state or liquid crystalline systems.

A nucleus with spin $I>\frac{1}{2}$ may possess an electric quadrupolar moment, eQ, and may be surrounded by an efg in a given sample. In a classical description, the energy resulting from the interaction between a charge distribution of density ρ and an external potential V can be written as (Slichter, 1980):

$$E = \int \rho(r).V(r)dv \qquad (I.2.8)$$

The quantum mechanical equivalent of Equation (I.2.8) may take the form (Slichter, 1980):

$$H_Q = \frac{C_Q}{4} (V_0A_0 + V_{\pm 1}A_{\mp 1} + V_{\pm 2}A_{\mp 2}) \qquad (I.2.9)$$

with $C_Q = \frac{eQ}{I(2I-1)}$, where I is the total nuclear quantum number. In Equation (I.2.9) the V_{-k} are the components of the irreducible efg tensor estimated at the deuterium site and A_k the components of the second rank irreducible tensor operator, formed by applying the Wigner-Eckart theorem (Slichter, 1980) on a set of nuclear wave functions.* The terms A_k and

* An example of the use of the Wigner-Eckart theorem to calculate the quadrupolar Hamiltonian is given in Appendix A.

V_{-k} are formulated below:

$$V_0 = \left(\frac{\partial^2 V}{\partial z^2}\right) \qquad \text{a)}$$

$$V_{\mp 1} = \pm \sqrt{\frac{2}{3}} \left[\left(\frac{\partial^2 V}{\partial x \partial z}\right) \mp i\left(\frac{\partial^2 V}{\partial y \partial z}\right)\right] \qquad \text{b)}$$

$$V_{\mp 2} = \frac{1}{\sqrt{6}} \left[\left(\frac{\partial^2 V}{\partial x^2}\right) - \left(\frac{\partial^2 V}{\partial y^2}\right) \mp 2i\left(\frac{\partial^2 V}{\partial x \partial y}\right)\right] \qquad \text{c)} \qquad \text{(I.2.10)}$$

$$A_0 = (3I_z^2 - I^2) \qquad \text{d)}$$

$$A_{\pm 1} = \mp \sqrt{\frac{3}{2}} \left(I_\pm I_z + I_z I_\pm\right) \qquad \text{e)}$$

$$A_{\pm 2} = 2\sqrt{6}\, I_\pm^2 \qquad \text{f)}$$

where $I_\pm = I_x \pm i I_y$ represent the raising and lowering operators, respectively.

Now, it is possible to write the Hamiltonian describing the state of a nucleus ($I > \frac{1}{2}$) coupled to an electric field gradient when a static magnetic field $\vec{H}_0$ and an rf field $H_1(t)$ are applied (Equations I.2.9 and I.2.3):

$$H = -\gamma\hbar \vec{I} \cdot (H_0 + H_1(t)) + \frac{C_Q}{4} \sum_{-2}^{2} (-1)^k V_{-k} A_k \qquad \text{(I.2.11)}$$

This formulation is general and H can be estimated in any axis system. However, it is convenient to express Equation (I.2.11) in the laboratory-fixed coordinate system, $L(x_0,y_0,z_0)$, such as $\vec{H}_0$ lies along the z_0-axis. The quadrupolar term will therefore be evaluated in L, so we need to add the superscript L in the V_{-k} and A_k terms. The efg tensor is commonly defined in the principal coordinate system, $P(x',y',z')$, bound to the nucleus, such as the z'-axis lies along the C-^{2}H bond vector. In the axis system, P, the efg tensor is symmetric and traceless ($V^P_{\pm 1}=0$). To calculate H in the laboratory frame one needs to express the V^P_{-k} elements in the frame L. This may be accomplished using Wigner-rotation matrices* (Rose, 1957):

$$V^L_{-k} = \sum_{\ell=-2}^{2} \mathcal{D}_{\ell,-k}\,(\alpha,\beta,\gamma) V^P_\ell \qquad \text{(I.2.12)}$$

where $\mathcal{D}_{\ell,-k}$ is a second rank Wigner-matrix element and α,β and γ the Euler angles as defined by Rose (1957) to rotate from the principal axis system P to the laboratory axis system L.

Using Equation (I.2.12) H_Q becomes:

$$H_Q = \frac{C_Q}{4} \sum_{k=-2}^{2} (-1)^k A^L_k \sum_{\ell=-2}^{2} \mathcal{D}_{\ell,-k}(\alpha,\beta,\gamma) V^P_\ell \qquad \text{(I.2.13)}$$

---

* An expression of the second rank Wigner matrix is shown in Appendix B.

This expression can hopefully be simplified by keeping only the terms which commute with H_z, that is, those which commute with I_z. One can easily see that only A_0^L fulfills this condition. Equation (I.2.13) transforms then to:

$$H_Q = \frac{C_Q}{4} A_0^L [\mathcal{D}_{0,0}(\alpha,\beta,0) V_0^P + \mathcal{D}_{\pm 2,0}(\alpha,\beta,0) V_{\pm 2}^P] \qquad (I.2.14)$$

where the symmetric and traceless properties of V^P have been used ($V_{\pm 1}^P = 0$) and where $\gamma = 0$ since when $k=0$, the $\mathcal{D}_{\ell,0}(\alpha,\beta,\gamma)$ elements are independent of γ.

I.2.4 Motional Averaging

Equation (I.2.14) is only valid for rigid molecules and could be used to describe, for instance, the spectral shapes of a polycrystalline sample containing deuterium atoms (Seelig, 1977).

If there are molecular motions, Equation (I.2.14) has to take into account the time-dependence of anisotropic interactions. This is reflected in H_Q by a time-averaging of the Euler angles. In solution, that is, isotropic medium, the Wigner-matrix elements have their mean value averaged to zero; H_Q cancels and will no longer affect the Zeeman energy levels; the possibility of extracting data from the perturbation of the Zeeman resonance lines is therefore lost.

Nevertheless the quadrupolar interaction still exists in solution and will play an important role in relaxation. In anisotropic media such as lamellar liquid crystals the Euler angles are still time-averaged but not necessarily to zero. One can hope to obtain information from the splitting of the Zeeman lines. One of the aims of deuterium-NMR in membrane research is to relate the quadrupolar splittings to the local order of the lipid components. A convenient way to picture the macromolecular model membrane sample is to think of a multitude of microdomains oriented at random, these microdomains being represented by a piece of a planar bilayer. Natural membranes possess only one bilayer and it is usually assumed that the radius of curvature is large enough such that the hypothesis of local planar bilayer domains remains correct.

In the liquid crystalline phase, the local bilayer normal, $\vec{n}$, is an axis of symmetry. It is then possible to use the local symmetries of the phase to relate the motions of the principal axis system, P, to an axis system, B, fixed to the bilayer. In order to describe the motions at several levels in the lamellar liquid crystalline phase one needs then to replace the initial transformation from P to L by two transformations: from P to B and from B to L. Thus, instead of Equation (I.2.12) one has:

$$V^{L}_{-k} = \sum_{m=-2}^{2} \mathcal{D}_{m,-k}(\alpha_b,\beta_b,\gamma_b) \sum_{\ell=-2}^{2} \mathcal{D}_{\ell,m}(\alpha_p,\beta_p,\gamma_p) V^{P}_{\ell} \qquad \text{(I.2.15)}$$

where $(\alpha_p,\beta_p,\gamma_p)$ are the Euler angles to rotate the components of the efg tensor from P to the bilayer-bound axis system, B, and $(\gamma_b,\beta_b,\gamma_b)$ the Euler angles required for the rotation from B to the laboratory-fixed axis system, L. Equation (I.2.14) now becomes:

$$H_Q = \frac{C_Q}{4} A^{L}_{0} \mathcal{D}_{0,0}(0,\beta_b,0) \left[\overline{\mathcal{D}_{0,0}(\alpha_p,\beta_p,0)} V^{P}_{0} + \overline{\mathcal{D}_{\pm 2,0}(\alpha_p,\beta_p,0)} V^{P}_{\pm 2}\right] \qquad \text{(I.2.16)}$$

where the bars indicate that the $\mathcal{D}_{\ell,m}$ Wigner-matrix elements are time-averaged through the time-dependence of the Euler angles (α_p,β_p) and where the fact that the z_0-axis of the laboratory frame, L, is an axis of symmetry has been used (H_Q independent of α_b) (Davis, 1983). There is no time average on the $\mathcal{D}_{0,0}(0,\beta_b,0)$ element; indeed one assumes here that the local-bilayer-normal frame of reference is not reorienting fast enough to induce a time dependence of the Euler angle β_b. This important assumption is directly related to the lateral diffusion of molecules within the bilayer. Indeed, these lateral motions are identical to bilayer normal reorientations from the NMR viewpoint. Consequently, if the rate of lateral diffusion is high enough and/or the radius of curvature of the bilayer small enough, the $\mathcal{D}_{0,0}(0,\beta_b,0)$ matrix element has to be time-averaged. However, for

simplicity, the assumption of the time-independence of this matrix element will be made. The possibility of violation of this assumption will be examined in Chapter II.2.

In its principal frame the efg is usually defined such as $V_0^p = V_{zz} = eq$ and so that the z'-axis is directed along the C-^{2}H bond. An asymmetry parameter can thus be identified as (Seelig, 1977):

$$\eta = \frac{V_{xx} - V_{yy}}{V_{zz}} \qquad \text{(I.2.17)}$$

where the V_{ii} terms represent the second derivatives of the efg with respect to i at the deuterium site. Equation (I.2.16) can thus be rewritten as:

$$H_Q = eq \frac{C_Q}{4}(3I_z^2 - I^2) \mathcal{D}_{0,0}(0,\beta_b,0) [\overline{\mathcal{D}_{0,0}(\alpha_p,\beta_p,0)} + \frac{\eta}{\sqrt{6}} \overline{\mathcal{D}_{\pm 2,0}(\alpha_p,\beta_p,\theta)}] \qquad \text{(I.2.18)}$$

Replacing the Wigner-matrix elements by their value, the solution of the spin Hamiltonian gives, to first order, the energy levels of a spin-1 system:

$$E_m = - h\nu_0 m + \frac{e^2qQ}{4I(2I-1)} (3m^2 - I(I+1)) \tfrac{1}{2}(3\cos^2\beta_b - 1) \qquad \text{(I.2.19)}$$

$$\times \overline{[\tfrac{1}{2}(3\cos^2\beta_p - 1) + \tfrac{1}{2}\eta\cos 2\alpha_p \sin^2\beta_p]}$$

In Equation (I.2.19) the effect of the rf field $\vec{H}_1(t)$ has not been taken into account. It can easily be seen that in the

absence of the quadrupolar interaction, the Zeeman term of Equation (I.2.19) gives three equally spaced energy levels corresponding to m = + 1, 0, -1, and leads to a single absorption line at the frequency ν_0 (Figure I.2-1). From Equation (I.2.19), one can see that the effect of the quadrupolar term is to split that single line by the value:

$$\Delta\nu = \frac{3}{2}\frac{e^2qQ}{h}\tfrac{1}{2}(3\cos^2\beta_b-1)\ \overline{[\tfrac{1}{2}(3\cos^2\beta_p-1) + \tfrac{1}{2}\eta\cos 2\alpha_p\sin^2\beta_p]} \qquad (I.2.20)$$

If all nuclei have the same orientation with respect to $\vec{H}_0$ (unique value of the angles β_b, β_p and α_p) the quadrupolar interaction will split the Zeeman spectrum into two lines whose frequency separation is $\Delta\nu$. This situation is illustrated in Figure I.2-1. However, in a macroscopic sample one often deals with random dispersions: all orientations are possible. This can be pictured as a multiple of microdomains whose $\vec{n}$-direction is distributed over the surface of a sphere (Figure I.2-2a). Their probability distribution is $P(\beta_b) = \tfrac{1}{2}\sin(\beta_b)$. Hence, in a randomly dispersed sample, one will observe all the resonance lines due to the variation of β_b from 0° to 90° with respect to $\vec{H}_0$, weighted by the probability $P(\beta_b)$. The shape of the observed spectrum is called a "powder pattern" (Seelig, 1977). Examples of such shapes are given in Figure I.2-2 for several values of the asymmetry parameter η.

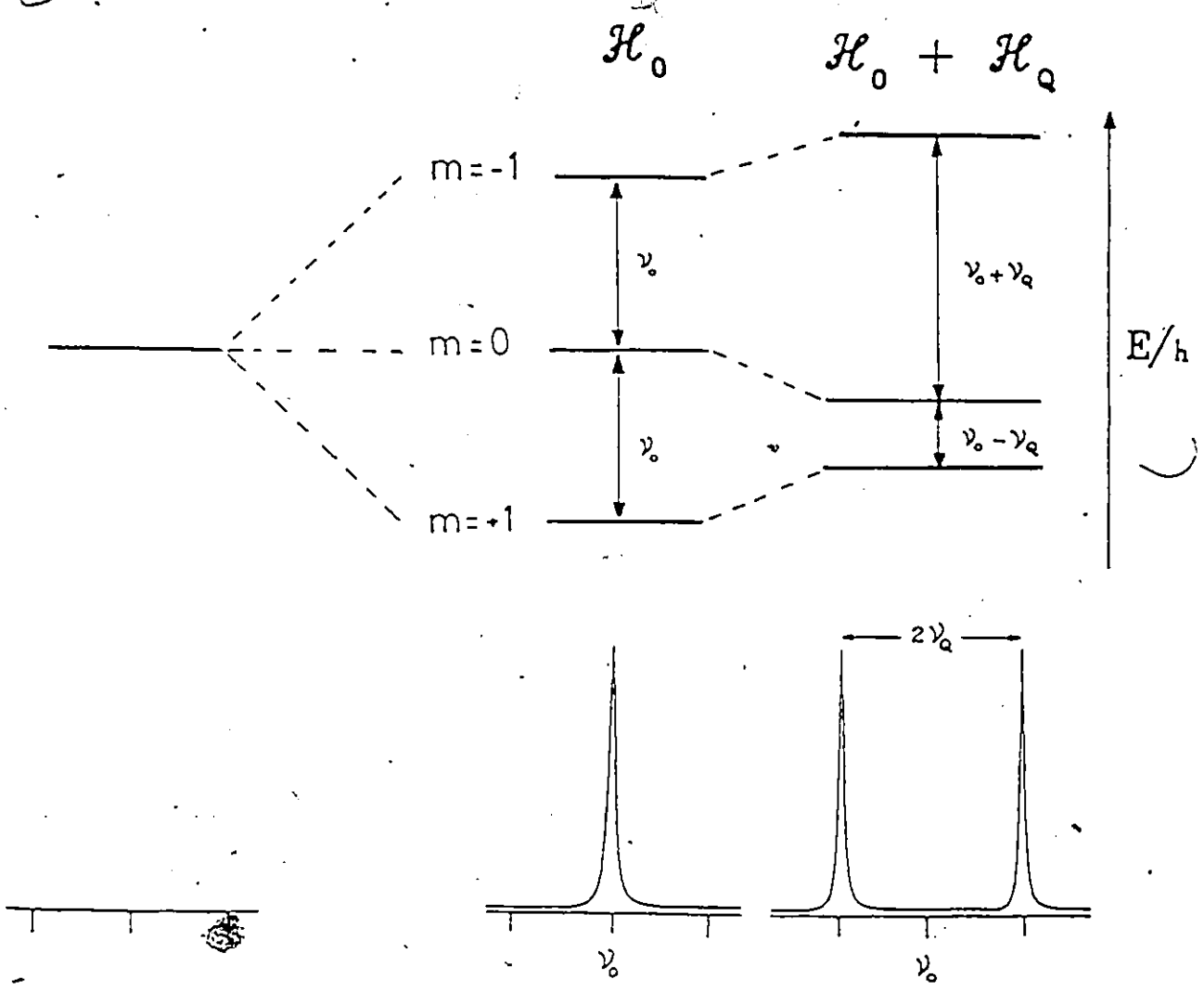

Fig. I.2–1. Energy levels for a spin–1 in a high magnetic field.
The quadrupolar interaction gives rise to two transitions at frequencies $\nu_0 \pm \nu_Q$ (see text).

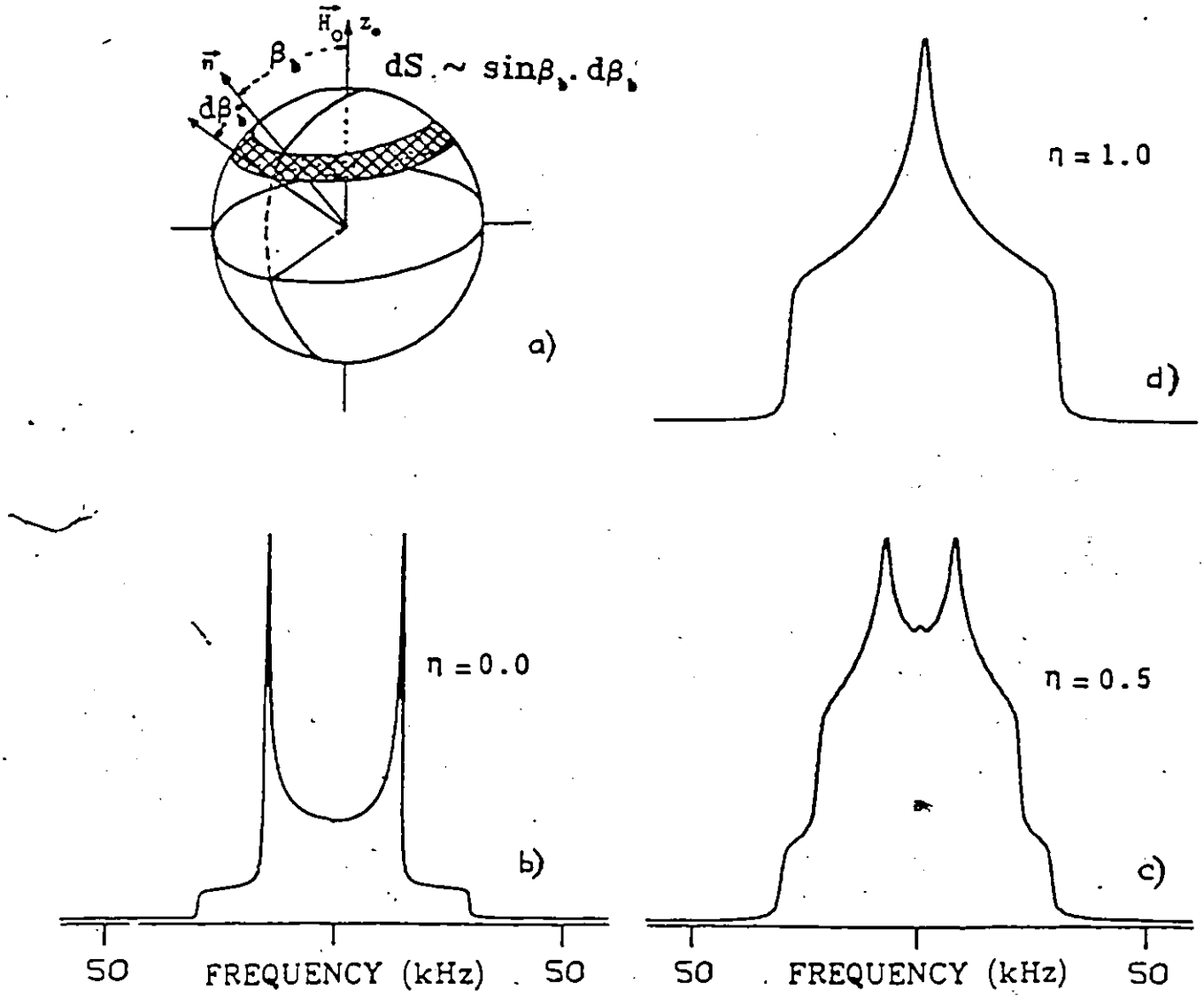

Fig. L2–2. Theoretical spin–1 quadrupolar powder patterns.
a) Random distribution of $\vec{n}$–directions over the surface of a sphere.
b),c) and d) Theoretical spectral shapes for several values of the asymmetry parameter η (see text).

I.2.5 The Order Parameter Tensor

The term in brackets of Equation (I.2.20) exhibits the concept of "orientational averages". When using spectroscopic techniques to study ordered anisotropic systems, it can be useful to describe the average orientational order, in the presence of molecular motions, in terms of an order parameter tensor (Davis, 1983). The concept of order parameters, S_{ij}, has been originally introduced by Saupe to describe the fluctuations of second-rank tensors in a most general way (Saupe, 1964).

Let us attach a cartesian coordinate system $P(x', y', z')$ to the C-^{2}H bond and a second axis system $B(a,b,c)$ such that c lies along the bilayer normal $\vec{n}$. The degree of orientational order of this C-^{2}H bond may be defined in terms of the order tensor (de Gennes, 1974):

$$\overline{S_{ij}^{uv} = \tfrac{1}{2}(3\cos\theta_{iu}\cos\theta_{jv} - \delta_{uv}\delta_{ij})} \qquad (I.2.21)$$

where $\cos\theta_{iu}$ and $\cos\theta_{jv}$ are the direction cosines defining the orientation of the C-^{2}H bond vector with respect to the axis system B, with i,j=1,2,3 (or x',y',z'); u,v=a,b,c. δ is the Kronecker symbol.

In the liquid crystalline phase, the bilayer normal, $\vec{n}$, is an axis of symmetry so, $S_{ij}^{aa} = S_{ij}^{bb}$ and $S_{ij}^{ab} = 0$ by

symmetry. In addition, if the two layers are identical (the a-b plane being a plane of reflexion), $S_{ij}^{cb} = S_{ij}^{ca} = 0$. The symmetry of the lamellar liquid crystalline phase reduces then to the order tensor S_{ij} ($S_{ij} = S_{ij}^{cc} = -2S_{ij}^{aa} = -2S_{ij}^{bb}$). The order tensor of any rigid molecule has, therefore, five independent components. Using the expression of S_{ij}, Equation (I.2.20) can be rewritten as:

$$\Delta\nu = \frac{3}{2} A_Q \tfrac{1}{2}(3\cos^2\beta_b - 1)[S_{33} + \frac{1}{3}\eta(S_{11} - S_{22})] \quad (I.2.22)$$

where $A_Q = \frac{e^2qQ}{h}$ is called the static quadrupolar coupling constant. If the molecule has a three-fold or higher axis of symmetry, $\eta=0$ and Equation (I.2.22) reduces to:

$$\Delta\nu = \frac{3}{2} A_Q \tfrac{1}{2}(3\cos^2\beta_b - 1)S_{33} \quad (I.2.23)$$

Equation (I.2.23) can also hold if the molecular motions are such that $S_{11} = S_{22}$, independent of the size of η (Davis, 1983). For C-^{2}H bonds in liquid crystalline bilayers of phospholipids it has been observed that $\eta \lesssim 0.05$ (Derbyshire, et al., 1969; Barnes, et al., 1973; Fung, 1974). Therefore S_{33} may also be called S_{C-^2H} and can provide a measure of the angular excursions of the C-^{2}H bond vector with respect to the director axis c (or $\vec{n}$).

I.2.6 Relaxation

The preceding paragraphs showed that in anisotropic fluids the quadrupolar splitting, $\Delta\nu$, for deuterons, substituted for hydrogens bonded to carbon gives a direct measure of the order parameter S_{C-2H}, hence an estimation of the structure and dynamics of molecules engaged in biological membranes.

The dynamics of such systems can also be studied through the determination of the nuclear magnetic relaxation times.

It is well known that for a system of non-interacting spins, $I=\frac{1}{2}$, there are two relaxation times - the spin-spin, T_2, and the spin-lattice, T_1. For spin I=1 nuclei, with non zero quadrupolar interaction (for example, in liquid crystals), one can measure 5 independent relaxation times: two T_1 and three T_2 (Jeffrey, 1981). The spin-lattice relaxation time T_{1Z} is associated with the return of the Zeeman energy to its equilibrium value, while T_{1Q} is linked to the decay of the quadrupolar energy.

A complete description of the relaxation times in a spin I=1 system as well as their derivation from the time dependence of the density matrix has been recently published by Jeffrey (1981). We will therefore report the theoretical expression of T_{1Z} and T_2 (since these relaxation times have

been measured herein) and refer the reader to the above quotation for further details:

$$\frac{1}{T_{1Z}} = K(J_1(\omega_0) + 4J_2(2\omega_0))$$

$$\frac{1}{T_2} = K(\frac{3}{2}J_0(0) + \frac{3}{2}J_1(\omega_0) + J_2(2\omega_0)) \qquad \text{(I.2.24)}$$

with $K = \frac{1}{8}[\frac{eQ}{\hbar}]^2$ and where the spectral density functions, $J_j(j\omega_0)$, have the same meaning as defined by Jeffrey.

T_2 can be seen as the relaxation time obtained from a measurement of the linewidth in the absence of temperature, field and other inhomogeneities. T_2 also describes the decay of the quadrupolar echo as a function of the pulse spacing between the two rf pulses of field $\overrightarrow{H_1}(t)$ used to form the echo (see following paragraph) (Davis, et al., 1976).

In biological membranes several motions can take place. We have seen that S_{C-^2H} was able to measure the angular fluctuations of the $C-^2H$ bond with respect to the director of the motion (usually, the bilayer normal). The main difference between T_{1Z} and T_2 resides in the presence of the $J_0(0)$ density function in the equation for the spin-spin relaxation rate. As it can be seen from its argument, this density function monitors the motions occurring at low frequencies. It appears thus that T_2 is more sensitive to slow motions than T_{1Z}. Therefore, the measurement of relaxation times

will lead an insight complementary to that of S_{C-^2H} in the study of molecular motions.

A brief description on how to measure these relaxation times will be given in Chapter I.3.

I.2.7 The Quadrupolar Echo

The most important limitation of solid state NMR is the recovery time of the receiver. As an example, the dead time required by the receiver to observe a spectrum with a width of 250 kHz must be less than $1/2\pi \times 250000 \simeq 0.6$ μs, which is impossible to obtain since it takes several microseconds for a resonant circuit to ring down to the noise level (after a pulse of rf field). Recording the spectrum in such conditions will perturb the FID (Free Induction Decay) leading to distorded lineshapes. This drawback can be overcome by forming an echo, that is, obtaining a complete refocusing of the magnetization at a time well beyond the spectrometer recovery time (Figure I.2-3) (Hahn, 1950).

In order to describe how this echo can be produced, we will outline the state of the system during the entire pulse sequence of Figure I.2-3. The density matrix formalism provides a way of picturing the spin system at a given time and describes the effect of external excitations such as rf pulses. In what follows, only the important steps are shown,

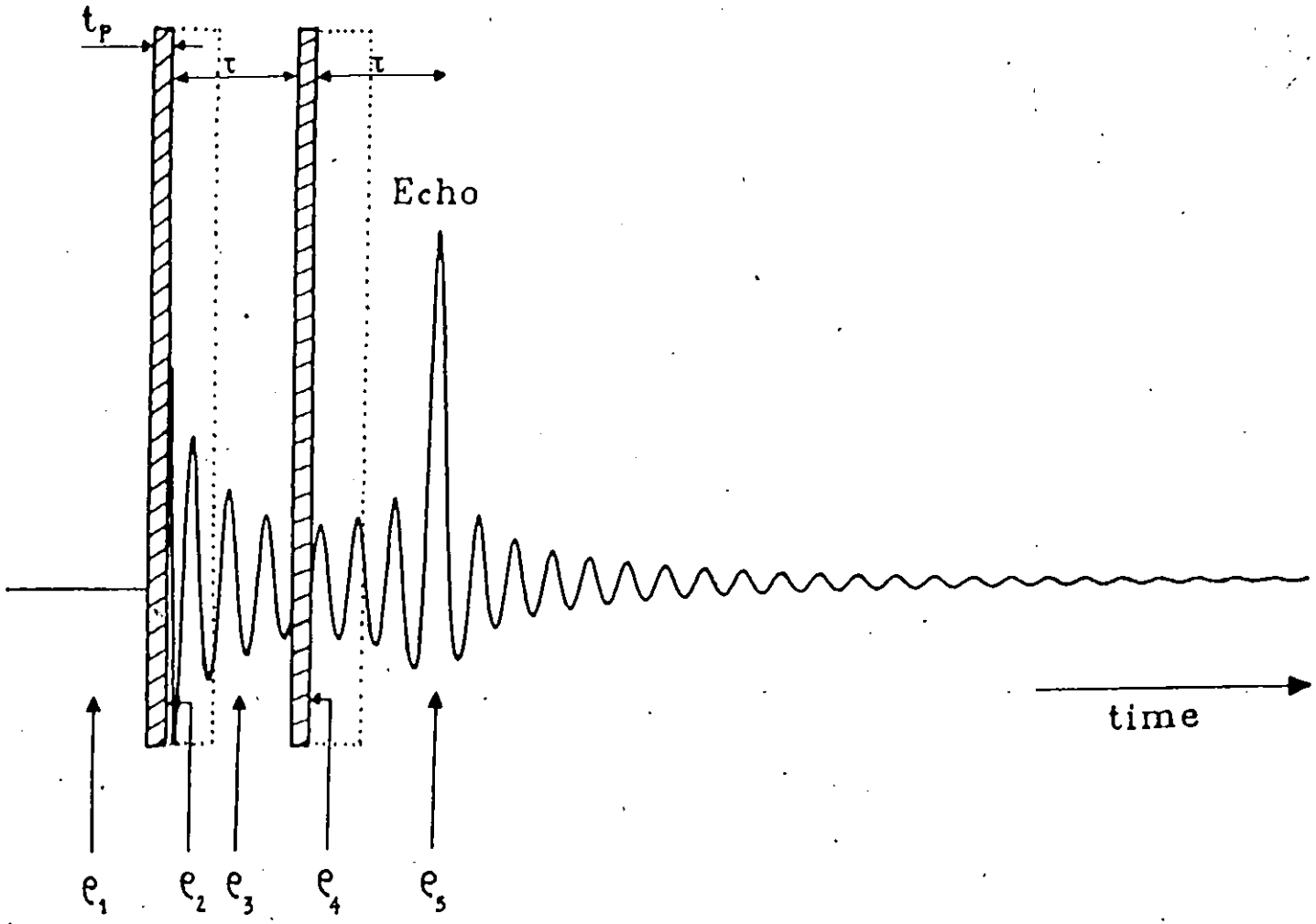

Fig. I.2–3. The quadrupolar echo in a powder sample. The dotted contours represent the dead time of the receiver following the application of two $\pi/2$ rf pulses (hatched areas).

for further details one can refer to Rance (1980), Jeffrey (1981), Davis (1983) and Bax (1982).

At the Boltzmann equilibrium the density matrix operator, ρ, representing the spin system (the phase coherence of the spin system) can be written as:

$$\rho_1(0) = I_z \qquad \text{(I.2.25)}$$

The time evolution of the density operator, $\rho(t)$, is given by the solution of the Liouville-von Neuman equation:

$$\frac{\partial \rho}{\partial t} = - \frac{i}{\hbar} [H, \rho] \qquad \text{(I.2.26)}$$

where H is the Hamiltonian responsible to the evolution and where the square brackets denote the commutator of H and ρ. A formal solution to Equation (I.2.26) is given by:

$$\rho_2(t) = \exp \{-iHt/\hbar\} \rho_1(0) \exp \{iHt/\hbar\} \qquad \text{(I.2.27)}$$

with $H = - \omega_1 \hbar I_x + \frac{1}{3} \omega_Q \hbar (3I_z^2 - I^2)$, where x (chosen arbitrary) indicates the phase of the applied rf pulse and $\omega_Q = \frac{3}{4} A_Q \frac{1}{2}(3\cos^2\beta_b - 1) S_{C-2H}$. Equation (I.2.27) shows that one can calculate the state of the density matrix at a time t from the knowledge of the density matrix at a time anterior to t. Proceeding thus, step-by-step, one will obtain the density matrix at the time of the echo.

Assuming that $\omega_1 >> |\omega_Q|$ during the time of the pulse, t_p, Equation (I.2.27) leads, after some algebra, to:

$$\rho_2(t) = I_z \cos\omega_1 t + I_y \sin\omega_1 t \qquad \text{(I.2.28)}$$

For a 90° pulse, where $\omega_1 t_p = \pi/2$, the above equation becomes:

$$\rho_2(t_p) = I_y \qquad \text{(I.2.29)}$$

One can therefore see that the sole effect of the $\pi/2_x$ pulse of rf field is to rotate the equilibrium magnetization onto the y direction (of the rotating frame).

After that pulse and during the time τ, the density matrix will evolve under the influence of the quadrupolar interaction, H_Q, to give:

$$\rho_3(t) \propto I_{y,1} \cos\omega_Q \tau - I_{y,2} \sin\omega_Q \tau \qquad \text{(I.2.30)}$$

where the $I_{p,k}$ are the fictitious spin-$\frac{1}{2}$ operators as defined by Vega and Pines (1977). The state of the density matrix after the application of a second rf pulse ($\pi/2_y$) is analogous to what has been calculated before:

$$\rho_4(\tau+t_p) \propto I_{y,1} \cos\omega_Q \tau + I_{y,2} \sin\omega_Q \tau \qquad \text{(I.2.31)}$$

and the evolution of ρ_4 after this second rf pulse gives:

$$\rho_5(\tau+t) \underline{\alpha} I_{y,1}\cos\omega_Q(t-\tau) - I_{y,2}\sin\omega_Q(t-\tau) \qquad (I.2.32)$$

The signal measured in a NMR experiment, after the second pulse, is proportional to the trace of the density matrix:

$$S_i(t) \underline{\alpha} < I_i(t) > = Tr(\rho_5(t)I_i)$$

hence:

$$S_x(t) = 0$$

$$S_y(t) \underline{\alpha} \cos\omega_Q(t-\tau)\exp\{-(t+\tau)/T_2\} \qquad (I.2.33)$$

The exponential term in $S_y(t)$ accounts for spin-spin relaxation (Jeffrey, 1981). In the above density matrix description the relaxation terms were not mentioned for simplicity. From Equation (I.2.33) it is easily seen that the maximum signal on $S_y(t)$ will occur at $t=\tau$. This result is called the quadrupolar echo. The signal recorded from the center of the echo onwards is a reproduction of the FID reduced by $\exp\{-2\tau/T_2\}$. The Fourier transformation of this signal (from the top of the echo) gives an undistorted spectrum as in Figure I.2-2.

REFERENCES TO CHAPTER I.2

Abragam, A. (1961), Principles of Nuclear Magnetism, Oxford University Press, London.

Barnes, R.G. and Bloom, J.W. (1973), Mol. Phys, 25, 493.

Bax, A. (1982), Two-Dimensional Nuclear Magnetic Resonance in Liquids, Delft University Press, London.

Carrington, A. and McLachlan, A.D. (1967), Introduction to Magnetic Resonance, Harper and Row, London.

Davis, J.H., Jeffrey, K.R., Bloom, M., Valic, M.I. and Higgs, T.P. (1976), Chem. Phys. Lett., 42, 390.

Davis, J.H. (1983), Biochim. Biophys. Acta, 737, 117.

de Gennes, P. (1974), The Physics of Liquid Crystals, Oxford University Press, London.

Derbyshire, W., Gorvin, T. and Warner, D. (1969), Mol. Phys. 17, 401.

Fung, B.M. (1974), in Critical Evaluation of Chemical and Physical Structural Information (D.R. Lide and M.A. Paul, eds.), National Academy of Sciences, Washington, D.C.

Hahn, E.L. (1950), Phys. Rev., 80, 580.

Jeffrey, K.R. (1981), Bull. Magn. Reson., 3, 69.

Rance, M. (1980), Ph.D. Thesis, University of Guelph, Ont., Canada (1957).

Rose, M.E. (1957), Elementary Theory of Angular Momentum, Wiley, New York.

Saupe, A. (1964), Z. Naturforsch., 19a, 161.

Sclichter, C.P. (1980), Principles of Magnetic Resonance, Springer-Verlag, New York.

Seelig, J. (1977), Quart. Rev. Biophys., 10, 353.

Vega,S. and Pines, A. (1977), J. Chem. Phys., 66, 5624.

CHAPTER I.3

MATERIALS AND METHODS

I.3.1 Introduction

The solid state ^{2}H-NMR experiment on model membranes begins with the organic synthesis of the deuterium labelled molecules, continues through the membrane preparation and the acquisition of a ^{2}H-NMR signal under the optimum conditions, and ends up by a mathematical treatment of the NMR observables. In order to maximize the success of the experiment, none of these steps must be neglected. To be able to rely on the data, the purity of the compounds is as important as the number of iterations in a spectral deconvolution. This chapter will describe all these stages in their logical order.

1.3.2 Organic Syntheses

1.3.2a Fatty Acid Syntheses

The fatty acids used in phospholipid synthesis were either made or bought when commercially available.

Dihydrosterculic Fatty Acid

The method of Jarrell, et al. (to be published) was basically followed.

The Zinc-Copper Couple

16 g of Zn powder was poured into boiling glacial acetic acid (50 ml) and stirred for 1 m. 3.2 g of Cu(II) $OAc_2.H_2O$ were dispersed in the same quantity of boiling acetic acid and added to the Zn reaction flask. The reaction mixture was heated and stirred until the blue colour had turned to brown-pink (2-3 m). The mixture was then allowed to settle and the acidic solution decanted. The remaining solids (powder) were washed 5 times with 100 ml of glacial acetic acid and 5 times with 100 ml of cold diethyl ether. After the last ether wash, the Zn-Cu couple was covered with dry diethyl ether (dried under metallic sodium) and stored under dry argon.

The Reaction

4.0 g of methyl oleate (Sigma, St. Louis, USA) and 32 ml or CH_2I_2 (distilled under vacuum and stored under metallic copper) were mixed with 30 ml of dry diethyl ether. The Zn-Cu couple was warmed and stirred and the methyl oleate-CH_2I_2 ether solution was added dropwise over a period of 30 m. After addition, the reaction mixture was refluxed under argon for 20 h. The reaction was then cooled and the ether solution was decanted. The residual solids were washed 3 times with 20 ml of dry ether. The combined ether solutions

were also washed 3 times with cold 1N HCl and 5 times with water. The resulting ether solution was dried over anhydrous sodium sulfate and the solvent evaporated under reduced pressure. The residue was passed through a column of Fluorisil (F-100, 100g, 60-100 Mesh) paked in hexane. The elution solvent was a hexane-ether mixture (70:30) (v:v). The fractions were checked by gas-chromatography (g.c.) for methyl oleate and methyl dihydrosterculate. The fractions containing the methyl dihydrosterculate were pooled, and the solvent removed under reduced pressure. The residue was dissolved in 100 ml of 80% ethanol containing 5% (weight) KOH. The solution was stirred and gently refluxed for two hours. The reaction was then cooled to 0°C and acidified (pH=4) with cold 1N HCl. The ethanolic solution was removed under reduced pressure and the solids were treated with 100 ml of ether. The ether mixture was washed 3 times with cold water and dried with Na_2SO_4. The ether was then evaporated and the DS acid purified by distillation (distillation temperature range: 120-130°C under 0.7-0.5 Torr). The final yield was 3.2 g of DS acid (80%). A sample of this acid was converted into the methyl ester analog and a g.c. was taken, revealing that the compound was 96% pure. The melting point of the DS acid was 33-36°C.

The deuterium labelled DS acids were made by Dr. H.C. Jarrell, using the above procedure, starting from the deuterated oleic acids which were generous gifts of Dr. A.P. Tulloch, NRC,

Saskatoon.

The deuterium labelled myristic acids (perdeutérated [$^2H_{27}$] and [14-$^2H_3$]) were purchased from Larodan Lipids, Sweden. The [4-$^2H_2$] and [4,14-$^2H_5$] myristic acids were a generous gift of Dr. H.C. Jarrell and the deuterated palmitic acids were kindly provided by Dr. A.P. Tulloch.

1.3.2b Phospholipid Syntheses

1,2-Dimyristoyl-sn-glycero-3-phosphocholine (DMPC)

The following synthesis is a modification of the procedures reported by Gupta, et al. (1977) and Oldfield, et al. (1978).

The complex of sn-glycero-3-phosphocholine and cadmium chloride (GPC.$CdCl_2$) was prepared as described by Chadha (1970). GPC.$CdCl_2$ (10 mmole) was dispersed in 50 ml of distilled water and lyophilized overnight. The resulting fluffy powder was further dried under high vacuum (0.5 Torr) at 56°C for about 3 hours. Myristic acid (Sigma, St. Louis, USA) was converted to its anhydride according to the method described by Salinger and Lapidot (1966). N,N-dimethylformamide (DMF) was refluxed for 30 m with calcium hydride (CaH_2) and distilled under dry argon atmosphere. The GPC.$CdCl_2$ was dissolved in hot (~45°C) freshly distilled DMF (70 ml), dry

myristic acid anhydride (25 mmole) and dry N,N-dimethyl-4-aminopyridine (21 mmole) were then added and the reaction flask sealed under dry argon atmosphere. The reaction, protected from light, was stirred for 3 hours at 30°C. Reaction completion was verified by thin layer chromatography (TLC) on silica gel plates in the solvent system chloroform: methanol:water, 65:25:4 (v:v), by comparison with a DMPC standard (Sigma, St. Louis, USA) using phosphate and iodine stains (Kates, 1972). The solvent was evaporated under reduced pressure and the solid residue treated with methanol:chloroform:water, 5:4:1 (v:v), (200 ml) and passed through a Rexyn ion exchange column (30 g, Rexyn 102 (H), Fisher). The elution was completed with 400 ml of the same solvent. The solvent was removed and the DMPC purified with a chromatographic column as described in the PDSPC synthesis (Dufourc, et al., 1983). The fractions were pooled and evoporated to dryness to yield 9.1 mmole of white crystals of DMPC (91%). Further purity of the lipid was monitored by measure of the gel to liquid-crystal transition temperature, T_c, of a DMPC-excess water mixture; T_c was 23.5°C and the width of the transition was less than 2°C, as determined by differential scanning calorimetry (DSC).

1-Myristoyl-sn-glycero-3-phosphocholine (lyso MPC)

Phospholipase A_2 was used to convert the DMPC into the lyso MPC. DMPC, 7 mmole, was dissolved in 20 ml of methanol and 630 ml of diethyl ether were added. Venom (45 mg) Crotalus Adamanteus (Sigma, St. Louis, USA) was dissolved in 10 ml of a buffer solution (220 mmole of NaCl, 20 mmole of $CaCl_2$, 1 mmole of EDTA, adjusted to pH 7.5 by dropwise addition of 0.1M HCl) and added to the ether solution. The mixture was vigorously stirred and addition of the same buffered quantity of venom was repeated after 10 and 20 m, respectively. The reaction was stirred for two hours and allowed to settle for 1 h. The solvent was then evaporated and the solid residue further dried under vacuum. Isolation of lyso MPC proceded as for DMPC, using the same stepped gradient of solvent for elution. Purity was checked by TLC by comparison with a lyso MPC standard (Sigma, St. Louis, USA). The collected fractions yielded, after removal of solvent, 5.2 mmole of lyso MPC (74%).

The lyso PPC (1-Palmitoyl-sn-glycero-3-phosphocholine) was purchased from Sigma, St. Louis, USA. The acylation of either the lyso MPC or PPC was realized using the procedure described below.

1-Palmitoyl-2-deutero DS-sn-glycero-3-phosphocholine (PDSPC)

Lipids were prepared by a modification (Dufourc, et al., 1983) of a reported procedure (Gupta, et al., 1974).

The fatty acid anhydride of specifically labelled DS acid (Jarrell, H.C., Tulloch, A.P. and Smith, I.C.P., to be published) (0.68 mmole) was obtained by standard procedures (Salinger & Lapidot, 1966). The yield of acid anhydride was estimated by infrared spectroscopy (IR) and found to be ~95%. Lyso-PC (0.20 mmole) was dispersed in 5 ml of distilled water and lyophilized overnight. The resulting fluffy powder was further dried under high vacuum at 56°C for 3 hours. The DS acid anhydride (0.35 mmole) and N,N-dimethyl-4-aminopyridine (DMAP) (0.40 mmole) were dried separately under vacuum for 3 hours. The lyso-PC was then dissolved in 5 ml of hot (45°C) chloroform (freshly distilled twice, over phosphorus pentoxide (P_2O_5)). The DMAP and the DS acid anhydride were then quickly added to this solution and the reaction flask closed under a dry argon atmosphere. The reaction was protected from light and stirred for 4 hours at 30°C. Completion of the reaction was checked by thin layer chromatography (TLC) as described for the DMPC synthesis (see above). The colorless reaction mixture was poured into a 1 cm diameter chromatographic column (20 g of silicic acid, Bio-sil A 100-200 Mesh packed in chloroform) and eluted stepwise with 100 ml

of chloroform, 200 ml of chloroform/methanol (1,1, v/v) and 300 ml of chloroform/methanol (1/3, v/v) at a flow rate of 1-2 ml/min. The eluates were tested by TLC on silica gel plates using the procedure already described. The first fraction of PDSPC appeared after the column had been eluted with 340 ml of the solvent mixtures. The fractions containing pure PDSPC were pooled and evaporated to dryness. There was no detectable chain migration (vide infra).

The following compounds were synthesized according to the above procedure:

[2'-$^2H_2$]	PDSPC	[sn-2-$^2H_{27}$]	DMPC
[5'-$^2H_2$]	PDSPC	[4'-$^2H_2$]	DMPC
[8'-$^2H_2$]	PDSPC	[14'-$^2H_3$]	DMPC
[9',10'$^2H_2$]	PDSPC	[4',14'-$^2H_5$]	DMPC
[11'-$^2H_2$]	PDSPC		
[19'-$^2H_2$]	PDSPC		
[16'-$^2H_2$]	PDSPC		
[11'-$^2H_2$]	POPC		

where the prime means that the numbered carbon, bearing the deuterons, belongs to the sn-2 acyl chain. Yields after isolation of the lipid ranged between 91% and 97%.

1-deutero palmitoyl-sn-glycero-3-phosphocholine (deuterated lyso PPC)

The deuterated fatty acids are very expensive when purchased or very time-consuming when synthesized. In order to minimize the amount of deuterated fatty acid and the reaction time, and to avoid the use of phospholipase A_2, direct sn-1 acylation was accomplished.

The GPC.$CdCl_2$ and the DMF were dried as described above. To 5 ml of DMF were added 0.6 mmole of GPC.$CdCl_2$. The solution was gently warmed and stirred, under an argon atmosphere, until dissolution of the GPC.$CdCl_2$. The DMAP (0.5 mmole) and the deuterated palmitic acid anhydride (0.5 mmole, previously dissolved in 2 ml of warm DMF) were then added. The clear solution was stirred for 2 m under an argon atmosphere. The reaction was quenched by addition of 2 ml of water and checked by TLC as already described. The TLC plates revealed a small formation of DPPC. The lyso PPC was isolated as already described in the DMPC synthesis. The yield was around 40%.

1-deutero palmitoyl-2-DS-sn-glycero-3-phosphocholine

The deuterated lyso PPC's were acylated with the non-deuterated dihydrosterculic acid anhydride by means of the procedure previously described. Six compounds were synthesized:

[3-$^2H_2$] PDSPC

[6-$^2H_2$] PDSPC

[8-$^2H_2$] PDSPC

[10-$^2H_2$] PDSPC

[13-$^2H_2$] PDSPC

[15-$^2H_2$] PDSPC

where the number in square brackets represents the carbon belonging to the sn-1 acyl chain.

All the lipid syntheses described above yield very pure lipids with less than 4% chain migration. Such a chain migration was controled by phospholipase A_2 treatment of the lipid and subsequent mass spectrometric analysis of the isolated fatty acid (Perly, B., Dufourc, E.J. & Jarrell, H.C., to be published).

1.3.2c Cholesterol Synthesis

The method reported by Gruenke and Craig (1979) was slightly modified to increase the yields and to allow separation of the deuterated α and β isomers of Δ^5-cholesten-3-ol.

The Δ^4-cholesten-3-one was prepared from cholesterol (Aldrich, Milwaukee, USA) according to Fieser (1963).

Sodium hydride (NaH) (80 mg, 3.3 mmole) was dispersed in 10 ml of monodeuterated methyl alcohol (MeO^2H) and then

added to the Δ^4-cholesten-3-one (5 g, 13 mmole). The resulting mixture was then stirred and refluxed overnight under dry nitrogen (N_2). The solvent was evaporated under dry N_2 and 10 ml of fresh MeO^2H were then added. The reaction was still refluxed 10 hours, and this cycle repeated once. The reaction mixture was then cooled and 2.5 ml of deuterated water (^2H_2O) were added. The resultant mixture was treated with sodium sulfate (Na_2SO_4) and filtered in a hot filter funnel. The yellowish solution was evaporated from MeO^2H. On adding the Na_2SO_4, a solid residue precipitated. This residue was washed twice with CCl_4 in order to recover the deuterated Δ^4-cholesten-3-one trapped in the solid. This second crop was evaporated from CCl_4. Both crops were dissolved in CCl_4 and a proton (^1H)-NMR spectrum was taken for each of the crops. The two proton spectra were identical and were compared with the proton spectrum of the unlabelled Δ^4-cholesten-3-one. Deuterated and non-deuterated compounds showed the same spectrum except in the region 2.25-2.60 ppm (C-2 protons) and at 5.57 ppm (vinylic hydrogen at C-4) where the deuterated compounds exhibit a complete loss of NMR signals. This loss is characteristic of deuterium incorporation at the C-2 and C-4 positions of the sterol body. Both crops were then poured together and evaporated to dryness to yield 3.5 g of [2,2,4,6,6-$^2H_5$]Δ^4-cholesten-3-one (70%).

The Δ^4-cholesten-3-one was then mixed with 4 ml of isopropenyl acetate and two drops of concentrated sulfuric acid (H_2SO_4) were added. The reaction mixture was stirred and refluxed for 1 hour under N_2 atmosphere. Anhydrous sodium acetate ($NaCH_3COO$) (0.3 g) was added to the solution and the mixture extracted with $CHCl_3$. The chloroform was evaporated to yield 3.2 g of yellow crystals of enol acetate. The enol acetate was then dissolved in 40 ml of tetrahydrofuran (THF). The resultant solution was gently stirred and a solution of 3.2 g of $NaBH_4$ in 25 ml of MeO^2H containing 2 ml of H_2O was then added dropwise. After addition, the reaction mixture was refluxed 1 hour. The solution was then cooled, 40 ml of concentrated HCl were added and the mixture quickly poured into 150 ml of H_2O. The aqueous mixture was extracted three times with 100 ml of methylene chloride (CH_2Cl_2). The subsequent CH_2Cl_2 fractions were combined and the solution evaporated to yield 2.9 g of yellowish crystals. During the washing phases, all the solutions were checked by TLC, on the solvent system described below, to ensure a minimum loss in sterol derivatives.

The compounds were then isolated by column chromatography as described below. Silicic acid (Bio-Rad, 100-200 mesh) (250 mg) was mixed in hexanes and loaded onto a 4 cm diameter column. The reaction mixture was diluted in 40 ml of hexanes: ether (95:5) (v/v) and warmed to obtain a complete

dissolution. This solution was then poured on top of the column and the compounds were eluted at a rate of 5 ml/min using a stepped gradient of solvent:

Volume	% Ether in Hexanes
1 L	5%
2.5 L	10%
7.5 L	15%

The compounds were characterized by TLC on silica gel plates (Merck). The developing system was an Hexane:Ether:Acetic acid (50:50:1) (v/v) mixture. The sterols spots were visualized as red blobs on a white background by means of a sterol spray (Kates, M., 1972): concentrated H_2SO_4:glacial CH_3COOH (50:50) diluted once in water. The eluted compounds were identified by comparison with standard samples of α and β Δ^5-cholesten-3-ol (Schwarz-Mann, New York, and Sigma Co., St. Louis, USA, respectively).

The deuterated α-cholesterol or epi-cholesterol was eluted with 4.5 L whereas the deutero β-cholesterol (Δ^5-cholesten-3β-ol) was obtained after 6 L of total elution. The fractions showing only one spot on TLC and belonging to the same compound were poured together and evaporated to dryness. Recrystallization from ethanol yielded 120 mg and 1.1 g of α and β isomers of the deuterated cholesterol

respectively (~25% yield based on the undeuterated Δ^4-cholesten-3-one as starting material). The melting points of the α and β isomers were 136-138°C and 147-149°C, respectively. A mass spectrum of each of the two isomers was obtained and revealed incorporation of 4.5 deuterons in both cases. Using mass spectral data, and high resolution deuterium NMR data, the percentage of incorporation was estimated to be ~85% at the C-2, C-2, C-4, C-4, C-6 positions and 20% at the C-3 position.

I.3.3 Membrane Preparation

The multilamellar dispersions of PDSPC were made by hydrating the lipids with excess deuterium-depleted water with agitation on a vortex mixer: samples were freeze-thawed and mixed until they appeared to be homogeneous and reproducible ^{2}H-NMR spectra were obtained.

Due to the lack of solubility of Ampho B in the usual organic solvents, the method used to prepare model membranes containing this antibiotic was rather different from that reported above. For consistency, all the membranes made for the Ampho B study were prepared in a same way, even if they did not contain the drug. The method will be illustrated for a membrane of DMPC, Cholesterol and Ampho B.

100 mg of DMPC and 24.4 mg of cholesterol (30 mole per cent with respect to the lipid) were dissolved in 3 ml of methanol:chloroform 1:2 (v:v). 58.3 mg of Ampho B (1:1 molar equivalent with cholesterol) were dissolved in 3 ml of dimethylsulfoxide (DMSO). Both solutions were mixed together and the solvent was removed under vacuum at -10°C. The resulting residue appeared as a gel and was dispersed in 5 ml of distilled water. The mixture was vortexed, cooled and warmed (≤ 40°C) several times and finally lyophilyzed overnight. This cycle was repeated once. The solids appeared then as a yellow powder. To make the model membrane, this powder was hydrated with 0.5 ml of deuterium-depleted water on a vortex mixer in the same manner described for PDSPC lipids. The samples were protected from light throughout the entire procedure and frozen at -20°C if not used immediately.

The stability of Ampho B was checked by U.V. spectroscopy either on freshly made or one month old samples: the model membrane was lyophilyzed and a small quantity of sample was weighed accurately and diluted in DMSO. Comparison was made with a standard: pure Ampho B diluted in DMSO (the dilution was such that the concentrations of Ampho B in the sample and in the standard were equal). Over a period of one month there was no detectable change either in amplitude or shape of the U.V. spectrum of the sample, with respect to that of the standard.

The samples containing Ampho B had a pH of around 6.5. No variation in pH was found, before or after the NMR experiment.

I.3.4 ^{2}H-Nuclear Magnetic Resonance Spectroscopy

^{2}H NMR results were acquired at 46.063 MHz using a Bruker CXP-300 spectrometer and a "home-built" probe (R.A. Byrd, unpublished). Spectra were recorded by means of a modified quadrupolar echo sequence. The basic quadrupolar echo sequence (Davis, et al., 1976) consists of an initial $\pi/2$ pulse applied along the x-axis of the rotating frame, followed by a $\pi/2$ pulse along the Y direction after a time τ. The echo signal occurs at a time τ after the second pulse (see I.2.7). To avoid extraneous signals, the echo-sequence was modified by changing the phases of the two $\pi/2$ pulses by 90° on successive repetitions, and alternatively adding and subtracting the signals in the computer. Quadrature detection was used to record the quadrupolar echo signals. Typical values of one echo sequence were 4.5-5.5 μs pulse length for the $\pi/2$ pulses and 40-60 μs delay between the μ/2 pulses. Prior to recording the echo signal the spin-lattice relaxation time was quickly estimated and the recycle time of the acquisition sequence set to $5T_{1z}$ thus assuring that the spectra were fully relaxed with respect to T_{1z}.

The frequency of the spectrometer was carefully set at the center of the quadrupolar powder pattern, thus folding the spectra about their centers increased the signal-to-noise ratio by a factor of $\sqrt{2}$. Folded and unfolded spectra were compared to ensure that no distortions had been introduced by the folding procedure. Samples were enclosed in a glass jacket, in the NMR probe, where the temperature was electronically regulated to within $\pm 0.5^{\circ}C$. The model membranes were allowed to stabilize at a given temperature at least 15 m prior to recording the NMR signals.

1.3.4a Spin-Lattice Relaxation Time Measurements

The most commonly used pulse sequence for determining the T_{1Z} by Fourier transform methods is the $180^{\circ}-\tau_1-90^{\circ}-\tau_2$ sequence, also referred as the inversion-recovery technique (Carr & Purcell, 1954). When using echo sequence, it transforms to: $(180^{\circ}-\tau_1-\text{echo sequence}-\tau_2)_n$. Since the pulse sequence has to be repeated n times to enhance the S/N ratio by $\sqrt{n}$, the system was allowed sufficient time to relax to its equilibrium state ($\tau_2 \geq 5T_{1Z}$).

To perform an experiment to measure T_{1Z}, a series of FID was acquired in a way similar to that described in I.3.4; the only variable was the time τ_1 between the 180° inverting pulse and the first $\pi/2$ pulse of the echo sequence. The data

acquired in an automated sequence were processed as described in Section I.3.5. Specific regions of the spectra could be integrated to determine whether T_{1Z} was varying across the powder spectrum (that is, orientational dependence).

If the spin-lattice relaxation can be described by a single exponential process (assuming quadrupolar relaxation) then the macroscopic longitudinal magnetization, $M(\tau_1)$, as a function of τ_1 is given by:

$$M(\tau_1) = M_0\{1-2\exp\{-\tau_1/T_{1Z}\}\] \qquad (I.3.1)$$

where M_0 is the equilibrium magnetization. To correct for imperfect 180° pulses (that is, pulses which do not exactly invert the magnetization such that $M(0) = -M_0$) Equation (I.3.1) may be modified to:

$$M(\tau_1) = M_0\ [1-A\exp\{-\tau_1/T_{1Z}\}] \qquad (I.3.2)$$

where the parameter A is substituted for the 2 which appears in Equation (I.3.1).

Equation (I.3.2) was used to fit the experimental data.

I.3.4b Spin-Spin Relaxation Time Measurements

The rate of transverse relaxation by T_2 was measured by monitoring the decay of the quadrupolar echo as a function

of the spacing τ between the two rf pulses of the echo sequence. In a typical experiment, a certain number of FID were acquired for different values of τ and stored on disk. The entire experiment was accomplished automatically. To determine the rate of decay, each free-precession signal was subject to various signal conditioning procedures as described in Section I.3.5, and then Fourier-transformed to obtain spectra which were subsequently plotted. To analyse these spectra, selected portions or windows of the powder pattern lineshape could be integrated thereby allowing measurement of the rate of decay of different regions of the spectrum.

If the spin-spin relaxation process can be described by a single exponential decay, the dependence of the transverse magnetization $M_y(2\tau)$ on τ is given by (see Chapter I.2):

$$M_y(2\tau) = M_y(0)\exp\{-2\tau/T_2\} \qquad \text{(I.3.3)}$$

where $M_y(0)$ is the transverse magnetization at $2\tau=0$. In order to obtain T_2 this equation was fitted using the integrated values of each spectrum for each window. $M_y(0)$ was taken to be the integrated value corresponding to the shortest τ.

I.3.5 The Data Treatment

The NMR data collected on the CXP-300 were transferred from the Bruker ASPECT-2000 computer to a Nicolet 1280 data processor (Byrd, R.A. and Rance, M., unpublished).

The data points before the top of the echo were discarded and the Fourier Transformation (FT) (part of the routines in the Nicolet 1280 NMR software) was applied to this resulting FID, giving rise to undistorted deuterium powder patterns.

These frequency-domain data were mathematically analyzed by means of spectral moment calculations or spectral deconvolution (dePaking) calculations. The principles of these two methods are outlined below.

I.3.5a The Spectral Moments

The deuterium powder pattern, $G(\omega)$, results from the convolution of a given lineshape function, $F(\beta_b,\omega)$, with the probability distribution, $P(\beta_b)$ (see Section I.2.4). This is written as (Seelig, 1977):

$$G(\omega) = \int_0^{\pi/2} F(\beta_b,\omega) * \sin\beta_b \cdot d\beta_b \qquad \text{(I.3.4)}$$

One usually chooses to measure the frequency separation, $\Delta\nu_Q$, between the peaks ($\beta_b=90^\circ$) of the powder pattern and relate

it to the S_{C-2_H} order parameter through Equation (I.2.23). This can be accomplished directly or through the estimation of the moments of the spectrum. The moments will give, in addition, information about lineshape changes.

The nth moment is defined as (Davis, 1979):

$$M_n = \int_0^\infty \omega^n G(\omega)\, d\omega / \int_0^\infty (\omega)\, d\omega \qquad \text{(I.3.5)}$$

where the fact that the deuterium powder pattern shapes are symmetric has been used. One can consider only positive frequencies with respect to the Larmor frequency, ω_0 (set to 0 here), and therefore, have non vanishing odd moments. In practice, the integration is replaced by a summation over finite values since this is the form in which the data exist in the computer memory. One can also relate the moments theoretically with $\Delta\nu_Q$. Indeed, combining Equations (I.3.4) and (I.3.5), one obtains upon integration:

$$M_n = A_n \omega_Q^{\,n} = A_n (2\pi)^n \Delta\nu_Q^{\,n} \qquad \text{(I.3.6)}$$

where the A_n are constants from the integration ($A_1 = 2/3\ \sqrt{3}$, $A_2 = 1/5$, etc.). The assumption that the individual lineshapes $F(\beta_b, \omega)$ can be approximated by delta functions has been made when integrating. For a single powder pattern, it can be seen that it is equivalent to measure any of the moments

or the observed quadrupolar splitting, $\Delta\nu_Q$. If there is more than one environment for the deuteron within the sample, there will be more than one quadrupolar splitting. In certain cases, one can have a statistical distribution of $\Delta\nu_Q$ and therefore Equation (I.3.6) will be violated. This provides a way to estimate spectral inhomogeneities (for example, several liquid-crystalline phases) within the powder pattern. Any deviation from Equation (I.3.6) may be monitored by means of a parameter, Δ_2, representing the relative variance of the distribution of $\Delta\nu_Q$ (Davis, 1979):

$$\Delta_2 = \frac{A_1^2 M_2}{A_2 M_1^2} - 1 = \frac{M_2}{1.35\ M_1^2} - 1 \qquad \text{(I.3.7)}$$

A value of Δ_2 greater than 0 will therefore be indicative of spectral inhomogeneities in the powder pattern. This assertion needs, however, to be tempered since one never deals with infinite signal-to-noise ratio in the experimental spectra. Any significance of Δ_2 must always be coupled with the quality of the spectral features (high signal-to-noise ratio, flat baseline and choice of the cut-off frequency - limit beyond which there is only zero intensity -).

Δ_2 may be also different from zero for reasons which are not due to a distribution of quadrupolar splittings or to the experimental conditions described above. To obtain

Equation (I.3.6), it was assumed that the width of the individual lines within the powder pattern was zero. This is far from being true. In order to account for the natural linewidth of each orientation, one can calculate Equation (I.3.6) assuming, for instance, a Gaussian broadening. The two first moments of the broadened spectrum, M_1^B and M_2^B are thus given by (see Appendix C for details):

$$M_1^B = M_1, \quad M_2^B = \sigma^2 + M_2 \tag{I.3.8}$$

where σ is the Gaussian linewidth. A broadened Δ_2, Δ_2^B, can also be defined:

$$\Delta_2^B = \frac{\sigma^2}{1.35\ M_1^2} + \Delta_2 \tag{I.3.9}$$

One sees therefore that if the Gaussian linewidth is of the order of magnitude of the quadrupolar splitting, the Δ_2 estimated from the experimental moments (with Equation (I.3.7)) will be greater than zero, even if one does not have a distribution of $\Delta\nu_Q$. However, for one order of magnitude difference between σ and $\Delta\nu_Q$, the Δ_2 parameter can still be interpreted in terms of spectral inhomogeneities.

I.3.5b DePaking

Due to the convolution mentioned in the above section, the value of $\Delta\nu_Q$ measured on the spectrum does not represent "truly" the separation between the resonances for the $\beta_b=90^\circ$ orientations. In order to remove this influence, the β_b dependent lineshape function, $F(\beta_b,\omega)$, was expressed in terms of the same lineshape function, for a fixed value of β_b (Bloom, et al., 1981). For instance, let us define $F(90^\circ,\omega) = F_{90^\circ}(\omega)$. Hence,

$$F(\beta_b,\omega) = N(\beta_b)\, F_{90^\circ}\left(\frac{\omega}{1-3\cos^2\beta_b}\right) \qquad (I.3.10)$$

where F_{90° is the lineshape function for the $\beta_b=90^\circ$ orientation and $N(\beta_b) = 1/(1-3\cos^2\beta_b)$ a normalization constant. Combining Equations (I.3.10) and (I.3.4) one obtains:

$$G(\omega) = \tfrac{1}{2}\int_0^{\pi/2} [3x(\omega-x)]^{-\frac{1}{2}} F_{90^\circ}(x)\,dx, \qquad (I.3.11)$$

with $x = \dfrac{\omega}{1-3\cos^2\beta_b}$ and where ω represents only the positive angular frequencies originating from one transition (m=0 to m=1 for instance). One sees from Equation (I.3.11) that the powder spectrum is expressed as a function of only one orientation. Therefore, by knowing $G(\omega)$ one can obtain $F_{90^\circ}(x)$, the spectrum for $\beta_b = 90^\circ$. Equation (I.3.11), when translated

into computer language, is only a finite summation over the data points:

$$g(n) = \sum_{k=1}^{n} A(n,k)\, f_{90^\circ}(k), \qquad \text{(I.3.12)}$$

where the $g(n)$ and $f_{90^\circ}(k)$ are the discrete contributions to the powder and oriented spectra, respectively, and where $A(n,k)$ is a finite estimation of $(3k(n-k))^{-\frac{1}{2}}$. The computing process "reads" the frequencies from the right to the left hand side of the powder pattern and begins to solve Equation (I.3.9) when encountering a non-zero-intensity data point. While doing so, the program will "find", in addition to $F_{90^\circ}(x)$, the shoulder ($\beta_b=0^\circ$) belonging to the other transition (m=-1 to m=0). This additional undesired contribution can be suppressed by using the first estimation of the $f_{90^\circ}(k)$ to calculate it from Equation (I.3.12) and then to subtract it from the experimental spectrum. The calculation is started again with this corrected experimental spectrum. Bloom et al. found that the calculation converged with 3 iterations, that is, a well defined doublet was obtained from a powder pattern lineshape.

The quadrupolar splitting was estimated by fitting empirically the dePaked lines with a Gaussian or Lorentzian lineshape function. The routine used for fitting belongs to the Nicolet 1280 NMR software.

The original dePaking program (Rance, M., 1981, unpublished result) was modified to process a series of spectra keeping their primary intensity (used in T_{1Z} or T_2 analyses).

All the calculations described in this thesis were processed either on Nicolet 1280 or IBM/TSS370 computers.

REFERENCES TO CHAPTER I.3

Bloom, M., Davis, J.H. and Mackay, A.L. (1981), Chem, Phys. Letters, 18, 198.

Carr, H.Y. and Purcell, E.M. (1954), Phys. Rev., 94, 630.

Chadha, J.S. (1970), Chem. Phys. Lipids, 4, 104.

Davis, J.H., Jeffrey, K.R., Bloom, M., Valic, M.I. and Higgs, T.P. (1976), Chem. Phys. Lett., 42, 390.

Davis, J.H. (1979), Biophys, J., 27, 339.

Dufourc, E.J., Smith, I.C.P. and Jarrell, H.C. (1983), Chem. Phys. Lipids (in press).

Fieser, L.J. (1963), Organic Syntheses, Coll. Vol. IV, 195.

Gruenke, L.D. and Craig, J.C. (1979), J. Labelled Compounds and Radiopharmaceuticals, 16, 495.

Gupta, C.M., Radhakrishnan, R. and Khorana, H.G. (1977), Biochemistry, 74, 4315.

Kates, M. (1972), Techniques of Lipidology, North-Holland Publishing Co., Amsterdam.

Oldfield, E., Meadows, M., Rice, D. and Jacobs, R. (1978), Biochemistry, 17, 2727.

Salinger, Z. and Lapidot, Y. (1966), J. Lip. Res., 7, 174.

Seelig, J. (1977), Quart. Rev. Biophys., 10, 353.

PART II

CYCLOPROPANE-CONTAINING LIPIDS

CHAPTER II.1

CYCLOPROPANE-CONTAINING LIPIDS

1. ORGANIZATION

II.1.1 Introduction

Fatty acids containing a cyclopropane ring, for example, the dihydrosterculic acid (DS) (Figure II.1-1a), are found in a variety of organisms such as bacteria and protozoa (Christie, 1969). These acids appear in the structural lipids and there is considerable evidence that they are synthesized from the corresponding unsaturated fatty acids by addition of a "C_1" fragment (Hofmann, et al., 1959). The donor of the CH_2 group was found to be a methionine, such as S-adenosylmethionine, which is a known source of methyl groups in the biosynthesis of natural products (O'Leary, 1962). This biosynthetic pathway would explain in fact why cyclopropane-containing fatty acids have the same positional distribution as monoenoic fatty acids in PL. It is well established that these unsaturated acids are present in phospholipids such as PE (Figure II.1-1b), which is the principal PL in most bacteria, at the sn-2 position. However, it is not known why the cyclopropane moiety is preferred to the double bond and why the bacteria perform such an energy expensive reaction to form cyclopropane fatty acids. Most intriguing

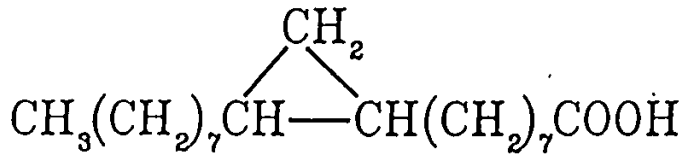

a)

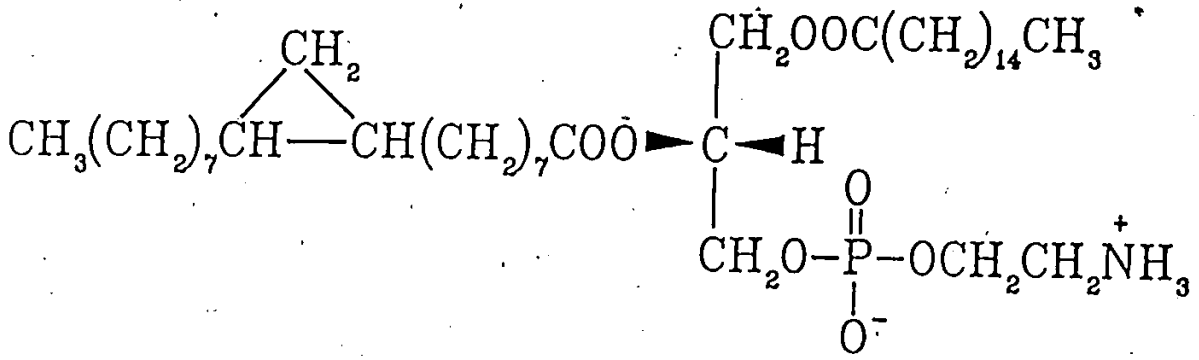

b)

Fig. II.1–1. a) Structure of the cis–9,10–methyleneocta–decanoic acid (dihydrosterculoyl acid) occuring in bacterial membranes.
b) Structure of the 1–palmitoyl–2–dihydrosterculoyl–sn–glycero–3–phosphoethanolamine occuring naturally in bacterial species.

is the fact that the cyclopropane-containing acids appear in bacterial cultures at the latter stages of the growth (E. coli, Law, et al., 1963; Serratia marcescens, Kates, et al., 1964). It has been suggested that when the production of cyclopropane acids has ceased the fatty acid composition in the membrane is stationary (Law, et al., 1963). In other words, the growth is stationary when a certain concentration of cyclopropane-containing fatty acids is reached.

A recent differential thermal analysis (DTA) study (Silvius and McElhaney, 1979) on cyclopropane versus monoenoic-containing PC leaded to the conclusion that the effects of replacement of a double bond by a cyclopropane were subtle.

In order to have a better understanding of the cyclopropane-containing lipids, the synthesis of specifically deuterium (^2H)-labelled PC was achieved (Dufourc, et al., 1983). The PL chosen as a model membrane was the 1-palmitoyl-2-dihydrosterculoyl-sn-glycero-3-phosphocholine (PDSPC). The deuteration was accomplished as described in Chapter I.3 on both fatty acyl chains in a total of 14 carbon positions. This work was undertaken in order to develop a basis for studies on the more complex biological systems such as Acholeplasma laidlawii (Jarrell, et al., 1983).

II.1.2 Organization of the sn-2 DS Chain in PDSPC

II.1.2a Theoretical Background

It is widely considered that the lipids in model and natural membranes exist in one or another liquid crystalline state; the structural properties of these molecules can therefore be described in terms of order parameters (Saupe, 1964). As has been shown in Chapter I.2, each rigid subunit of a molecule can be associated with a symmetric, second rank, traceless, order parameter tensor $\underline{S}$. The ^{2}H-NMR observables in model membranes can be related to this tensor through Equation (I.2.23), rewritten here as:

$$\Delta\nu = \frac{3}{2} A_Q \tfrac{1}{2}(3\cos^2\beta_b - 1) S_{33} \qquad \text{(II.1.1)}$$

where the order parameter tensor element $S_{33} = \tfrac{1}{2}\overline{(3\cos^2\beta_p - 1)}$ represents the angular fluctuations of the C-^{2}H bond vector with respect to the axis of motion ($\vec{n}$) (see Figure II.1-2). Petersen and Chan (1977) split S_{33} into two components:

$$S_{33} = S_\alpha S_\gamma = \tfrac{1}{2}\overline{(3\cos^2\alpha - 1)}\,\tfrac{1}{2}\overline{(3\cos^2\gamma - 1)} \qquad \text{(II.1.2)}$$

where the bar denotes a time average, γ represents the angle between the C-^{2}H bond vector and the instantaneous segmental chain orientation, and α is the angle between the instantaneous segmental

chain orientation and the director of the motion $\vec{n}$, taken to be the normal to the bilayer surface.* In order to use the same conventions as Petersen and Chan, we set $\theta'=\beta_b$. The angles α, γ and θ' are shown in Figure II.1-2. The S_{C-^2H} order parameter is usually derived from Equation (II.1.1).

$$\Delta\nu_Q = \Delta\nu_{\theta'=90^o} = \frac{3}{4} A_Q S_{C-^2H} = \frac{3}{4} A_Q S_\alpha S_\gamma \qquad \text{(II.1.3)}$$

For rigid molecules such as cyclopropane or cholesterol Equation (II.1.3) transforms to

$$\Delta\nu_Q = \frac{3}{4} A_Q \overline{\frac{(3\cos^2\alpha-1)}{2}} \; \frac{(3\cos^2\gamma-1)}{2} \qquad \text{(II.1.4)}$$

where the oscillations of the γ angle are of sufficiently small amplitude, given the constraints of the rigid cyclopropane structure, to allow Equation (II.1.4) to be valid over a wide range of temperatures. The term $\overline{((3\cos^2\alpha-1)/2)}$ is often referred as the molecular order parameter, S_{mol}.

It might appear crude to split S_{C-^2H} into two components S_α and S_γ; however, by doing so one will be able to distinguish between pure angular fluctuations of the entire rigid unit (S_α order parameter) and the geometrical orientation of a particular $C-^2H$ bond with respect to the instantaneous axis of motion.

* The α and γ angles should not be confused with the Eulerian angles used in the appendices.

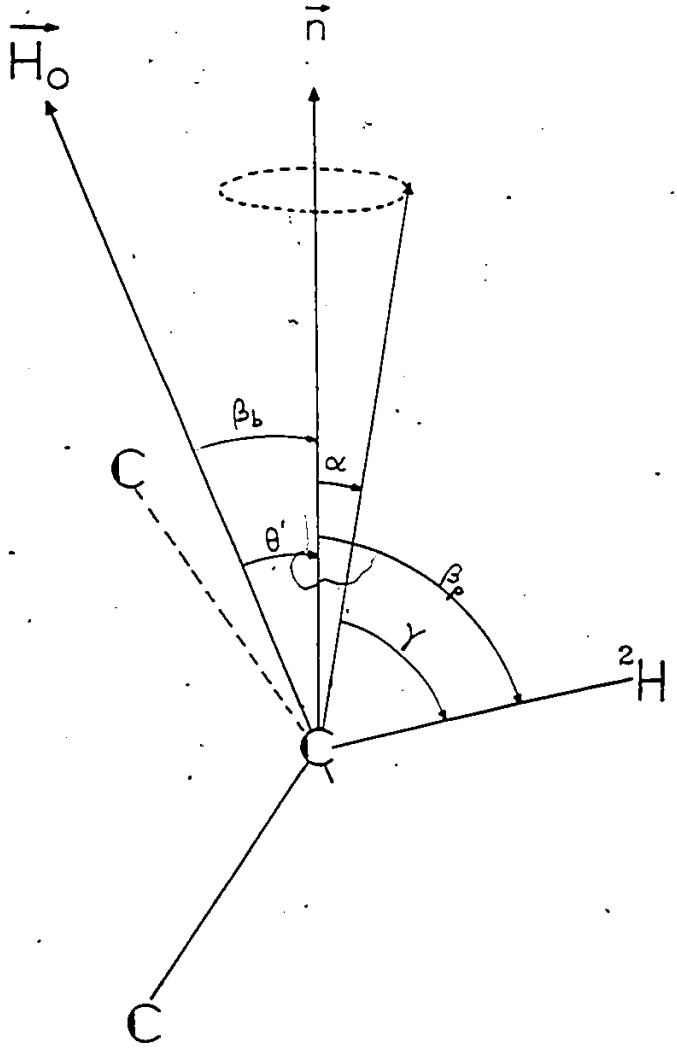

Fig. II.1–2. The angles β_p, β_d, θ', α and γ used to define the motional averaging (see text).

II.1.2b The Liquid-Crystalline Phase

Deuterium spectra of seven different samples were recorded as a function of temperature over the range 0-40°C. Only two samples showed a single quadrupolar powder pattern, those in which the dihydrosterculic acid chains were labelled at the C-5' or the C-16' positions. The other samples exhibited a superposition of two quadrupolar powder patterns, except for those labelled at C-9', 10' and C-19' which showed additional spectral features (vide infra). Spectra from the seven samples at 20°C are shown in Figure II.1-3. In all cases, the spectral shapes are characteristic of axially symmetric motions (η=0) of lipids in a liquid crystalline phase, as described by Seelig (1977). The spectra shown in Figure II.1-3 were "dePaked" as described in Materials and Methods and the resulting calculated spectra are given in Figure II.1-4.

DePaked spectra exhibiting several splittings were analyzed by the curve fitting routine described in Materials and Methods: in all cases, the two pairs of major lines for each dePaked spectrum had equal area, within the experimental error (2-3%).

DePaked spectra corresponding to the [19'-$^2H_2$] and [9',10'-$^2H_2$] labelled positions show, in addition to the major lines, small features, noted as "*" in Figure II.1-4,

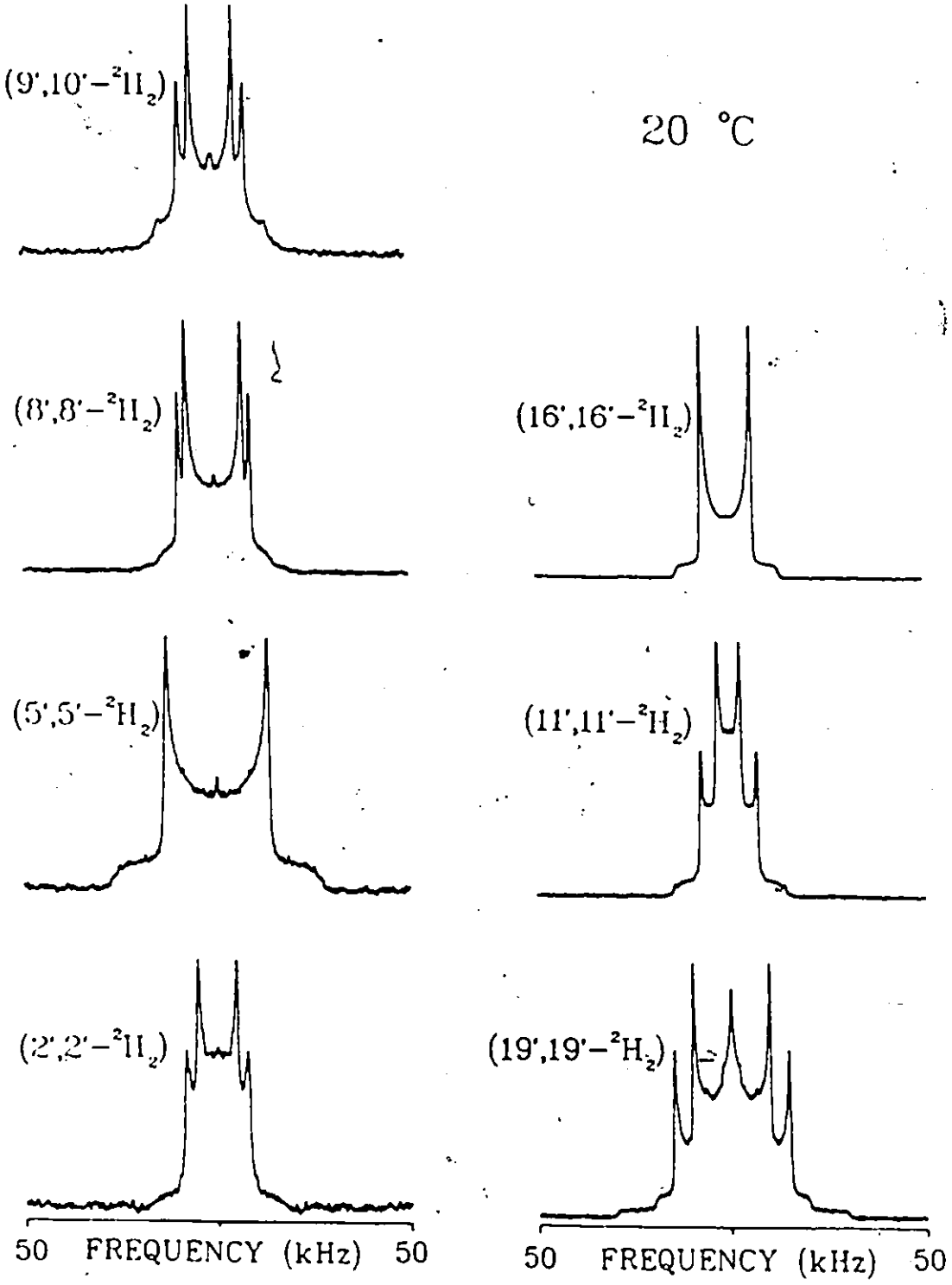

Fig. II.1-3. ^2H-NMR spectra of PDSPC model membranes at 20 °C. The dihydrosterculoyl chains are deuterated at the positions indicated. Typical experimental parameters: $\pi/2$ pulse length of 5 μs; pulse spacing of 60 μs; recycle time 0.1 to 0.2 s; 250 kHz spectral window; 20,000 accumulations.

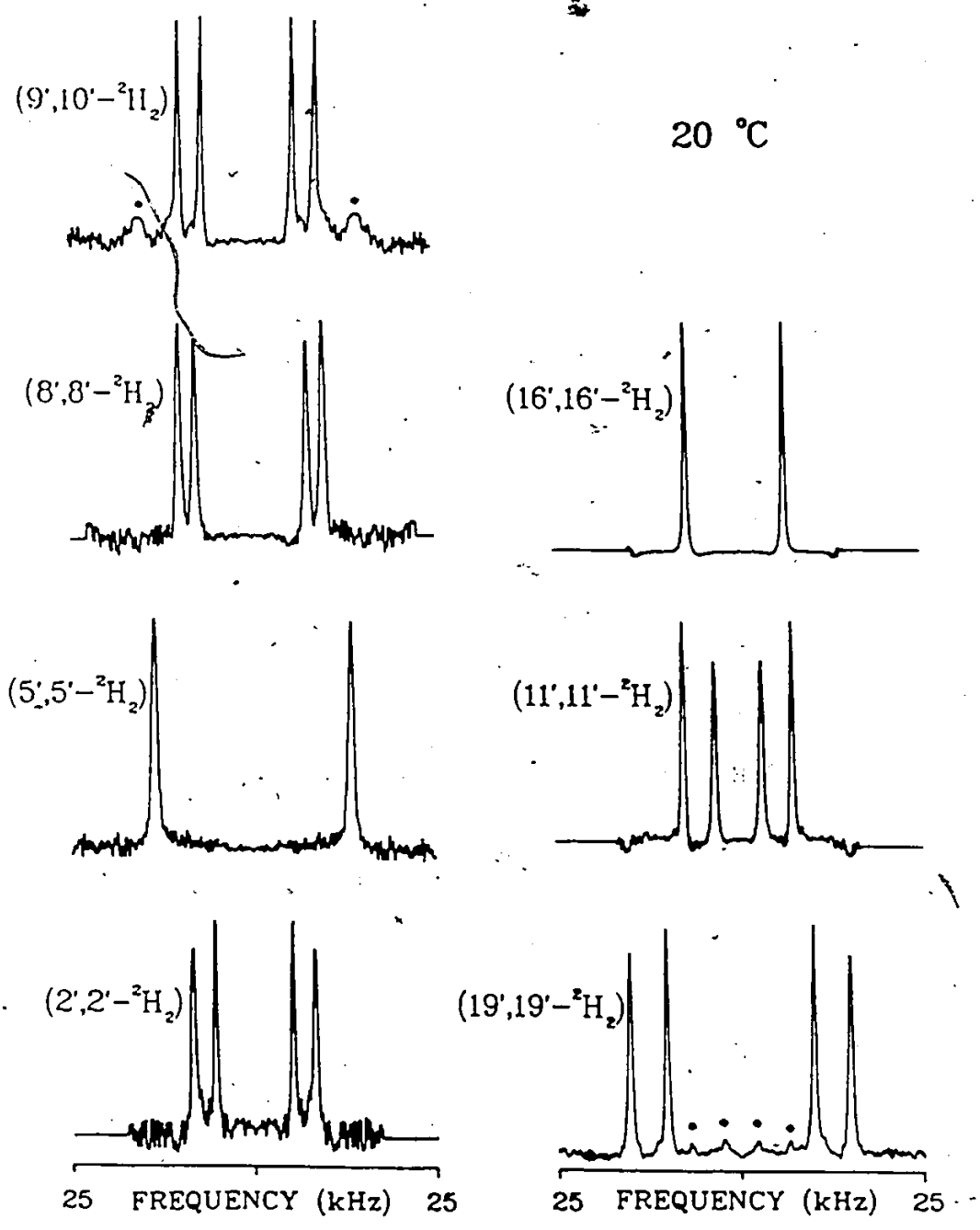

Fig. II.1-4. Same as in Fig. II.1-3, but all the spectra were dePaked. Processing parameters: deconvolution on 200 to 500 data points using 3 iterations (see text).

corresponding to quadrupolar splittings of 4.6, 14 and 29 kHz, respectively. The additional components were attributed to the trans isomer of the PDSPC, by comparison with the results reported by Seelig and Waespe-Šarčevič (1978) for 1-palmitoyl-2-elaidoyl-sn-glycero-3-phosphocholine (PEPC) deuterated at the trans double bond (trans-9',10'-$^2H_2$). Previous gas-chromatographic data also indicated that the DS acids deuterated at the 9,10 and 19 positions were contaminated by ~3-4% of their respective trans isomer (Jarrell, H.C., Tulloch, A.P. and Smith, I.C.P., to be published). The peaks noted "*" correspond to about 6-7±3% of the total spectral area, which is consistent with their assignment to the trans isomer of DS in the PDSPC.

In the earlier study of PEPC it was observed that the deuterons at C-9' and C-10' are equivalent, that is, that their respective C-^{2}H bonds have the same average orientation with respect to the axis of motion. A calculation analogous to that derived for the cis PDSPC (see appendices) showed that the C-^{2}H bonds at C-9' and C-10' in the trans PDSPC are oriented at approximately 90° to the director of the motion, $\vec{n}$, whereas the C-^{2}H bonds of the C-19' deuterons are close to the magic angle (54.7°).

In the temperature range 0-40°C the powder spectra for all labelled positions had the shape characteristic of axial symmetry. The quadrupolar splittings of the peaks, $\Delta\nu_Q$,

for the lipid in the liquid crystalline phase were measured from the dePaked spectra as a function of temperature and as a function of the label position (Figure II.1-5).

It is noteworthy that the $\Delta\nu_Q$ estimated from dePaked spectra is thought to be the "true" quadrupolar separation since this value is free from the convolution operation (Seelig, 1977) defining the powder spectrum. In Figure II.1-6 we plot the quadrupolar splitting ratio, $\Delta\nu^k_{Q,T_j}/\Delta\nu^k_{Q,T_o}$, where $\Delta\nu^k_{Q,T_j}$ and $\Delta\nu^k_{Q,T_o}$ are the quadrupolar splittings of the kth position at a given temperature, T_j, and at 0^oC, respectively, as a function of the temperature T_j. Both Figures II.1-5 and II.1-6 show a decrease in quadrupolar splitting with increasing temperature, except for the [2'-$^2H_2$] derivative where the inner splitting, denoted as $2'_i$, increases with increasing temperature. The temperature behaviour of $\Delta\nu_Q$ may be explained with the use of Equation (II.1.3) which can be rewritten as

$$\Delta\nu_Q = \frac{3}{4} A_Q S_\alpha S_\gamma; \qquad \text{(II.1.5)}$$

hence, $\Delta\nu_Q$ might vary according to the angular excursions of the C-^{2}H bond with respect to the instantaneous segmental chain orientation (S_γ) or to the angular fluctuations of the instantaneous segmental chain orientation with respect to the director (S_α). In other words, the $\Delta\nu_Q$ variation would be governed by "segmental" (S_α) and "geometrical" (S_γ) factors,

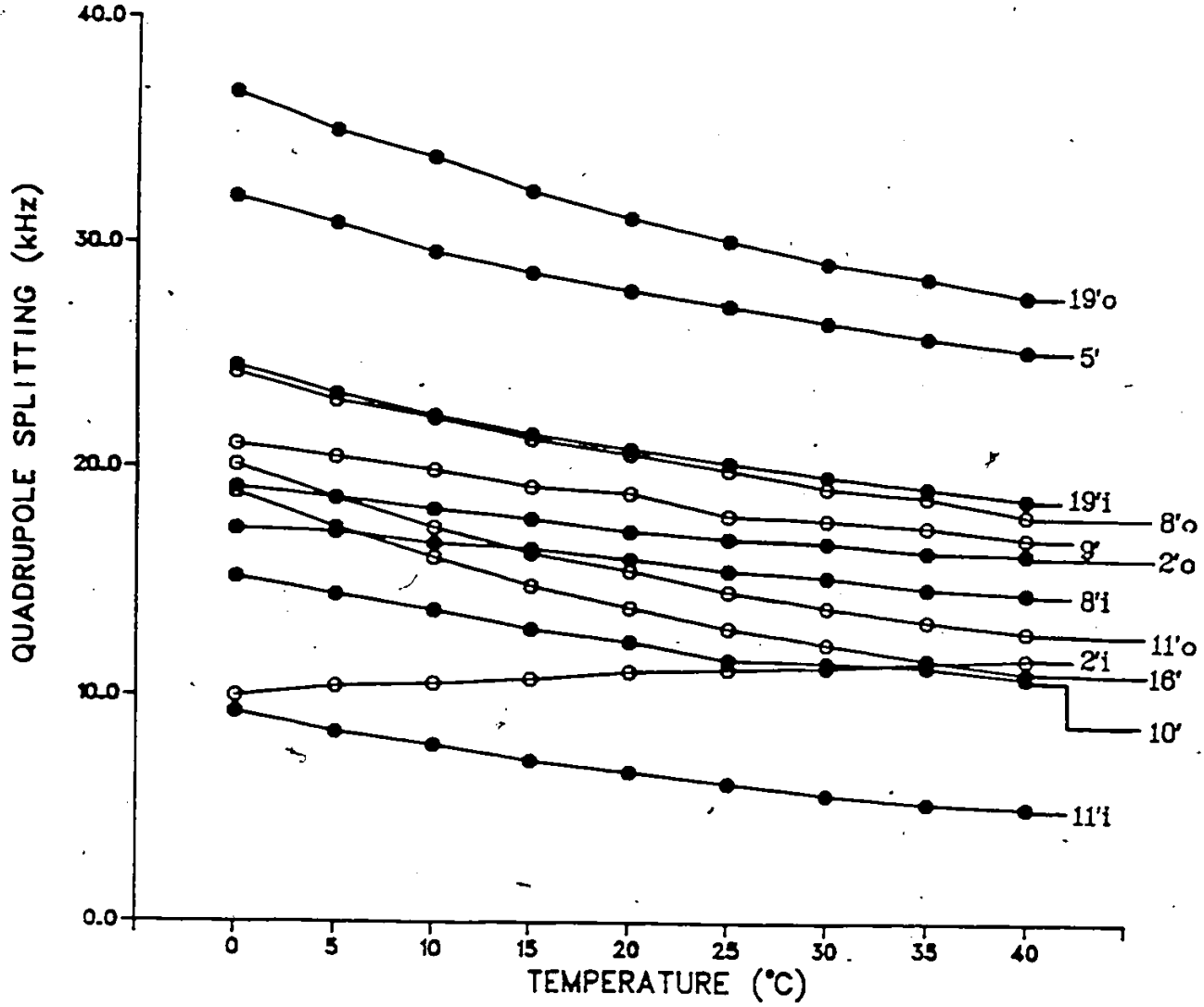

Fig. II.1–5. Temperature dependence of the quadrupolar splittings for specifically deuterium-enriched PDSPC model membranes. Labeled positions are indicated by means of carbon numbering. Subscript o = outer splitting, subscript i = inner splitting. The size of the symbols gives an estimate of the experimental error. The assignment of the 9', 10' positions is arbitrary.

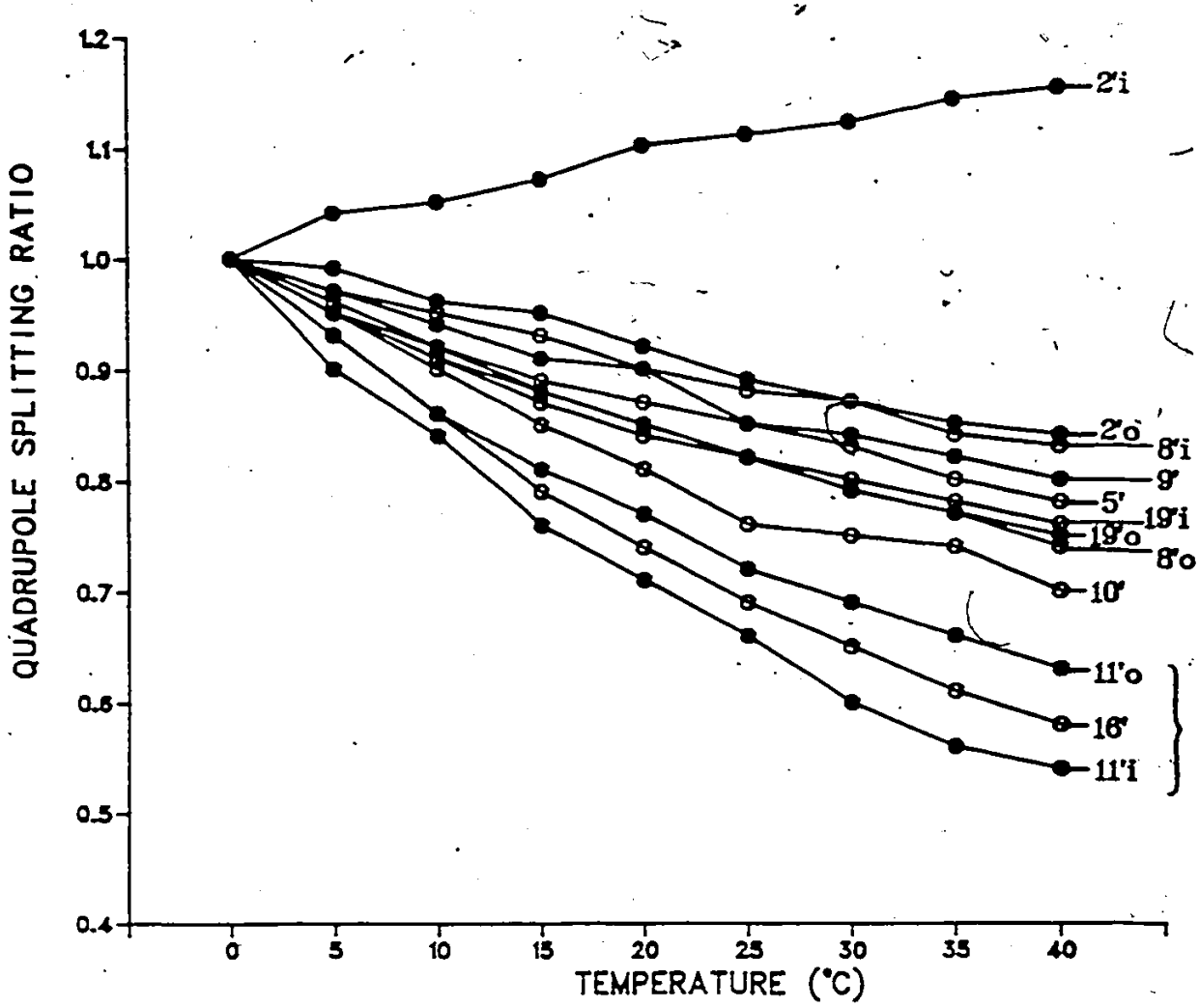

Fig. II.1–6. Temperature dependence of the quadrupolar splitting ratios: $\Delta\nu^{k}_{Q,T_j}/\Delta\nu^{k}_{Q,T_o}$; k = kth ^{2}H labeled position of PDSPC model membranes; j = jth temperature and T_o = 0 °C. Other notations as given in Fig. II.1–5.

so that when the temperature increases S_α and S_γ decrease for the positions down the chain. The general $\Delta\nu_Q$ decrease which is observed in Figures II.1-5 and II.1-6 for all labelled positions except the [2'-$^2H_2$] could be attributed to an increase in amplitude and/or rate of the motions of the chains (chain tilting, translational diffusion, rotational diffusion and gauche-trans isomerization, for example). Deuterons at positions beyond the cyclopropane ring, C-11' and C-16', give rise to more pronounced decreases in $\Delta\nu_Q$ than do the others, over the same temperature range, indicating that the lower half of the DS chain is subject to greater angular excursions about the axis of motion, $\vec{n}$, than is the upper half.

The temperature behaviour of $\Delta\nu_Q$ for the deuterons at the C-2' position seems to be even more complex. Engel and Cowburn (1981) have shown by specific labelling with deuterium at the pro-R position of the sn-2 chain that the two quadrupolar splittings observed for the 1-palmitoyl-2-[2'-$^2H_2$] palmitoyl-sn-glycero-3-phosphocholine arose from spatial inequivalence of the two deuterons, rather than from two long-lived conformations for the methylene segment. The authors estimated the average orientations of the C-^{2}H bonds for the two deuterons: the C-^{2}H bond of the pro-R deuteron is normal to the extended chain axis, while the C-^{2}H bond of the pro-S deuteron makes an angle of approximately 34 degrees. The integrated area of both pairs of peaks is identical for the

[2'-$^2H_2$] PDSPC, suggesting a similar explanation in this case. Hence the $\Delta\nu_Q$ identified as 2_0 might be attributed to the pro-R deuteron and that noted 2_i to the pro-S. Any excursion from the 90° average orientation of the pro-R deuteron would lead to a decrease in S_γ and hence a decrease in $\Delta\nu_Q$ with temperature. A change from 34° to 30° in the average orientation of the pro-S deuteron would lead to an 18% increase in S_γ. Therefore the apparently abnormal temperature behaviour of the pro-S $\Delta\nu_Q$ would be simply due to a counterbalancing effect of the S_γ on the S_α order parameter. Such behaviour has already been observed for the pro-S deuteron in [2'-$^2H_2$] POPC by Seelig and Waespe-Šarčević (1978).

II.1.2c The Low Temperature Region

^2H spectra were recorded from the [5'-$^2H_2$]-PDSPC sample over the temperature range -20°C to 0°C (Figure II.1-7). Above -5°C the spectra are characteristic of lipids in the liquid crystalline phase. As the temperature is lowered, a second component, with a width of about 100 kHz appears, which dominates the spectrum at -20°C. The presence of two components in the low temperature spectra indicates that two phases coexist within the bilayer with an interconversion rate which is less than the difference between the quadrupolar splittings ($10^5 s^{-1}$) (Rance, et al., 1980).

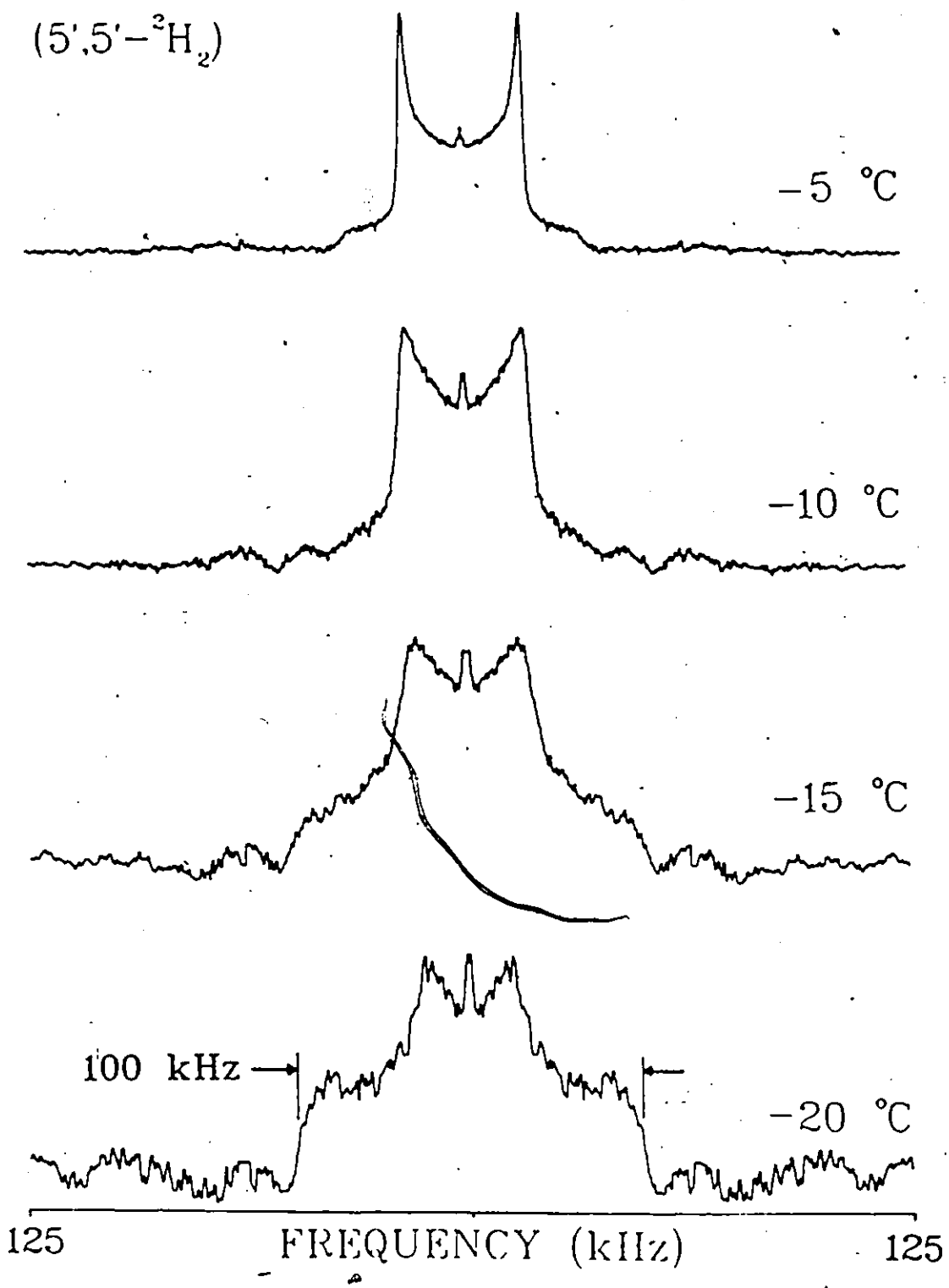

Fig. II.1-7. Temperature dependence of spectra for the [5'-$^2H_2$] PDSPC sample. Same experimental parameters as in Fig. II.1-3.

It can be seen from the spectra in Figure II.1-7 that the central component, indicative of lipid in the liquid crystalline phase, undergoes a broadening as the temperature decreases. This, in fact, suggests a reduction in the spin-spin relaxation time, T_2, in the neighbourhood of the phase transition which occurs at about -15°C. Such behaviour has already been observed in A. laidlawii membranes (Rance, et al., 1980) and interpreted as a diffusional effect (if T_2 is governed by diffusion of molecules from one domain to the next). These authors attributed the lowering of T_2 at the phase transition to the fact that a molecule could jump from a liquid crystalline to a gel state domain. In previous ^2H NMR studies of the membranes of A. laidlawii at temperature just below that of the liquid-crystal to gel phase transition, the broad spectral component due to the gel phase lipid had a width of ca. 60 kHz (Rance, et al., 1980; Smith, et al., 1979). This is the value expected for an all-trans chain rotating rapidly about its long axis. Further decrease in temperature led to broadening towards the 127 kHz expected for cessation of motion. The present spectra, Figure II.1-7, have quite different behaviour. The large spectral component which appears during the transition has a width of ca. 100 kHz, demonstrating that very little motional averaging of the quadrupolar splitting tensor is taking place, that is, there is no intermediate state between liquid crystallinity and

immobility of the chains. This may be due to the bulk of the cis cyclopropane group. However, even at -20°C, the central feature of the spectrum persists; the source of this phenomenon has not yet been elucidated and requires further investigation. The persistance of the central component was also observed in NMR spectra of A. laidlawii membranes enriched in oleic acid (Rance, et al., 1980). Low temperature data for POPC are not available, but Seelig and Waespe-Sarcevič (1978) have reported that the gel-to-liquid crystal phase transition is centered at -5°C, which is comparable to the -10 to -15°C we found as the range of the transition of PDSPC from a highly ordered to a liquid crystalline phase.

II.1.2d The Order Parameter Profile

Figure II.1-8 shows the quadrupolar S_{C-^2H} order parameter as a function of the label position at 25°C. The S_{C-^2H} were calculated according to Equation (II.1.3) assuming a ^2H quadrupolar coupling constant of 170 kHz (Stockton, et al., 1975) for all labelled positions except for C-9', C-10' and C-19'. For the latter A_Q was measured on the corresponding fatty acids at -50°C and estimated to be 183 kHz ± 10 kHz. This value is in good agreement with the 184 kHz reported by Millet and Dailey (1972) for the perdeuterated cyclopropane molecule. In this figure, we also reported the S_{C-^2H} values

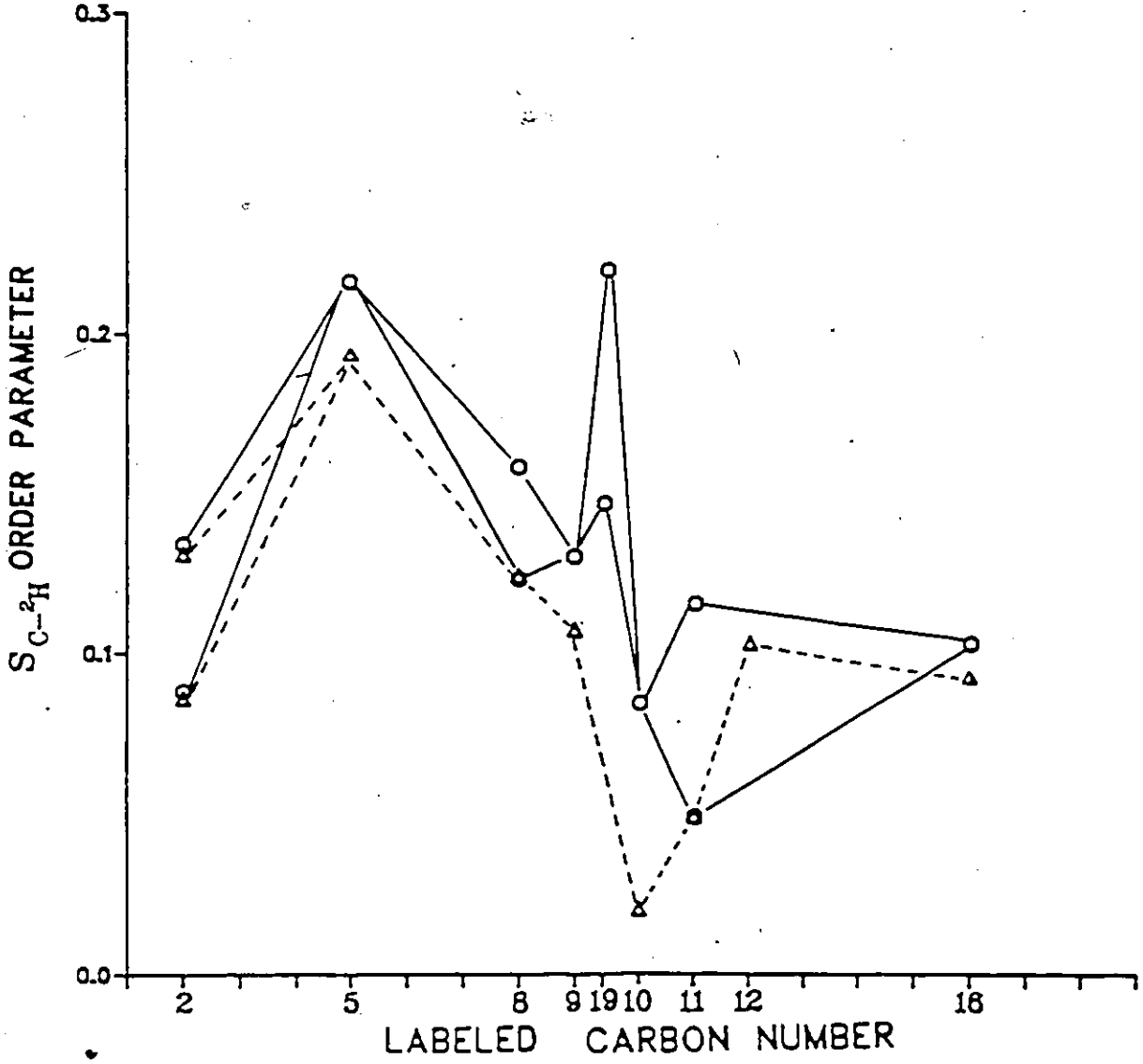

Fig. II.1–8. Variation of the deuterium order parameter S_{C-^2H} with position of labeling.

o – PDSPC data at 25°C (the assignment of the 9' and 10' positions is arbitrary).

▽ – POPC data at 27°C, from Seelig and Waespe–Šarčevič (1978). C–5' and C–16' S_{C-^2H} values are From Perly, Smith and Jarrell (to be published).

for the POPC at 27°C (C-2', C-8', C-9', C-10', C-11' and C-12' from Seelig and Waespe Sarcevič, 1978) and at 25°C (C-5' and C-16', Perly B., Smith, I.C.P. and Jarrell, H.G., to be published).

In principle, the deuterons at each of positions 8', 19', 11', could give rise to two quadrupolar splittings, if there were two different conformations of the chain at these positions, in slow exchange. Engel and Cowburn (1981) have ruled out this possibility in the case of the [2'-$^2H_2$]-DPPC and it is more likely that, in our case, all the multiple splittings arise from different average orientations of the C-^{2}H bonds of the individual deuterons. As was previously mentioned, the integrated areas of the two pairs of major peaks were identical within each sample, which seems to confirm the hypothesis of geometrical rather than conformational effects in the S_{C-^2H} profile. Figure II.1-8 does not differentiate between purely geometric effects (S_γ) and segmental fluctuations (S_α), as defined in the theoretical background. The molecular or "segmental" order parameter, S_α, as defined in the theoretical background is a measure of the statistical motions of the various subunits in the fatty acyl chain. In other words, S_α measures the angular excursions of each subunit to the axis of motion: the lower is S_α, the greater are the angular excursions. Generally, when measuring S_{C-^2H} one cannot separate S_α from S_γ (Equation II.1.5). When dealing

with rigid subunits such as the cyclopropane ring, S_γ is no longer time-averaged: each C-^{2}H bond has a fixed geometry with respect to the rigid body. One can then assume that S_α is the same for the whole unit. For instance, the cyclopropane deuterons have the same S_α but different S_γ, resulting in different S_{C-2_H}. If we have enough observables (at least 3 independent S_{C-2_H} order parameters) we can calculate S_α by estimating each individual "geometrical" term, S_γ. An analysis based on molecular order parameters, S_{mol} (or S_{33}, or S_α), will lead us to a geometry-free interpretation of the behaviour of molecules such as PDSPC with respect to the motions involved in a lipid multilayer.

Seelig and Waespe-Šarčevič (1978) and Taylor, et al. (1981), have reported two different methods for obtaining such molecular ordering interpretations. Their methods were adapted for this specific analysis (see Appendices D and E; respectively). For each method the same cyclopropane-bound coordinate system, $\underline{C}$, was chosen. The first method relates the observable S_{C-2_H} order parameters to $\underline{\underline{S}}^{\underline{C}}$ order matrices. These matrices were then diagonalized and the correct answer was chosen on the basis of the uniaxial properties of the lipid membrane (η=0). The second method (Appendix E) was used to calculate the orientations of the cyclopropane unit by comparison of calculated and experimental quadrupolar splitting ratios. The molecular order parameter was also

obtained from this latter method. In the case of the 9', 10' and 19' positions, S_{mol} was estimated using the two methods. Both methods converged to a value of $S_{mol} = 0.59 \pm 0.04$ and an orientation defined by $\beta = 89^{\circ} \pm 2^{\circ}$ and $\gamma = -59^{\circ} \pm 2^{\circ}$ (see Appendix A for a definition of the angles β and γ). Positions 8' and 11' were treated by method E (method D is not applicable in this case, since at least three independent order parameters are required for defining the order matrix in the methylene-bound coordinate system and we only have two observables) to yield $S_{mol} = 0.36 \pm 0.04$, $\beta = 19^{\circ} - 31^{\circ}$, $\gamma = 70^{\circ} - 85^{\circ}$; $S_{mol} = 0.20 \pm 0.06$, and $\beta = 70^{\circ} - 86^{\circ}$, respectively. These results are reported in Figure II.1-9. The S_{mol} reported for the positions C-5' and C-16' were taken to be $-2\ S_{C-^2H}$ (it was assumed that for these positions, the $^2HC^2H$ plane was at 90° to the instantaneous chain orientation). The S_{mol} profile observed for the PDSPC is quite unusual. The cyclopropane ring seems to induce ordering at its own level and disordering in its neighbourhood (positions 8' and 11'). In addition, a break in the molecular order parameter profile seems to occur after position 10', as already suggested by the temperature behaviour of the quadrupolar splitting ratios (see Figure II.1-6). This behaviour is quite different from that reported by Seelig and Waespe-Šarčevič for POPC bilayers (Seelig and Waespe-Šarčevič, 1978). These authors indicated that there was no

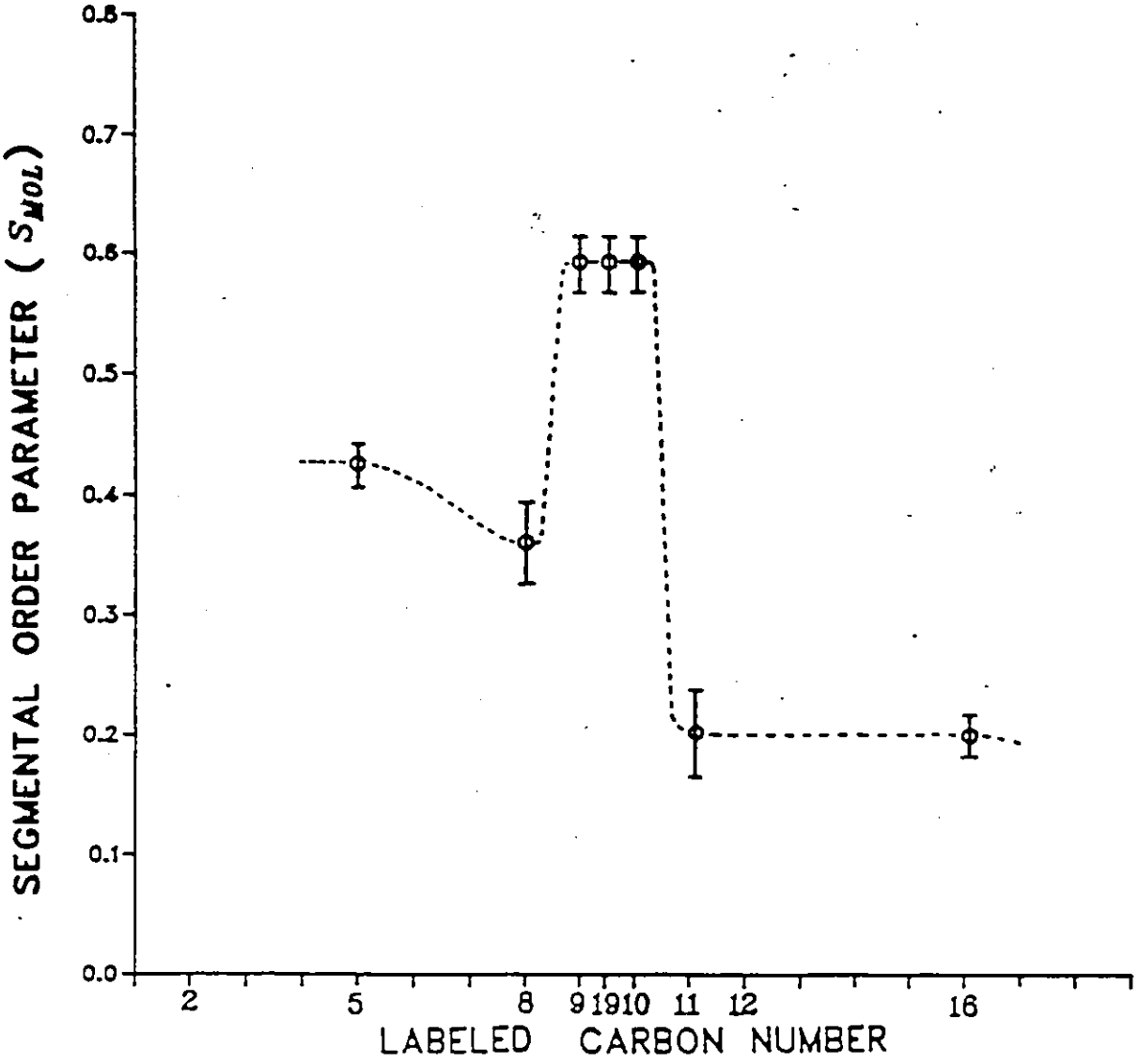

Fig. II.1–9. Variation of the deuterium segmental order parameter, S_{MOL}, with position of labeling for PDSPC samples at 25°C. The bars give an estimate of the error.

perturbation in the molecular order parameter profile and quote a value of S_{mol} = 0.37 for the deuterons at the C-9' and C-10' positions in POPC.

It has to be emphasized that these mathematical calculations do not make any assumption about the orientations of the axis of motion, $\vec{n}$. Both methods, indeed, allow the observables, defined in an arbitrary axis system, to be related to the molecular order parameter defined in the axis system (denoted "*") in which the motion has axial symmetry: the two methods "search" for this axis system. The assumption made to construct Figure II.1-9 is that the motion is fast enough such as the z* axis found for each subunit of the sn-2 DS chain lies along the same direction, $\vec{n}$.

Finally, we must mention that the calculations assume no distortions in the cyclopropane bond angles. Further refinement of the data could be made if the actual geometry of the cyclopropyl moiety within the fatty acid chain were known with more accuracy.

II.1.2e The [11'$^2H_2$] Label in POPC and PDSPC

The above results indicate that the cyclopropyl function induces a tilt of the sn-2 chain of PDSPC in the region of the cyclopropane ring which gives rise to a non-equivalence of the deuterons at the 8' and 11' positions. Seelig and

Waespe-Šarčevič (1978) suggested a ~7° tilt for the double bond of POPC, and that this would also affect the 8' and 11' positions. By analogy with the PDSPC, this tilt might induce a similar non-equivalence of the 11'-deuterons. In order to investigate this possibility the 1-palmitoyl-2-[11'-$^2H_2$] oeloyl-sn-glycero-3-phosphocholine ([11'-$^2H_2$] POPC) was prepared and the ^{2}H-NMR spectrum obtained at 25°C, as shown in Figure II.1-10. The dePaked spectrum clearly reveals that the deuterons are equivalent. Thus, the deuterons at the position C-11' in POPC have the same average orientation with respect to the axis of motion. It is interesting to notice that the apparent linewidths of the two components of the PDSPC sample, as shown in Figure II.1-10, are slightly different, explaining the difference in intensity of the two doublets of the dePaked spectrum of [11'-$^2H_2$] PDSPC. However, as we have already mentioned, the areas of the inner and outer doublets are identical within the experimental error.

Figure II.1-10 clearly outlines the differences between POPC and PDSPC systems from the ^{2}H-NMR viewpoint. This figure simply points out that the spatial orientation of the functional group (double bond or cyclopropane) must be drastically different in both systems in order to account for such spectral discrepancies.

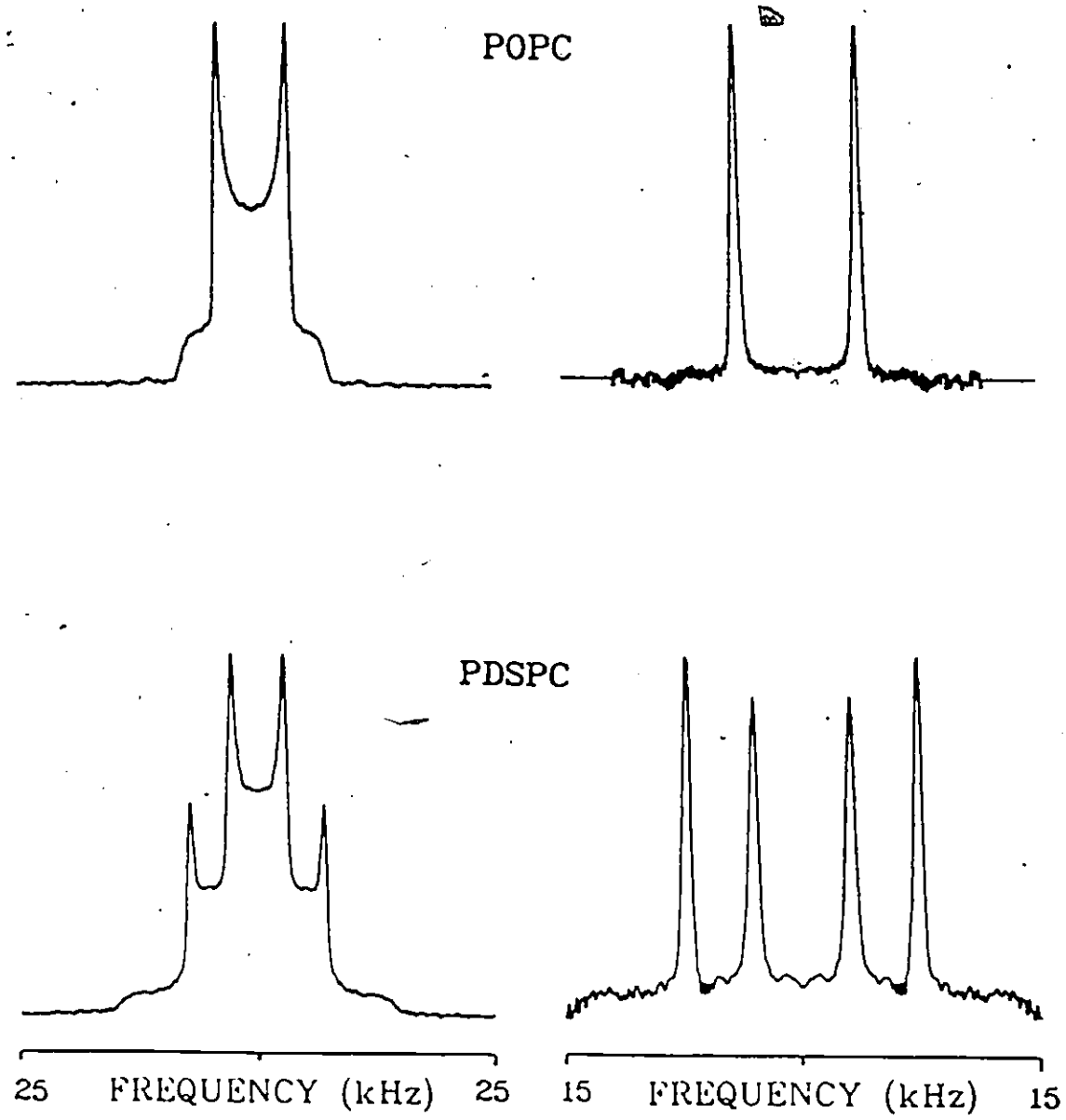

Fig. II.1–10. ^{2}H–NMR spectra and the corresponding dePaked spectra of the [11′–^{2}H$_2$] labeled position of both the POPC and PDSPC model membrane systems at 25°C. Same experimental parameters as in Fig. II.1–3.

II.1.2f Concluding Remarks

Bilayers of PDSPC exhibit properties quite different from those of other phospholipid-water systems investigated so far, especially in their temperature behaviour and their order-position profile in the liquid crystalline phase.

The packing of the molecules at low temperatures leads to ^{2}H-NMR spectral features different from those of the well known gel phase of model and natural membranes investigated so far; a highly ordered component clearly appears at -20°C, indicative of very restricted motions of the fatty acyl chains.

The cyclopropane function induces a large perturbation in the molecular order parameter profile: an increase of S_{mol} at the cyclopropane level, and a decrease of S_{mol} in its neighbourhood (positions C-8', C-11'). The cyclopropane ring appears to act as a boundary between two regions of the fatty acyl chain within the lipid layer: one region (from position 2' to the cyclopropane level) having restricted motions and a second (from the cyclopropyl unit to the end of the chain) more susceptible to fluctuations.

The calculated average orientation of the cyclopropane unit shows that the 9', 10' carbon-carbon bond is almost perpendicular to the axis of motion. If the normal to the bilayer is the axis of motional averaging, which seems to be widely verified so far in liquid-crystalline lipid phases,

the C-9', C-10' bond is almost parallel to the bilayer surface.

II.1.3 Organization of the sn-1 Palmitic Chain in PDSPC

II.1.3a The Liquid Crystalline Phase

The deuterium spectra of six different samples ([3-$^2H_2$], [6-$^2H_2$], [8-$^2H_2$], [10-$^2H_2$], [13-$^2H_2$] and [15-$^2H_2$] PDSPC) were recorded at 25°C. Figure II.1-11 shows some of these spectra as an example. All the samples, in the six labelled positions, showed a single quadrupolar powder pattern whose shape is characteristic of axially symmetric motions of lipids in a liquid-crystalline phase (Seelig, 1977). In order to obtain the "true" quadrupolar splitting, $\Delta\nu_Q$, all spectra were dePaked according to the procedure described in Materials and Methods. DePaked spectra are shown in Figure II.1-11. It is clear from the dePaked spectra that the two deuterons at any given position in the palmitic chain are equivalent, that is, they have the same spatial orientation with respect to the instantaneous chain orientation. The quadrupolar splittings have been reported in Figure II.1-12 as a function of the labelled carbon number. Figure II.1-12 shows also the quadrupolar splittings of the sn-2 DS-labelled positions (Section II.1.2b) for comparison.

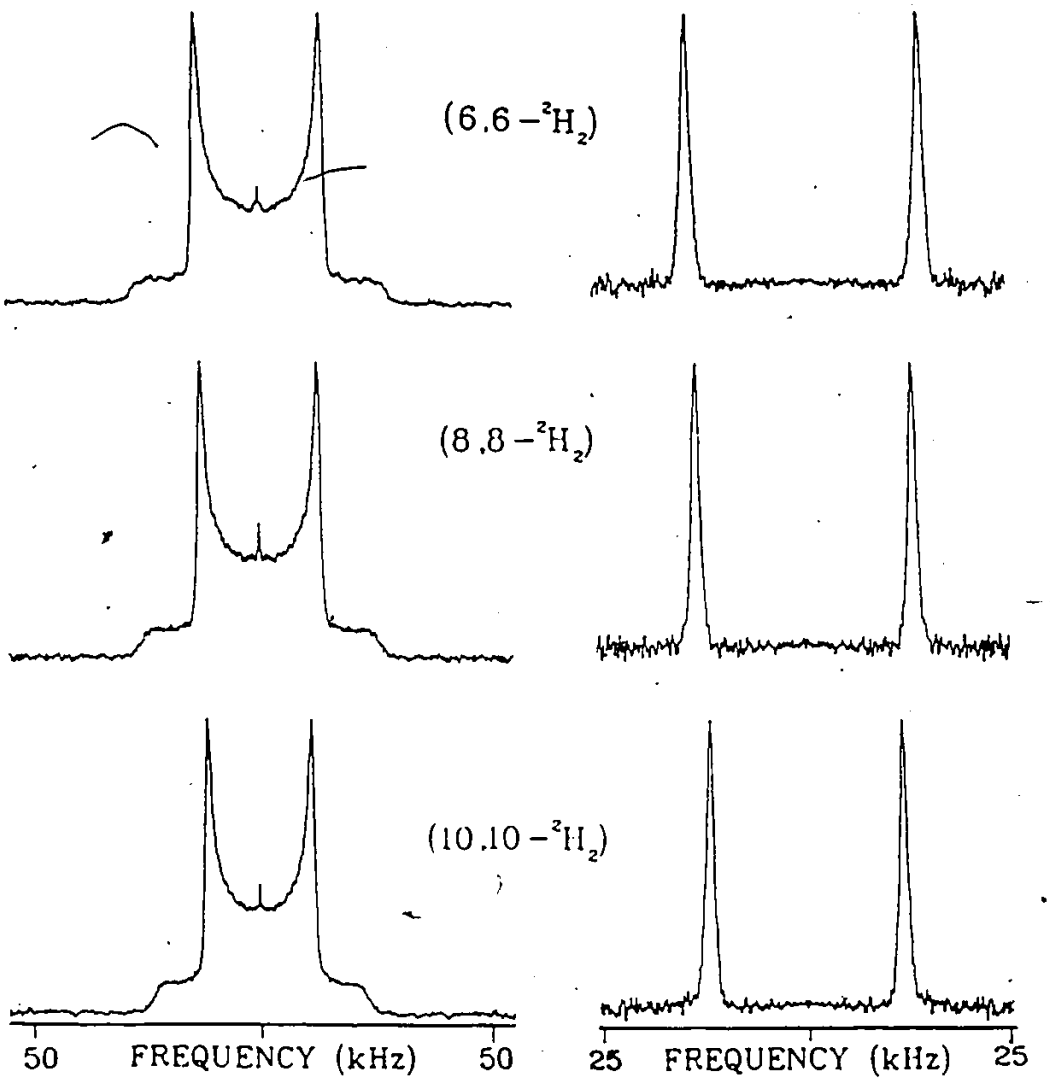

Fig. II.1–11. ^{2}H–NMR spectra and dePaked spectra of PDSPC model membranes at 25°C. The palmitoyl chains are deuterated at the positions indicated. Same experimental parameters as in Fig. II.1–3.

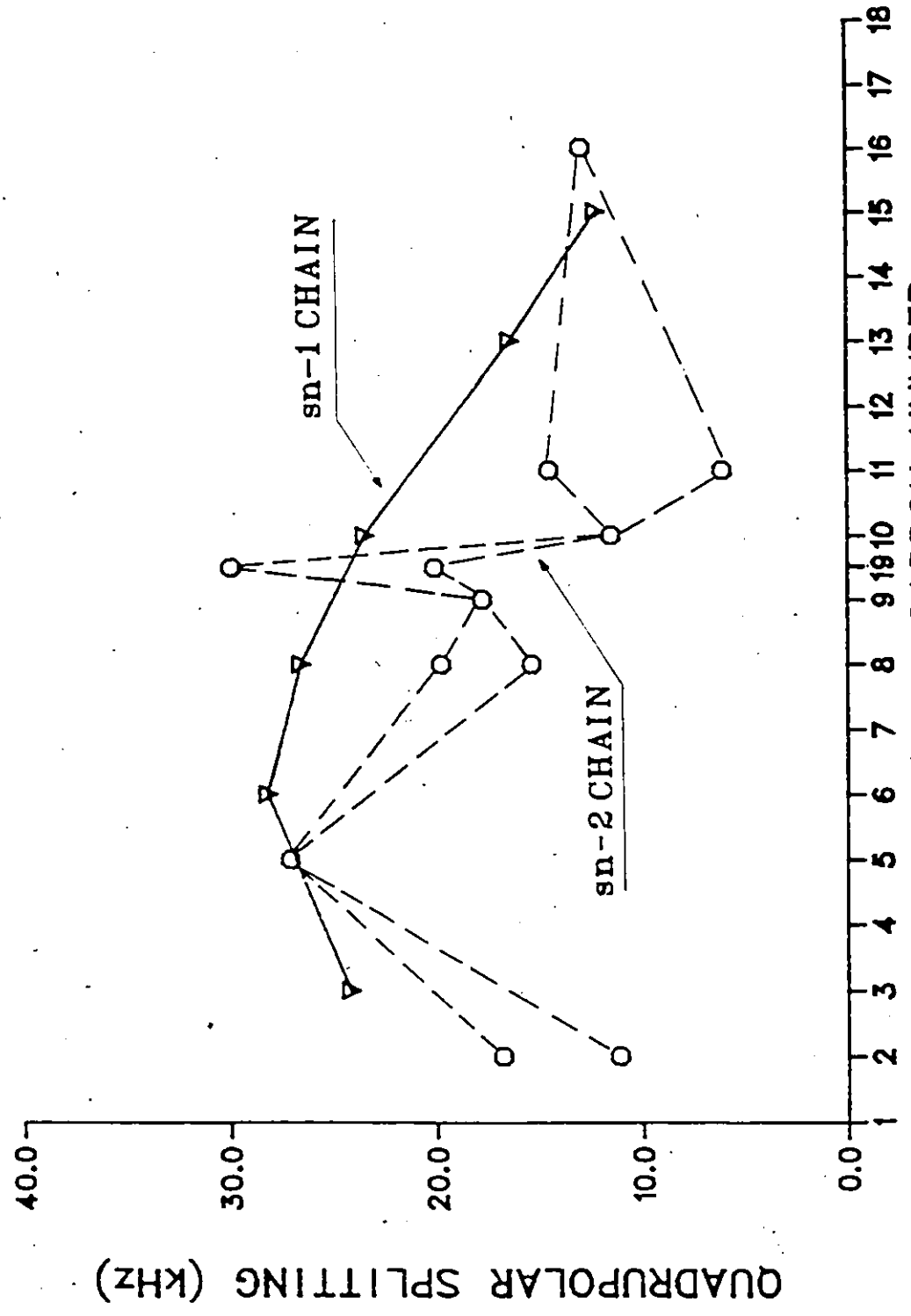

Fig. II.1–12. Variation of the quadrupolar splitting $\Delta\nu_Q$, with the position of labeling, at 25° C.
O – Dihydrosterculoyl sn–2 chain.
▽ – Palmitoyl sn–1 chain.

The first element which comes to the eye is the dramatic difference in profile between both chains. The sn-1 palmitic chain has an essentially monotonic order-position profile, whereas the sn-2 DS chain shows the perturbation induced by the cyclopropane ring. The quite complex order-position profile of the sn-2 chain can be simplified by calculating the S_α (or S_{mol}) order parameter (Section II.1.2b). Figure II.1-3 shows this "geometry corrected" molecular order profile for the sn-2 DS chain. The values reported for the molecular order parameter of the sn-1 chain in Figure II.1-3 are taken to be $-2\ S_{C-^2H}$; in doing do, we assumed that the individual $C-^2H$ bonds of this chain were oriented at 90° with respect to the instantaneous segmental chain orientation. There is no reason a priori for such a choice. It could be possible that the cyclopropane ring, in the sn-2 chain, perturbs the sn-1 chain in a way such that the deuterons at positions 8 or 10 are still equivalent but oriented at 80° or 70° with respect to the instantaneous chain orientation. S_γ would therefore be smaller than -0.5 and consequently S_α greater than $-2\ S_{C-^2H}$. However, such a molecular order profile has already been encountered in DMPC or DPPC bilayers: indeed, it was observed that the plateau region (up to carbon 10) was progressively broken when the temperature was raised above the phase transiton temperature, T_c (Oldfield et al., 1978; Seelig & Seelig, 1974). For PDSPC bilayers,

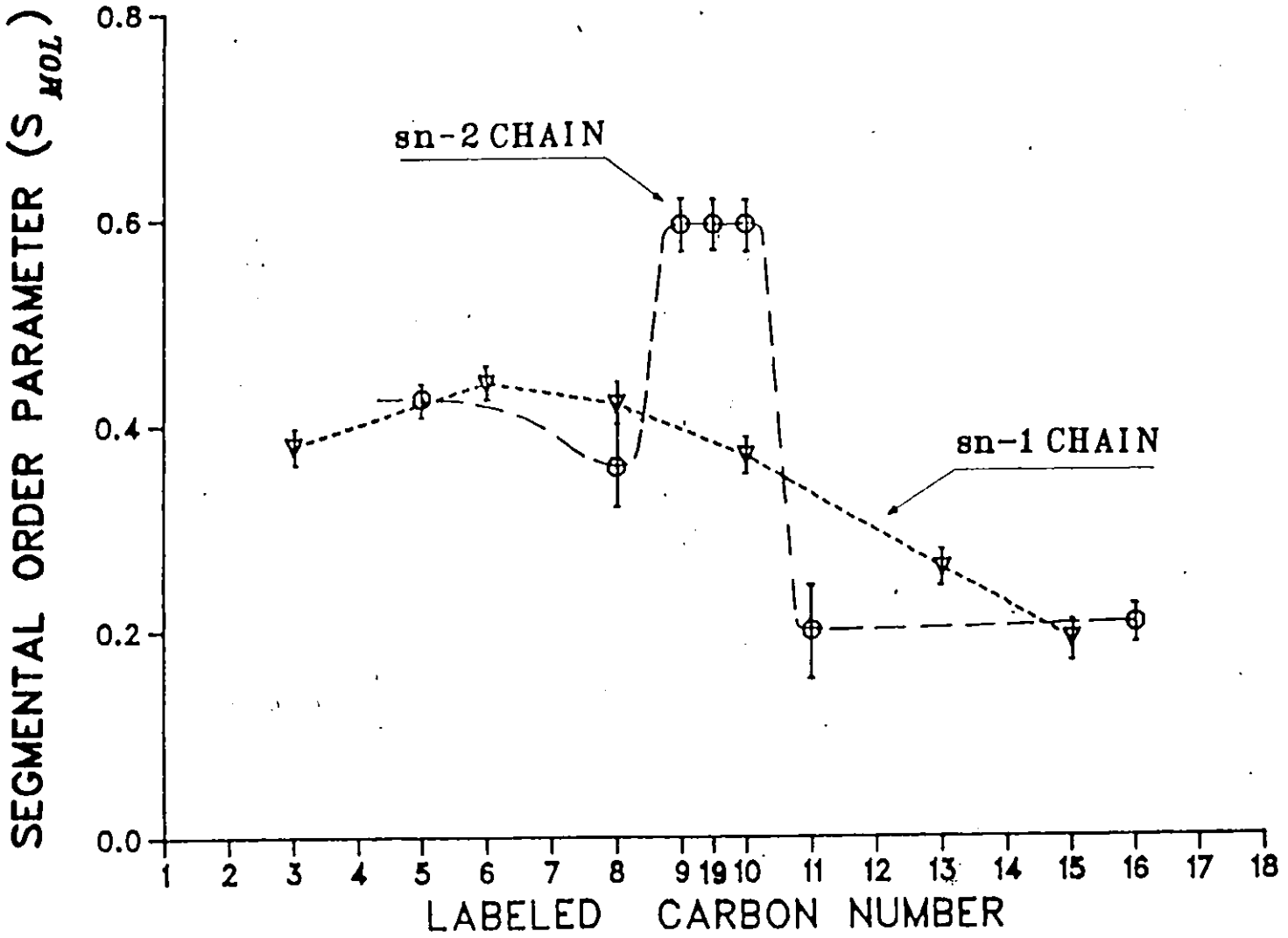

Fig. II.1–13. Variation of the segmental order parameter, S_{MOL} , with position of labeling for PDSPC model membranes at 25°C. Same notations as in Fig. II.1–12.The bars give an estimate of the error.

25°C represents a temperature ~35°C above their phase transition temperature (-10°C to -15°C). It is not surprising thus to find such a slope and almost no plateau in the molecular order profile of the sn-1 palmitic chain. Further details are developed in the next section.

II.1.3b The Plateau Region of the sn-1 Palmitic Chain

Figure II.1-14 represents the temperature behaviour of deuterons at 6, 8 and 10 positions (near the end of what plateau exists at 25°C). Figure II.1-14a shows the absolute variation of the quadrupolar splittings when the temperature is increased whereas Figure II.1-14b exhibits their change relative to carbon 6 when the temperature is raised. This figure shows clearly the progressive loss of plateau character from -10°C to 60°C. At -10°C, just above the transition temperature the 6, 8 and 10 positions show an almost horizontal line, very similar to that observed for DPPC bilayers at 41°C (Seelig, et al., 1974). Therefore, the assumption that $S_\gamma = -0.5$ made in the precedent section seemed to be justified. A more detailed analysis of Figure II.1-14b reveals that the loss of plateau character proceeds in two steps: from -10°C to 5°C only position 10 shows a decrease in its quadrupolar splitting, relative to carbon 8 and 6 positions, whereas above 5°C the plateau character is

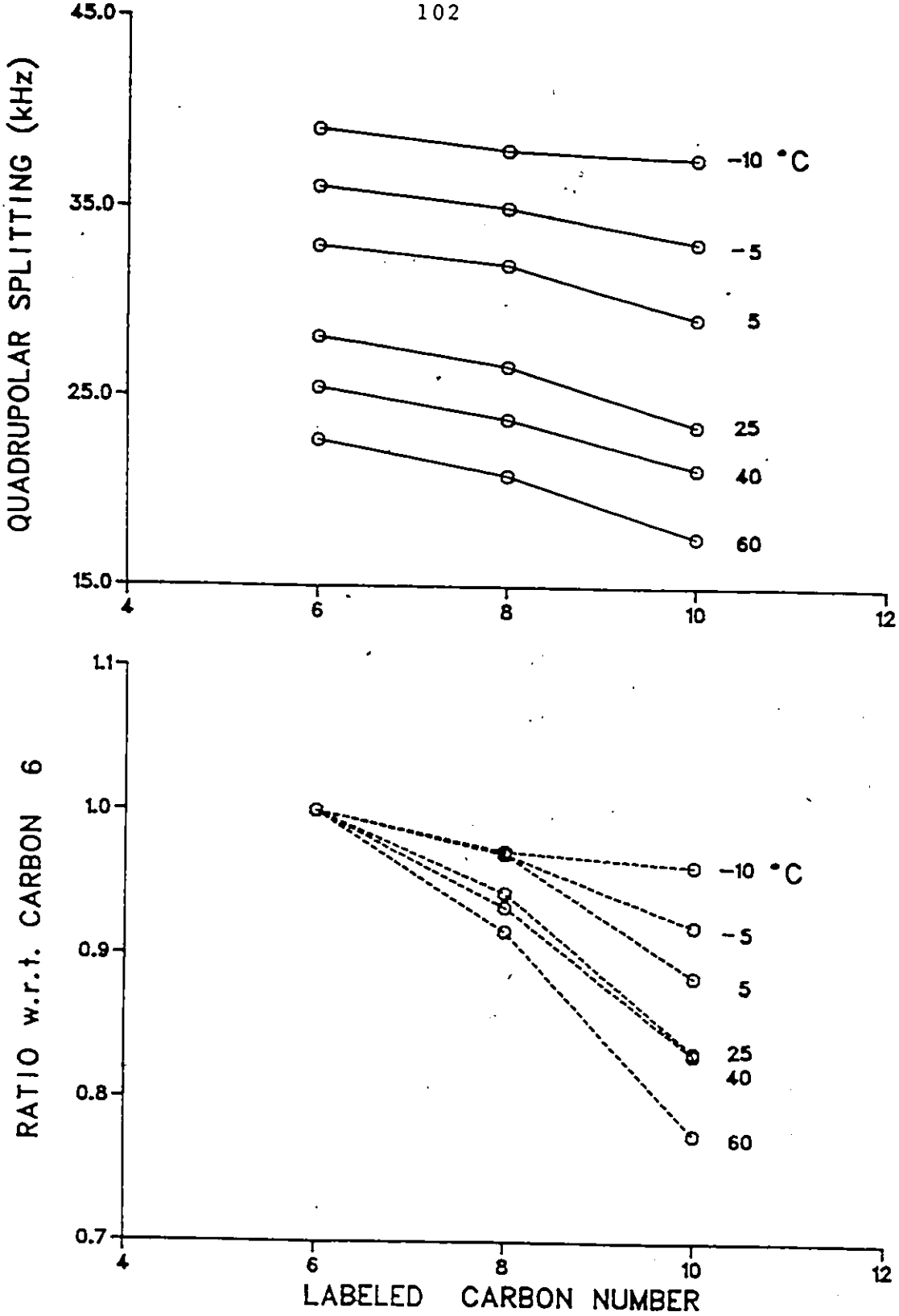

Fig. II.1-14. Temperature dependence of quadrupolar splittings for specifically deuterium-enriched PDSPC model membranes (palmitoyl sn-1 chain).
Top: quadrupolar splittings as a function of the labeled positions, at the indicated temperatures.
Bottom: quadrupolar splitting ratios as a function of the labeled positions. The ratio is made with respect to the quadrupolar splitting at C8, at a given temperature.

definitively lost. Such behaviour was not observed in bilayers of lipids with only straight saturated acyl chains: the plateau was more rapidly broken at temperatures 5 or 10°C above T_c. It appears therefore that the presence of a cyclopropyl function at the sn-2 chain preserves the plateau of the sn-1 chain, at least until the position 8, in a range of 15-20°C above T_c.

II.1.3c Temperature Behaviour of the sn-1 and sn-2 Chains

The previous sections showed that even if the cyclopropane moiety were not perturbing the order profile of the sn-1 chain, it seemed to inhibit the temperature-induced decrease of the plateau quadrupolar splittings found in fully saturated systems. In order to understand what is happening between the two chains, spectra of the [6-$^2H_2$] PDSPC were recorded between -10°C and 70°C and compared with those obtained for the [5'-$^2H_2$] PDSPC system by Dufourc, et al. (1983). All spectra within that range had axially symmetric shape and were dePaked as described in Materials and Methods. The corresponding quadrupolar splittings are reported in Figure II.1-15a. The bottom of that figure, (b), shows, for both labeled positions the quadrupolar splitting ratio, $\Delta\nu^k_{Q,T_j}/\Delta\nu^k_{Q,T_{-10}}$, where $\Delta\nu^k_{Q,T_j}$ and $\Delta\nu^k_{Q,T_{-10}}$ are the quadrupolar splittings of the kth position at the

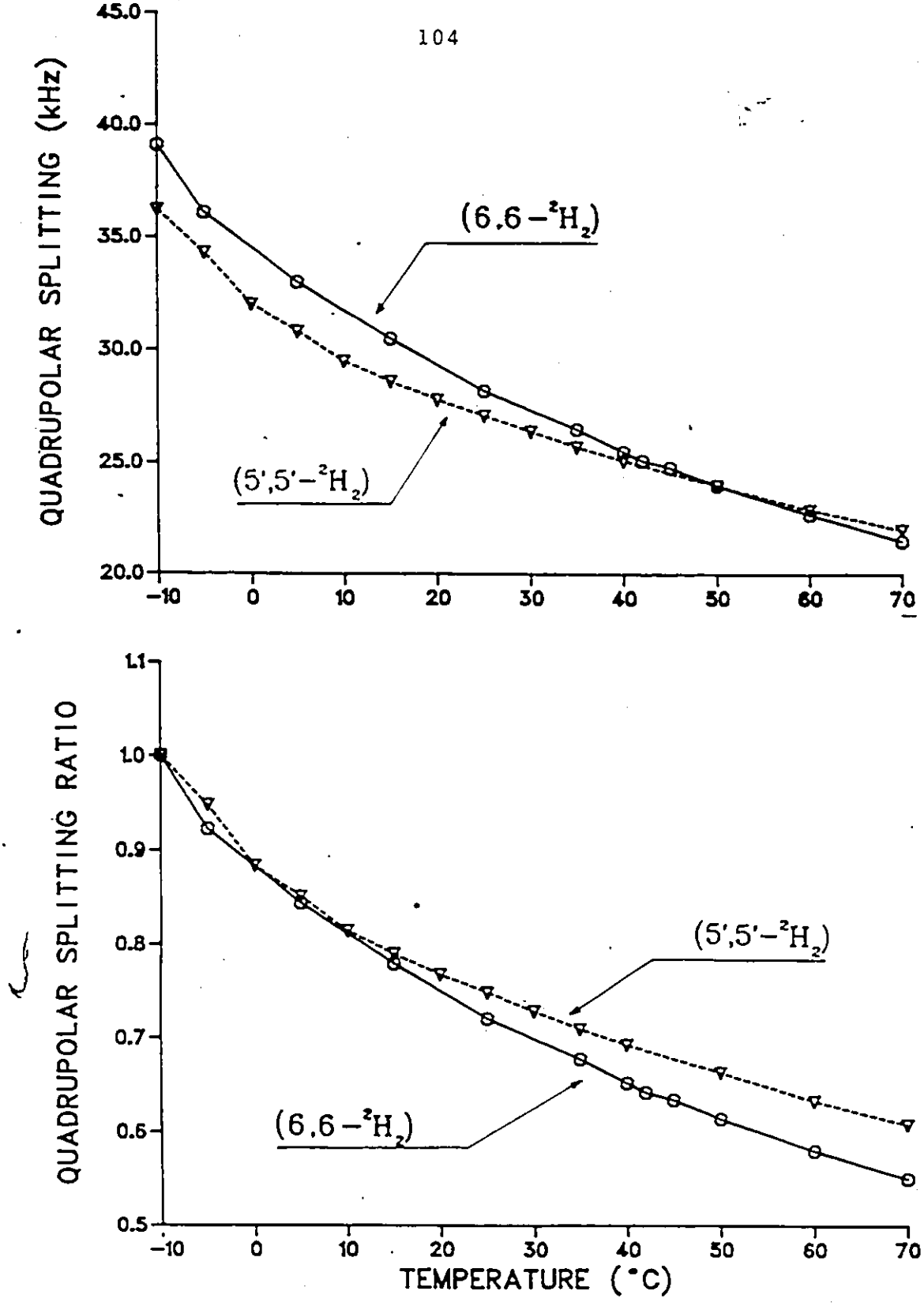

Fig. II.1-15. Temperature dependence of the quadrupolar splittings of specifically deuterium-enriched PDSPC molecules.
Top: quadrupolar splittings at the indicated labeled positions.
Bottom: quadrupolar splitting ratios (same definition as in Fig. II.1-6, with $T_o = -10°C$).
The symbols give an estimate of the error.

temperature T_j and T =-10°C, respectively. Figure II.1-15 reveals that the temperature dependence of both chains is quite different: the sn-2 chain at position 5' is less sensitive to temperature changes than the sn-1 chain at position 6. At low temperatures, the palmitic chain exhibits higher quadrupolar splittings than the DS chain. It also appears from Figure II.1-15 that both 6 and 5' positions have an identical decrease in their $\Delta\nu_Q$ for 20 to 30°C above T_c and that past 20°C, the palmitic chain at C-6 exhibits a stronger relative decrease (Figure II.1-15b) than the DS 5' position. This latter fact indicates that the local order is more rapidly lost at position 6 than 5', when the temperature is raised. It has been shown (Section II.1.2b) that the temperature variation of the upper half of the sn-2 chain (from the cyclopropane ring to the glycerol backbone) was quasi-identical for all its C-^{2}H bonds. One can thus draw the conclusion that the sn-1 palmitic chain loses its local order more easily than the sn-2 DS chain, when the motions of the entire system are increased, that is, when the temperature is raised.

It is well known that in phospholipids the two chains are not physically equivalent (Seelig and Seelig, 1975), that is, the CH_2 segments of the sn-1 chain are closer to the center of the bilayer than are the corresponding segments of the sn-2 chain. This appears to be also the case in PDSPC

model membranes (Dufourc, et al., 1983). Henceforth, it seems quite surprising to notice that the palmitic chain at position 6 has a higher $\Delta\nu_Q$ than the DS chain at position 5' (see Table II.1-1). It is instructive to compare the PDSPC system with the POPC and DPPC systems under conditions where they are in the same physical state, that is, subjected to the same average molecular forces. According to theories of phase transitions such a situation is encountered at equal temperatures relative to those of the phase transitions, T_c. Consequently, the quadrupolar splittings of positions 5 and/or 6 for both chains of the three model membranes mentioned above have been reported in Table II.1-1 at temperatures just above their respective phase transitions. This table clearly indicates that there is no difference in $\Delta\nu_Q$ between both chains in DPPC whereas the marked difference in quadrupolar splitting observed between the palmitic and dihydrosterculic chains in PDSPC is also present between the palmitic and oleic chains in POPC, at exactly the same labelled positions. Furthermore, at the same reduced temperature, one can classify the three systems in a scale of increasing order as: DPPC < POPC < PDSPC. The converse classification is almost true at the same absolute temperature, for example, 41°C. In order to account for the increase in order between DPPC and POPC, at the same temperature above their respective T_c, Seelig and Seelig (1977) brought out the idea that the C=C bond of the oleic chain

Table II.1-1

QUADRUPOLAR SPLITTINGS AT ABSOLUTE AND RELATIVE TEMPERATURES

Model Membrane System	T_c °C	$\Delta\nu_Q$, (T) Relative Temperature kHz, (°C)	$\Delta\nu_Q$, (T) Absolute Temperature kHz, (°C)	References
PDSPC sn-1 [6 -$^2H_2$]	[-10,-15]	39.2, (-10)	25.0, (42)	
PDSPC sn-2 [5'-$^2H_2$]	[-10,-15]	36.2, (-10)	25.2, (40)	Dufourc, et al., 1983
DPPC sn-1 [5 -$^2H_2$]	41	29.5, (41)	29.5, (41)	} Seelig and Seelig, 1974
DPPC sn-2 [5'-$^2H_2$]	41	29.5, (41)	29.5, (41)	
POPC sn-1 [5 -$^2H_2$]	- 5	33.8, (- 1)	24.5, (42)	} Seelig and Seelig, 1977
POPC sn-1 [6 -$^2H_2$]	- 5	35.1, (- 1)	24.9, (42)	
POPC sn-2 [5'-$^2H_2$]	[-5, 0]	31.2,(0)		Perly, et al., 1983

Comparison of quadrupolar splittings for different systems at relative and absolute temperatures. Data from Dufourc, et al. and Perly, et al. are from dePaked spectra. $\Delta\nu_Q$ from Seelig and Seelig (1977) were calculated from the value of S_{mol}, taking A_Q = 170 kHz.

induces a stiffening in the plateau region of the palmitic chain in POPC. Our results are consistent with this hypothesis. The cyclopropane ring would thus by its stiffening effect (it has been demonstrated that the ring has a higher S_{mol} than all other sn-2 positions (Section II.1.2d) increase the $\Delta\nu_Q$ of both chains and preserve the plateau region of the palmitic chain at temperatures well above that of the phase transition, T_c.

Figure II.1-15a shows that this stiffening effect is detectable at position 6 up to 40°C (50°C above T_c). If the cyclopropane ring reduces the angular fluctuations of the sn-1 chain as does the double bond, it is not obvious why the plateau region of its own chain is less ordered at low temperatures than that of the palmitic chain. Some insight may be gained on considering the calculated average orientation of the cyclopropane. It was shown that the 9'-10' bond of the ring is almost oriented at 90° to the instantaneous chain orientation (Section II.1.2d). For clarity, the spatial orientation, extracted from these calculations, is sketched roughly in Figure II.1-16, for $S_{mol} = 1$. The aim of this figure is not to represent the exact configuration of the chains, but rather to give an idea of the cylinders of influence (assuming axial symmetry) of each chain subunit. One sees thus that the cylinder of influence (the bulkiness) of the cyclopropyl unit has a larger radius than those of

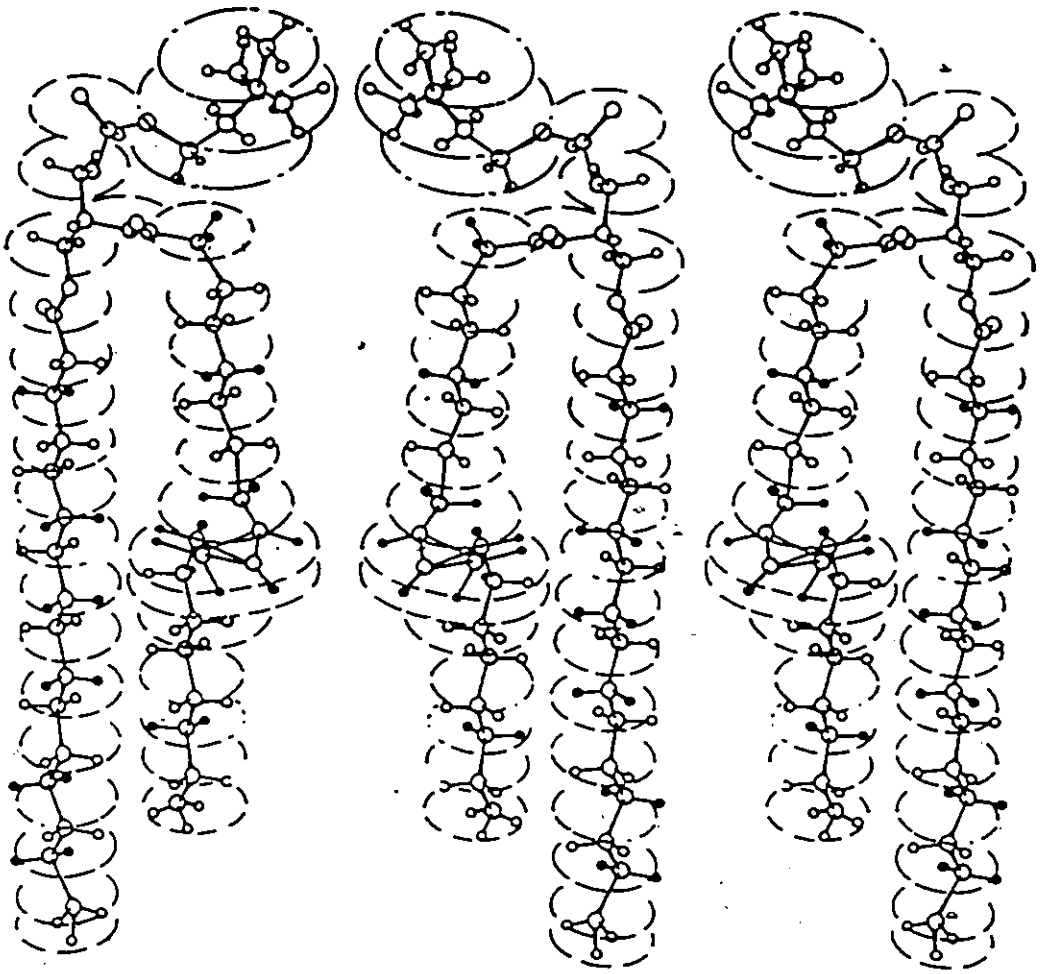

Fig. II.1–16. Hypothetical configuration of PDSPC molecules embedded in a model membrane, when $S_{MOL} = 1$. The filled circles represent the labeled positions. The dashed circles show the cylinder of influence of each subunit (see text).

the other segments of the chains. It might then be thought that at low temperatures, when the chains begin to pack together, there is still "free" space around the upper half of the sn-2 chain, thus allowing more angular fluctuations than in the corresponding positions of the sn-1 chain. According to that model, one would expect a lower local order for the DS plateau than for the palmitic plateau.

II.1.3d The Phase Transition

By monitoring the spectral changes at the [5'-$^2H_2$] position, when lowering the temperature, it was shown that the phase transition of PDSPC model membranes occurred around -10° to -15°C (Dufourc, et al., 1983). A similar study was carried out for the position [6-$^2H_2$]. The corresponding spectra are shown in Figure II.1-17. For comparison, the spectrum of the [5'-$^2H_2$] PDSPC at -20°C is also shown in this figure. Spectra at -20°C were recorded using a 500 kHz spectral width, a $\pi/2$ pulse width of 6 µs and a 35 µs spacing between the $\pi/2$ pulses of the echo sequence. The Figure II.1-17 shows that the spectra at position 6 begin to lose their axially symmetric shape at -10°C and that at -20°C the gel phase is clearly present. One notices also that at -20°C the liquid-crystalline phase still appears in the spectrum. However, the most striking is the marked

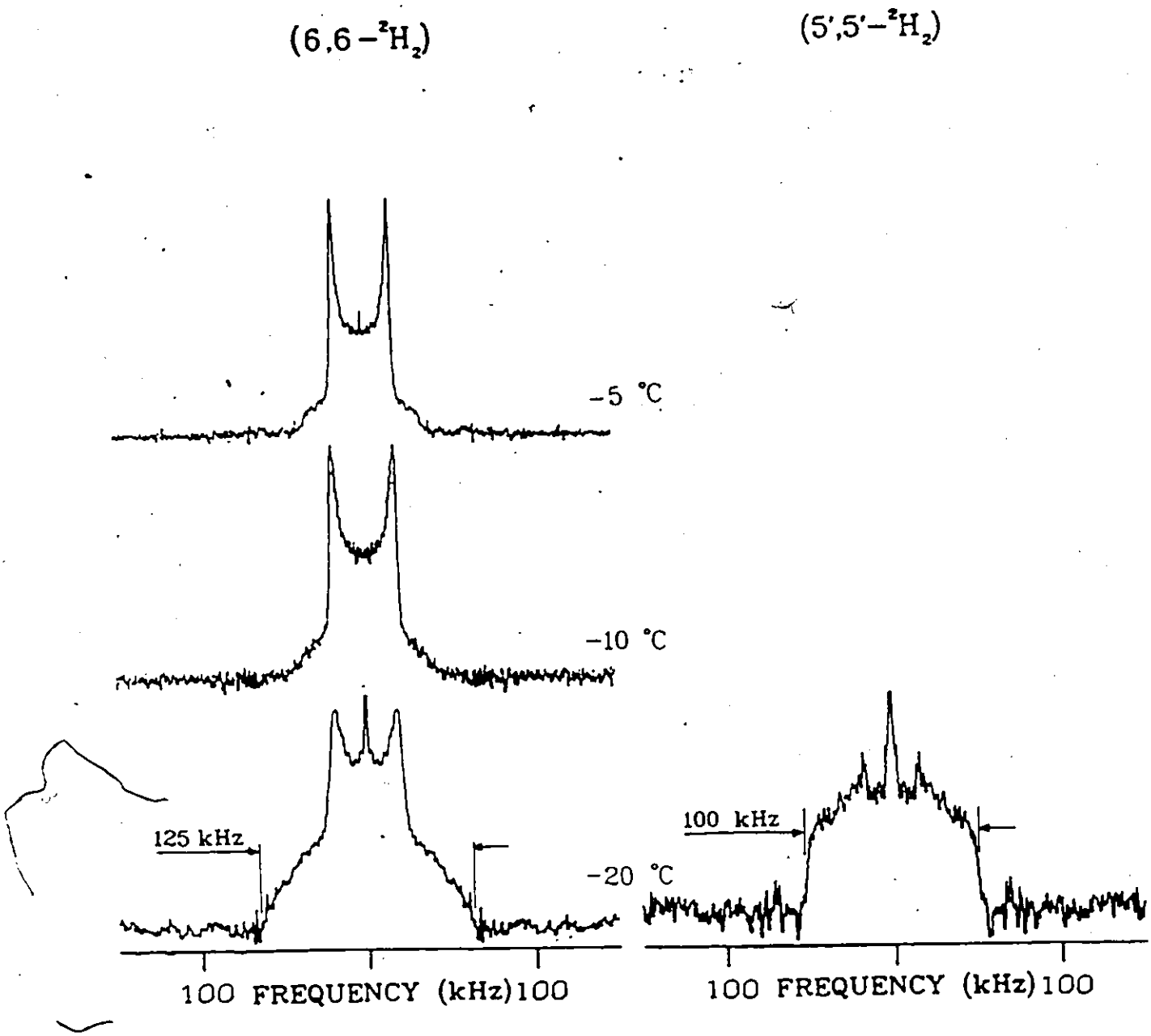

Fig. II.1-f7. Spectral shapes of $[6-^2H_2]$ and $[5'-^2H_2]$ PDSPC model membranes at low temperatures. Same experimental parameters as in Fig. II.1-3 except for spectra recorded at -20°C where the spectral window was 500 kHz.

difference in spectral features between the sn-1 and sn-2 positions at -20°C. The maximum width observed for the spectrum of the [6-$^2H_2$] PDSPC is ca. 125 kHz whereas the [5'-$^2H_1$] PDSPC spectrum has a maximum width of ca. 100 kHz. Although the dramatic differences in spectral shapes between position 6 and 5', at -20°C, are not well understood, one might try, however, to explain the spectral width differences as follows. The 125 kHz broad feature in the sn-1 spectrum indicates the cessation of angular fluctuations of that chain. In other words, $S_\alpha = 1$, $S_\gamma = -0.5$ for some molecules in the system. This latter situation has already been encountered for straight chain saturated lipids in the gel phase (Smith, et al., 1979; Davis, 1983). The 100 kHz maximum width appearing in the spectrum of the sn-2 chain at position 5' may be explained at least in two ways: either there are residual angular fluctuations, hence $S_\alpha \sim 0.8$ ($S_\gamma = -0.5$), or there are no angular fluctuations ($S_\alpha = 1$) but the C-^{2}H bonds at position 5' and at -20°C are tilted with respect to the instantaneous chain orientation, giving rise to $S_\gamma = -0.4$. Such a value of S_γ would imply a 15° tilt of these C-^{2}H bonds with respect to the bilayer normal, at -20°C. Although the present data do not allow a decision between these two hypotheses, the latter brings out the question of whether or not this supposed tilt would be present in the liquid crystalline phase. Such a tilt

would also explain why the sn-1 plateau appears more ordered than that of the sn-2 chain. The hypothesis of a tilt at position 5' in PDSPC should also hold for the [5'-$^2H_2$] POPC since the same spectral differences are observed between sn-1 and sn-2 positions for both systems (see Table II.1-1). However, it seems improbable that, in the liquid-crystalline phase, either the C=C or the cyclopropane induce a tilt of the C-^2H bond 4 carbons away from them. Furthermore, spectra of [5'-$^2H_2$] POPC at temperatures below the phase transition were showing a maximum width of ca. 125 kHz (Perly, B., personal communication). It appears therefore that the 100 kHz width observed for the [5'-$^2H_2$] PDSPC sample at -20°C is a characteristic of that position in the gel phase. It should also be mentioned that the hypothesis of a free space around the sn-2 chain (see previous section), in the liquid crystalline phase, and which holds also for the POPC system would tend to support the hypothesis of residual flexibility of the PDSPC sn-2 upper half chain at -20°C.

II.1.3e Concluding Remarks

The study of the sn-1 palmitoyl chain organization in PDSPC model membranes brings new details to the understanding of this system. It has been observed that the plateau region of the sn-1 chain is preserved at high temperatures above the phase transition whereas the plateau of

straight chain saturated model membrane systems such as DPPC is not. At low temperatures, the sn-1 plateau is more ordered than the corresponding sn-2 position. However, the sn-1 chain appears to be more sensitive to increases in temperature than is the sn-2. From these observations, the hypothesis has been advanced that the ring possesses a bulky cylinder of influence which induces a stiffening of the sn-1 plateau region and which provices free space for the upper-half of its sn-2 chain.

Finally, one can classify the DPPC, POPC and PDSPC model membrane systems in a scale of increasing order, at equivalent temperatures above their respective T_c, as follows: DPPC < POPC < PDSPC. However, at the same absolute temperature, say ~41°C, this classification is almost reversed: POPC $\lesssim$ PDSPC < DPPC.

REFERENCES TO CHAPTER II.1

Christie, W.W. (1969), in F.D. Gunstone (ed.), Topics in Lipid Chemistry, Vol. 1, 1.

Davis, J.H. (1983), Biochim. Biophys. Acta, 737, 117.

Dufourc, E.J., Smith, I.C.P. and Jarrell, H.C. (1983), Chem. Phys. Lipids (in press).

Engel, A.K. and Cowburn, D. (1981), FEBS Lett., 126, 2, 169.

Hofmann, K., L'Leary, W.M., Yoho, C.W. and Liu, T.Y. (1959), J. Biol. Chem., 234, 1672.

Jarrell, H.C. and Smith, I.C.P. (1983), in preparation.

Kates, M., Adams, G.A. and Martin, S.M. (1964), Canad. J. Biochem., 42, 461.

Law, J.H., Zalkin, H. and Kaneshiro, T. (1963), Biochim. Biophys. Acta, 70, 143.

Millet, F.S. and Dailey, B.P. (1972), J. Chem. Phys., 56, 7, 3249.

Oldfield, E., Meadows, M., Rice, D. and Jacobs, R. (1978), Biochemistry, 17, 2727.

O'Leary, W.M. (1962), J. Bact., 84, 967.

Perly, B., Smith, I.C.P. and Jarrell, H.C. (1983), in preparation.

Petersen, N.D. and Chan, S.I. (1977), Biochemistry, 16, 12, 2657.

Rance, M., Jeffrey, K.R., Tulloch, A.P., Butler, K.W. and Smith, I.C.P. (1980), Biochim. Biophys. Acta, 600, 245.

Saupe, A. (1964), Z. Naturforsch., 19, 161.

Seelig, J. (1977), Quart. Rev. Biophys., 10, 353.

Seelig, A. and Seelig, J. (1974), Biochemistry, 13, 23, 4839.

Seelig, A. and Seelig, J. (1975), Biochim. Biophys. Acta, 406, 1.

Seelig, A. and Seelig, J. (1977), Biochemistry, 16, 1, 45.

Seelig, J. and Waespe-Šarčevič, N. (1978), Biochemistry, 17, 3311.

Silvius, J.R. and McElhaney, R.N. (1979), Chem. Phys. Lipids, 25, 125.

Smith, I.C.P., Butler, K.W., Tulloch, A.P., Davis, H.J. and Bloom, M. (1979), FEBS Lett., 42, 390.

Stockton, G.W., Polnaszek, C.F., Leitch, L.C., Tulloch, A.P. and Smith, I.C.P. (1974), Biochem. Biophys. Res. Comm., 60, 844.

Taylor, M.G., Akiyama, T. and Smith, I.C.P. (1981), Chem. Phys. Lipids, 29, 327.

CHAPTER II.2

CYCLOPROPANE-CONTAINING LIPIDS

2. DYNAMICS

II.2.1 Introduction

The deuterium quadrupolar splitting, $\Delta\nu_Q$, is determined by the average conformation of the particular C-^{2}H bond and the amplitude of the angular fluctuations of that segment. Knowledge of $\Delta\nu_Q$ thus provides structural information about the membrane system. Deuterium NMR relaxation time measurements yield, on the other hand, complementary information on the dynamics of the lipid molecules. Although a large number of ^{2}H-NMR structural studies appear in the scientific literature, few ^{2}H relaxation time measurements have been published. There are at least two reasons for the paucity of relaxation data: the relaxation measurements are time consuming and the theoretical basis is still under development. However, some aspects of relaxation of a spin-1 system, and their application to anisotropic media, have recently been reported by Jeffrey (1981) and Brown (1982), respectively.

II.2.2 Deuterium Spin-Lattice Relaxation of PDSPC Molecules

II.2.2a Theoretical Background

In his model, Brown attempted to picture the relaxation rates in terms of acyl chain motions. Assuming the most general anisotropic rotational diffusion model to describe the segmental or molecular reorientations in lipid bilayers, he derived the rates of spin-lattice relaxation as a function of fluctuations of limited amplitude of the C-^{2}H bond vectors with respect to the axis of motion. Brown extended his model to account for slow fluctuations of the local director with respect to the macroscopic bilayer normal (Brown, 1982).

In the case where the spin-lattice relaxation is only due to fast motions, assuming that the auto correlation function for C-^{2}H bond fluctuations (which gives rise to the T_{1z} relaxation) can be described by a single exponential decay with a time constant τ_c and assuming that these motions fall into the short correlation limit, that is, $\omega_0^2\tau_c^2 << 1$, Brown derived the following expression for the spin-lattice relaxation rate:

$$\frac{1}{T_{1z}} = \frac{3}{8}(2\pi)^2 A_Q^2 [1-S_{C-^2H}^2]\tau_c. \qquad \text{(II.2.1)}$$

A similar equation had been derived by Brown, Seelig and Häberlen in 1979, predicting that T_{1z} would vary across the powder spectrum. However, it has been shown (Brown & Davis, 1981) that this was not the case, and our data support the latter point of view (vide infra).

II.2.2b ^2H Spin-Lattice Measurements on the sn-1 and sn-2 Chains of the PDSPC Model Membrane System

The spin-lattice relaxation rates were measured for each of the ^2H-labeled positions along both dihydrosterculic and palmitic chains, at 25°C. The relaxation data were obtained by the inversion-recovery technique, as described in Materials and Methods. In all cases, the spin-lattice relaxation process was characterized by a single exponential function. A typical set of spectra is shown in Figure II.2-1 to illustrate the method and to give an idea of the high S/N ratio needed in such experiments. T_{1z} values were extracted by fitting the equation $M(\tau_1) = M_0 (1-A\exp\{-\tau_1/T_{1z}\})$ with the integrated areas of certain regions of the spectral shape, namely "windows" around the $\theta' = 0°$, 90° and 54.7° orientations. θ' represents the angle between the director and the magnetic field whereas $M(\tau_1)$ and M_0 represent the longitudinal magnetization at times τ_1, and at the equilibrium, respectively. The adjustable parameter A was used to account for the imperfections of the 180° inverting pulse. An example of fitting

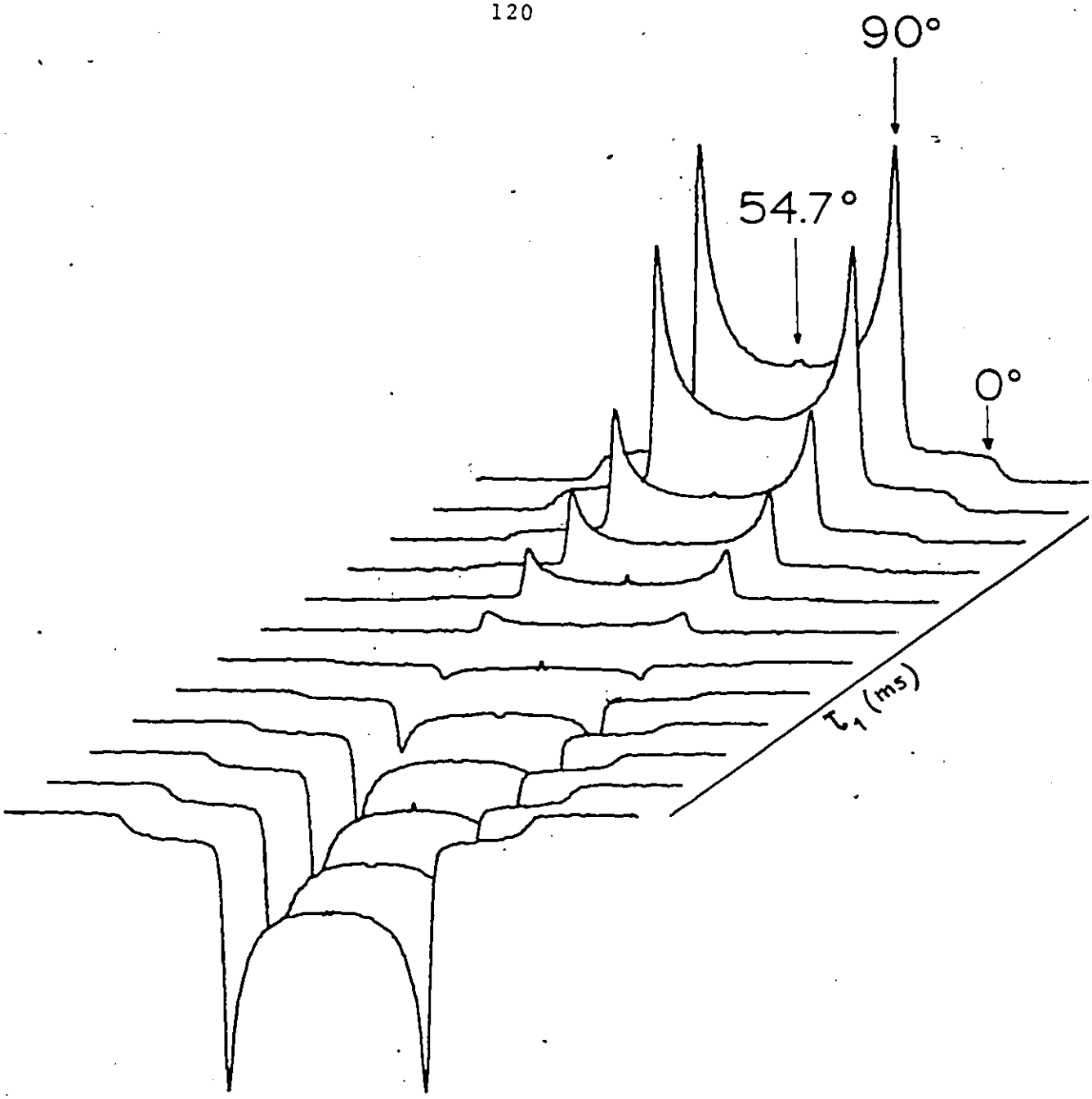

Fig. II.2–1. Example of stacked plot of spectra resulting from the inversion recovery technique for measuring T_{1Z} of the $[16'-^2H_2]$ PDSPC sample, at 25°C.

the exponential decay is shown in Figure II.2-2. Spin-lattice relaxation times for all other positions were recorded and analyzed in the same way. The results are summarized in Table II.2-1. Among all spectra recorded, those of [16'-$^2H_2$] PDSPC show the "greater" angular dependence in T_{1z} (Figure II.2-2). The second moment, M_2, is also plotted as a function of τ_1 in Figure II.2-2 and demonstrates that M_2 is independent of τ_1, within the experimental error. The invariance of the second moment shows that there is no systematic change in the shape of the spectrum for τ_1 values between 1 and 50 ms. The apparent angular dependence in Figure II.2-2 is therefore due to the inaccuracy involved when measuring areas near the 0° orientation. When, at certain positions, the spectrum exhibit two or more quadrupolar splittings, the entire set of spectra was dePaked and the remaining oriented lines were treated as described above to obtain the T_{1z} of the individual components. It should be mentioned here that a direct measure of T_{1z} on powder spectra having several components, that is, several powder patterns superimposed, will lead to an inaccurate estimate of the T_{1z} of each individual powder pattern. This systematic error is of course a function of the T_{1z} of each component and will be really important if the differences in T_{1z} are large. Figure II.2-3 shows the stacked plot of spectra to measure T_{1z} on the [19'-$^2H_2$] PDSPC sample as well as its dePaked analog. On this sample, systematic error would have been in

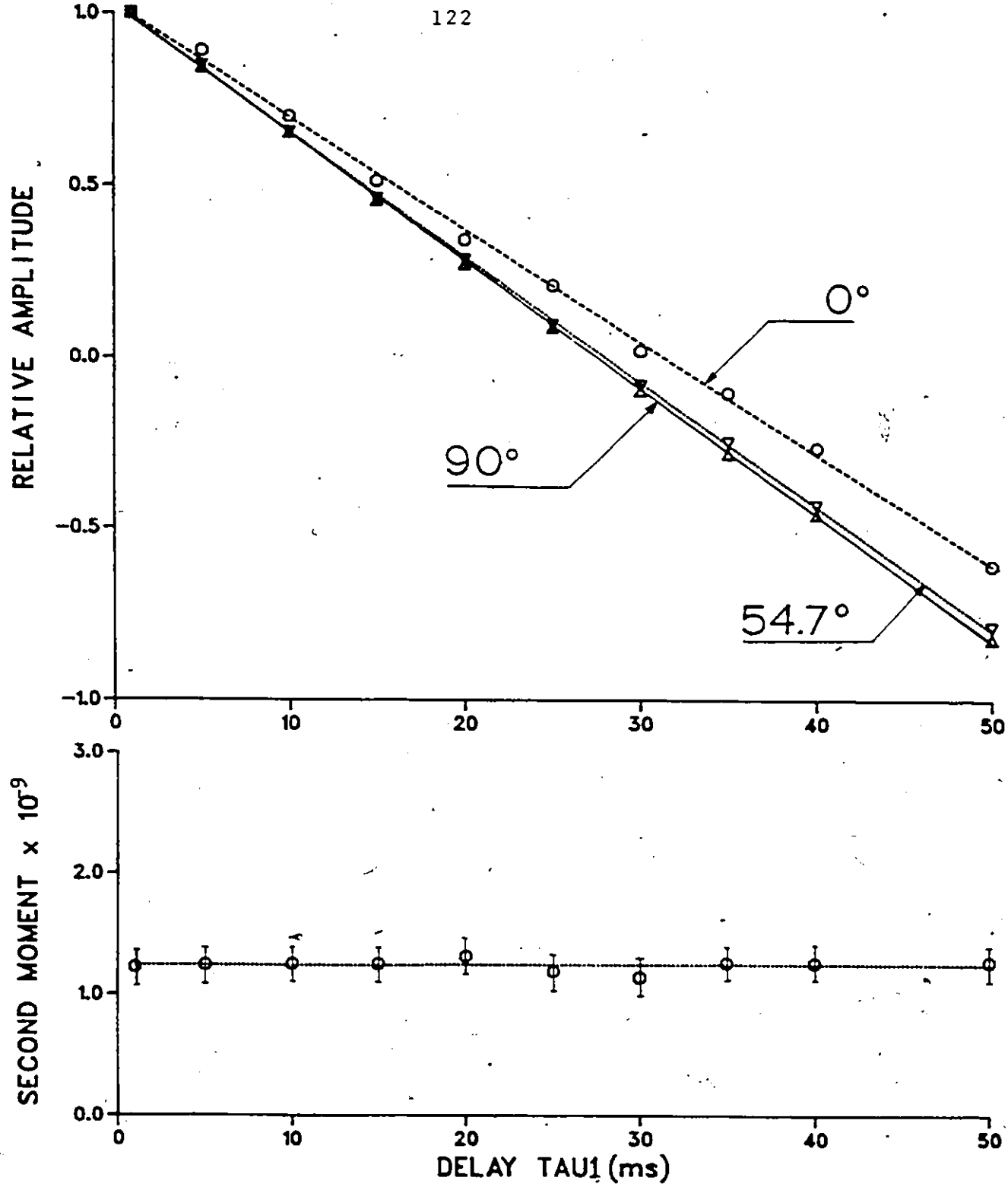

Fig. II.2-2. Top: typical T_{12} measurement for macroscopic orientations (angles $\theta = \beta_b = 0°, 90°, 54.7°$) indicated in Fig. II.2-1. The relative amplitude represents the value $Ln(1-M(\tau_1)/M_\infty)/LnA$ (see text). The data are normalized to the value at the smallest τ_1.

Bottom: variation of the second moment of spectra of Fig. II.2-1 as a function of the delay τ_1.

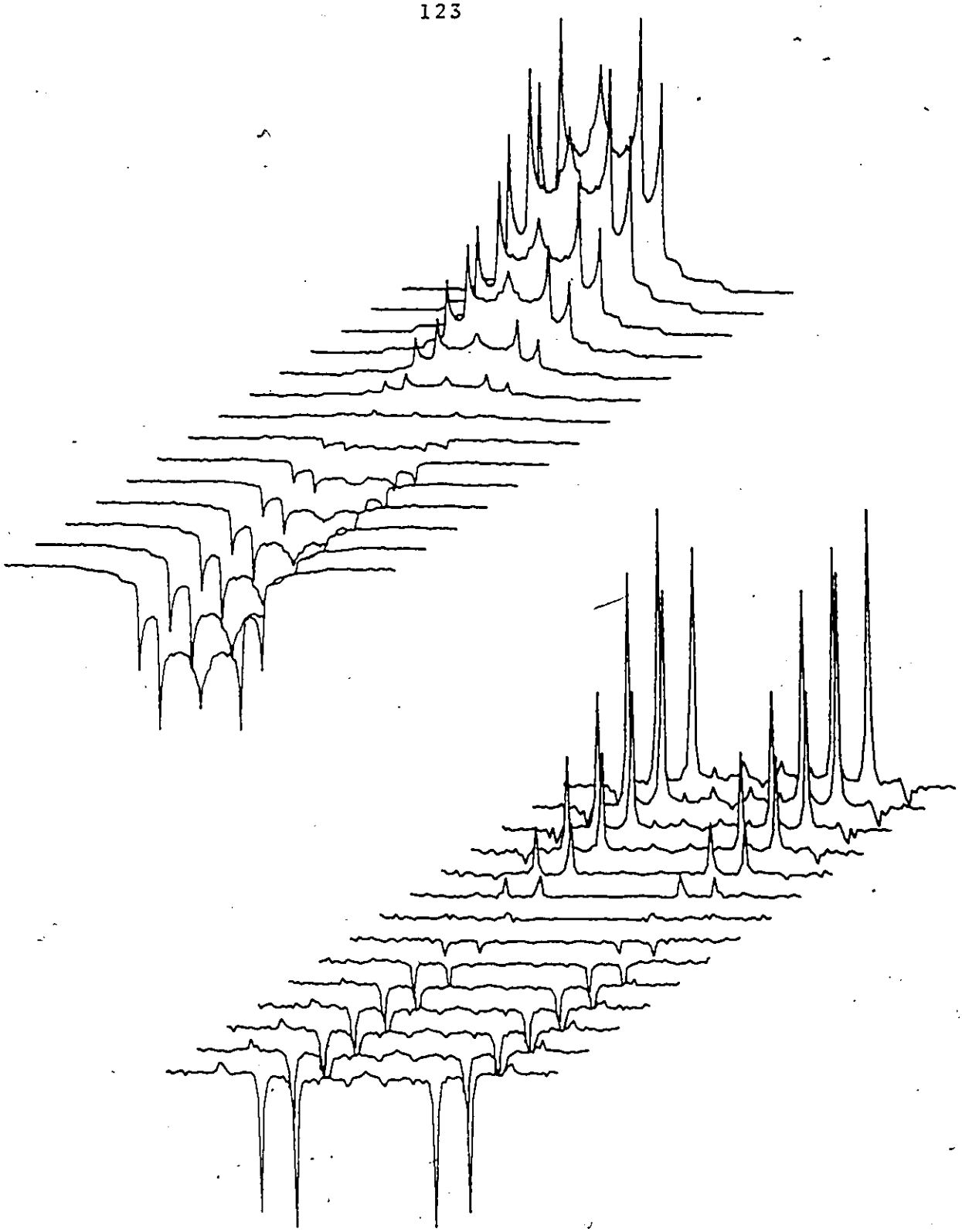

Fig. II.2–3. Stacked plot of spectra (top) and de Paked analog (bottom) resulting from a T_{1z} experiment. The data are from the [19'–$^2H_2$] PDSPC sample at 25°C.

Table II.2-1

RELAXATION TIMES OF PDSPC AND POPC[a] AND MODEL MEMBRANES, AT 46.1 MHz

Labeled Carbon Position	T (°C)	$\lvert S_{C-^2H} \rvert$	T_{1z} [c] (ms)	τ_c [d] (sec)
PDSPC sn-1 [3 -$^2H_2$]	25	0.190	16.6	1.5×10^{-10}
PDSPC sn-1 [6 -$^2H_2$]	25	0.221	20.1	1.2×10^{-10}
PDSPC sn-1 [8 -$^2H_2$]	25	0.209	20.7	1.2×10^{-10}
PDSPC sn-1 [10 -$^2H_2$]	25	0.184	21.8	1.1×10^{-10}
PDSPC sn-1 [15 -$^2H_2$]	25	0.096	72.0	0.33×10^{-10}
PDSPC sn-2 [5'-$^2H_2$]	25	0.216	16.5	1.5×10^{-10}
PDSPC sn-2 [8'-$^2H_2$]	25	0.123	13.8	1.7×10^{-10}
PDSPC sn-2 [8'-$^2H_2$]	25	0.158	14.0	1.7×10^{-10}
PDSPC sn-2 [9'-$^2H_2$] [b]	25	0.130	9.6	2.1×10^{-10}
PDSPC sn-2 [19'-$^2H_2$]	25	0.146	8.4	2.5×10^{-10}
PDSPC sn-2 [19'-$^2H_2$]	25	0.219	9.4	2.3×10^{-10}
PDSPC sn-2 [10'-$^2H_2$] [b]	25	0.084	8.5	2.4×10^{-10}
PDSPC sn-2 [11'-$^2H_2$]	25	0.049	14.1	1.7×10^{-10}
PDSPC sn-2 [11'-$^2H_2$]	25	0.115	14.2	1.7×10^{-10}
PDSPC sn-2 [16'-$^2H_2$]	25	0.103	44.9	0.53×10^{-10}
POPC sn-2 [5'-$^2H_2$]	36	0.183	24.1	1.0×10^{-10}
POPC sn-2 [9'-$^2H_2$]	36	0.099	20.9	1.1×10^{-10}
POPC sn-2 [10'-$^2H_2$]	36	0.017_7	17.6	1.2×10^{-10}
POPC sn-2 [16'-$^2H_2$]	36	0.083_4	67.8	0.35×10^{-10}

[a] From Perly, et al., to be published.

[b] The assignments of these positions is arbitrary (and could be inverted).

[c] The accuracy on the T_{1z} is about ± 2-3%. The values reported above are measured on the peaks for $\theta' = 90^\circ$.

[d] From Equation (II.2.1) (see text), with A_Q = 175 kHz and 183 kHz for C-^{2}H segments on double bonds (Seelig, 1977) and on cyclopropane (Dufourc, et al., 1983), respectively, and 170 kHz (Seelig, 1977) otherwise.

the order of 2-3% on each T_{1z}, that is, the higher T_{1z} would have been underestimated by 2-3% whereas the smaller T_{1z} would have been overestimated by the same percentage, if dePaking had not been used. This error is negligible here since the T_{1z} of the two components are very similar.

The relaxation rates of both sn-1 and sn-2 chain labels are reported in Figure II.2-4 as a function of the labeled carbon. To date, this is the only example where the relaxation rate profiles of the sn-1 and sn-2 chains of the same lipid in a model membrane are compared. The results are quite astonishing: whereas the sn-2 DS chain shows a considerable reduction in the rate of relaxation at the cyclopropane level, the sn-1 palmitic chain exhibits essentially a plateau at the corresponding positions. An almost identical picture has been found with order parameter (S_{mol}) profiles (see Chapter II.1). Using Equation (II.2.1) one can make the order "correction" and obtain the correlation time of the movement. This has been done and the subsequent results are shown in Table II.2-1: the profiles observed in Figure II.2-4 would not change considerably if the correlation times were reported, instead of the relaxation rates. It can therefore be concluded that the cyclopropyl unit motions are slow and rather strongly correlated. Furthermore, the discontinuity in the relaxation rate profile observed in sn-2 is not seen in sn-1. It appears that the motions are therefore more

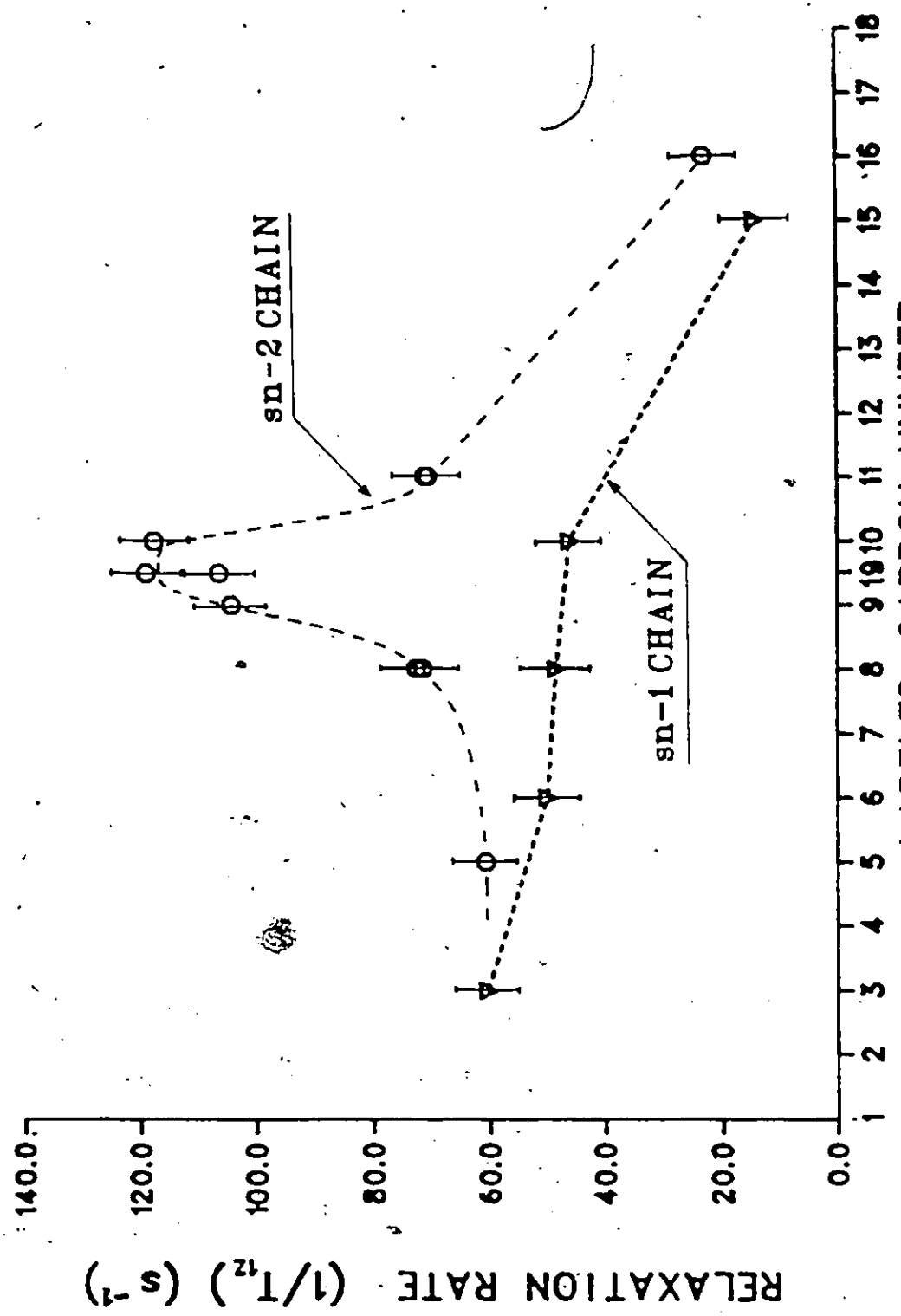

Fig. II2-4. Comparison of the relaxation rates of both sn-1 and sn-2 chains of PDSPC, as a function of labeled positions, at 25°C.

correlated through bonds than through space. This latter assertion questions the hypothesis of a mean field bilayer pressure, favouring the extension of the chains perpendicular to the bilayer surface, to account for the plateau (C3 to C9) of correlation times found in DPPC multilayers (Brown, et al., 1979). If such a field exists in PDSPC model membranes its form may be expected to be rather complex. Even if the sn-1 plateau relaxation rate profile is not perturbed by the slow cyclopropane motions, the correlation times of all sn-1 positions are higher than the corresponding correlation times of DPPC (Brown, et al., 1979). This indicates that the cycle slows down the motions of the sn-1 chain in preserving the plateau entity. It is also interesting to notice that the relaxation rate at C3 is the highest among all sn-1 labeled positions. This observation reflects the fact that the relaxation rates are fastest near the beginning of the chains, due to the anchoring effect of the glycerol moiety. The latter is indeed known to have a high correlation time, at least twice as long as that of the plateau positions in DPPC (Brown, et al., 1979). The relaxation rates for all sn-2 positions are higher than those in the corresponding sn-1 labels, indicating that the cyclopropane ring system is most efficient in slowing down the rates of motion of its own chain, rather than those of its neighbours. Furthermore, one notices in Figure 11 that positions adjacent to the cycle (namely C8' and C11') "feel" this

reduction in motional rates much more than positions far away from it (C5' and C16'). This result is not surprising since one knows from structural studies that the cyclopropyl moiety perturbs positions 8' and 11' (by inducing orientational nonequivalences of the deuterons bound to these carbons) but not positions 5' and 16'. The general slow motions of the sn-2 positions could also be correlated with the fact that this chain was found to be less sensitive to temperature variations (change in rate and/or amplitude of motions) than the sn-1 chain (see Section II.1.3). A high rate of relaxation, that is, a high correlation between segmental motions, would thus seem to occur concomitantly with a lesser temperature sensitivity.

Carbon-deuterium bonds attached to the same carbon atom, or to a rigid unit such as the cyclopropane moiety are expected to have the same correlation time. On that basis, the validity of Equation (II.2.1) can be checked. From Table II.2-1, it appears that this equation gives the same correlation time for deuterons at C8' and C11' whereas there is a ~15% discrepancy for cyclopropyl deuterons. In order to account for this fact one might consider that given the slow motions of the cyclopropane, movements other than molecular rotations, torsional oscillations and bond stretching and bending could contribute to the spin-lattice relaxation. The present data could thus be re-analysed by adding

to Equation (II.2.1) terms accounting for non-collective or collective modes of low frequency motions (lateral diffusion, whole lipid bilayer reorientation ...) as described by Brown (1982).

II.2.2c Temperature Dependence of the [19'-$^2H_2$] PDSPC

The spin-lattice relaxation time was measured on the [19'-$^2H_2$] PDSPC sample over the temperature range ~5°C to 45°C.

The results are plotted in Figure II.2-5a. One can notice that the curvature of the plots is progressively reduced from 45°C to -5°C indicating that a minimum in T_{1z} would be observed around -30°C, -40°C, if the function were monotonic. The marked increase in relaxation time when the temperature is increased over 15°C implies that the motions most responsible for the relaxation process have correlation times such that $\omega_0^2\tau_c^2 << 1$. Assuming that τ_c has an Arrhenius-type dependence, $\tau_c = \tau_0 \exp\{E_a/RT\}$, where E_a is the activation energy for processes causing the molecular motions, that is, determining the spin-lattice relaxation rate, one can determine from the temperature dependence of Ln (T_{1z}) the magnitude of E_a. From the slopes of Figure II.2-5b the average activation energy was 12.3 ± 1.0 kJ.mol^{-1}, half way between the 14.6 ± 1.3 kJ.mol^{-1} and the 10.5 kJ.mol^{-1} found for E_a

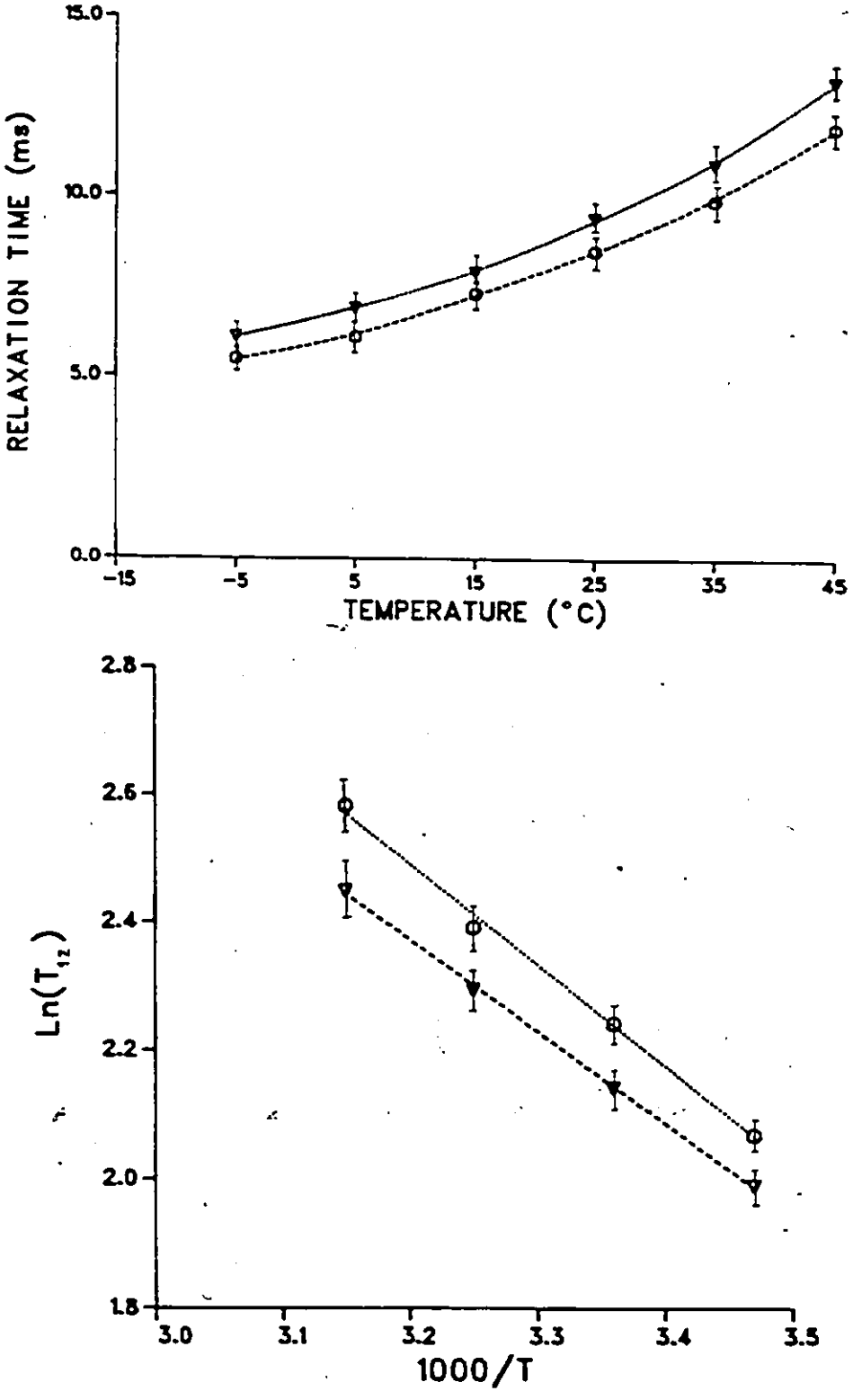

Fig. II.2–5. Top: temperature dependence of T_{1Z}. The data are from the $[19\text{-}^{2}H_{2}]$ PDSPC model membrane system. Bottom: Arrhenius plot of T_{1Z}. Same data as top.

in bilayers and isotropic solutions of DPPC, respectively (Brown, et al., 1979).

II.2.2d Comparison of Relaxation Rate Profiles Between Several Model Membrane Systems

As we mentioned earlier, biological systems should be compared when submitted to the same average molecular forces. It is believed that such a situation exists when the systems under study are at the same temperatures with respect to those of their phase transitons. Although few deuterium relaxation data are available, we reported in Figure II.2-6 the relaxation rates as a function of the labelled carbon position of sn-2 PDSPC at 25°C, sn-2 POPC at 36°C (Perly, et al., to be published) and DPPC at 80°C and 54.4 MHz (Brown, et al., 1979). All relaxation rates were thus monitored at 35-40°C above the gel to liquid-crystalline phase transition of each of the three systems. Again, the behaviour of these model membranes is significantly different. The most obvious general comment is that the rates of relaxation increase from the fully saturated to the cyclopropane-containing lipids. On the basis of Equation (II.2.1) one can therefore classify the three systems in a scale of increasing correlation time of the chain motions as:

DPPC < POPC < PDSPC,

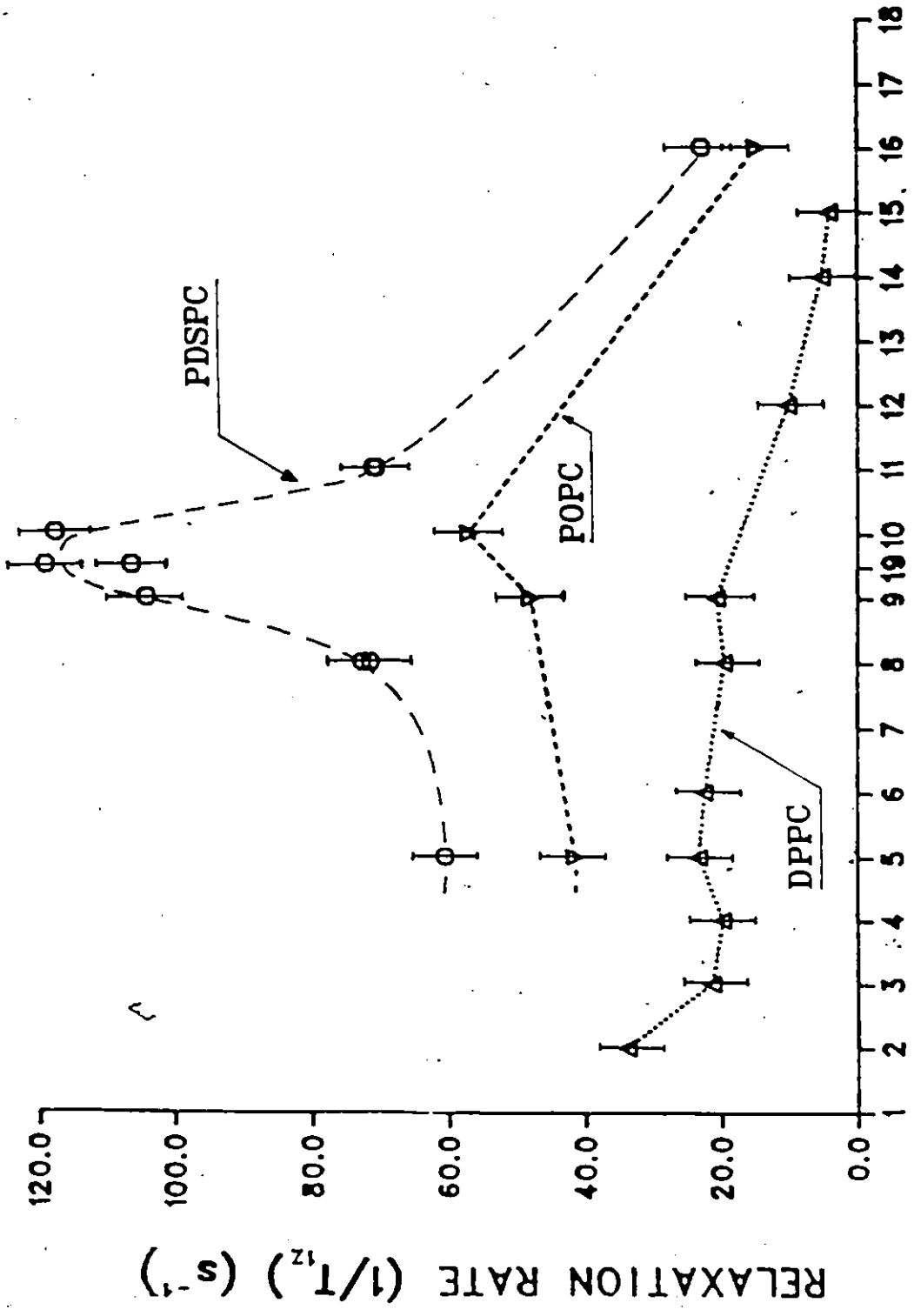

Fig. II.2-6. Comparison of the relaxation rate profiles for several model membrane systems.
O -- sn-2 PDSPC at 25°C and 46.1 MHz.
▽ -- sn-2 POPC at 36°C and 46.1 MHz (Perly et al. to be published).
Δ -- DPPC at 80°C and 54.4 MHz (Brown et al.,1979).

at the same relative temperature. The above classification for the rates of motions is therefore the same as it was found for the amplitudes of the motions, at the same temperatures above T_c. A more detailed study of the rate profiles of Figure II.2-6 shows that, at the functional level, that is, the double bond or the cyclopropane, there is an increase in the rate of relaxation with respect to the positions preceding the functional group. Therefore, one can conclude that the C=C slows down the motions, as does the cyclopropane moiety, but by a much lesser amount. In PDSPC, the increase in correlation time at the cyclopropane level can be correlated with an increase of the segmental molecular order parameter (decrease in the C-^{2}H bond amplitude fluctuations) (see previous section). Seelig and Waespe-Šarčevič (1978) corrected the C9', C10' S_{C-^2H} order parameters for the geometrical orientation of the double bond with respect to the instantaneous axis of motion and found that the S_{mol} of the C=C was on the plateau level. However, they were not able to do so using only information from ^{2}H-NMR (as was done for the geometrical correction of the cyclopropane S_{C-^2H}'s). These authors obtained the missing observable from infrared linear dichroism measurements of the C=C stretching frequency in egg yolk lecithin at room temperature (Fringeli, 1977). Since egg yolk lecithin contains about 70% wt. POPC one might question whether this external datum

corresponds truly to that for a 100% POPC system. When separating the geometric from the segmental order contributions in the cyclopropane S_{C-2_H}, Dufourc, et al. (1983) used two different methods. One of them gives the unique solution $(S_{mol})_{\alpha}$ and is only applicable when one has enough observables (S_{C-2_H}) consistent with the symmetry of the molecule and when these observables are different enough in magnitude to allow accurate calculations. The other is less specific and does not give a unique solution but can be used as long as one has two observables for the same rigid unit. However, the accuracy, and the convergence of the method, decreases with decreasing number of observables for the rigid body. It was shown that this latter method contains, among other solutions, the unique solution given by the former. Although the first method is not applicable for only the ^{2}H-NMR observables of the 9'-10' double bond, the second was tried for the POPC data at 36°C (see table II.2-1, positions (9' and 10')). Keeping the same axis system as defined by Seelig and Waespe-Šarčevič for the C=C, two main solutions were found: $S_{mol} = 0.36 \pm 0.03$ and $S_{mol} = 0.47 \pm 0.03$. The resultant orientations of the double bond were slightly different from that calculated previously: instead of a 7-8° one-dimensional tilt found by the above authors, a small two-dimensional tilt was observed, that is, the axis of motion was not exactly in the double bond plane. Although

one cannot decide between these two solutions one notices that one of them would lead to a S_{mol} value for the double bond distinctively above the plateau of segmental order parameters for positions anterior to it, in agreement with the increase in relaxation rate observed in Figure II.2-6, at the C=C level. It appears thus from the above discussions that the relaxation rate profile is strongly dependent on the segmental order parameter profile (S_α or S_{mol}) in contrast with earlier conclusions (Brown, et al., 1979). The spin-lattice relaxation in lipid multilayers depends therefore on both the local ordering and the rate of motions.

II.2.2e Concluding Remarks

The comparison of relaxation rates between the sn-1 palmitic and sn-2 dihydrosterculic deuterium-labelled chains of PDSPC model membranes showed that the cyclopropyl moiety perturbs the correlation time profile of the sn-2 chain by inducing a considerable slowing down of the motions, at its own level and at the neighbouring C-^{2}H bonds. The sn-1 chain, though exhibiting much slower motions than DPPC at the same relative temperature, did not show the huge perturbation seen in the sn-2 chain profile; instead, a plateau of correlation times, up to C10 was observed. This observation leads to the conclusion that the motions are more correlated through bonds than through space. The finite perturbation

induced by the cycle on the sn-2 chain appears in addition to be lost with distance. The cyclopropane moiety thus anchors the motions at its own level in preserving the plateau entity of the neighbouring chains. The net effect is a stronger correlation of the motions of the entire system, leading the model membrane to be less sensitive to gradient of motions such as those caused by sudden temperature jumps.

The shapes of the relaxation rate profiles for sn-1 and sn-2 were quasi-identical to those found for the segmental order parameter profiles of these chains. This second observation leads to the assertion that the spin-lattice relaxation rate is strongly dependent on the local ordering of the system.

Comparisons of sn-2 chain relaxation rate profiles for PDSPC, POPC and DPPC, at the same relative temperature and almost the same magnetic field, showed that these systems could be classified on a scale of increasing correlation time as:

DPPC < POPC < PDSPC.

The small perturbation of the sn-2 relaxation rate profile of POPC at the double bond level led to a review of the earlier calculation of S_{mol} of the C=C. It was found that indeed the double bond in POPC could exhibit a slightly

higher S_{mol} than that of the plateau region of the oleoyl chain. The inherent underdetermination of the method of calculation did not allow, however, a decision among other solutions, and thus whether the above slight increase in S_{mol} was the unique solution.

II.2.3 Deuterium Spin-Spin Relaxation of PDSPC Molecules

The spin-spin relaxation time, T_2, was estimated on seven labeled samples (sn-2 chain of PDSPC) as described in Materials and Methods. The T_2 spectral set was integrated, after Fourier transformation of the signal from the top of the spin-echo outwards, by windows, namely macroscopic orientations around $\theta' = 0^\circ$, 90° and 54.7°; as described for T_{1z}. The resultant areas were fitted to the expression: $M(2\tau) = M(2\tau_{min}) \exp\{-2\tau/T_2\}$ where $M(2\tau)$ and $M(2\tau_{min})$ are the transverse magnetizations at time 2τ and $2\tau_{min}$, respectively, and where τ_{min} represents the shortest pulse spacing between the two $\pi/2$ pulses required to form the spin-echo. Figure II.2-7 shows an example of a T_2 data set, as well as an example of a fit of the above equation for various orientations θ'. One clearly sees that there is a marked angular dependence of T_2. The T_2 data are reported, for the sn-2 positions, in Table II.2-2. This table shows, for the cases were it was possible to measure them, the values of T_2

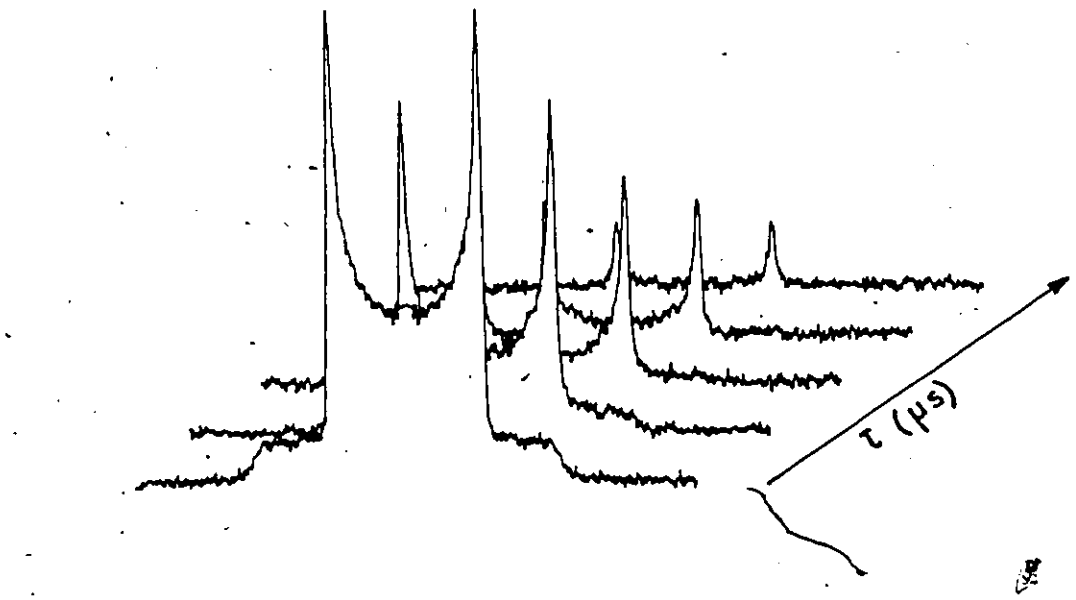

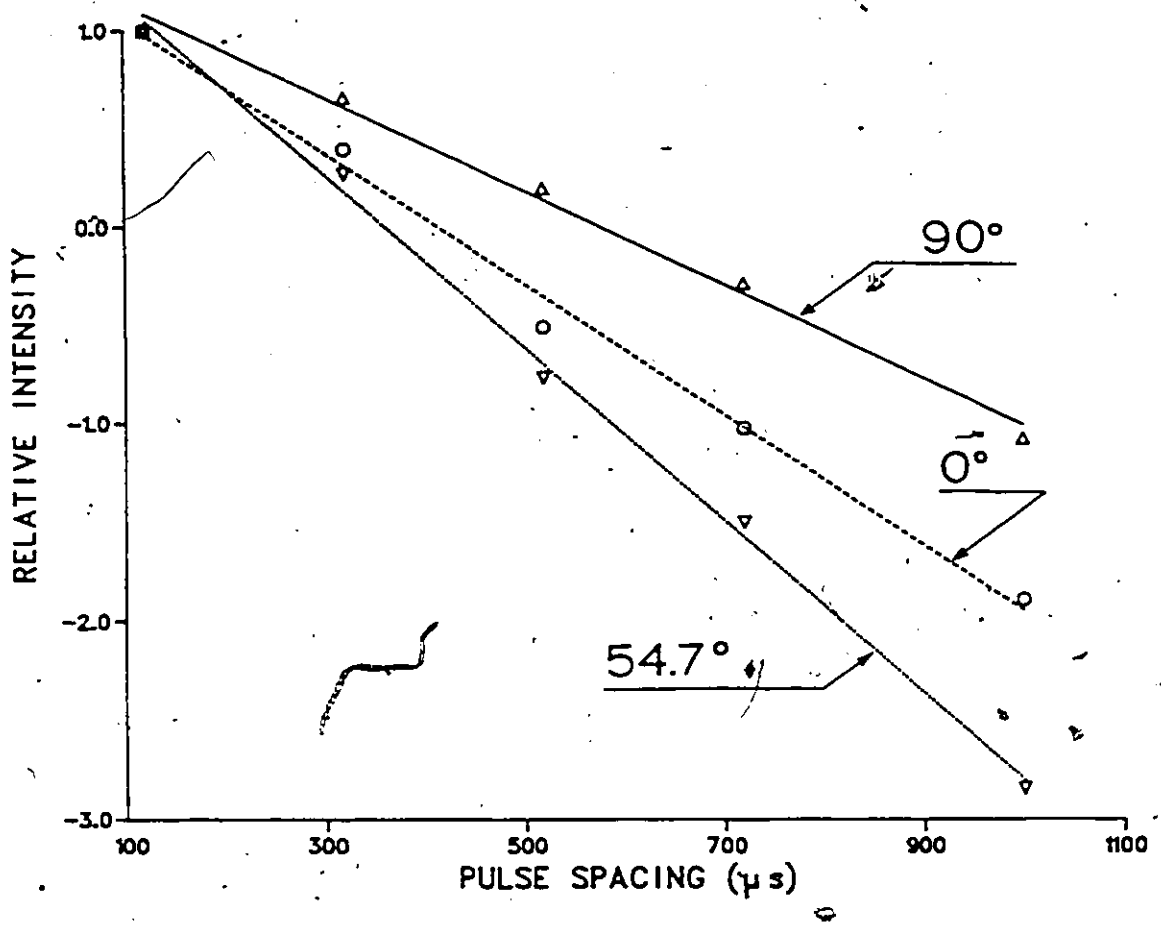

Fig. II2-7. Top: example of stacked plot of spectra for measuring T_2. The data are from $[5'-^2H_2]$ PDSPC at 25°C.
Bottom: example of T_2 measurement at several regions on the powder pattern. The relative intensity represents $\mathrm{Ln}(M(2\tau)/M(2\tau_{min}))$. The data, from top, are normalized to the value at the smallest τ, τ_{min}.

Table II.2-2

SPIN-SPIN RELAXATION TIMES FOR sn-2 PDSPC

Labeled Carbon	S_{C-^2H}	T	$T_2(\mu S)$[a]			$1/\pi T_2(90^o)$	$deP(90^o)$[b]	$T_2(90^o)/T_2(0^o)$
		(^oC)	0^o	90^o	54.7^o	(Hz)	(Hz)	
[5'-$^2H_2$]	0.216	25	290	470	250	680	900	1.62
[8'-$^2H_2$]	0.158	25	(340)	810		390	650	(2.38)
[8'-$^2H_2$]	0.123	25		790		400	650	
[9'-$^2H_2$]	0.130	25	(430)	580		550	550	(1.35)
[10'-$^2H_2$]	0.084	25		590		540	500	
[19'-$^2H_2$]	0.219	25	470	750		420	700	1.60
[19'-$^2H_2$]	0.146	25	510	900		350	550	1.76
[11'-$^2H_2$]	0.115	25	580	1000		320	550	1.72
[11'-$^2H_2$]	0.049	25		1030		310	650	
[16'-$^2H_2$]	0.154	- 5	310	700	530	460	900	2.26
[16'-$^2H_2$]	0.113	10	500	840	420	380	730	1.68
[16'-$^2H_2$]	0.103	25	650	1070	540	300	480	1.65
[16'-$^2H_2$]	0.092	35	430	560	320	570	640	1.30

[a] Accuracy of T_2 measurements ~10% for the 90^o and 54.7^o orientations, ~20% for the 0^o orientation.
[b] Linewidth estimated by fitting the dePaked spectrum, fit accuracy ~10%.
[c] Ratio between T_2 at 90^o and 0^o orientations, respectively.

at 0°, 90° and 54.7°. The ratio between T_2 at 90° and T_2 at 0° shows that we do not have a $P_2(\cos\theta')$ angular dependence ($P_2(\cos\theta') = \frac{1}{2}(3\cos^2\theta'-1)$; this ratio is equal to 2 when the $P_2(\cos\theta')$ dependence is fulfilled. The discrepancy between the line width estimated from dePaking ($\theta'=90^{\circ}$) and the line width from the T_2 experiment at $\theta' = 90^{\circ}$ is also another proof that the $P_2(\cos\theta')$ dependence is violated (the dePaking algorithm assumes a $P_2(\cos\theta')$ angular dependence of the individual line widths within the powder pattern). The line width that one can obtain from dePaking is therefore not the "true" line width at $\theta' = 90^{\circ}$, for our set of spectra. One also notices that the T_2 at the magic angle, $\theta' = 54.7^{\circ}$, is the shortest of all the spectrum, at $25^{\circ}C$. This fact leads to the conclusions that the spin-spin relaxation rate is the most efficient when the bilayer normal is oriented at 54.7° with respect to the static magnetic field direction. One can also say that this efficiency is not due to a $P_2(\cos\theta')$ type angular dependence, instead, one might think that collective or non-collective modes of motion (for example, lateral diffusion of the lipid molecule in the bilayer) provide a better way to relax near the magic angle. The type of angular dependence appears also to vary with temperature (see Table II.2-2, position [16'-$^2H_2$]). However, the present data are not sufficient to investigate in detail the spin-spin relaxation mechanisms. A complete lineshape analysis, by simulation of T_2 experiments would therefore be

necessary; such a study is out of the scope of this work. The only result one can point out is the lack of pure $P_2(\cos\theta')$ dependence in the T_2 relaxation process. A similar conclusion has already been obtained by Rance in ^{2}H-NMR studies of A. laidlawii membranes (1981).

REFERENCES TO CHAPTER II.2

Brown, M.F. (1982), J. Chem. Phys., 77, 1576.

Brown, M.F., Seelig, J. and Haeberlen, U. (1979), J. Chem. Phys., 70, 5045.

Brown, M.F. and Davis, J.H. (1981), Chem. Phys. Lett., 79, 431.

Dufourc, E.J., Smith, I.C.P. and Jarrell, H.C. (1983), Chem. Phys. Lipids (in press).

Fringeli, U.P. (1977), Z. Naturforsch., C32, 20.

Jeffrey, K.R. (1981), Bulletin of Magnetic Resonance, 3, 69.

Seelig, J. (1977), Quart. Rev. Biophys., 10, 353.

Seelig, J. and Waespe-Šarčevič, N. (1978), Biochemistry, 17, 3311.

Rance, M. (1981), Ph.D. Thesis, University of Guelph, Guelph, Ont., Canada.

CHAPTER II.3

CYCLOPROPANE-CONTAINING LIPIDS

3. CONCLUSION

The Role of Cyclopropane Rings in Membrane Lipids

Despite the title which would seem to state a definitive answer with respect to the occurrence of cyclopropane moieties in membranes, our aim is to define more or less clearly the structural consequences of three-membered rings in fatty acyl lipid chains, and to attempt to relate these to functional aspects. It is well known now that the living membranes need to possess certain physical characteristics to function properly as binding sites, selective permeability barriers, in-out transporters or nerve influx carriers. However, most important is for the membrane to be stable in a physical state where it can perform the above functions, that is, insensitive to gross external perturbations such as sudden changes in pH, gradients of temperature or other physical modifications leading to large structural and dynamical changes which may in certain cases yield to the disruption of the membrane and therefore the death of the cell. The gel phase does not allow the functions mentioned above to work properly, the reference state of a living membrane is rather the so-called "fluid" state, that is, the liquid crystalline phase.

The experimental observations reported herein lead us to think that the cyclopropane possesses some of these characteristics; in order to understand it we shall compare the behaviour in temperature of a fully saturated lipid, for example, DPPC or DMPC, with respect to that of a cyclopropane-containing lipid, for example, PDSPC. The first property needed for the lipid is that it has to be in the "fluid" phase state of reference about the living temperature range, T_L (35^o-45^o), that is, the gel to liquid crystalline phase transition temperature, T_c, must be far from this range of temperatures. The fully saturated lipids can pack so easily that their T_c is high and increases when the chain length increases. The palmitoyl chain which is the most commonly occurring in nature induces T_c to be near T_L in DPPC-like lipids. In contrast, the cyclopropyl moiety, whose cylinder of influence (bulkiness) prevents an easy packing of the chains by possibly providing a free space around its sn-2 plateau positions (which could therefore be thought as a reservoir of motion, when lowering temperatures) induces T_c far away from T_L. The cyclopropyl group provides thus a good fluid phase at T_L. Figure II.3-1 is an attempt to describe the above pictorially. The waving cylinders are supposed to represent the amplitude of the chain flexibility (the local ordering). At the same low absolute temperature, the PDSPC-like systems possess more motional amplitude (more

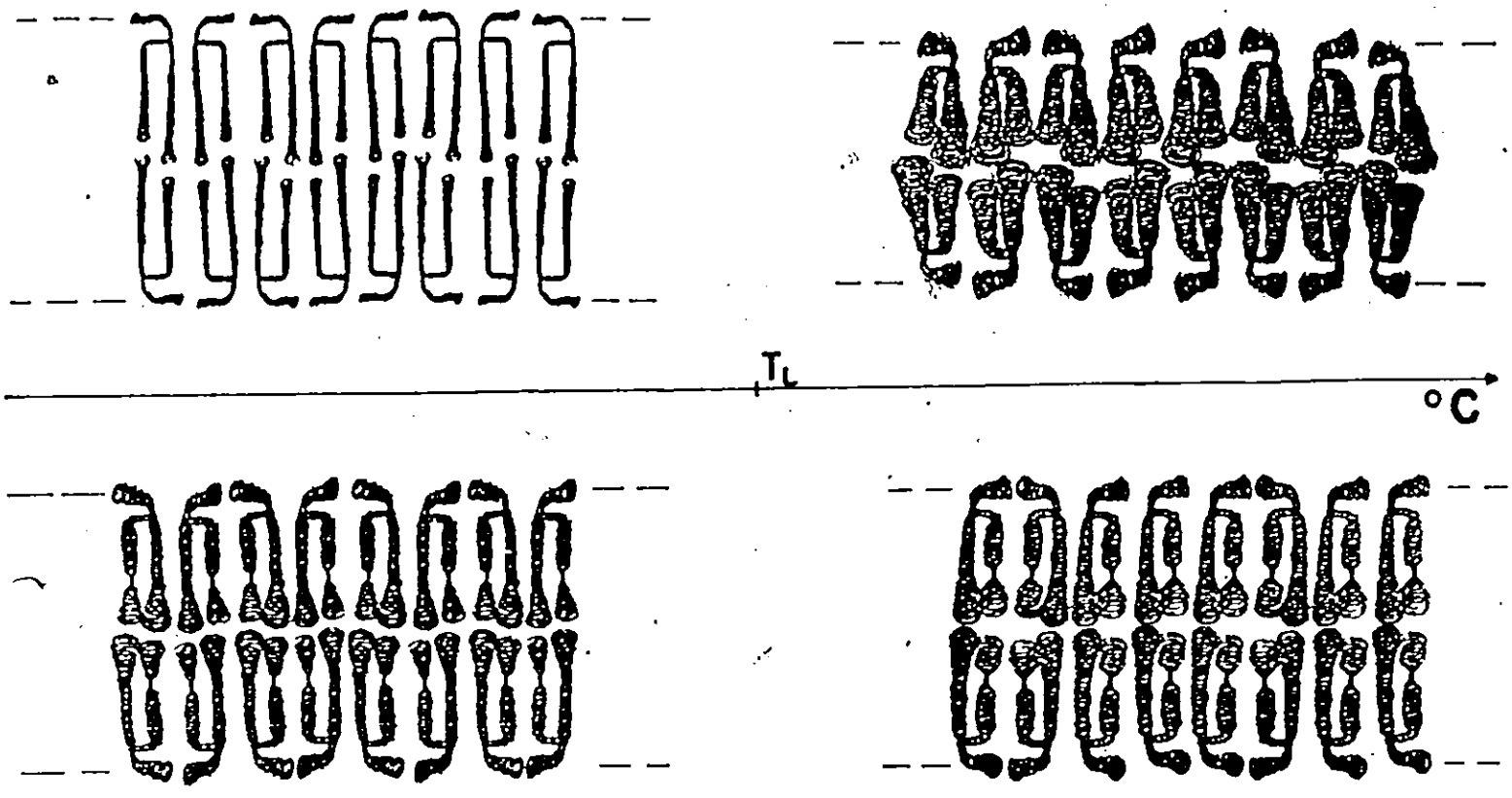

Fig. IL3–1. Graphic representation of segmental order parameters for DPPC–like (top) or PDSPC–like (bottom) model membrane systems. The waving cylinders are attempts of representing the amplitude of the angular fluctuations of the individual C–^{2}H bonds. The constriction seen in the acyl chains (bottom) represents the low amplitude fluctuations of the cyclopropane ring.

disorder) than the DPPC-like model membranes. One might think that if the cyclopropane perturbs the membrane packing, it would lead to an easy membrane disruption at high temperatures. This is not the case; indeed, it has been demonstrated herein that the cyclopropane induces a high correlation of the motions: the flexibility of the chains does not change greatly over 20 or 30°C temperature intervals; the best example is the preservation of the sn-1 plateau (up to the eighth carbon position) some 20°C above T_c. Figure II.3-1 represents also the membrane organization at high temperatures. One sees that the local ordering of PDSPC-like membranes does not change appreciably with temperature variations, whereas the DPPC-like lipids exhibit two really different pictures at low and high temperatures about T_L. Over the same temperature interval, the fully saturated lipids undergo rather important structural and dynamical modifications whereas the cyclopropane-containing membranes do not. The ring by its high local order and by the long correlation time for its motions acts therefore as a barrier preventing the propagation of the motions. One can therefore understand that changing the temperature by 10 or 20°C will not affect the structural and dynamical properties of cyclopropane containing membranes. The cyclopropyl moiety has therefore a regulatory role with respect to the amplitude and the rates of the motions involved in membrane stability. However, although we can begin to

understand the behaviour of PDSPC-like membranes around T_L, the nature of their packing at lower temperatures is not quite clear. The hypothesis of free space around the sn-2 plateau region in PDSPC must be checked: if the cyclopropane ring prevents the other chains from coming close to the carbon atoms of the sn-2 chain, in the plateau region, something else has to fulfill the same function at the glycerol backbone level. One might thus think that the shape of the PDSPC low temperature spectra is head group dependent, that is, the PC head group prevents the other PDSPC molecules from approaching closely at the glycerol level. ^{2}H-NMR low temperature studies of PDSPE model membranes (which possess a head group significantly smaller than PDSPC) might help evaluate the hypothesis of free space around the carbon atoms of the sn-2 plateau in PDSPC.

With regards to the biological synthesis of the cyclopropane ring system from a double bond, one can imagine from the shapes of Figure II.2-6, that the unsaturated lipids are precursors of membrane stabilization by the above processes. One may expect that the double bonded systems possess the properties of cyclopropane-containing lipids, but to a lesser degree. The final evolutionary stage in membrane growth would thus occur when these unsaturated fatty acids had been converted into their cyclopropane-containing analogs, the membrane reaching at the same time its highest stability with respect to external perturbations.

It is also interesting to notice that this so-called evolutionary process arises from an increase in order at the functional level (the C=C or the cyclopropane), that is, a decrease in entropy at that level. This remark can be related to the thermodynamics of irreversible processes; this branch of thermodynamics states that one can have decreases in entropy while being far from equilibrium. It might well happen that the unsaturated systems, in certain membranes, represent this state "far from equilibrium"; the system will therefore evolve towards the equilibrium stage through the biosynthesis of cyclopropane.

To conclude, we would like to emphasize that the observations and models formulated herein are of course over-simplified views of what happens in real life. A necessary control for the conclusions found for model membrane lipids must be accomplished through experiments on real membrane systems.

PART III

CHOLESTEROL IN MEMBRANE LIPIDS

CHAPTER III.1

CHOLESTEROL IN MEMBRANE LIPIDS

1. ORGANIZATION

III.1.1 Introduction

Cholesterol is a major component of the plasma membranes where it is often present at equimolar ratio with the phospholipids (Gomperts, 1977). Like lipids it has amphiphatic properties due to the presence of a hydroxyl group and a hydrophobic body (the steroid skeleton and the aliphatic tail attached at C17). It is therefore expected that cholesterol will orient itself normal to the membrane surface in order to maximize the hydrophilic and hydrophobic interactions.

Although the dynamics and conformational properties of cholesterol-containing membranes have been extensively investigated by a wide variety of techniques such as ESR (Smith, 1971; Schreier-Mucillo, et al., 1973) or ^{2}H-NMR (Stockton, et al., 1976; Stockton & Smith, 1976; Gally, et al., 1976; Brown & Seelig, 1978; Oldfield, et al., 1978; Taylor, et al., 1981, 1982) there is no clear cut answer with respect to "what cholesterol does to a lipid membrane" or "what does the lipid to the sterol"? A lot of the above studies concluded that the cholesterol has a

"condensing" effect on the lipid fatty acyl chains, above the gel-to-liquid crystalline phase transition temperature, T_c, of the given lipid and a disordering action below T_c. In some cases, it was reported that the gel-to-liquid crystalline phase transition of the lipid was removed by addition of high amounts of cholesterol (Davis, et al., 1979).

Several modes of action have been postulated. One of them uses the ordering-disordering properties to suggest that the sterol molecule controls the membrane "fluidity" (Madden, et al., 1979) whereas another alternative invokes a direct cholesterol-protein or cholesterol-lipid interaction without modification of the so-called "viscosity" of the membranes (Dahl, et al., 1981). The work presented herein is an attempt to understand better the cholesterol-lipid interactions at the molecular level and therefore provide a way of checking the validity of the above models. This study was also undertaken in order to define a basis for the analysis of cholesterol-polyene antibiotic-lipid interactions (Dufourc, et al., to be published).

^{2}H-NMR has proven to be a suitable technique to obtain molecular information such as the chain flexibility of lipid molecules or the rates of the molecular motions involved in relaxation processes (Davis, 1983). Through the synthesis of specifically deuterated DMPC or α and β-cholesterol (Figure III.1-1), and ^{2}H-NMR, the cholesterol-lipid

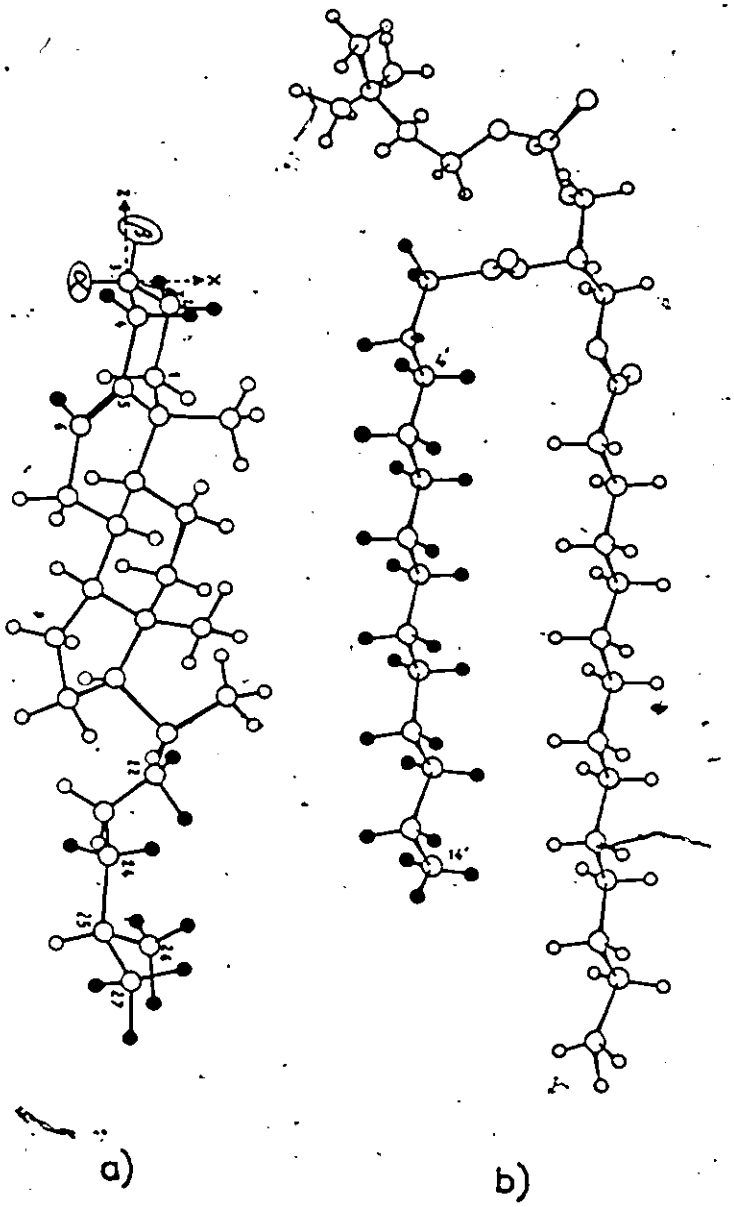

Fig. III.1-1. Structures of DMPC (b) and cholesterol (a) molecules. α= H, β= OH: β-cholesterol; α= OH, β= H: α-cholesterol. The filled circles represent the available deuterium labels. The sterol-fixed axis system (x,y,z) has its origin at C3.

interaction was studied from both the lipid and the cholesterol viewpoints, at several bilayer depths (that is, the plateau and the tail or center of the bilayer regions).

III.1.2 Theoretical Background

As has been demonstrated in the theory of deuterium nuclear magnetic resonance (Section I.2.5), the quadrupolar splittings of the powder pattern can be related to the order parameters through the equation (Davis, 1983):

$$\Delta\nu = \frac{3}{2} A_Q \frac{1}{2} (3 \cos^2\beta_b - 1)[S_{33} + \frac{1}{3} \eta (S_{11} - S_{22})] \qquad \text{(III.1.1)}$$

where β_b represents the macroscopic orientation of the axis of motion (usually taken to be the bilayer normal) with respect to the magnetic field direction, S_{ii} ($i = 1,2,3$) the order parameter tensor elements (the C-^{2}H bond fluctuations) and η the asymmetry parameter (the indication whether the electric field gradient (efg) at the nucleus site is axially symmetric). This equation reduces to the well-known axially symmetric case if $\eta = 0$ (efg tensor axially symmetric at the nucleus site) and/or $S_{11} = S_{22}$ (axially symmetric motions):

$$\Delta\nu = \frac{3}{2} A_Q \frac{1}{2} (3 \cos^2\theta' - 1) S_{C-^2H} \qquad \text{(III.1.2)}$$

In Equation (III.1.2) we used the notions introduced by Petersen and Chan (1977) for C-^{2}H ($\beta_b = \theta'$, $S_{33} = S_{C-^2H}$) with $S_{C-^2H} = S_\alpha S_\gamma$ (see Figure II.1-2 and Section II.1.2a for definition of the angles α, γ, θ' and of S_α and S_γ). For C-^{2}H bonds linked to a rigid structure one can consider that S_α is identical for all of them. However, these bonds can give rise to different S_{C-^2H} depending upon their geometrical orientation (different S_γ) with respect to the instantaneous axis of motion (vide infra).

III.1.3 DMPC - β-Cholesterol Interactions, the Plateau Region

III.1.3a Asymmetric Shapes at Low Temperatures

In order to monitor the interactions near the top of the bilayer, ^{2}H-NMR spectra of β-cholesterol-DMPC mixtures (3:7 molar ratio) were obtained; the deuterium atoms were either on the 4' carbon position (sn-2 chain) or on the 2,2, 3,4,4,6 carbon positions of the steroid rigid body (the A, B rings). Spectra were recorded in the temperature range 0°-65°C. Above 10°C, both the lipid or the cholesterol spectra exhibit axially symmetric powder pattern shapes (Figure III.1-2). One can therefore conclude that above 10°C the lipid and cholesterol undergo fast axial motion: increasing the temperature leads to an increase in the degree of spatial

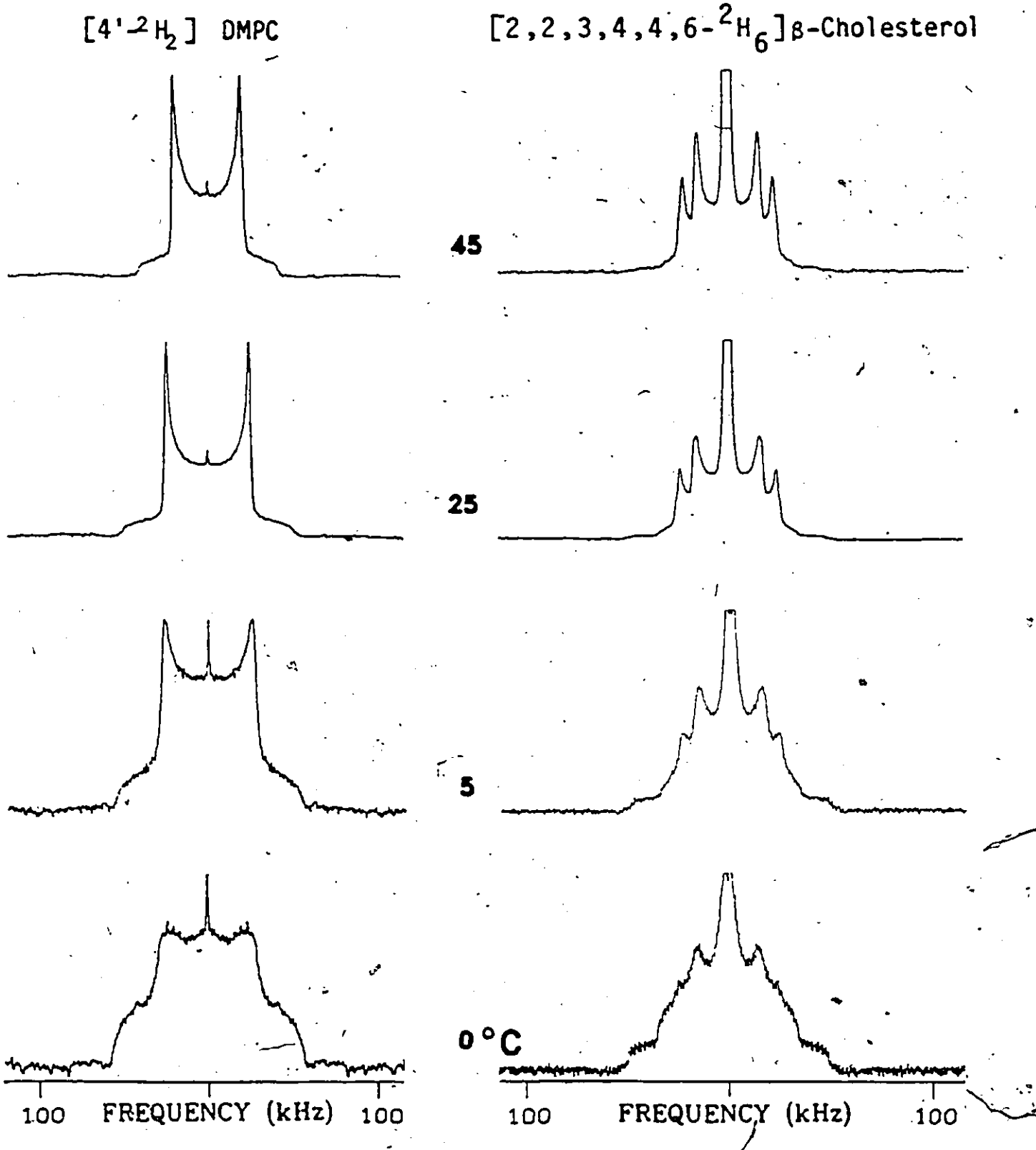

Fig. III.1-2. Temperature dependence of ^{2}H-NMR spectra of the β-cholesterol:DMPC (3:7 molar ratio) system. Experimental parameters: π/2 pulse length of 4 μs; pulse spacing of 60 μs; recycle time of 50 ms for deuterated cholesterol and of 100 ms for deuterated DMPC; 500 kHz spectral window and 18,000 accumulations.

averaging of the quadrupolar interaction, that is, the spectra reduce in width, keeping the same shape, as the temperature is raised. This behaviour will be further detailed in the next section.

Below 10°C, the spectra change in shape and increase their width as the temperature is lowered. Such spectral shapes have already been described (Seelig, 1977; Davis, 1983) or encountered in long hydrocarbon chains (Taylor, et al., 1983) and are characteristic of the lack of axial symmetry. Since $\eta = 0$ for C-^{2}H bonds in liquid crystalline bilayers (see Section I.2.5), it appears more likely that these axially asymmetric shapes are due to the loss of the fast rotational diffusion around the molecular long axis. Although the spectral shapes at low temperatures do not show a purely asymmetric powder pattern, possibly due to a mixture of axially and non axially-symmetric-like phases or to a substantial increase in the powder pattern linewidths, approximate calculations to simulate these spectra were performed and led to an apparent asymmetry parameter value of about 0.2, at 0°C.

It is interesting to notice that the ^2H powder spectra of both the lipid and cholesterol lose their axially symmetric shape at the same temperature, ca. 5°C, indicating therefore that the DMPC-β-cholesterol system is homogeneous with respect to the type of motions involved to average the quadrupolar interactions, at low temperatures. It is also noteworthy that the axially symmetric liquid-crystalline phase of the lipid is extended 15-18°C below the pure DMPC gel-to-liquid-crystalline phase transition temperature, that is, 23°C.

III.1.3b Temperature Dependence of the Segmental Order Parameter in the DMPC-β-Cholesterol Model Membrane System

Above 10°C, both the lipid and the β-cholesterol deuterium spectra exhibit an axially symmetric shape. The powder spectra were therefore dePaked as described in Materials and Methods, to obtain a spectral simplification, that is, only one orientation ($\theta' = 90°$). Figure III.1.3 shows an example of dePaked spectrum for β-cholesterol at 25°C. One notices that even if all the peaks are not resolved, the measurement of the splittings is far easier on the dePaked spectrum than on the power pattern. This

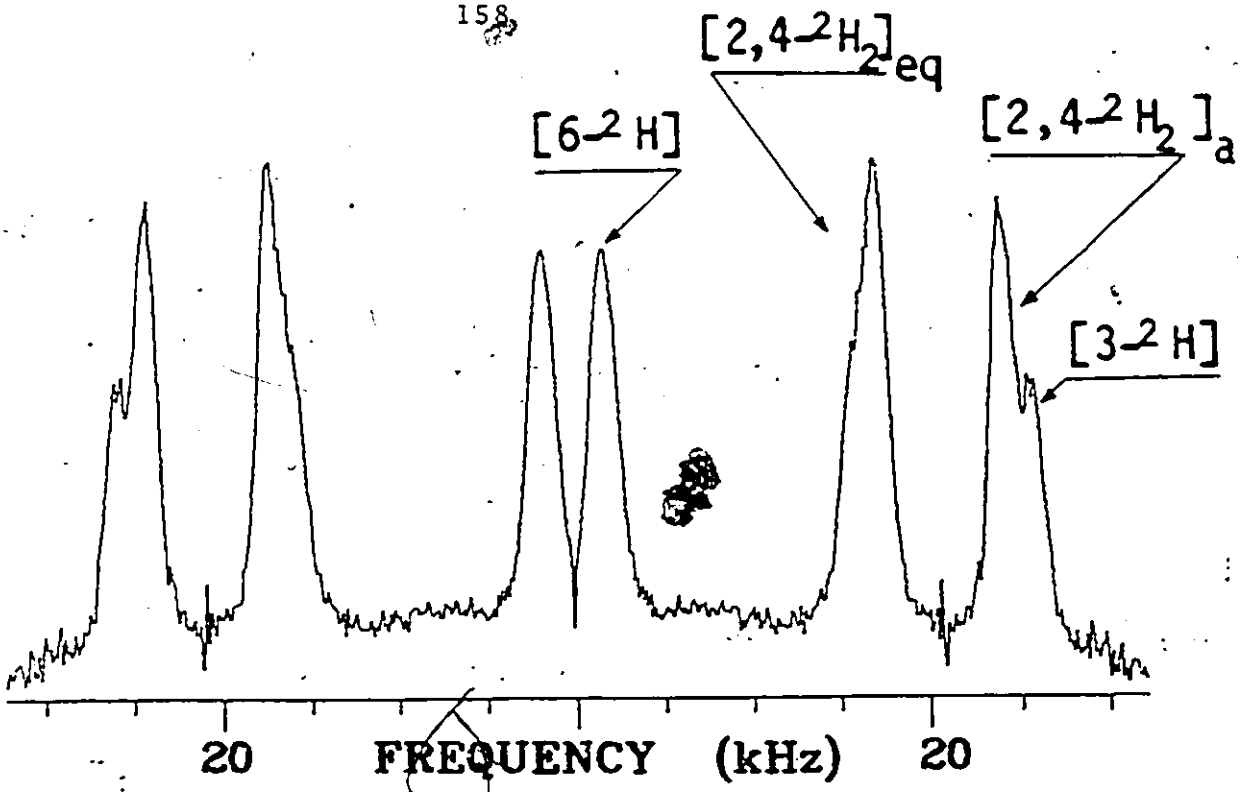

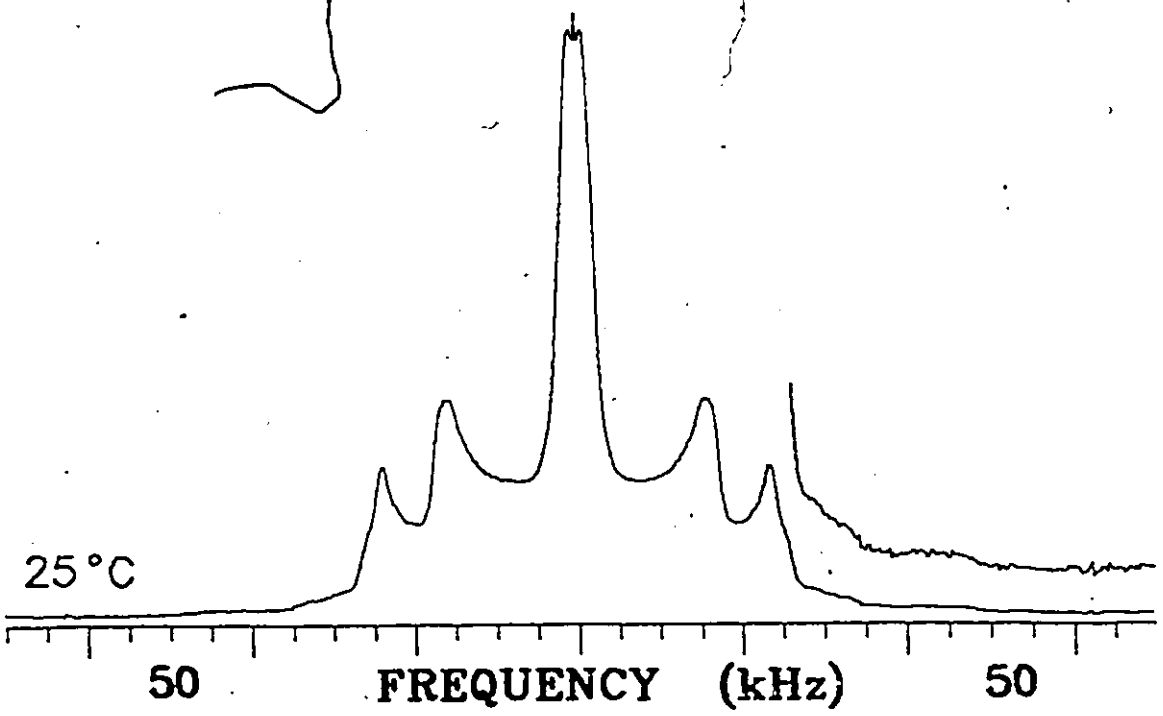

Fig. III.1-3. ^{2}H-NMR spectrum (bottom) and dePaked spectrum (top) of [2,2,3,4,4,6-$^2H_6$] β-cholesterol in DMPC (3:7 ratio), at 25°C. Same experimental parameters as in Fig. III.1-2. Processing parameters: deconvolution on 800 points; 3 iterations.

procedure was used for all spectra, above 10°C, and the results were compiled in Table III.1-1. The assignment of the β-cholesterol deuterons was made on the basis of the calculations below and correspond to those proposed by Taylor, et al. (1981). The C-^{2}H bonds of the sterol rigid body give very different quadrupolar splittings despite the fact that it can be considered that they undergo the same angular fluctuations, that is, they have the same segmental order parameter S_α (or S_{mol}). This is simply due to their different geometrical orientation with respect to the instantaneous segmental axis of motion. Hopefully, this geometrical dependence can be removed and one can obtain the pure angular fluctuations of the C-^{2}H bonds. In order to have access to the S_{mol} information, two methods, at least, can be used (Dufourc, et al., 1983). One of them consists of writing from the S_{C-^2H} order parameters and the molecular atomic coordinates, the order matrix in an arbitrary axis system linked to the rigid body and subsequently diagonalizing this matrix in order to obtain it in its axially symmetric form, thus reflecting the axial properties of the model membrane. The other defines the orientation of the axis of motion as a function of 2 angles, β and γ, of the arbitrary molecule-fixed coordinate system and "searches" for these angles. The latter gives thus S_{mol}, once the orientation of the axis of motional averaging is known. Each

Table III.1-1

DEUTERIUM QUADRUPOLAR SPLITTINGS OF THE DMPC-β-CHOLESTEROL SYSTEM,[a] PLATEAU REGION

Labeled Positions	Temperature (°C)											
	5	10	15	20	25	30	35	40	45	50	55	65
β-cholesterol[b]												
[6-^{2}H]		4.0	3.8	3.6	3.4	3.2	3.2	3.2	2.7	2.5	2.4	2.2
[3-^{2}H]		52.2	52.2	52.2	51.5	51.2	51.0	50.8	48.8	48.3	48.1	46.4
[2-^{2}H]eq[d]		34.6	34.6	34.2	34.2	34.2	33.8	33.6	32.1	31.9	31.3	30.3
[4-^{2}H]eq[d]		32.2	32.2	32.0	32.0	31.8	31.6	31.4	32.1	31.9	31.3	30.3
[2,4-^{2}H$_2$]ax		49.4	49.0	48.6	48.2	48.0	47.4	47.0	46.0	45.2	44.6	43.4
DMPC[b]												
[4'-^{2}H$_2$]	(54.7)[c]	54.2	53.2	52.5	50.8	48.8	46.9	44.4	42.1		37.9	

[a] Data from dePaked spectra, in kHz.
[b] Accuracy of the splittings ~1-2%.
[c] Estimated on the powder spectrum, accuracy ~5%.
[d] The assignment of these deuterons is arbitrary and could be reversed.

method has its particular drawbacks: the first requires, in the most general case, five ^{2}H-NMR observables but gives a unique answer; the second does not require as many S_{C-^2H}, but may give rise to several answers. Whereas the first allows a "blind" search, the second requires a hint to choose the correct solution. Due to the lack of symmetry of the cholesterol molecule, a matrix analysis would then require the maximum number of S_{C-^2H} order parameters, five. Although, theoretically, this method could be applied to the present set of data, the quadrupolar splittings are not different enough in magnitude to allow accurate calculations: the best solution led to a value of $S_{mol} \sim 1.2, \pm 0.4$ which is clearly incorrect. The second method, although less general, was applied using as a hint the fact that the cholesterol molecule has to orient almost vertically to the membrane surface in order to maximize the hydrophobic and hydrophilic interactions. This method, applied to cholesterol, is detailed in Appendix F. At 25°C, the final result was $S_{mol} = 0.80 \pm 0.03$ and an orientation of the cholesterol molecule within the bilayer such that the C_3-^{2}H bond vector makes an average angle $\theta = 84^\circ \pm 2^\circ$ with respect to the axis of motion, that is, the cholesterol molecule is indeed quasi-perpendicular to the membrane surface. This result agrees well with a value of $S_{mol} = 0.78$ reported by Oldfield, et al. (1978) at 23°C for β-cholesterol in the same system mixture;

arbitrarily assuming $\theta(C_3-^2H) = 90^\circ$. Our findings for the β-cholesterol-DMPC (3:7) system correlate also well with those obtained by Taylor, et al. (1981) ($S_{mol} = 0.87$, $\theta(C_3-^2H) = 79^\circ \pm 2^\circ$) for β-cholesterol in the β-cholesterol-egg PC (1:1) mixture at 25°C.

These calculations have been extended to all spectra for temperatures comprised between 10° and 65°C. The subsequent S_{mol} have been plotted as a function of temperature in Figure III.1.4. In this figure we have also reported the S_{mol} of the lipid labeled at the C4' position in presence and absence of 30% molar β-cholesterol. Since the average orientation of a methylene $C-^2H$ bond with respect to the instantaneous segmental axis of motion can be taken to be 90°, that is, the $C-^2H$ bond angular reorientations are equiprobable around $\gamma = 90^\circ$, $S_{mol} = -2\ S_{C-^2H}$ for the lipid at C4' (Seelig & Seiderberger, 1974). The first noticeable feature on Figure III.1.4 is the quasi temperature independence of the β-cholesterol molecular order parameter, S_{mol}^{chol}, between 10°C and 40°C; even at 65°C, the change in S_{mol}^{chol} is less than 10% with respect to the value at 10°C. The segmental order parameter of the lipid at C4' in the presence of β-cholesterol, $S_{mol,chol}^{4'}$, changes rather drastically over the same temperature range. Below $T_c = 23^\circ C$, the temperature of the gel to liquid crystalline phase transition of the pure lipid, the change in $S_{mol,chol}^{4'}$ with temperature is slight,

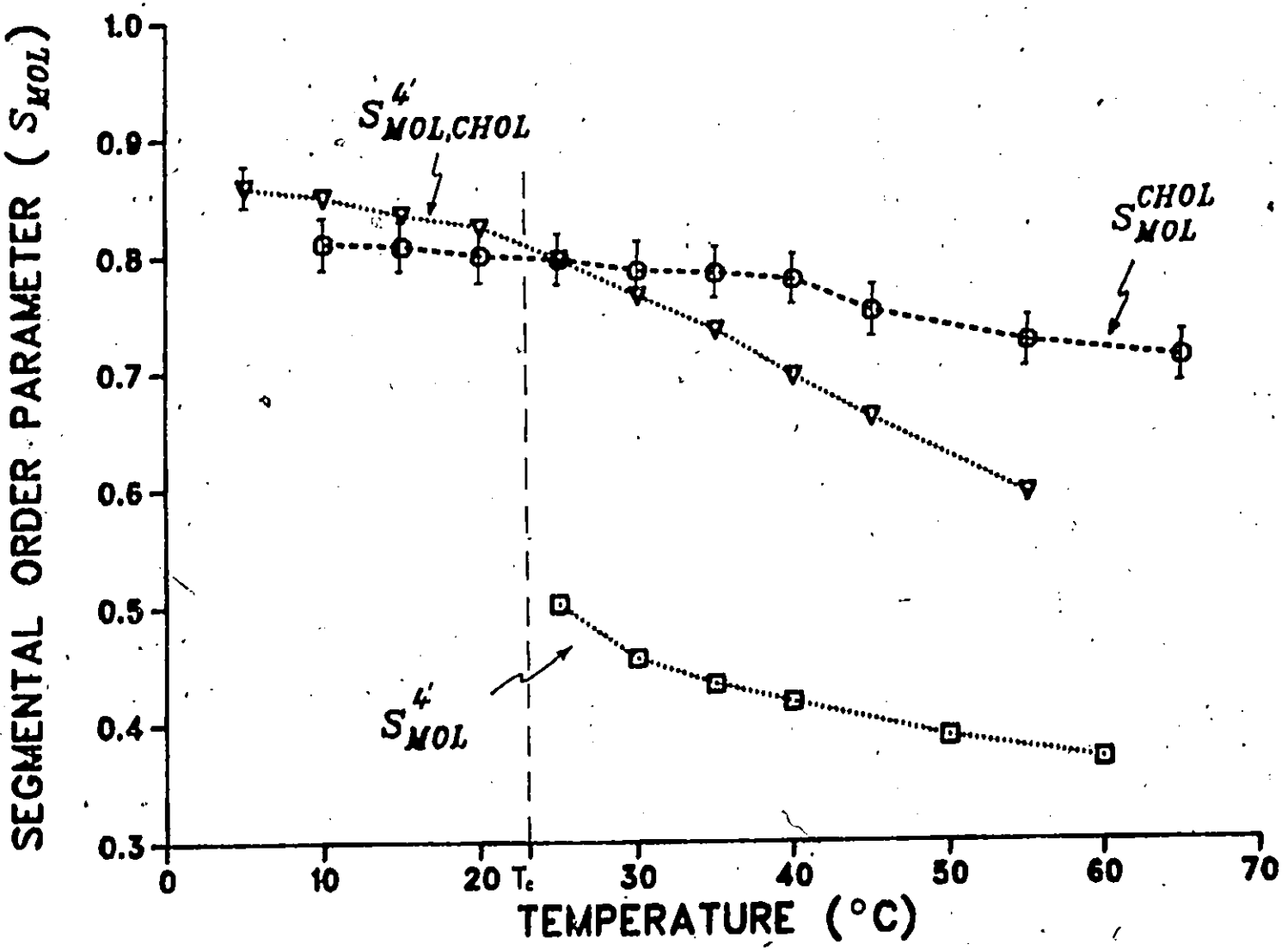

Fig. III.1–4. Temperature variation of the segmental order parameter, S_{MOL} , of the β–cholesterol:DMPC (3:7) system.
$S^{4'}_{MOLCHOL}$ = S_{MOL} of DMPC at C4' in the presence of sterol
$S^{4'}_{MOL}$ = Same as $S^{4'}_{MOLCHOL}$, without cholesterol.
S^{CHOL}_{MOL} = S_{MOL} of the four rings of cholesterol in DMPC.
The bars and symbols give an estimate of the error.

whereas above 23°C the drop in $S^{4'}_{mol,chol}$ with increasing temperature is rather marked. Despite this apparent "memory" of the pure lipid phase transition, it is difficult to conclude, based on the available data, that there is indeed a phase transition occurring at ca. 23°C. One can nevertheless remark that around T_c, the former gel to liquid crystalline phase transition temperature of the lipid, the lipid chain flexibility changes noticeably its rate of variation with temperature. Below T_c the amplitude of the angular fluctuations of the C-^{2}H segments at C4' are almost the same as those of the cholesterol body. It has to be remembered that below T_c the lipid chains would not show any C-^{2}H angular fluctuations at all if the β-cholesterol were not present (Davis, 1979). One may therefore interpret the "fluidizing" effect as a disordering effect: the β-cholesterol, through its almost temperature-independent "wobbling", forces the lipid chains to fluctuate even below 23°C, since it fluctuates itself. Since between 10°C and 23°C $S^{chol}_{mol} \sim S^{4'}_{mol,chol}$, it appears therefore that the cholesterol controls, through its own motions, the motions of the entire system, in this temperature range. Above ~23°C, the $S^{4'}_{mol,chol}$ behaves similarly to $S^{4'}_{mol}$ (segmental order parameter at the C4' position in the absence of β-cholesterol), except that the $S^{4'}_{mol,chol}$ profile is shifted towards high values of the segmental order parameter. It is interesting to notice that

at high temperatures S_{mol}^{chol} is markedly higher than $S_{mol,chol}^{4'}$. This leads to the comment that at high temperatures the system is characterized by two kinds of angular fluctuations, that is, those of the lipid and of β-cholesterol. Roughly put, this system could be compared to icebergs floating in a "sea" of lipids. This point is rather important and we would like to emphasize that measuring the molecular order parameter of the β-cholesterol at, for instance, 65°C would not give information about the chain flexibility. One would measure the property of the probe in the system rather than measure the property of the system.

With regards to the condensing effect of β-cholesterol, one can indeed confirm that due to its higher S_{mol}^{chol}, this latter orders the lipid, above T_c. However, the control of $S_{mol,chol}^{4'}$ (the chain flexibility) appears less efficient above T_c than below T_c.

From a pure mathematical viewpoint, it might be interesting to consider the profiles in Figure III.1.4 as abstract curves: the $S_{mol,chol}^{4'}$ profile could thus be the result of a rather odd convolution between the S_{mol}^{chol} and the $S_{mol}^{4'}$ curves, the β-cholesterol acting as a sort of "smoothing" function.

III.1.4 DMPC-β-Cholesterol Interactions, the Tail Region

III.1.4a Deuterium Nonequivalence in the Cholesterol Tail

The amplitude of the motions near the center of the bilayer was monitored by recording deuterium spectra from both the lipid and the β-cholesterol molecules (7:3 molar ratio). The deuterium atoms were on either the 14' position of the DMPC sn-2 chain or the 22-, 24-, 26- and 27- positions of the aliphatic β-cholesterol tail. Figure III.1-5 shows the temperature variation of the [14'-$^2H_3$]DMPC and the [24-$^2H_2$]-β-cholesterol spectra whereas Figure III.1-6 shows the deuterium powder patterns of the β-cholesterol tail at positions 22, 24, 26 and 27, at 25°C. Several interesting features can be noticed in Figure III.1-6. Firstly, one remarks the presence of multiple powder patterns for positions near the end of the tail, that is, positions [24-$^2H_2$] and [26,27-$^2H_6$]. The nonequivalence of the terminal methyl groups of β-cholesterol (Figure III.1-6d) has already been demonstrated by Taylor, et al. (1982) using egg PC as a substrate. These authors observed that the degree of nonequivalence was progressively diminished with increasing concentration of β-cholesterol; at 30 mole per cent of β-cholesterol the two methyl groups gave essentially a single deuterium powder pattern. At first sight, the spectrum of

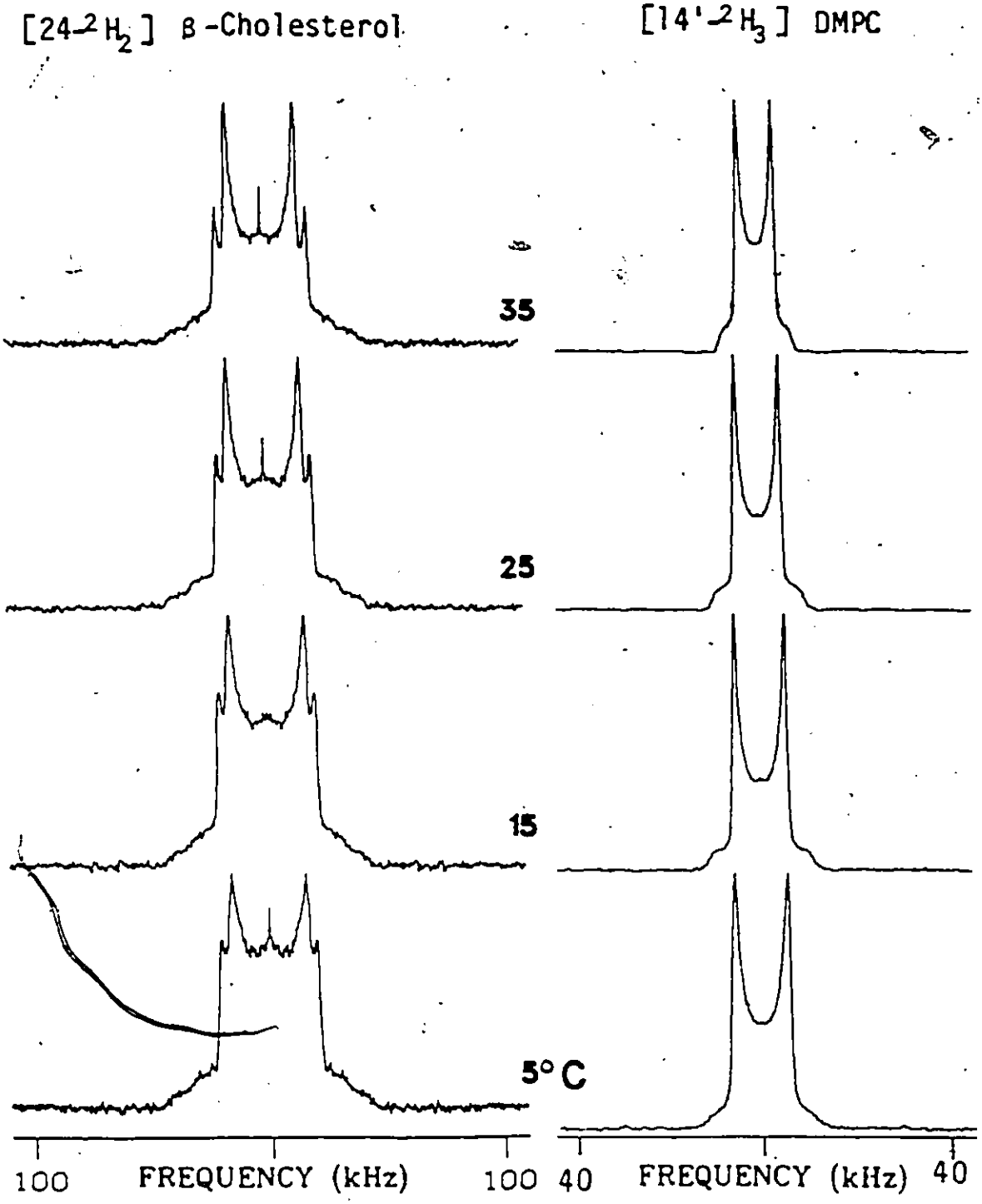

Fig. III-5. Same as in Fig. III-2 for different deuterium-labeled positions. Same experimental parameters as in Fig. III-2 except recycle time of 100 ms for deuterated sterol and 1s for [14'-$^2H_3$]DMPC; 250 kHz spectral window for deuterated DMPC.

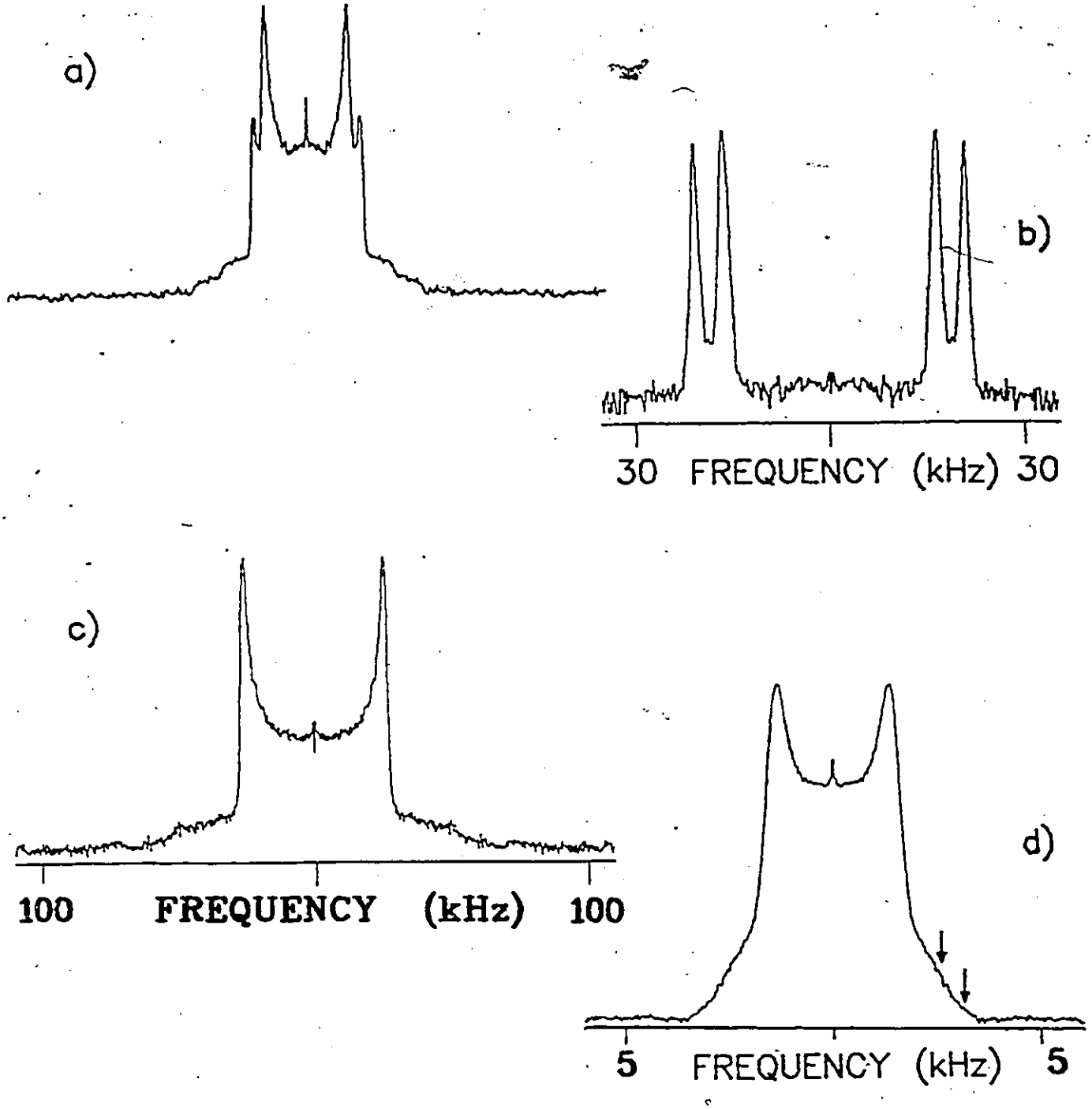

Fig. III.1–6. ^{2}H–NMR spectra of β–cholesterol in DMPC (3:7) at 25 °C.
a) [24–$^2H_2$] β–cholesterol.
b) Same as a), dePaked.
c) [22–$^2H_2$]β–cholesterol.
d) [26,27–$^2H_6$]β–cholesterol.

Figure III.1-6d could be considered to be a single powder pattern; however, the high S/N ratio allows us to distinguish two shoulders (that is, two $\theta' = 0^{\circ}$ orientations), indicated by arrows. It is worthwhile to mention that the frequency of the spectrometer was carefully offset such that no distorsion was induced by folding the spectrum. The dePaking procedure was tried on this spectrum but the two components could not be resolved; this is simply due to the fact that the difference in quadrupolar splitting is of the order of magnitude of the individual component linewidths.

The two deuterons at C24 are also nonequivalent but their respective powder patterns are well separated (Figure III.1-6a) and the dePaked spectrum (Figure III.1-6b) shows that the two pairs of lines have the same area, within the experimental error. Furthermore, there was no change in the relative areas of the dePaked lines for position 24 over the temperature range 5°-65°C thus ruling out the possibility of two long-lived conformations. The more likely explanation is that the two deuterons at C24 have different average orientations with respect to the instantaneous segmental axis of motion. Such a case has already been encountered (Engel & Cowburn, 1981; Dufourc, et al., 1983) and is quite general for the two deuterons at the C2' sn-2 position in phospholipids. The method used to calculate the average orientation of the rigid sterol moiety was used here to calculate the order and average orientation of the two deuterons

at C24, with respect to the instantaneous segmental axis of motion. Although not very accurate since only two splittings are available, this method led to two principal solutions: $S_{mol} = 0.66 \pm 0.04$, $\theta_1 = 88 \pm 4^{\circ}$, $\theta_2 = 74 \pm 4^{\circ}$ and $S_{mol} = 0.66 \pm 0.04$, $\theta_1 = 36 \pm 4^{\circ}$, $\theta_2 = 73 \pm 4^{\circ}$, where S_{mol} is the segmental order parameter of the methylene unit at C24 and θ_1, θ_2 the average angles made by the two deuterons with respect to the segmental axis of motion. It is interesting to notice that both solutions give the same order parameter with different orientations of the [24-$^2H_2$] segment: one of them is such as the deuterons are almost at 90° with respect to the axis of motion (similar to methylenes in a lipid fatty acyl chain) whereas the other would involve the normal to the ^2H-C24-^2H plane almost perpendicular to the axis of motion. Although the choice between these two solutions is rather difficult, the orientation involving an extended cholesterol side chain conformation seems the more plausible, based on the following.

The two deuterons at C22 exhibit a single powder pattern, that is, they possess the same average orientation with respect to the instantaneous axis of motion. Assuming that this orientation is 90° the segmental order parameter at C22 will be equal to $-2\ S_{C-^2H}$ which leads to $S_{mol} = 0.83 \pm 0.01$, at 25°C. This value agrees well with the molecular order parameter found in the previous section for the rigid steroid structure, that is, $S_{mol} = 0.80 \pm 0.03$, at the same

temperature. This indicates that one can consider the cholesterol acyl chain, up to C22, to be as rigid as the four ring structure, that is, the rigid cholesterol cylinder-like body can be extended up to carbon 22. Moreover, one can also consider that the entire cholesterol side chain is highly ordered since at C24, two carbons from the end of the chain, the segmental order parameter is equal to 0.66. These findings confirm unambiguously the earlier hypothesis which suggested that the β-cholesterol side chain was rigid (Darke, et al., 1972; Shimshik & McConnel, 1973).

With regards to the low temperature spectra, one notices in Figure III.1-5 that the [24-$^2H_2$]-β-cholesterol spectrum begins to show small features indicative of axial asymmetry at 5°C, as it was found for the rigid cholesterol body in the previous section. Conversely, and in contrast to [4'-$^2H_2$] DMPC at low temperatures (see previous section), the terminal methyl of DMPC does not show these features. However, it is difficult to compare the motions of methylene and methyl groups. It is well known that the methyl unit provides an additional averaging of the quadrupolar interaction through rotation about its C_3 axis. It is possible that when the motions approach axial asymmetry for the methylene units, the additional motion of the methyl group preserves the axial symmetry of its motions. This is of course an oversimplified view of the methyl motions. The change in shape

of the [14'-$^2H_3$] DMPC spectra (which is not well understood), when the temperature is lowered, suggests also that a qualitative and quantitative description of these motions would require a detailed lineshape analysis beyond the scope of the present study.

III.1.4b Fluidizing-Condensing Effect of the β-Cholesterol Side Chain

The hypothesis that only the cholesterol rigid skeleton is responsible for the fluidizing-condensing effect in lipid-cholesterol mixtures (Rothman & Engelman, 1972) can be verified by comparing the temperature behaviour of the cholesterol tail positions with respect to the lipid positions at the same depth in the membrane, that is, near the center of the bilayer; the only available variable temperature data, to-date, are the quadrupolar splittings of [24-$^2H_2$] cholesterol and of [14'-$^2H_3$] DMPC. As we have already mentioned in the previous section, it is difficult to compare methylene and methyl motions. However, Stockton, et al. (1976) proposed to relate the motions of these two groups with respect to the same axis of motion, that is, the bilayer normal. To do so, the $S_{mol}^{CH_3}$ can be defined as (Stockton, et al., 1976):

$$S_{mol}^{CH_3} = -6\, S_{C-^2H_3}. \qquad \text{(III.1.3)}$$

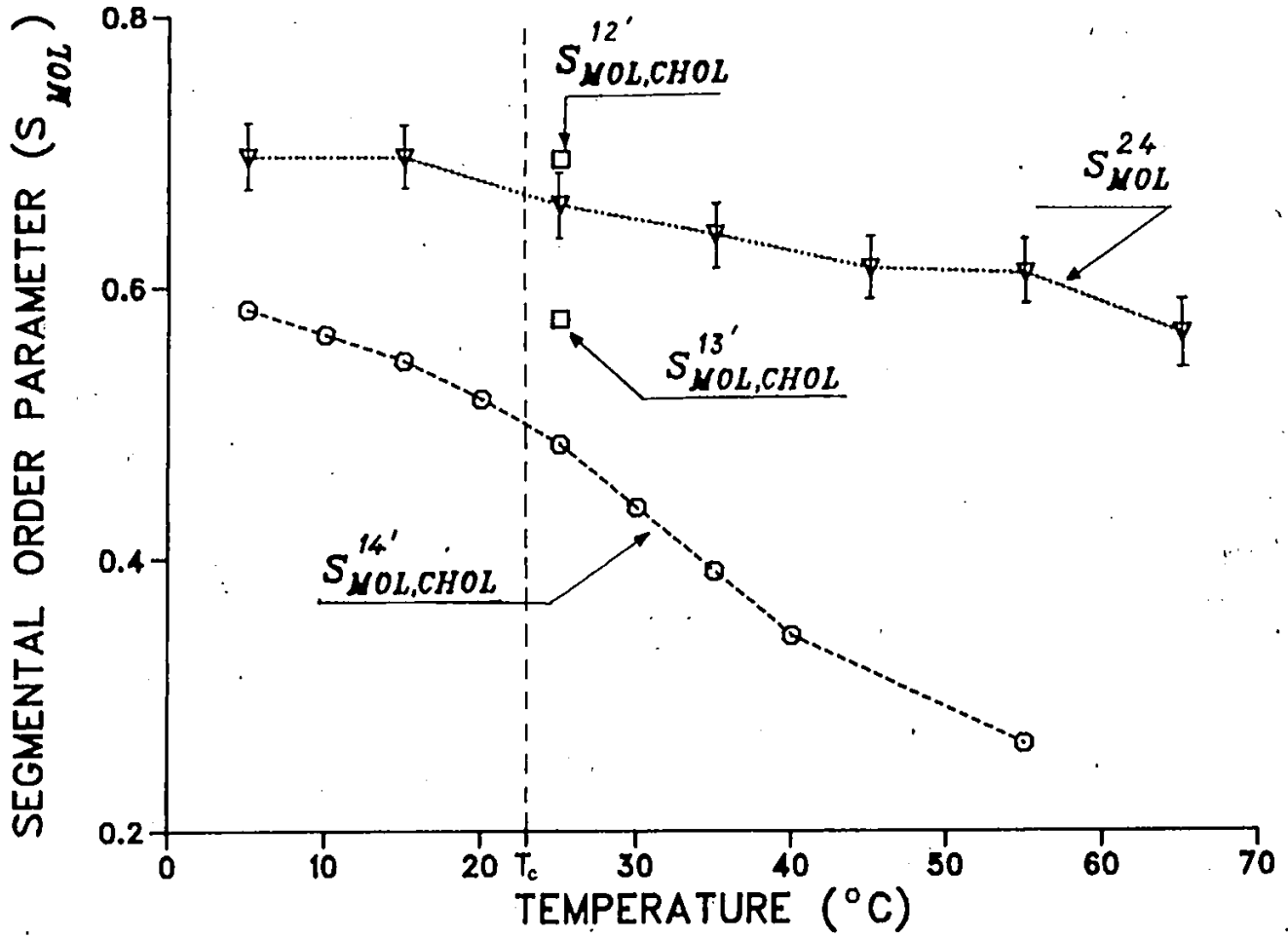

Fig. III.1–7. Temperature variation of the segmental order parameter, S_{MOL}, of the β-cholesterol:DMPC model membrane system.
S^{24}_{MOL} = S_{MOL} of sterol labeled at C24, in DMPC.
$S^{14'}_{MOL,CHOL}$ = S_{MOL} of DMPC labeled at C14', in the presence of cholesterol.
$S^{12'}_{MOL,CHOL}$ and $S^{13'}_{MOL,CHOL}$, same as $S^{14'}_{MOL,CHOL}$ with DMPC labeled at C12' and C13', respectively.

In the following qualitative analysis, we shall use Equation (III.1.3) but we would like to point out that possibly due to the additional averaging brought by the methyl free rotation, $S_{mol}^{CH_3}$ might be underestimated. Figure III.1-7 shows the segmental order parameter of the lipid in the presence of β-cholesterol at C14', $S_{mol,chol}^{14'}$ and the segmental order parameter of the β-cholesterol at C24, S_{mol}^{24}, in the temperature range 5°-65°C. Also shown is the segmental order parameter for lipid positions C12' and C13' (Dufourc, et al., to be published), for the same system at 25°C, in order to compare the magnitude of S_{mol} for lipid and cholesterol methylene units. The similarity in profile between Figure III.1-7 and Figure III.1-4 is striking: the S_{mol}^{24} shows almost the same temperature insensitivity that the S_{mol}^{chol} whereas the lipid at C14' exhibits the same phase transition "memory" around 23°C as it was observed for the $S_{mol,chol}^{4'}$ in Figure III.1-4. This leads to the conclusion that even if the amplitudes of the C-^{2}H angular fluctuations are different in magnitude, their temperature dependence is identical for all lipid and cholesterol positions, respectively. The marked difference in magnitude, at 25°C, between the $S_{mol,chol}^{14'}$ and S_{mol}^{24} may be accounted for by the fact that the C-$^2H_3$ lipid unit undergoes different types of motional averaging than does the C-$^2H_2$ of the cholesterol tail, at C24. The segmental order parameters at positions 12' and 13' show that indeed,

around 25°C, the amplitude of the angular fluctuations of the C-$^2H_2$ lipid units are of the same order of magnitude as the cholesterol side chain methylene units. The role of cholesterol discussed for the plateau region can therefore be generalized throughout the membrane bilayer thickness. In addition, due to the rigidity of its side chain, the entire cholesterol molecule can be considered as a rigid "cylinder" with molecular order parameter of ca. 0.7-0.8 when present at 30 mole per cent in DMPC. It would be interesting to investigate if the rigidity of the cholesterol side chain is dependent on cholesterol concentration.

With respect to the terminal methyl units at C26 and C27 the origin of the small quadrupolar splittings is not fully understood. Stockton, et al. (1976) have used $S_{mol} = -18\ S_{C-^2H}$ for the three choline methyl groups arguing that their S_{C-^2H} could be related to the instantaneous axis of motion by three geometric transformations, that is, $S_{C-^2H}^{(CH_3)_3} = S_\alpha S_{\gamma_1} S_{\gamma_2} S_{\gamma_3}$, where S_α is the segmental order parameter (S_{mol}) and where $S_{\gamma_i} = \frac{1}{2}(3\cos^2\gamma_i - 1)$, the $\gamma_i (i = 1,2,3)$ being the angles of the three subsequent axially symmetric transformations to rotate from the principal axis system bound to the C-^2H bond vector to the instantaneous segmental axis of motion, which is itself related to the average axis of motion, the bilayer normal, through S_α. According to these authors one will find, using Table III.1-2, $S_{mol}^{26,27} \sim$

Table III.1-2

DEUTERIUM QUADRUPOLAR SPLITTINGS OF THE DMPC-β-CHOLESTEROL SYSTEM,[a]
TAIL REGION

Labeled Positions	Temperature (°C) 5	10	15	20	25	30	35	40	45	55	65
β-cholesterol											
[22 -$^2H_2$]					53.1						
[24 -^2H]	(33.2)[d]		33.2		32.2		30.3		27.8	25.4	23.7
[24 -^2H]	(42.0)[d]		42.0		41.0		39.8		38.1	36.1	34.4
[26 -$^2H_3$]							2.7[c]				
[27 -$^2H_3$]							3.1[c]				
DMPC[b]											
[12'-$^2H_2$][e]							44.3				
[13'-$^2H_2$][e]							36.8				
[14'-$^2H_3$]	12.4	12.0	11.6	11.0	10.3	9.3	8.3	7.3		5.6	

[a] From dePaked spectra, in kHz.
[b] Accuracy of the splittings ~ 1-2%.
[c] Estimated on the shoulders of the powder spectrum.
[d] Estimated on the powder spectrum since this latter showed a non-symmetrical shape (see text), accuracy ~5%.
[e] From DMPC [$^2H_{27}$-sn-2]: β-cholesterol (7:3) (Dufourc, et al., to be published).

0.38-0.44 (segmental order parameters of the methyls at C26 and C27) which is in good agreement with the value found for $S^{14'}_{mol,chol}$, at 25°C. However, this calculation does not account for either the inequivalence at C26 and C27 or for additional motional averaging due to free methyl rotation and although $S^{14'}_{mol,chol} \sim S^{26,27}_{mol}$ the value of S_{mol} for methyl groups might simply be particular to methyl motions and not segmental chain fluctuations. Deuteration at C25 of the β-cholesterol side chain should give additional information, through ^{2}H-NMR, about the motions of the methyl groups at C26 and C27.

III.1.5 The α-Cholesterol-DMPC System

A recent study of the 3 β-thiocholesterol interactions with egg PC membranes (Parkes, et al., 1982) concluded that the 3 β-hydroxyl group of cholesterol determines, through its hydrogen bonding with phospholipids, the solubility of the sterol and its membrane ordering properties. The α-isomer of cholesterol (epicholesterol, see Figure III.1.1 is thus expected to exhibit weak hydrogen bonding with lipids, a limited solubility (Demel, et al., 1972), and little ordering effect on the phospholipid membranes. The results presented below are an attempt to clarify this latter assertion and to understand why α-cholesterol is not utilized in natural membranes.

III.1.5a Low Temperature Spectra of the α-Cholesterol-DMPC System

Deuterium spectra of the α-cholesterol:DMPC (3:7) mixture were obtained over the temperature range 10^{o}-65^{o}C. The ^{2}H labels were either on the lipid at positions C4' and C14' or on α-cholesterol at positions 2, 2, 3, 4, 4, 6. Figure III.1-8 shows some of the low temperature spectra for both the lipid and the α-cholesterol. One notices that above 20^{o}C, the spectra have axially symmetric shapes and that around 15^{o}C the axial asymmetry of the powder patterns begins to appear. Whereas the β-cholesterol:DMPC system shows axially symmetric lineshapes for 15-18^{o}C below T_c, epicholesterol at the same concentration extends the axially symmetric phase for only 5-8^{o}C below T_c. It can therefore be concluded that α-cholesterol is much less efficient than β-cholesterol with respect to the fluidizing effect on DMPC. This will be confirmed in the next section.

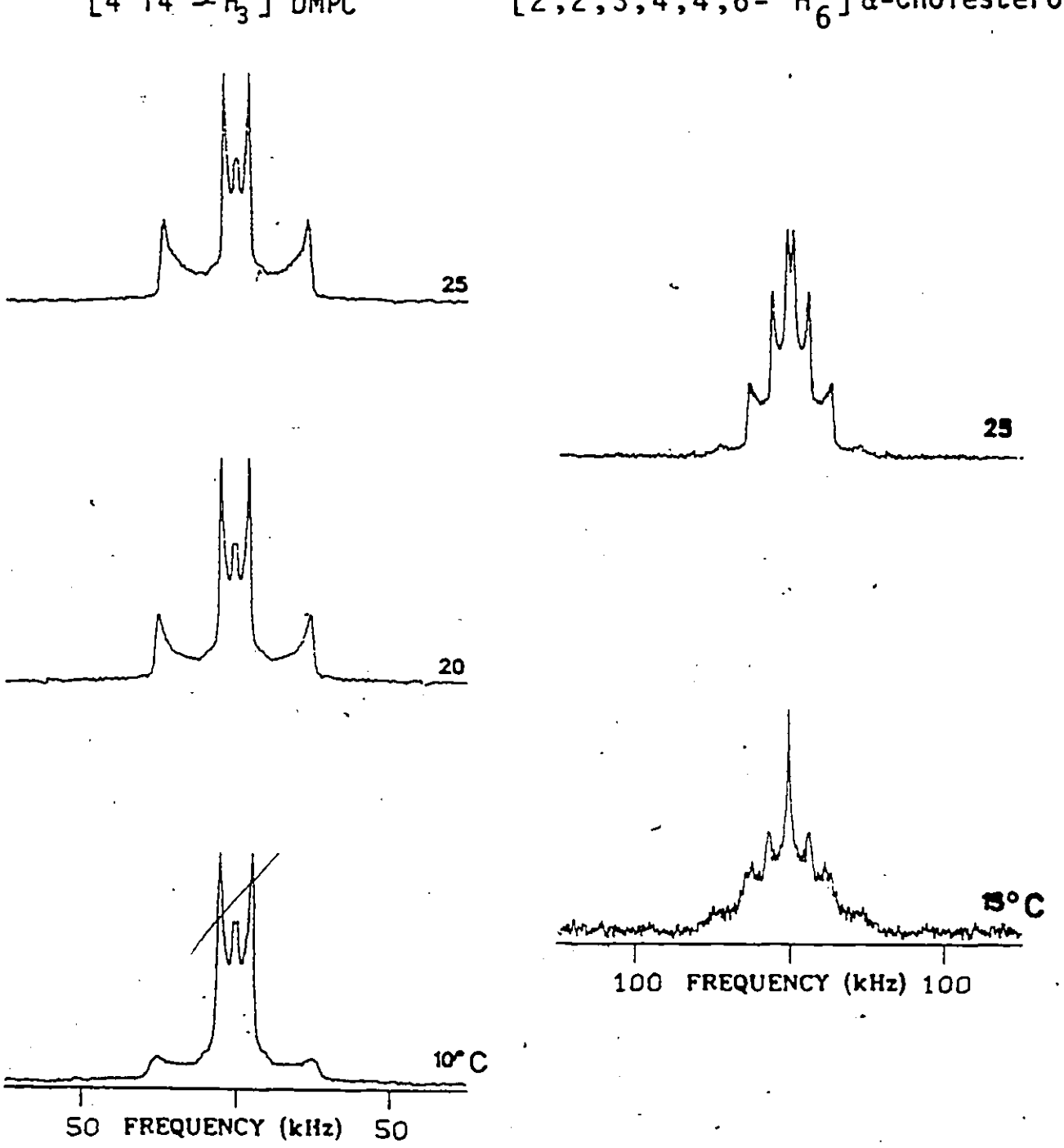

Fig. III.1–8. Low temperature ^{2}H–NMR spectra of the α–cholesterol:DMPC system (3:7 molar ratio). Same experimental pafameters as in Fig. III.1–2.

III.1.5b Reorientation of the α-Cholesterol in the Bilayer Membrane

Above 20°C all spectra exhibit axially symmetric shapes, and therefore the dePaking routine may be used. Figure III.1-9 shows some spectra of α-cholesterol with the corresponding spectra of β-cholesterol, at same temperatures. The dePaking routine is well illustrated on the top of Figure III.1-9: one indeed notices how the individual lines can be resolved on a dePaked spectrum even when they are barely seen in the powder pattern spectrum, for example, α-cholesterol at 65°C. The quadrupolar splittings were obtained by making use of the line fitting routine described in Materials and Methods and are reported in Table III.1-3. The assignment of the α-cholesterol splittings is based on the calculations described below and in Appendix F.

A first qualitative comment can be made regarding the relative change in both spectral width and shape of α-versus β-cholesterol, when the temperature is raised. From 25°C to 65°C the β-cholesterol splittings undergo a concomitant decrease for all labeled positions; this indicates that the molecular order parameter decreases without any molecular reorientation of β-cholesterol, that is, the C-^{2}H bonds exhibit the same average orientation with respect to the axis of motion either at 25°C or 65°C. In that same temperature range, certain α-cholesterol labeled positions

Table III.1-3

DEUTERIUM QUADRUPOLAR SPLITTINGS OF THE DMPC-α-CHOLESTEROL SYSTEM,[a] PLATEAU REGION

Labeled PPositions	Temperature (°C) 10	20	25	30	35	40	45	50	55	65
α-cholesterol[b]										
[6 -^{2}H]		5.0	5.8	6.0		7.8		9.4	9.8	10.2
[2 -^{2}H]$_{ax}$		53.5	54.7	54.1		52.2		49.3	48.8	46.6
[2 -^{2}H]$_{eq}$		26.5	24.9	24.2		20.5		15.1	15.1	13.1
[4 -^{2}H]$_{ax}$		53.5	54.7	54.1		52.2		49.3	48.8	46.6
[4 -^{2}H]$_{eq}$		26.5	24.9	24.2		23.0		20.0	20.0	18.6
DMPC[b]										
[4'-$^2H_2$]	(53.7)[c]	50.8	48.3	45.9	43.0		38.3		34.9	
[14'-$^2H_3$]	(12.0)	10.3	9.3	8.3	7.3		5.9		5.1	

[a] Data from dePaked spectra, in kHz.
[b] Accuracy on the splittings ~1-2%.
[c] Estimation on the powder pattern, accuracy ~5%.

show a decrease in quadrupolar splitting whereas others exhibit an increase when the temperature is raised (Figure III.1-9, top). One can therefore conclude that both S_{mol} and the average orientation of the α-isomer within the bilayer membrane are changing with temperature.

In order to quantitate these remarks, calculations analogous to those carried out for β-cholesterol (previous sections) were undertaken for α-cholesterol (see Appendix F). Unfortunately, it was not possible to obtain a unique answer, that is, to determine unambiguously the position of the axis of motion of α-cholesterol. As mentioned in Appendix F, two solutions were found. The first solution, named 1, is such that the OH group (in α) would be directed towards the aqueous surface whereas the second solution, 2, involves the hydroxyl group pointing towards the hydrophobic core (see sketches in Figure III.1-10). In order to decide which of these solutions is correct, an additional experiment involving α-cholesterol labeled at C3 would be needed. Indeed, the average orientation of the axis of motion of α-cholesterol in DMPC (3:7) predicts a quadrupolar splitting at C_3-^{2}H of ca. 40 kHz or ca. 100 kHz according to solutions 1 or 2, respectively (see Appendix F). Unfortunately, such a labeled compound is not available yet and the low ^{2}H incorporation at C3 (~20%) in [2,2,3,4,4,6-$^2H_6$]-α-cholesterol does not allow interpretation with certitude of the small

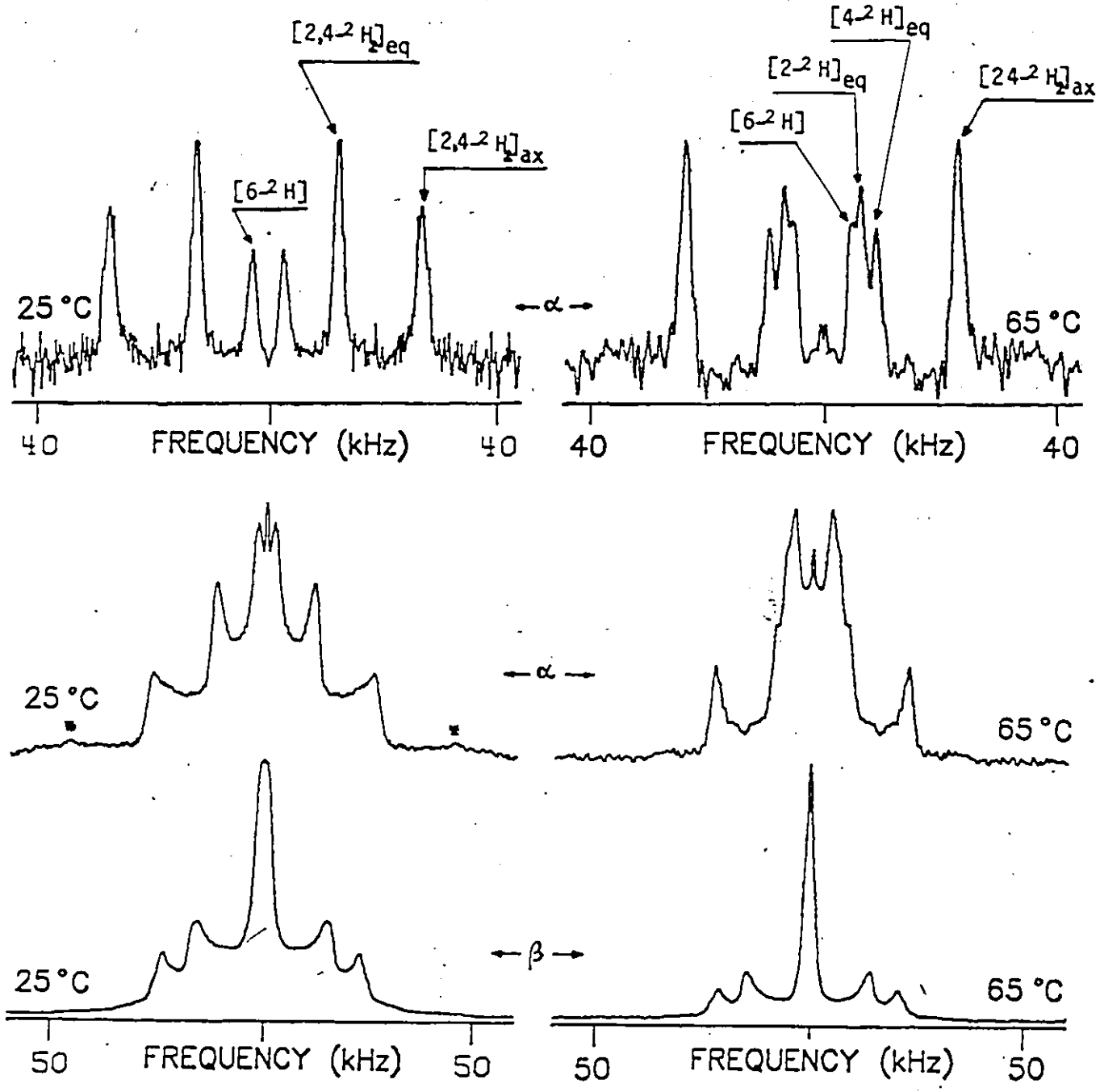

Fig. III.1-9. ^{2}H-NMR spectra of [2,2,3,4,4,6-$^2H_6$]α-(center) and β- (bottom) cholesterol in DMPC (3:7) at the indicated temperatures. Top spectra are dePaked analogs of center spectra. Same experimental and processing parameters as in Fig. III.1-3.

spectral feature of ca. 95 kHz in Figure III.1-9 (indicated by * in the spectrum of α-cholesterol at 25°C) as an argument in favour of solution 2. However, the general behaviour of α-cholesterol in model membranes may still be discussed according to the two solutions. In order to characterize the reorientation of α-cholesterol within the DMPC bilayer, it was chosen to follow the angular variation ($\theta(C_2-{}^2H_{eq})$) of a given C-^{2}H bond vector with respect to the axis of motion, $\vec{n}$, as a function of temperature. Figure III.1-10 reports such a variation for both α- and β-cholesterol. One notices that whereas there is no change in orientation of the β-cholesterol in DMPC from 10°C to 65°C, both solutions for α-cholesterol show that the $C_2-{}^2H_{eq}$ bond vector tends to reorient towards the magic angle, with respect to $\vec{n}$, as the temperature increases. This behaviour agrees well with the observation that the $\Delta\nu_Q$ for this bond decreases more rapidly than the other $\Delta\nu_Q$ values of α-cholesterol, on raising the temperature (Table III.1-3 and Figure III.1-9). It is interesting to notice that at physiological temperatures β-cholesterol sits vertically in the bilayer membrane whereas the α-isomer shows a marked tilt with respect to the membrane surface (see the sketch in Figure III.1.10). Such an orientation for α-cholesterol in DMPC can be understood by considering the hydrophilic and hydrophobic interactions as well as some simple mechanistic concepts. The hydroxyl

group in β-cholesterol can be expected to coincide with the axis of inertia of the entire molecule whereas in the α-isomer (assuming to first order that the α- and β-cholesterol have the same axis of inertia) this OH group is definitely not aligned along this axis. In order to maximize the hydrophobic and hydrophilic interactions, the β-molecule therefore sits vertically within the membrane; its OH group pointing towards the water surface. Such a situation satisfies both the hydrophilic-hydrophobic forces and the inertia equilibrium of the molecule, and can thus be expected to be very stable: it is therefore not surprising that β-cholesterol does not reorient even when the amplitude of allowed motion increases (Figure III.1-10). The α-isomer tends also to direct its OH group towards any hydrophilic region (the water surface or the C=0 of the lipids) and to do so it needs to take a tilted orientation with respect to the bilayer. On the other hand, the inertia of the molecule tends to align the α-cholesterol perpendicularly to the surface, parallel to the axis of motion of the membrane, that is, the bilayer normal. Therefore, the observed tilt would be the resultant of two constraints, the amphiphatic interactions and the inertia of the α-cholesterol, acting in different directions. At high temperatures, the amplitude of allowed motions increases leading to a decrease of the lateral bilayer pressure: the hydrophobic and hydrophilic interactions are

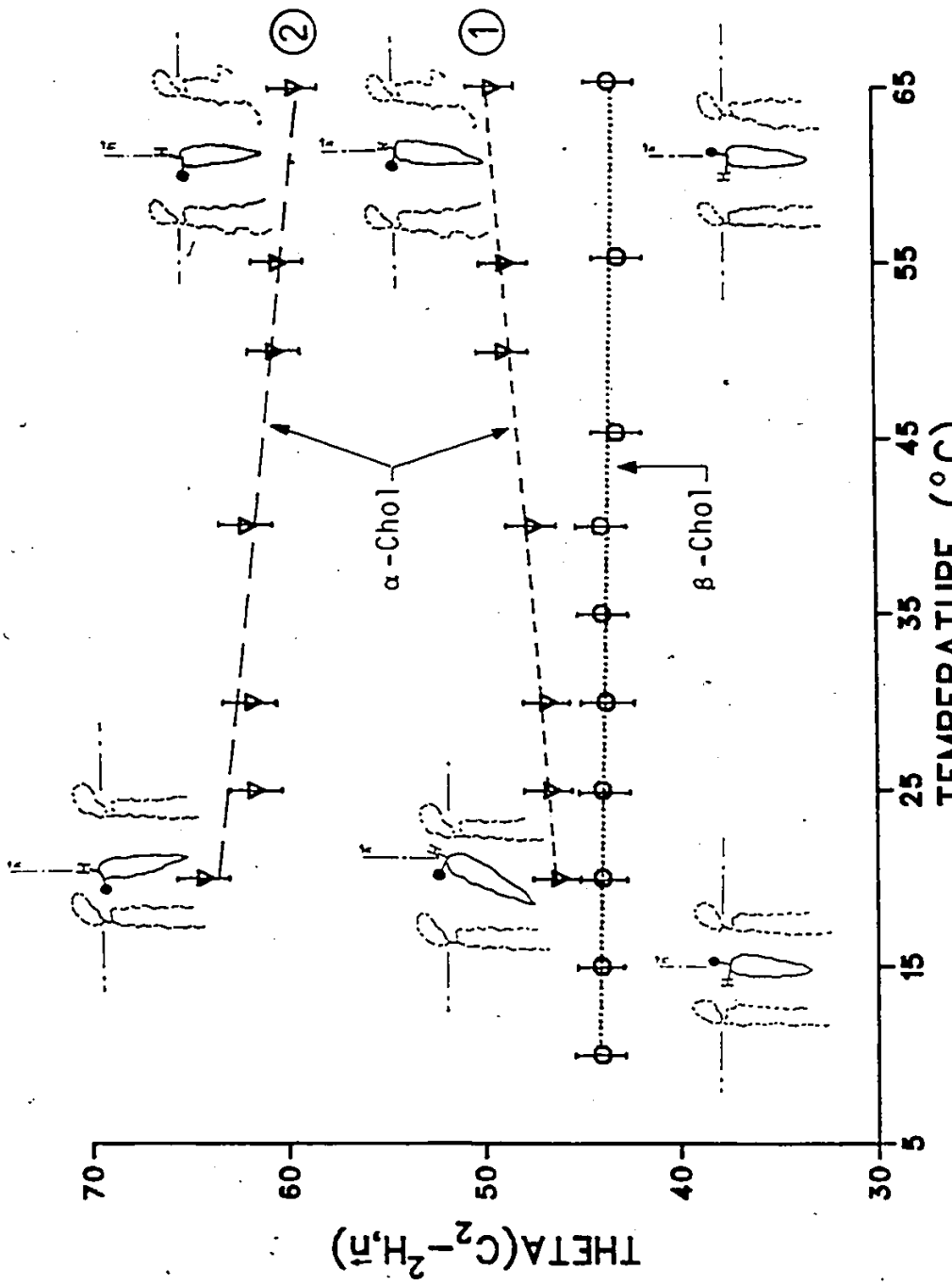

Fig. III.1–10. Temperature dependence of the angle $\theta(C_2-^2H, \vec{n})$ of α– or β–cholesterol in DMPC (3:7). The filled circles represent the OH group in α– or β–position.

therefore less demanding and the α-isomer of cholesterol will tend to align its axis of inertia towards the perpendicular to the bilayer surface (Figure III.1-10).

The above analysis, although approximate and simplistic, brings two remarks. Firstly, a small modification in the structure of cholesterol (OH in α or β) leads to rather important modifications of membrane organization. Secondly, the tilted position of α-cholesterol within the membrane could be the reason that this isomer of cholesterol is not present in natural membranes: it would disturb too much the parallel packing of the lipid chains.

III.1.5c Segmental Order Parameter Temperature Profile for the α-Cholesterol: DMPC System, the Plateau Region

The molecular order parameter of α-cholesterol (4 ring system) in DMPC, S_{mol}^{chol}, has been calculated using the procedure described for β-cholesterol. The results are reported in Figure III.1-11 together with the segmental order parameter of DMPC labeled at C4' with and without α-cholesterol, $S_{mol,chol}^{4'}$ and $S_{mol}^{4'}$, respectively. One notices firstly that α-cholesterol shows disordering-ordering properties similar to those observed for β-cholesterol (Figure III.1-4). It is interesting to compare Figure III.1-4 and Figure III.1-11. One indeed notices a greater temperature dependence of the angular fluctuations of α-cholesterol than

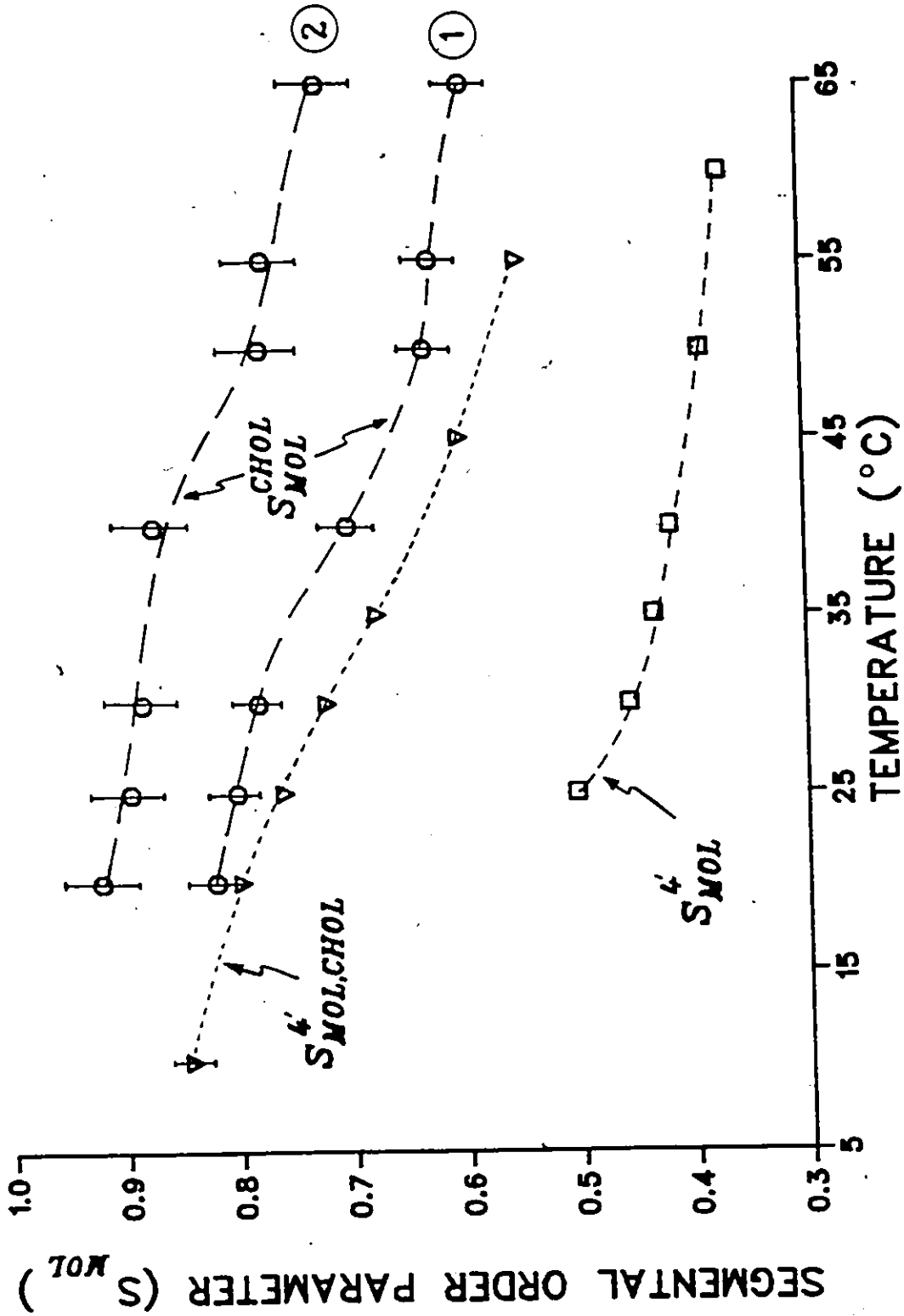

Fig. III.1-11. Temperature dependence of the segmental order parameter, S_{MOL}, in the system α-cholesterol:DMPC (3:7). S^{CHOL}_{MOL} = S_{MOL} of the four rings of cholesterol in DMPC. $S^{4'}_{MOLCHOL}$ = S_{MOL} of DMPC labeled at C4' in the presence of sterol.

$S^{4'}_{MOL}$ = Same as $S^{4'}_{MOLCHOL}$ in the absence of sterol.

was observed for the β-isomer. Unfortunately, the ambiguity of the calculation (see Appendix F) does not allow a choice of which of the S_{mol}^{chol} profiles (according to solutions 1 or 2) is correct. One must therefore postpone discussion of the relative amplitudes of angular fluctuations of α- or β-cholesterol until further experimental evidence is available. However, if one cannot compare the "wobbling" of both isomers, one can nonetheless follow the lipid response. The temperature profile of $S_{mol,chol}^{4'}$ (Figures III.1-4 and III.1-11) indicates that the lipids containing α- or β-cholesterol show almost the same segmental order parameters at low temperatures whereas above T_c, $S_{mol,chol}^{4'}$ is significantly lower in presence of the α-species than with the β-isomer. This observation seems to be general for all the labeled lipid positions since inspection of Tables II and III reveals that the quadrupolar splittings of C14'-labelled DMPC containing α-cholesterol are always lower than those observed in presence of the β-isomer, above T_c. To summarize the comparisons of the ordering capabilities of both isomers, one can state that the α-isomer is also able to regulate the motions of the lipid acyl chains but is less efficient in that role than β-cholesterol, especially at high temperatures. One also notices that the lipid mixed with 30 mole per cent α-cholesterol exhibits the so-called "memory" of its phase transition temperature, as was observed with the DMPC-β-cholesterol system.

III.1.6 Concluding Remarks

Deuterium solid state NMR of mixed systems such as DMPC:cholesterol model membranes is able to distinguish the local order of the various components embedded in the membrane. Such information allows a quantitation of the disordering-ordering effect of cholesterol in model membranes: through the quasi temperature independence of its "wobbling" β-cholesterol induces motion of the lipid acyl chains below T_c, and inhibits them above T_c. Cholesterol thus acts as a regulatory agent by maintaining the bilayer membrane in a liquid crystalline state where motions are axially symmetric and local order is increased, possibly to stabilize further the bilayer membrane against external perturbations such as sudden temperature jumps or high gradients of local pressure. In addition, the side chain of cholesterol has been found to be as ordered as the condensed ring structure. The latter finding completes the picture that the entire cholesterol molecule is a spinning and wobbling cylinder, moderating the angular fluctuations of the lipids, throughout the bilayer thickness.

Analysis of the ^{2}H-NMR observables of the DMPC:α-cholesterol system showed that, at physiological temperatures, the α-isomer of cholesterol makes a tilt with respect to the normal to the bilayer. This tilted configuration has been proposed as one of the reasons that α-cholesterol is not

biosynthesized, arguing that such a molecular tilt would disturb the parallel packing of the lipid chains and thus decrease membrane stability. With regards to the ordering effect of α-cholesterol on membrane lipids it can be concluded, from both the lipid and the cholesterol viewpoints, that the α-isomer, if it were present in natural membranes, would have a disordering-ordering action similar to that found for β-cholesterol. From its action on DMPC, it appears, however, that the α-isomer would be less efficient in this regulatory role than the β-species, especially at high temperatures.

Finally, although there is no indication that a phase transition occurs around 23°C, the segmental order parameter of DMPC shows a marked change in the slope of its temperature dependence around T_c, leading to the conclusion that the lipid has, even in mixed systems, a "memory" of its phase transition temperature. This "memory" was observed with both α- or β-cholesterol:DMPC systems.

A loss of axially symmetric shape of the deuterium powder spectra has been observed at low temperatures (5°C for β-cholesterol:DMPC and 15°C for α-cholesterol:DMPC) but it is difficult to attribute this finding solely to a loss of axially symmetric motions.

On the other hand, the extraordinarily small deuterium quadrupolar splittings observed for the terminal methyl

groups of the cholesterol side chain are not well understood and require further investigation.

REFERENCES TO CHAPTER III.1

Brown, M.F. and Seelig, J. (1978), Biochemistry, 17, 381.

Dahl, J.S., Dahl, C.E. and Bloch, K. (1981), J. Biol. Chem., 256, 87.

Darke, A., Finer, E.G., Flook, A.G. and Phillips, M.C. (1972), J. Mol. Biol., 63, 265.

Davis, J.H. (1979), Biophys. J., 27, 339.

Davis, J.H., Bloom, M., Butler, K.W. and Smith, I.C.P. (1979), Biochim. Biophys. Acta, 597, 477.

Davis, J.H. (1983), Biochim. Biophys. Acta, 737, 117.

Demel, R.A., Bruckdorfer, K.R. and Van Deemen, L.L.M. (1972), Biochim. Biophys. Acta, 255, 321.

DuFourc, E.J., Smith, I.C.P. and Jarrell, H.C. (1983), Chem. Phys. Lipids (in press).

Engel, A.K. and Cowburn, D. (1981), FEBS Lett., 126, 2, 169.

Gally, H.U., Seelig, A. and Seelig, J. (1976), Hoppe-Seyler's Z. Physiol. Chem., 357, 1447.

Gomperts, B. (1977), The Plasma Membrane, Academic Press Inc., London.

Madden, T.D., Chapman, D. and Quinn, P.J. (1979), Nature, 279, 538.

Oldfield, E., Meadows, M., Rice, D. and Jacobs, R. (1978), Biochemistry, 17, 2727.

Parkes, J.G., Watson, H.R., Joyce, A., Phadke, R. and Smith, I.C.P. (1982), Biochim. Biophys. Acta, 691, 24.

Petersen, N.O. and Chan, S.I. (1977), Biochemistry, 16, 12, 2657.

Rothman, J.E. and Engelman, D.M. (1972), Nature New Biol., 42, 237.

Schreier-Muccillo, S., Marsh, D., Dugas, H., Schneider, H. and Smith, I.C.P. (1973), Chem. Phys. Lipids, 10, 11.

Seelig, J. (1977), Quart. Rev. Biophys., 10, 353.

Seelig, J. and Neiderberger, W. (1974), J. Am. Soc., 96, 2069.

Shimshik, E.J. and McConnell, H.M. (1973), Biochemistry, 12, 2551.

Smith, I.C.P. (1971), Chimia, 25, 349.

Stockton, G.W., Polnaszek, C.F., Tulloch, A.P., Hasan, F. and Smith, I.C.P. (1976), Biochemistry, 15, 954.

Stockton, G.W. and Smith, I.C.P. (1976), Chem. Phys. Lipids, 17, 251.

Taylor, M.G., Akiyama, T. and Smith, I.C.P. (1981), Chem. Phys. Lipids, 29, 327.

Taylor, M.G., Akiyama, T., Saitô, H. and Smith, I.C.P. (1982), Chem. Phys. Lipids, 31, 359.

Taylor, M.G., Kelusky, E.C., Smith, I.C.P., Casal, H.L. and Cameron, D.G. (1983), J. Chem. Phys., 78, 5108.

CHAPTER III.2

CHOLESTEROL IN MEMBRANE LIPIDS

2. DYNAMICS

III.2.1 Introduction

As has been widely demonstrated, the amplitude of the C-^{2}H bond fluctuations (as monitored by the ^{2}H-NMR spectral lineshapes) can be related to the local order of a molecular segment (or a molecule) embedded in an anisotropic environment, for example, a biological membrane, thus providing information about membrane organization. ^{2}H-NMR is also capable, in principle, of establishing the characteristic time scales of these fluctuations, through the measurement of relaxation times. For instance, the ^{2}H spin-lattice relaxation rates, $1/T_{1z}$, of DPPC [$^2H_{62}$] (both sn-1 and sn-2 chains perdeuterated) (Davis, 1979) plotted as a function of the labeled chain position, exhibit a profile (especially the plateau of T_1 up to carbons 9 and 10) quasi-identical to that determined previously for the segmental order parameter versus chain position (Seelig and Seelig, 1974). From these relaxation data, Brown (1982) has been able to describe the rates of the lipid motions in terms of fast and slow motional components. The fast motions have been described with a single correlation time, τ_f,

whereas the relatively low frequency motions were modeled by 1) a single effective correlation time, τ_s, or 2) by a distribution of correlation times corresponding to collective fluctuations of the director of molecular ordering.

The main problem when extracting correlation times from relaxation measurements on anisotropic systems resides in separating the rates of motion from the ordering effects. For instance, it can be difficult to obtain the high and low frequency motions of methylene segments in lipid fatty acyl chains from only T_{1z} and the orientational order parameter. One often encounters the situation of more unknowns than equations. However, such a problem can be circumvented when dealing with rigid molecules, for example, cholesterol. Indeed, with enough deuterons on the four-ring structure, it can be expected that the slow and fast motions will be identical for each individual C-^{2}H bond vector, thus allowing a complete solution of the spin-lattice relaxation rate equation (vide infra).

The work presented herein is thus an attempt to describe the cholesterol motions, within a model membrane (DMPC), by making use of the theory derived by Brown (1982) for deuterium spin-lattice relaxation in biological membranes.

III.2.2 Theoretical Background

The models proposed by Brown (1982) were used throughout this study. For clarity, we shall reintroduce the basic definitions and only report the final equations. It is widely recognized that in model membranes and above T_c (the gel-to-liquid crystalline phase transition temperature) the molecular motions are axially symmetric. It is therefore assumed that in each subaxis system of Figure III.2-1*, the motions do possess axial symmetry. Figure III.2-1 shows the coordinate frames needed to describe the various motions: the transformations from one axis system to another are accomplished using second rank Wigner rotation matrices. One thus relates the local segmental motions to the laboratory axis system by four subsequent transformations: 1) a first transformation from the efg axis system, whose z-axis is aligned along the C-^{2}H bond, to the molecular system of the rotational diffusion tensor D(t), followed by, 2) a transformation from D(t) to the instantaneous director axis system n(t), followed by 3) a transformation from n(t) to the average director axis system n_0 (this third transformation allows small director fluctuations) and followed by 4) a final transformation

* Same notations as employed by Brown (1982).

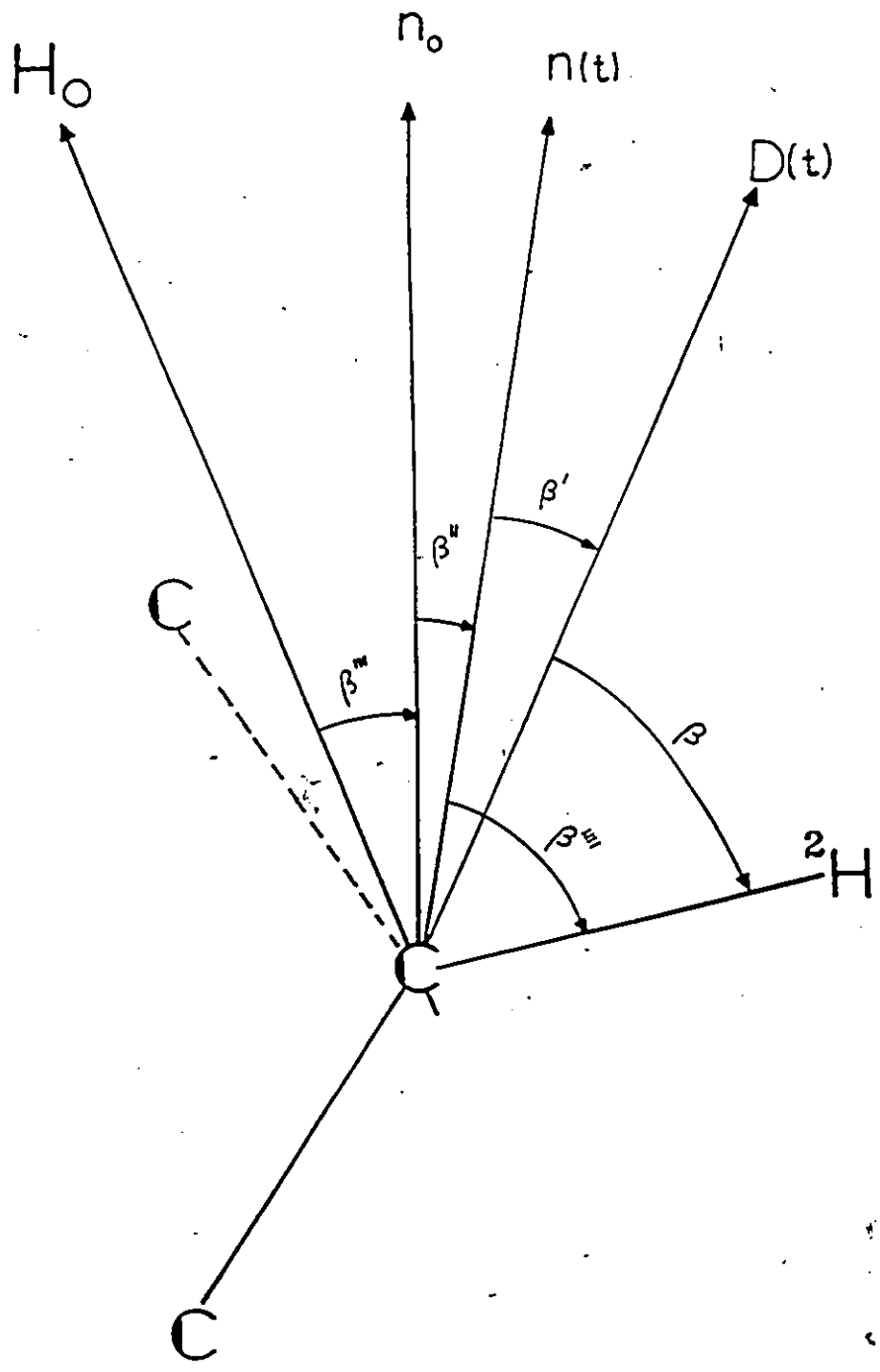

Fig. III.2–1. Angles for describing deuterium spin–lattice relaxation phenomena in lamellar liquid crystalline phases (from Brown, 1982).

from n_0 to the laboratory frame of reference (linked to H_0). According to Brown, we can distinguish 3 cases: i) relaxation due to fast motions, ii) relaxation due to both fast and slow motions, using a non-collective model for slow motions, and iii) relaxation due to fast and slow motions, using a collective model for slow motions. It has been found that in lamellar liquid crystalline phases, T_{1z} is orientationally independent (Brown & Davis, 1981); henceforth the spin-lattice relaxation rate measured in the laboratory axis system can thus be expressed in these three cases as follows:

i) Relaxation due to fast motions, $\frac{1}{T_{1z}} = \frac{1}{T_{1z\underline{f}}}$

$$1/T_{1z} = \frac{3}{80}(2\pi)^2 A_Q^2 \{(1-S^2)(j_{\underline{f}}(\omega_0) + 4j_{\underline{f}}(2\omega_0))\} \quad \text{(III.2.1)}$$

where $A_Q = \frac{e^2qQ}{h}$ is the deuterium quadrupolar coupling constant (A_Q = 170 kHz and 175 kHz for $-C-^2H_2$ and $=C-^2H$ segments, respectively (Seelig, 1977)). In Equation (III.2.1) $S = \mathcal{D}_{0,0}(\beta'''';\ t)$ is the observed S_{C-^2H} order parameter and $j_{\underline{f}}(p\omega_0) = 2\tau_{\underline{f}}/(1 + (p\omega_0)^2\tau_{\underline{f}}^2)$.

ii) Relaxation due to fast and slow motions, $\frac{1}{T_{1z}} = \frac{1}{T_{1z\underline{f}}} + \frac{1}{T_{1z\underline{s}}}$

The Non-collective Model

$$1/T_{1zf} = \frac{3}{80} (2\pi)^2 A_Q^2 \{(1-S^2/x^2)(j_f(\omega_0) + 4j_f(2\omega_0))\} \qquad \text{(III.2.2a)}$$

$$1/T_{1zs} = \frac{3}{80} (2\pi)^2 A_Q^2 \{\frac{S^2}{x^2}[(1-x^2)(j_s(\omega_0) + 4j_s(2\omega_0))]\} \qquad \text{(III.2.2b)}$$

where $S = \mathcal{D}_{0,0}(\beta''; t).\mathcal{D}_{0,0}(\beta''''; t)$ is now the new observed S_{C-2_H} order parameter and $x = \mathcal{D}_{0,0}(\beta''; t)$. One allows here the director fluctuations (monitored by β''), assuming that this slow motion can be described by a single correlation time τ_s (non-collective model). This assumption implies that the slow frequency motions can be viewed as "rigid body" angular displacements.

iii) Relaxation due to fast and slow motions, $\frac{1}{T_{1z}} = \frac{1}{T_{1zf}} + \frac{1}{T_{1zs}}$

The Collective Model

$$1/T_{1zf} = \frac{3}{80} (2\pi)^2 A_Q^2 \{(1-S^2)(j_f(\omega_0) + 4j_f(2\omega_0))\} \qquad \text{(III.2.3a)}$$

$$1/T_{1zs} = \frac{9}{80} (1 + 2\sqrt{2}) (2\pi)^2 A_Q^2 S^2 C\omega_0^{-\frac{1}{2}} \qquad \text{(III.2.3b)}$$

where $S = \mathcal{D}_{0,0}(\beta''''; t) = \mathcal{D}_{0,0}(\beta'; t).\mathcal{D}_{0,0}(\beta)$ is the observed S_{C-2_H} order parameter. C is a parameter related to the elastic constant of the bilayer, K, ($C = \frac{kT}{\pi K^{3/2}} \sqrt{\frac{\eta}{2}}$) (see Brown

(1982) for details). The assumption that the director reorientations were of small amplitude was made to calculate Equation (III.2.3), that is, $x^2 = \mathcal{D}_{0,0}(\beta''; t)^2 \simeq 1$. In addition, it was assumed that only $j_s(\omega_0)$ were contributing to the relaxation frequency dependence (Vold, et al., 1980). The collective model to describe low frequency motions does not provide a single correlation time, but rather a distribution of correlation times, τ_q ($\tau_q^{-1} = Kq^2/\eta$, where η is the viscosity and q the qth mode, see Brown (1982) and de Gennes (1974) for details).

III.2.3 Results

The spin-lattice relaxation times of [2,2,3,4,4, 6-$^2H_6$]-α- and β-cholesterol in DMPC (3:7) were measured by the inversion-recovery technique. Figure III.2-2 shows as an example a stacked plot of deuterated β-cholesterol powder patterns resulting from the inversion recovery experiment. While dealing with multiple powder patterns, that is, a superposition of powder spectra due to the presence of different deuterons, it is difficult to extract accurately the T_{1z} of each deuterium atom. If the T_{1z} of the individual deuterons are quite different in magnitude, a straight estimation of the spin-lattice relaxation times from the peak intensity of each powder pattern would lead to erroneous

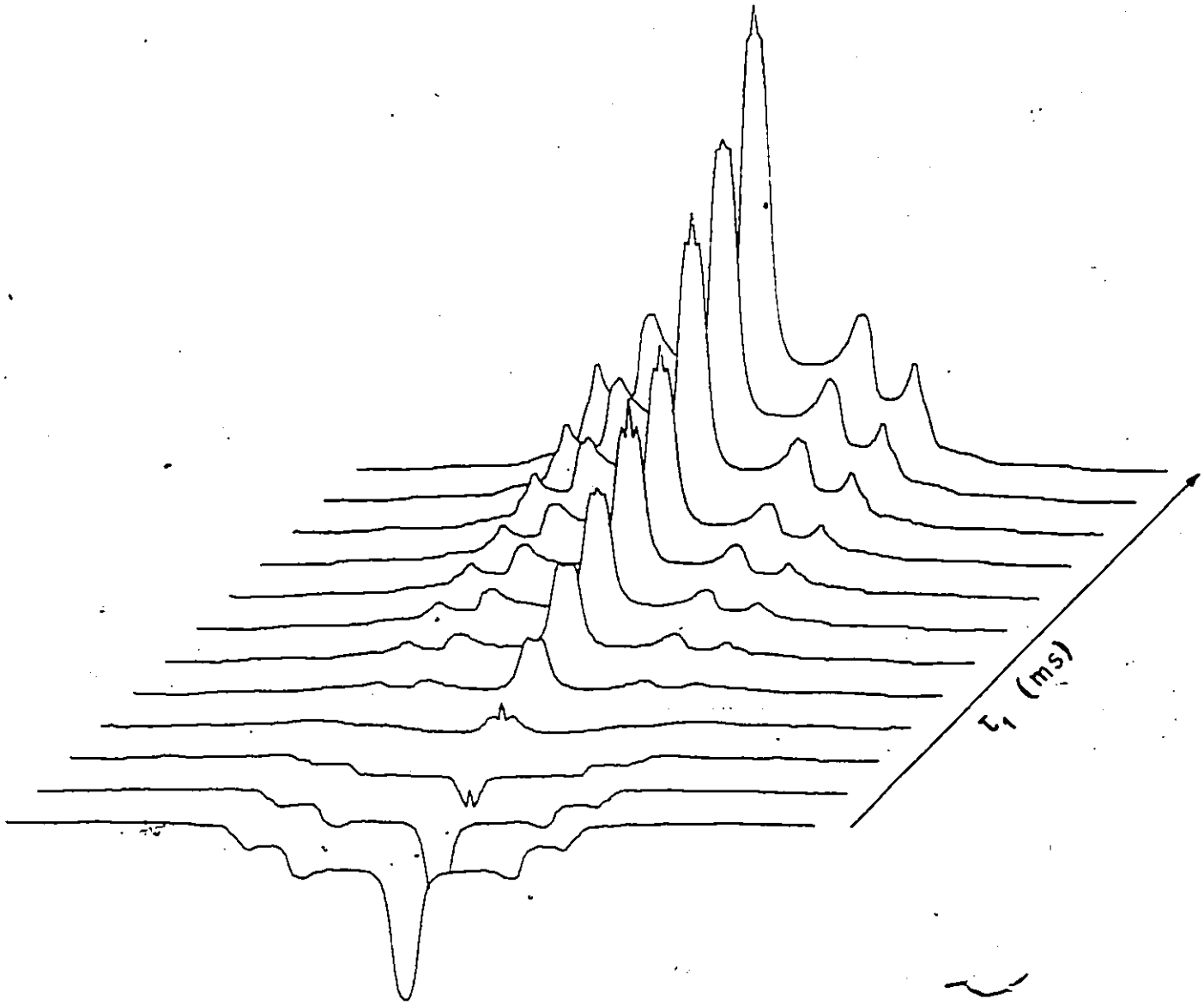

Fig. III.2–2. Stacked plot of spectra resulting from the inversion–recovery experiment for measuring T_{1z} of $[2,2,3,4,4,6-{}^2H_6]\,\beta$ –cholesterol in DMPC (3:7) molar ratio Same experimental parameters as in Fig. III.1–2.

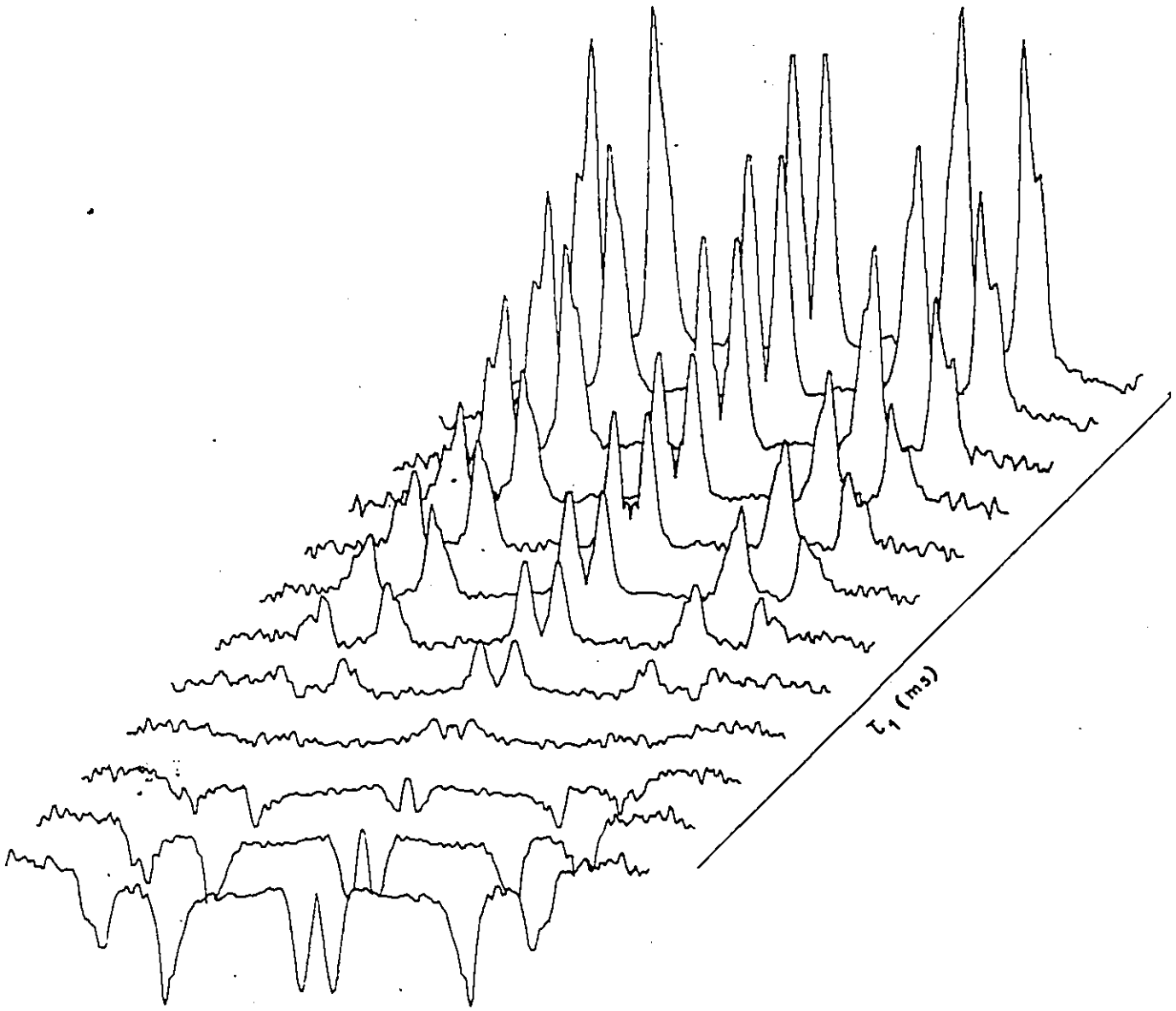

Fig. III.2-3. Same as Fig. III.2-2, but each subspectrum was dePaked using the same processing parameters as in Fig. III.1-3.

values of T_{1z} (the estimated peak intensity is the result of the weighted intensities of all the overlapping powder patterns). Therefore, one must dePake the entire set of powder patterns arising from the inversion-recovery experiment (Figure III.2-3). In order to use the dePaking algorithm in a correct fashion, the T_{1z} of a given powder pattern must not change across the powder pattern, that is, the T_{1z} for a given deuteron has to be orientationally independent. Such a situation appears, however, quite often in model membrane systems, for example, non-sonicated DPPC multilayers (Brown & Davis, 1981) or PDSPC lamellar dispersions (Dufourc, et al., to be published), and was assumed to occur also in the cholesterol:DMPC system. The peaks of each dePaked spectrum were integrated and the resulting area fitted to the equation: $M(\tau_1) = M_0 \ (1-A\exp\{-\tau_1/T_{1z}\})$ where $M(\tau_1)$ and M_0 represent the longitudinal magnetization at times τ_1 and at the equilibrium ($\tau_1 = \infty$), respectively, and where A is an adjustable parameter to account for imperfections of the 180° inverting pulse. Spin-lattice relaxation times were thus estimated at various temperatures for β- and α-cholesterol (Table III.2-1). Figure III.2-4 shows the T_{1z} temperature variation for some deuterons of the β-cholesterol four-ring structure: one clearly notices that although those deuterons exhibit different T_{1z}, they have the same behaviour in temperature, that is, they all show a minimum at around

Table III.2-1

SPIN-LATTICE RELAXATION TIMES[a] OF α- AND β-CHOLESTEROLS AT 46.1 MHz

Temperature (°C)	System β-cholesterol	Labeled Carbon Position				
		$[3\text{-}^2H]^c$	$[2,4\text{-}^2H_2]_{ax}$	$[4\text{-}^2H]_{eq}$	$[2\text{-}^2H]_{eq}$	$[6\text{-}^2H_2]$
15	T_{1z}	6.9	7.6	6.0	6.2	5.0
	$\lvert S_{C\text{-}^2H}\rvert$	0.409	0.384	0.253	0.271	0.030
25	T_{1z}	5.8	6.3	4.7	4.7	3.7
	$\lvert S_{C\text{-}^2H}\rvert$	0.409	0.378	0.251	0.268	0.027
35	T_{1z}	6.6	5.8	4.2	4.3	3.2
	$\lvert S_{C\text{-}^2H}\rvert$	0.400	0.372	0.248	0.265	0.026
50	T_{1z}	10.0	8.8	6.0	6.0	4.5
	$\lvert S_{C\text{-}^2H}\rvert$	0.379	0.355	0.250	0.250	0.019
60	T_{1z}	13.8	12.1	7.6	7.6	5.6
	$\lvert S_{C\text{-}^2H}\rvert$	0.375	0.347	0.244	0.244	0.018
	α-cholesterol					
25	T_{1z}		6.4	4.6	4.6	3.5
	$\lvert S_{C\text{-}^2H}\rvert$		0.434	0.195	0.195	0.046

[a] In ms. accuracy on T_{1z} ~5%.
[b] Accuracy on $\lvert S_{C\text{-}^2H}\rvert$ ~2-3%.
[c] Accuracy on T_{1z} ~10%.

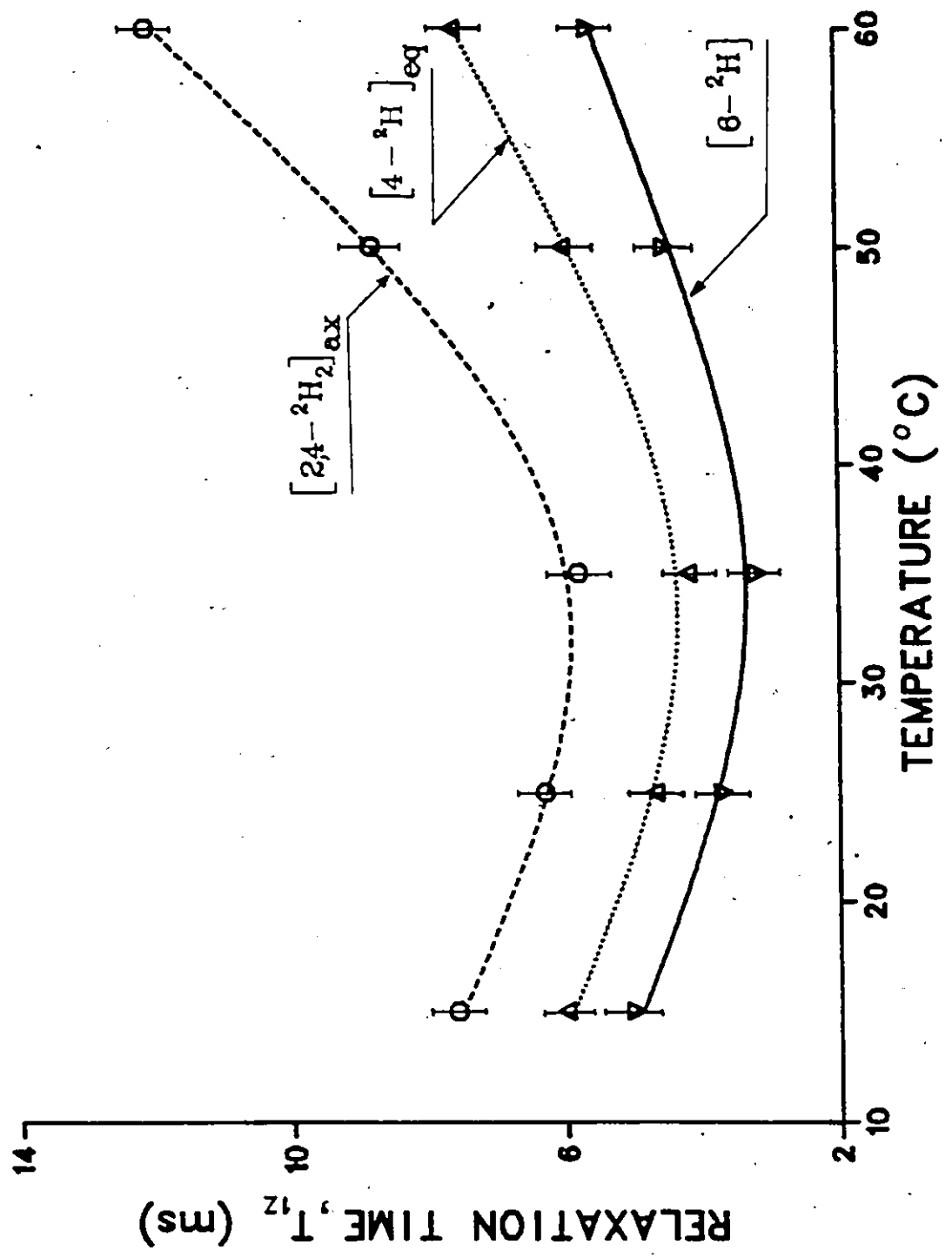

Fig. III.2–4. Temperature dependence of T_{12} of β-cholesterol in DMPC (3:7) at the indicated labeled positions. The bars give an estimate of the error.

32-35°C. This is an indication that they possess similar rates of motion. The minimum in T_{1z} indicates that the effective correlation time is $\tau_{eff} = \frac{1}{p\omega_0}$, that is, $\tau_{eff} = 3.45 \times 10^{-9}$s or $\tau_{eff} = 1.73 \times 10^{-9}$s depending whether $j(\omega_0)$ or $j(2\omega_0)$ dominate the rate of relaxation. It is also interesting to plot the rate of relaxation as a function of $S^2_{C-2_H}$ (Figure III.2.5). Indeed, one remarks that the spin-lattice relaxation rate is a linear function of $S^2_{C-2_H}$ for temperatures between 15°C and 60°C. The extrapolation to $S^2_{C-2_H} = 0$ leads to relaxation rates of 195 s^{-1}, 300 s^{-1} and 180 s^{-1} at 15°C, 35°C and 60°C, respectively. It is also interesting to notice that the relaxation rate increases when S_{C-2_H} decreases; the converse was found for DPPC bilayers (Brown, 1982).

III.2.4 Discussion

The values of τ_{eff}, obtained from the minimum in T_{1z} still correspond to rather rapid motions. The problem now arises to determine whether this minimum gives the value of τ_f or a combination of τ_f and τ_s (in the case where one can depict the motions with two distinct correlation times). These two possibilities are discussed below.

Assuming that the minimum corresponds to the fast motions, $\tau_{eff} = \tau_f$, at ~35°C $(p\omega_0)^2\tau_f^2 = 1$ and $j_f(p\omega_0) = \tau_f$.

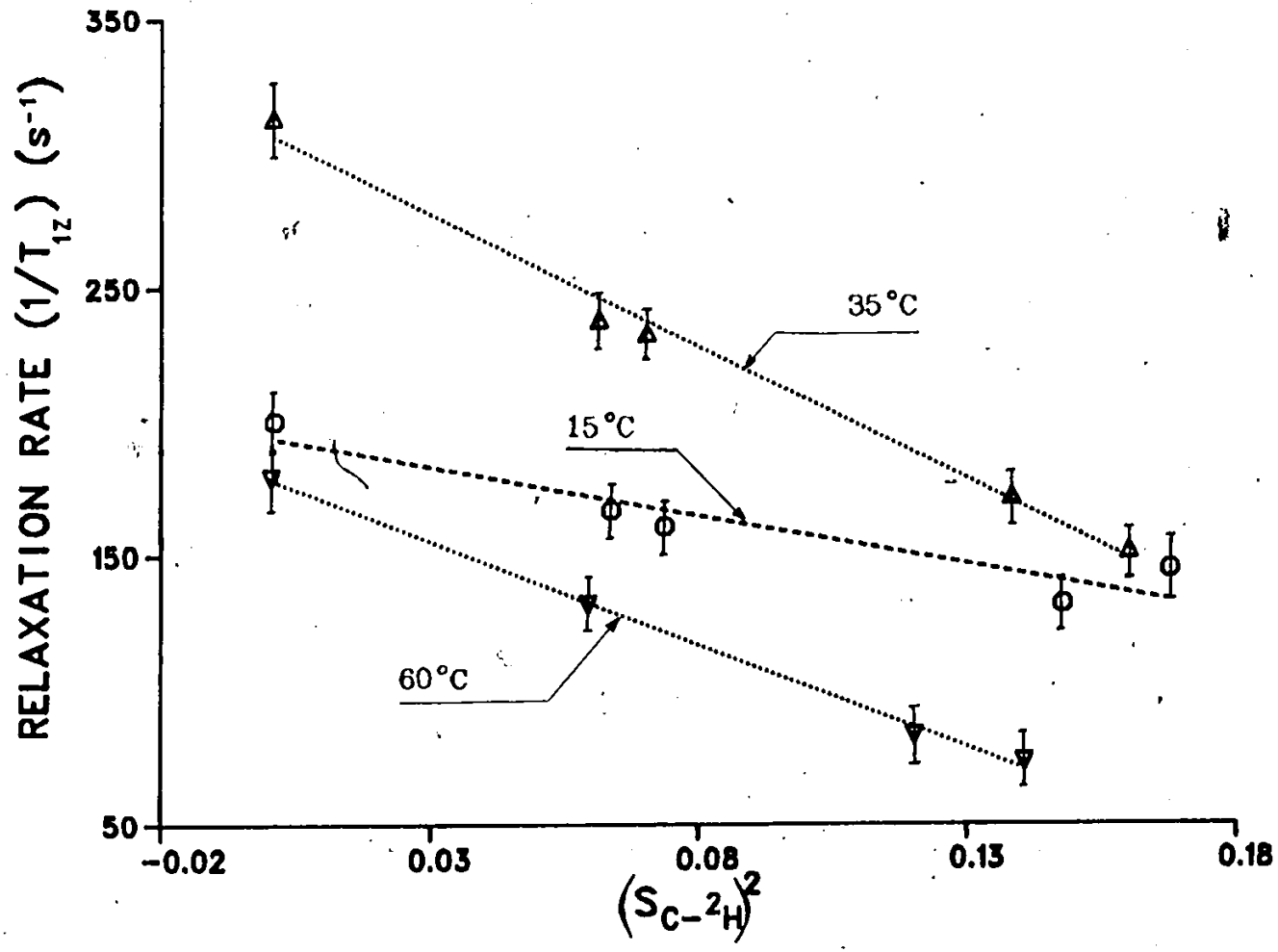

Fig. III.2–5. Variation of the relaxation rate $(1/T_{1z})$ as a function of $S^2_{C-^2H}$. A least squares linear regression was applied to the data points corresponding to a given temperature. The bars give an estimate of the error.

Equations (III.2.1), (III.2.2) and (III.2.3) thus transform to:

$$\text{i)} \quad \frac{1}{T_{1z}} = A(1-S^2)\tau_{\underline{f}} \qquad \text{(III.2.4)}$$

$$\text{ii)} \quad \frac{1}{T_{1z}} = A\{(1-S^2/x^2)\tau_{\underline{f}} + \frac{S^2}{x^2}(1-x^2)\frac{4}{5\omega_0^2\tau_{\underline{s}}}\} \qquad \text{(III.2.5)}$$

$$\text{iii)} \quad \frac{1}{T_{1z}} = A(1-S^2)\tau_{\underline{f}} + BS^2C\omega_0^{-\frac{1}{2}} \qquad \text{(III.2.6)}$$

where $A = \frac{3}{16}(2\pi)^2A_Q^2$ and $B = \frac{9}{80}(1 + 2\sqrt{2})(2\pi)^2A_Q^2$. In Equation (III.2.5) the slow motions were assumed to occur in the long correlation time limit, that is, $(p\omega_0)^2\tau_{\underline{s}}^2 >> 1$, hence $j(p\omega_0) = 2/(p\omega_0)^2\tau_{\underline{s}}$. The three models i), ii) and iii) yield for $S^2 = 0$ $\tau_{\underline{f}} = 1.40 \pm 0.05\ 10^{-9}$s, at 35°C. Such a value of $\tau_{\underline{f}}$ is lower than the calculated τ_{eff} from the minimum in T_{1z}. It appears therefore that the observed minimum is not solely due to the fast motions but is rather a mixture of fast and slow motions. Brown (1982) showed that the two minima observed for fast and slow motions were progressively transformed to one minimum when the ordering of the system was increased. It has already been shown that the molecular order parameter of β-cholesterol at 35°C is ~0.8 in the DMPC:β-cholesterol system (7:3) (Dufourc, et al., to be published) and therefore it is not surprising that such a situation occurs here.

Assuming* now that the fast motions are in the short correlation time limit, that is, $(p\omega_0)^2\tau_f^2 << 1$ hence $j(p\omega_0) = 2\tau_f$, and that the slow motions are still in the long correlation time limit, Equations (III.2.1), (III.2.2) and (III.2.3) transform to, at 35°C:

$$\text{i)} \quad \frac{1}{T_{1z}} = A(1-S^2)2\tau_f \qquad \text{(III.2.7)}$$

$$\text{ii)} \quad \frac{1}{T_{1z}} = A\{(1-S^2/x^2)2\tau_f + \frac{S^2}{x^2}(1-x^2)\frac{4}{5\omega_0^2\tau_s}\} \qquad \text{(III.2.8)}$$

$$\text{iii)} \quad \frac{1}{T_{1z}} = A(1-S^2)2\tau_f + B\,S^2C\omega_0^{-\frac{1}{2}} \qquad \text{(III.2.9)}$$

In the limiting case of no order ($S^2 = 0$), Equations (III.2.7), (III.2.8) and (III.2.9) lead to $\tau_f = 7.0 \pm 0.3 \times 10^{-10}$s, at 35°C. When $S_{C-2_H} \neq 0$, Equation (III.2.7) is trivially solved and Equations (III.2.8) and (III.2.9) are also easily solved since one has a maximum of three unknowns and 5 T_{1z} with their corresponding S_{C-2_H} order parameters (Table III.2-1). The unknowns are τ_f, x and τ_s for the non-collective model, ii) and τ_f and C for the collective model, iii). Table III.2-2 summarizes the results. The model including only fast motions does not give a correct answer: τ_f varies indeed with the S_{C-2_H} order parameter. Conversely, the two models including slow motions lead to a value of τ_f very close to that obtained by extrapolation to zero ordering, that is $7.0 \pm 0.3 \times 10^{-10}$s.

* See note added in proof, p. 219.

This is however not surprising since τ_f has been obtained by solving either Equations (III.2.8) or (III.2.9) by pairs (using 2 T_{1z} values). The non-collective model leads to a value of τ_s of 1.0×10^{-8}s which is higher than τ_f by about one order of magnitude but which represents slow motions that are not 'too slow'. Furthermore, the value $x^2 = (\frac{3\cos^2 \beta"(t)-1}{2})^2$ leads to an angle $\beta"(t)$ of ca. 40° which indicates that the director fluctuations are of quite large amplitude. One may therefore question whether the non-collective model describes the "small" director fluctuations in a correct fashion. The collective model (Equation III.2.9) does not provide a single correlation time but can however lead to the parameter C which is linked to the distribution of correlation times and to the elastic constant of the bilayer. Table III.2-2 shows that when using Equation III.2.9 one obtains a negative value of C. Such a result would imply a negative elastic constant which is not realistic. However, it has to be remembered that Equation (III.2.9) has been derived assuming that $(\mathcal{D}_{0,0}(\beta", t))^2 = x^2 = 1$. One may rewrite this equation including the finite director fluctuations:

$$\frac{1}{T_{1z}} = A(1-S^2/x^2)\tau_f + B\, S^2(\frac{1}{x^2} - 1)C'\omega_0^{-\frac{1}{2}} \qquad \text{(III.2.10)}$$

Table III.2-2

CALCULATION OF CORRELATION TIMES
FOR β-CHOLESTEROL IN DMPC AT 35°C

	Fast Motions (Equation (III.2.7))	Slow and Fast Motions[c]	
		Non-Collective (Equation (III.2.8))	Collective (Equations (III.2.9,10))
τ_f	$4.2 - 7.3 \times 10^{-10}$ s	$6.9 \pm 0.2 \times 10^{-10}$ s	$6.9 \pm 0.2 \times 10^{-10}$ s
τ_s		$1.0 \pm 0.2 \times 10^{-8}$ s	
x^2		0.138	0.138[b]
C^a			$\sim 2 \times 10^{-5}$ $s^{\frac{1}{2}}$
C'^b			$\sim 7 \times 10^{-6}$ $s^{\frac{1}{2}}$

[a] Calculated from Equation (III.2.9).
[b] Calculated from Equation (III.2.10).
[c] The numerical values obtained using the non-collective and collective models represent an average and were calculated from all T_{1z} of β-cholesterol in DMPC at 35°C (Table III.2-1).

Using Equation (III.2.10) one obtains then the same value of τ_f, that is, 6.9×10^{10} s and a positive value of C' (Table III.2-2). However, the validity of C' is difficult to check since there are little data available on bilayer elastic constants. By means of Equation (III.2.10) one finds the same value of x^2 as for the non-collective model and one may question again the assumption of director fluctuations of only small angles.

In order to estimate the relative contributions of the slow and fast motional components in the spin-lattice relaxation rate, one needs to calculate $1/T_{1zf}$ and $1/T_{1zs}$ (Table III.2-3). From the values of Table (III.2-3) one notices that depending on x^2, $1/T_{1zf}$ is either positive or negative when using Equations (III.2.8) and (III.2.10). The rate of relaxation by fast motions, $1/T_{1zf}$ is very sensitive to x^2; for instance, if $x^2 > 0.16$, all the $1/T_{1zf}$ values in Table III.2-3, according to Equations (III.2.8) and (III.2.10), would be positive. The negative values might simply arise from the inaccuracy of the experiment. As a general remark it appears that $1/T_{1z} \gtrsim 1/T_{1zf}$ and therefore a slow motional component exists. One notices that the relative slow contribution is not a constant for all deuterons, that is, it is dominant for [3-^{2}H] and [2,4-$^2H_2$] positions and negligible at [6-^{2}H]. This behaviour might be understood by considering the geometrical orientation of each C-^{2}H bond vector with respect to the average director, in

Table III.2-3

RATES OF RELAXATION[a] OF β-CHOLESTEROL IN DMPC AT 35°C

	$1/T_{1z}$ [b]	$1/T_{1zf}$ [d] Equation (III.2.8)	Equation (III.2.9)	Equation (III.2.10)	β [c]
[3-^{2}H]	152	- 47	248	- 47	85°
[2,4-$^2H_2$]$_{ax}$	172	- 1	254	- 1	82°
[4-^{2}H]$_{eq}$ [e]	238	164	277	164	42°
[2-^{2}H]$_{eq}$ [e]	233	145	275	145	71°
[6-^{2}H]	313	311	313	311	53°

[a] In s^{-1}.
[b] Experimental value.
[c] Calculated from $S_{C-^2H} = S_{\beta'} = S_{\beta}$, with $S_{\beta'} = 0.78$ at 35°C. (From Chapter III.1, using the following notations: $S_{\beta'} = S_{mol}$ and S_{γ}. The angles α and γ are those of Figure II.1-2).
[d] Calculated from Equations (III.2.8), (III.2.9) and (III.2.10) (see text).
[e] The assignment of these positions is arbitrary and could be reversed.

the absence of motion (angle β, Table III.2-3). A given director fluctuation will not have the same efficiency on a C-^{2}H bond oriented at 90° or at the magic angle with respect to n_0. In order to obtain the average contribution of the fast motions the director fluctuations would have to be related to the average orientation of the individual C-^{2}H bonds with respect to n_0. One also notices that Equation (III.2.9) leads $1/T_{1z\underline{f}} \geq 1/T_{1z}$. Such a result would imply the slow motional component to be negative; one can therefore conclude that, in the case of cholesterol, Equation (III.2.9) does not provide a good description of the spin-lattice relaxation rate and must be replaced by Equation (III.2.10).

From what has been discussed above, one notices that the mean relative contribution of the fast and slow components cannot be obtained from $1/T_{1z\underline{f}}$ and $1/T_{1z\underline{s}}$. However, assuming that the non-collective model gives a good enough approximation of the slow and fast correlation times and assuming that:

$$\frac{1}{\tau_{eff}} = \frac{1-a}{\tau_{\underline{f}}} + \frac{a}{\tau_{\underline{s}}} , \qquad \text{(III.2.11)}$$

the relative mean contribution of the fast and slow motional component may be calculated. In order to have 1.73×10^{-9} s $\leq \tau_{eff} \leq 3.45 \times 10^{-9}$ s, the weighting factor has to be such

that $0.65 \leq a \leq 0.84$. This finding would imply that the slow motional component dominates the spin-lattice relaxation of cholesterol in model membranes.

Equations (III.2.8) and (III.2.10) led to plausible answers, but it is not possible, based on the present data, to decide between these non-collective and collective models, respectively. However, one notices that the non-collective model has a ω_0^{-2} dependence, whereas the collective model predicts that $1/T_{1zs}$ varies as a function of $\omega_0^{-\frac{1}{2}}$. Therefore, in order to choose between the two models, another T_{1z} experiment is needed, using at least one different value of the magnetic field.

III.2.5 Concluding Remarks

The presence of a minimum, at 35°C, in the temperature dependence of T_{1z} of deuterated cholesterol in the β-cholesterol:DMPC system led to an effective correlation time between 1.73×10^{-9} s and 3.45×10^{-9} s. From the 6 deuterium labels on the four-ring structure of β-cholesterol, the plot of $1/T_{1z}$ *versus* $S^2_{C-2_H}$ showed that the rate of relaxation decreases linearly with increasing $S^2_{C-2_H}$.

These experimental data have been analyzed in terms of fast and slow motions according to the models proposed by Brown (1982). A plausible description of these motions has

been obtained with both the non-collective and the modified collective model (using finite and non-negligible director fluctuations, Equation (III.2.10)). Both models gave a value of the fast correlation time, τ_f, of 6.9×10^{-10} s. The non-collective model led to a τ_s, the correlation time of the slow motions, of 1×10^{-8} s whereas the collective model led to a value of the parameter C of about 7.10^{-6} $s^{\frac{1}{2}}$. From the value of τ_f and τ_s, and from the order of magnitude of τ_{eff}, the non-collective model was able to predict that the slow motions contributed for 65-84% to the effective motional correlation time.

However, these findings have to be tempered with the following remarks:

- the director fluctuations were found to be of quite large amplitude (β"; t) = 40^{o});
- the effect of the director fluctuations was perceived differently by each deuterium atom.

The latter remark is of importance since it means that $1/T_{1zf}$ varies according to the orientation of a given C-^{2}H bond with respect to the average director, n_0. Although giving a good enough idea of the magnitude of the motions, both the collective and the non-collective models fail in relating the

director fluctuations to the average orientation of a C-^{2}H bond vector with respect to n_0. One indeed believes that, since the deuterons of the four-ring cholesterol skeleton possess the same molecular order parameter, and since T_{1z} is orientationally independent, all T_{1z} should be equal (except those whose A_Q is different). The observed differences in T_{1z} might therefore be due to director fluctuations whose effect is determined by the orientation of the individual C-^{2}H bonds with respect to n_0. However, the derivation of such a model is out of the scope of this study and will not be presented herein.

Note added in proof:

Further experimental data led to the evidence that the minimum observed for cholesterol at 35°C is due to fast motions in contrast to what has been assumed on p. 211 and ff. (Dufourc and Smith, to be published).

REFERENCES TO CHAPTER III.2

Brown, M.F. (1982), J. Chem. Phys., 77, 1576.

Brown, M.F. and Davis, J.H. (1981), Chem. Phys. Lett., 79 431.

Davis, J.H. (1979), Biophys. J., 27, 339.

de Gennes, P.G. (1974), The Physics of Liquid Crystals, (Oxford University, London).

Seelig, J. (1977), Quart. Rev. Biophys., 10, 353.

Seelig, A. and Seelig, J. (1974), Biochemistry, 13, 23, 4839.

Vold, R.L., Vold, R.R., Poupko, R. and Bodenhausen, G. (1980), J. Magn. Reson., 38, 141.

PART IV

AMPHOTERICIN B AND MODEL MEMBRANES

CHAPTER IV.1

AMPHOTERICIN B AND MODEL MEMBRANES

1. GENERALITIES

IV.1.1 Introduction

In 1950, Hazen and Brown discovered a compound, Nystatin, which belonged to a new class of antibiotics. The distinguishing feature of this class of antibiotics was the observation that they had no effect on bacteria but were toxic to fungi (Hazen & Brown, 1951). Since that time, 70 other compounds have been isolated and identified as belonging to the similar structural class of antibiotics: the polyene antibiotics. The purpose of this section is to review the structure and chemistry of the class of polyene antibiotics, discuss that biological action on natural and real membranes and present the models currently proposed to describe the mechanism of their action. It will be finally shown which strategy will be used to possibly characterize these models by ^{2}H-NMR.

IV.1.2 Structures and Chemical Properties of Polyene Antibiotics

All the polyene antibiotics (P.A.) are characterized by having intense ultraviolet (UV) absorption spectra. The

chromophores responsible for this absorption have been unequivocally identified as conjugated double bonds (hence "polyene") (Figure IV.1-1). In addition to this conjugated double bond system, the P.A. are characterized by a large ring of carbon atoms (12-14 up to 35-37 carbon atoms; Norman, et al., 1976) whose closure is effected by the formation of an internal ester. The ring contains a hydrophilic zone due to the presence of an array of hydroxyl groups. Some P.A. may also possess glycosyl and charged groups, for example, Amphotericin B (Ampho B) and Nystatin. Inspection of the structures given in Figure IV.1-1 reveals that the hydrophilic and hydrophobic components provide an amphiphatic character to these macrolide rings. It is not surprising, therefore, that the P.A. will show limited solubility in both water and weakly polar organic solvents such as alcohols esters or ethers. In contrast, they may be dissolved in very polar organic solvents such as dimethylformamide or dimethylsulfoxide. Among all the P.A., Amphotericin B is the only polyene antibiotic for which both chemical structure and absolute configuration are known (Mechlinski, et al., 1970 and Ganis, et al., 1971).

IV.1.3 Action of P.A. on Natural and Model Membranes

In the early 1960s, evidence was found that P.A. could mediate a change in the cellular permeability of a

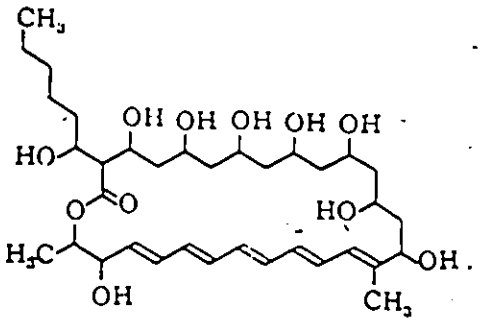

Filipin

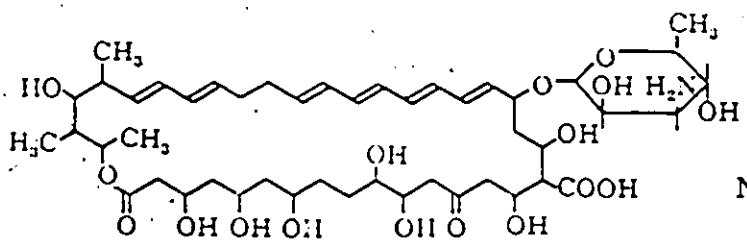

Nystatin

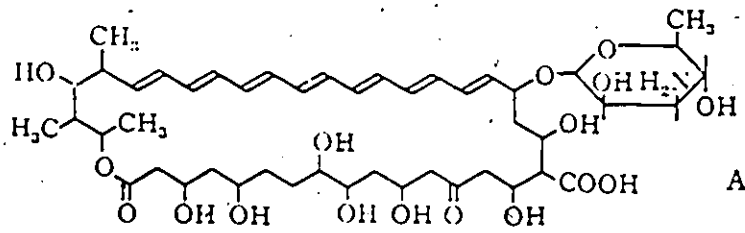

Amphotericin B

Fig. IV.1–1. Structure of the polyene antibiotics Filipin, Nystatin, and Amphotericin B (from Gomperts, 1977).

number of organisms, thus promoting a leakage of important cellular constituents and ultimately lysis and death of the cell (Kinsky, 1961, a,b). Since the plasma membrane is the structural unit of the cell responsible for the maintenance of cell permeability, it is a likely candidate for the site of action for the P.A. Gottlieb and coworkers (1958, 1961) found that the addition of sterols to the growth media of Saccharomyces cerevisiae prevented the characteristic Filipin-induced growth inhibition and permeability changes. Lampen, et al. (1962) were able to demonstrate a correlation between the binding of Nystatin to subcellular fractions of Saccharomyces cerevisiae and the sterol content of the particular fraction. These results led to the hypothesis that there was a physical-chemical interaction between the sterol and the polyene. Studies on model membranes allowed a better understanding of this interaction (Andreoli, 1973; de Kruijff, et al., 1974 a,b; de Kruijff and Demel, 1974; for a review see Norman, et al., 1976). Figure IV.1-2 shows the effect of Filipin and Ampho B on the release of K^+ and glucose from liposomes prepared with and without cholesterol. One notices that the presence of cholesterol is essential to the change in permeability induced by addition of the polyene. It is well known that the presence of cholesterol in liposomes composed of a single phospholipid species obliterates the gel to liquid-crystalline phase

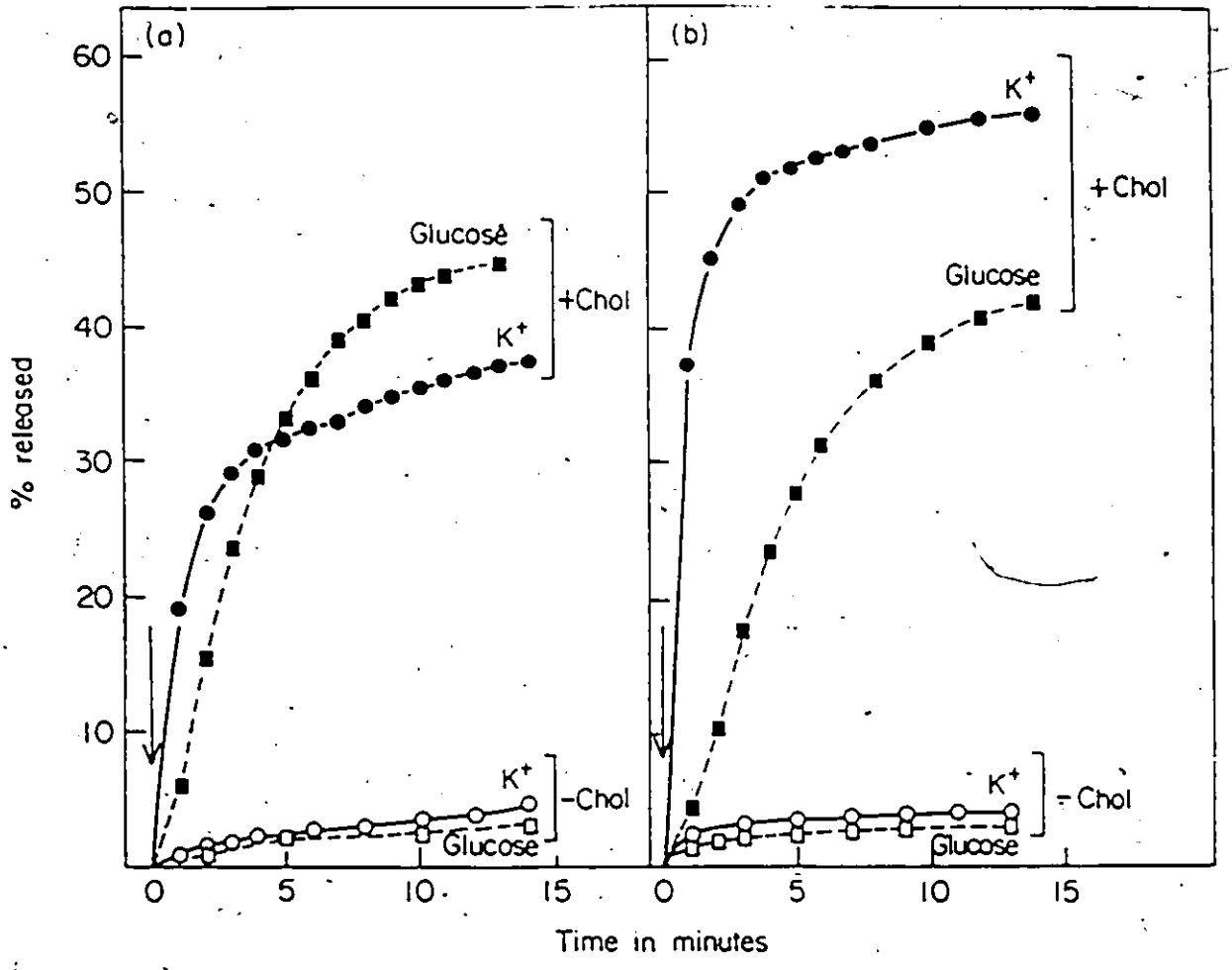

Fig. IV.1-2. Effect of Filipin (a) and Amphotericin B (b) on the realease of K^+ and glucose from liposomes prepared with and without 16 moles % of cholesterol. (from de Kruijff et al., 1974).

transition of the lipid as detected by DSC. The addition of Filipin to these cholesterol-containing liposomes was shown to restore the phase transition of the pure lipid (Normal, et al., 1972).

IV.1.4 Model for the Sterol-Polyene Antibiotic Interaction

The following will be essentially concentrated on the P.A. Amphotericin B, with reference to the review article of Norman, et al. (1976) for more details on other P.A.-sterol interactions. The permeability studies mentioned in the previous section showed that there was a limitation in the size of the released solutes: β-cholesterol-containing liposomes treated with Ampho B were just permeated by glucose, in fact glucose was the largest compound able to leak out. From these observations and the calorimetric studies already mentioned, several authors postulated the pore model (Andreoli, 1973; de Krujff and Demel, 1974). This model states that β-cholesterol and Ampho B form a 8:8 molecular complex, whose structure is shown in Figure IV.1-3 creating a pore of maximum diameter approximately 8Å. As one may notice in Figure IV.1-3, two such complexes are required to make a transmembrane channel leaky to solutes. In 1978, Van Hoogevest and de Kruijff refined this model by postulating that in situations where

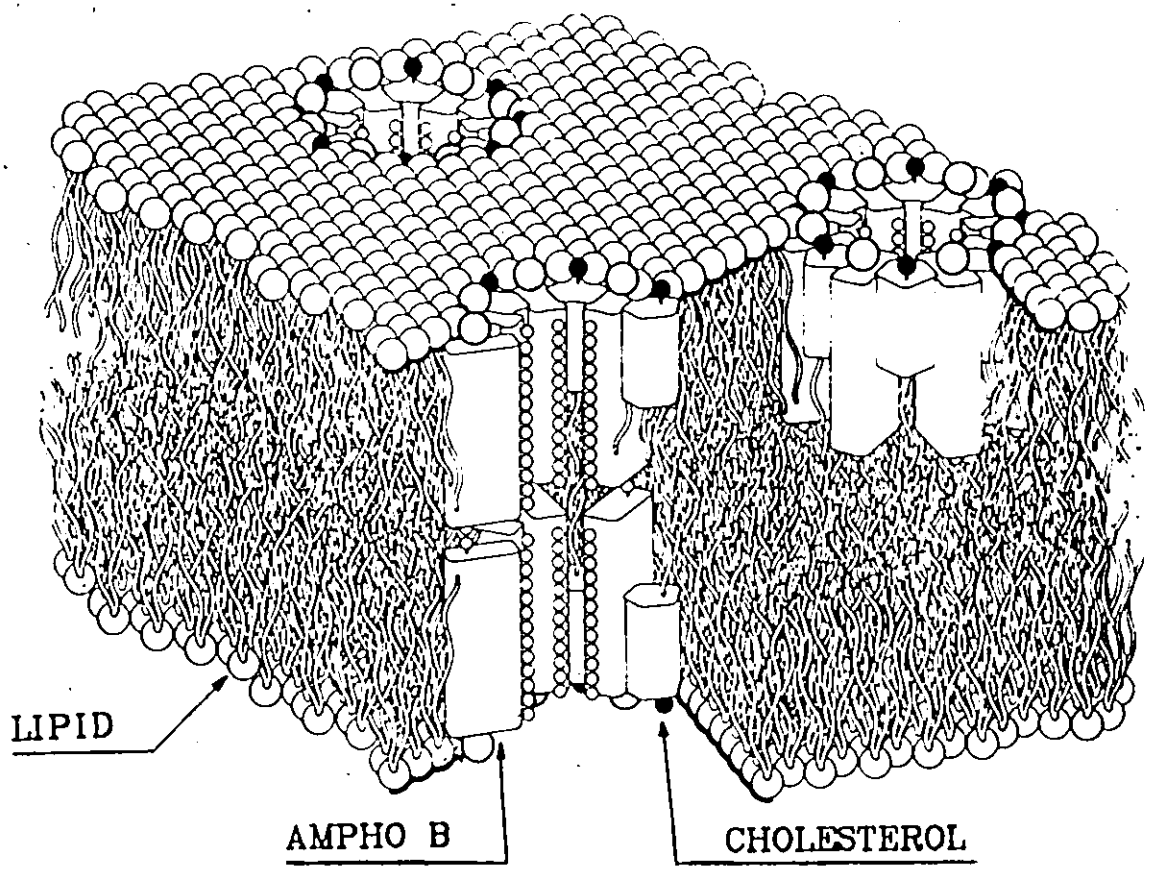

Fig. IV.1–3. The complex Amphotericin B:cholesterol as postulated by de Kruijff and Demel (1974).

the membrane was thin enough, one complex was sufficient to span the bilayer and therefore induce permeability.

IV.1.5 Study of the Pore Structure

Since the permeability and calorimetric studies did not demonstrate directly the pore structure, several other methods such as Electron Spin Resonance (ESR) or Circular Dichroism (CD) were used to gain insight on the effective geometry of the Ampho B-cholesterol complex. In 1979, Okhi, et al., observed little change in the order parameter, as measured by ESR, of PC spin probes in model membranes containing cholesterol, with and without Ampho B. Conversely, using epiandrosterone spin probes, the same authors observed that the ESR signal exhibited a new component with a large overall hyperfine splitting (but with a very small intensity compared with free epiandrosterone) when Ampho B was added to the membrane system. These authors concluded that the steroid probe was immobilized by the antibiotic. Oeshlschlager and Lacks (1980) studied the interaction between Ampho B and Ergosterol in egg PC using PC spin probes. They concluded that the complex Ampho B: Ergosterol could exist in the 1:2 as well as 1:1 (molar) forms. Bolard, et al. (1980) using CD techniques on the Ampho B: cholesterol: DMPC system came also to the conclusion of multiple Ampho B:

cholesterol complex forms (1:2, 1:1, ...). Although there is evidence that the Ampho B induces permeability changes only when sterols are present in the membrane, there is still no unequivocal information about the postulated pore geometry as well as its lifetime.

The aim of the present study is therefore to use ^{2}H-NMR to study the possible structure and dynamics of the supposed pore. The model membrane system which has been chosen for such an investigation is composed of DMPC, cholesterol and Amphotericin B. The first step of that three body problem was to study the influence of Ampho B on DMPC, the second was to investigate the action of cholesterol on DMPC (previous sections) and the third concerned the DMPC: cholesterol: Ampho B interactions. Since it was "relatively" easy to incorporate by organic syntheses deuterium atoms on both the lipid and the sterol molecules, the interactions were monitored either by DMPC or by cholesterols. Since the presence of an OH group in β of the steroid body seemed to be a requirement to the P.A.: sterol complex formation (from the permeability studies mentioned above) investigations have been carried out using both α- and β-isomers of cholesterol.

REFERENCES TO CHAPTER IV.1

Andreoli, T.E. (1973), Kidney International, 4, 337.

Bolard, J., Seigneuret, M. and Boudet, G. (1980), Biochim. Biophys. Acta, 599, 280.

de Kruifjj, B. and Demel, R.A. (1974), ibid., 339, 57.

De Kruijff, B., Gerritsen, W.J., Oerlemans, A., Demel, R.A. and Van Deenen, L.L.M. (1974a), ibid., 339, 30.

de Kruijff, B., Gerritsen, W.J., Oerlemans, A., Van Dijck, P.W.M., Demel, R.A. and Van Deenen, L.L.M. (1974b), ibid., 339, 44.

Ganis, P., Avitabile, G., Mechlinski, W. and Schaffner, C.P. (1971), J. Amer. Chem. Soc., 93, 4560.

Gottlieb, D., Carter, H.E., Sloneker, J.H. and Amman, A. (1958), Science, 128, 361.

Gottlieb, D., Carter, H.E., Sloneker, J.H., Wu, L.C. and Gandy, E. (1961), Phytopathology, 51, 321.

Hazen, E.L. and Brown, R. (1951), Proc. Soc. Exp. Biol. Med., 76, 93.

Kinsky, S.C. (1961a), Biochem. Biophys. Res. Commun., 4, 353.

Kinsky, S.C. (1961b), J. Bacteriol., 82, 889.

Lampen, J.O., Arnow, P.M., Borowska, Z. and Laskin, A.I. (1962), J. Bacteriol., 184, 1152.

Mechlinski, W., Schaffner, C.P., Ganis, P. and Avitabile, G. (1970), Tetrahedron Lett., 44, 3873.

Norman, A.W., Demel, R.A., de Kruijff, B. and Van Deenen, L.L.M. (1972), J. Biol. Chem., 247, 1918.

Norman, A.W., Spielvogel, A.M. and Wong, R.G. (1976), Adv. Lipid Res., 14, 127.

Oeshlschlager, A.C. and Laks, P. (1980), Can. J. Biochem., 58, 978.

Okhi, K., Nozawa, Y. and Ohnishi, S. (1979), Biochim. Biophys. Acta, 554, 39.

Van Hoogevest, P. and de Kruijff, B. (1978), Biochim. Biophys. Acta, 511, 397.

CHAPTER IV.2

AMPHOTERICIN B AND MODEL MEMBRANES

2. PURE LIPID SYSTEMS

IV.2.1 Ordering Effect of Amphotericin B on Pure Lipids

A sample containing Ampho B and [4'-$^2H_2$]-DMPC (3:7 molar ratio) was prepared according to the procedure described in Materials and Methods. Deuterium powder patterns were thus obtained for this sample between 5°C and 60°C. These spectra are compared in Figure IV.2-1 with the spectra of pure [4'-$^2H_2$]-DMPC at the same temperatures. At low temperatures (5°C), the spectra of lipids with and without Ampho B are quasi-identical, that is, they exhibit the spectral shape characteristic of the so-called gel phase of the pure lipid with a maximum spectral width of ca. 120 kHz. On increasing the temperature above 23°C (the gel to liquid crystalline phase transition temperature) the spectra of the pure lipid show well defined axially symmetric shapes indicative of a lipid in only one average environment whereas the sample containing Ampho B exhibits, in addition to the peak doublet, a broad spectral feature of ca. 120 kHz maximum width, at the corresponding temperatures. The relative percentage of these two components can be estimated either from spectral simulations or from the spectral moments.

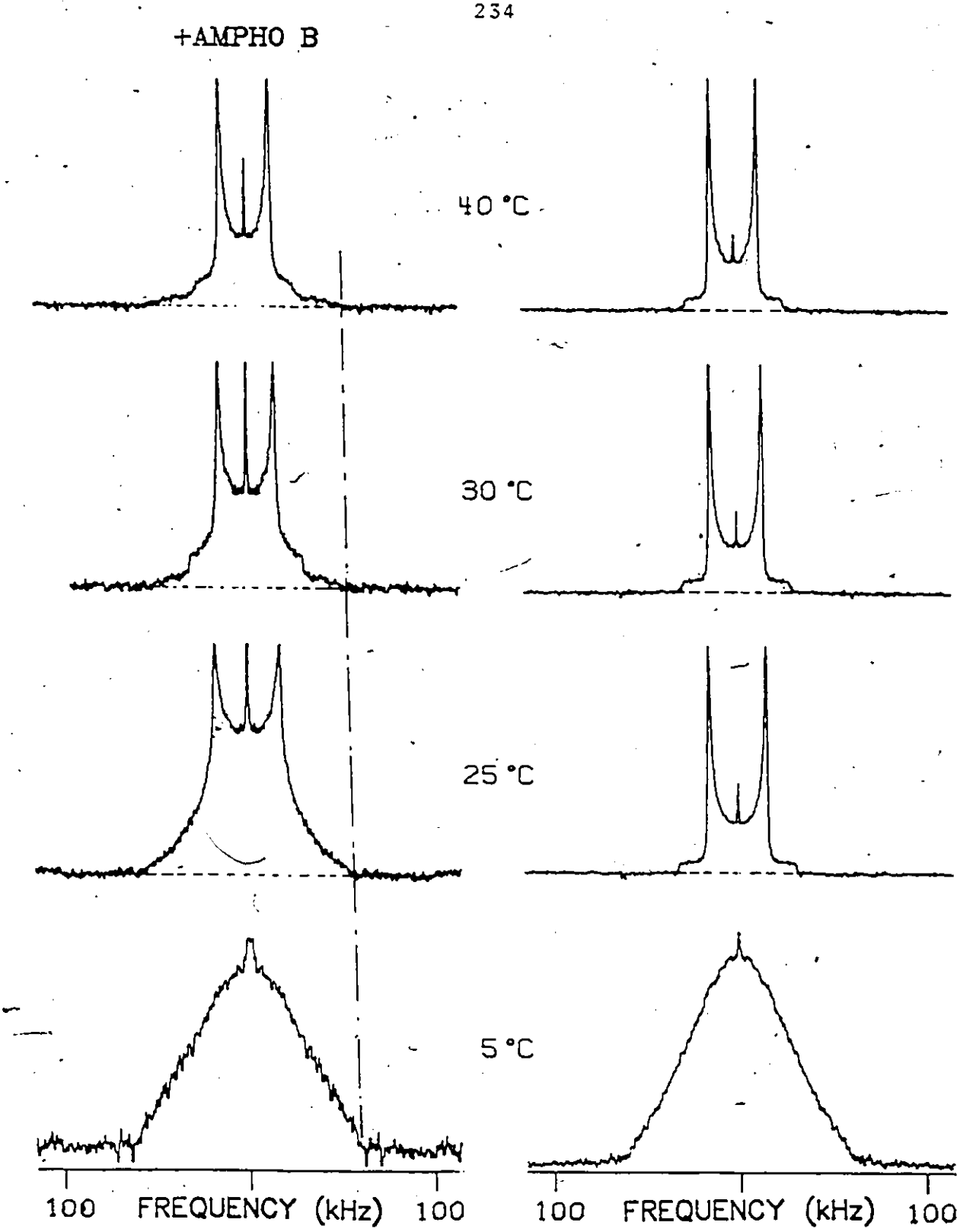

Fig. IV.2 1. ^2H-NMR spectra of $[4\text{-}^2H_2]$ DMPC model membranes in the presence or absence of Amphotericin B (30 mole %), as a function of temperature. Experimental parameters: $\pi/2$ pulse length of 4 μs; pulse spacing 60 μs; recycle time 100 ms; 250 kHz spectral window and 24,000 accumulations.

The major component which appears to be axially symmetric above 25°C was simulated using the quadrupolar splitting of the sharp peaks and a constant linewidth. The simulated spectrum was then subtracted from the total experimental spectrum and the remaining area was integrated and scaled according to the total area of the experimental spectrum. On the other hand, the first moment of the total spectrum, M_1^T, can be expressed as (Jarrell, et al., 1981):

$$M_1^T = a\, M_1^{Ax} + (1-a) M_1^{Im} \qquad \text{(IV.2.1)}$$

where M_1^{Ax} represents the first moment of the axially symmetric powder pattern (major component in the spectra above 25°C) and can be estimated from the quadrupolar splitting $\Delta\nu_Q$: $M_1^{Ax} = (2/3\sqrt{3})(2\pi)\Delta\nu_Q$. In Equation (IV.2.1) M_1^{Im} represents the first moment of the broad component and was taken to be the value of the experimental first moment at 5°C and a is the relative amount of the axially symmetric powder pattern. Above 25°C, the relative amount of the broad component estimated from both methods is 30 ± 6% and stays constant on increasing the temperature.

The presence of the broad component at all temperatures above 25°C indicates that 30% of the lipids are "immobilized" by the antibiotic. The temperature independence of this interaction is indicative of very strong binding.

The word "immobilized" means in our sense that there is no longer angular fluctuation of the C-^{2}H bonds, that is, the chains are "frozen" in all trans position, the only remaining motion being the rotational diffusion around the axis of motion. This situation is achieved when $\Delta\nu_{max}$ = 127.5 kHz (the maximum spectral width is defined such as β_b, the macroscopic orientation, is zero). Furthermore, the lipids which are not "immobilized" by the Ampho B possess larger quadrupolar splittings than in the absence of antibiotic, at corresponding temperatures. Figure IV.2-2 shows the temperature variation of $\Delta\nu_Q$ for the "mobile" lipids, with and without the P.A. Assuming that the C-^{2}H units of the 70% lipids which are not immobilized by the antibiotic have the same average orientations with respect to the director of the motion as those of the pure lipid, one can conclude that from 25°C to 40°C Ampho B induces ordering in the "mobile" lipid. However, this ordering action is no longer perceived at high temperatures; above 50°C the lipids of the Ampho B-containing membranes face two very different physical environments: in one of these domains the lipids are strongly coupled with the antibiotic whereas in the other they are as free as if they were in a pure lipid system. It is interesting to notice that these two domains behave differently with temperature: one of them is temperature dependent, that is, its local ordering is modulated by the

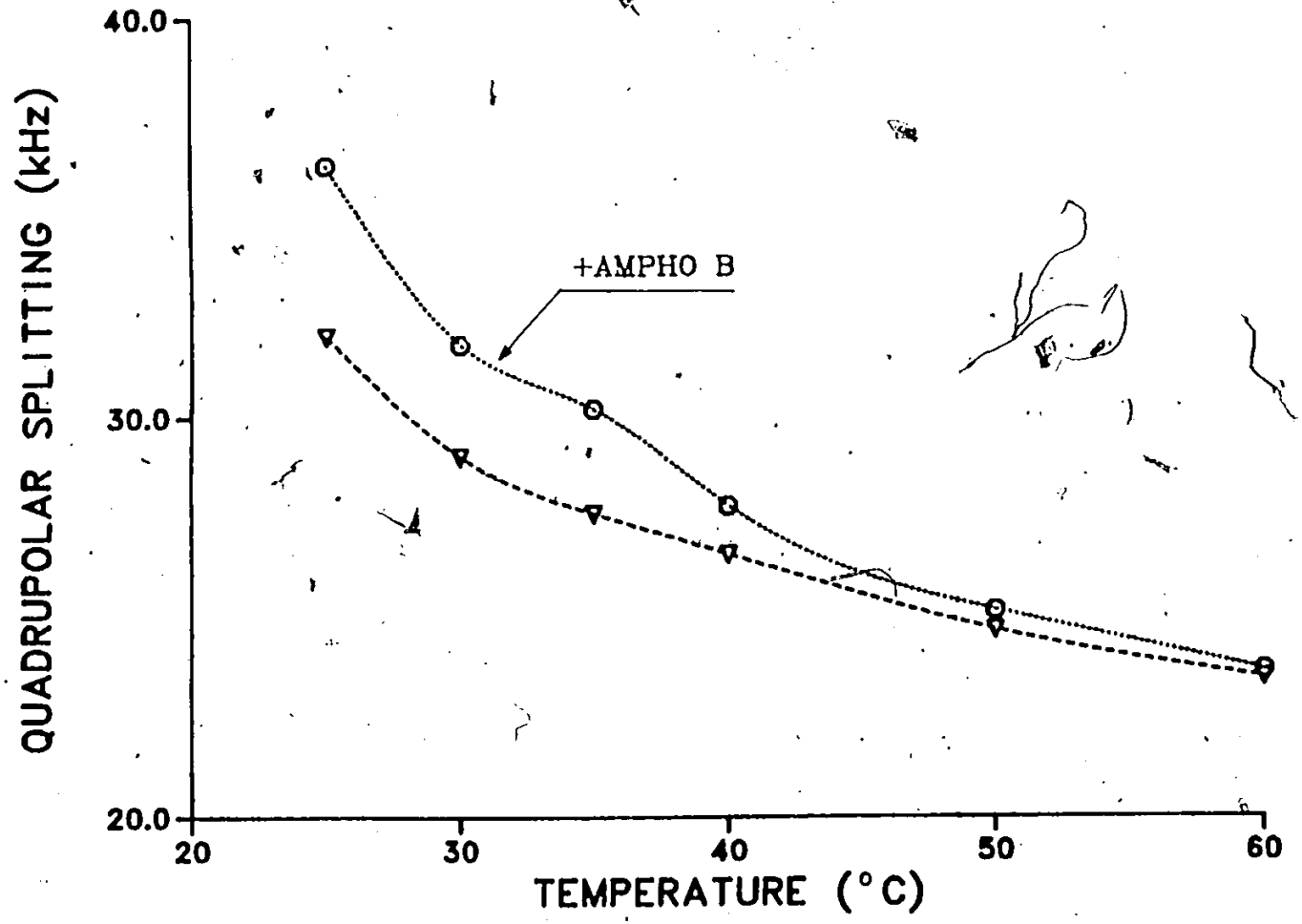

Fig. IV2-2. Temperature variation of the quadrupolar splittings of DMPC labeled at C4' in the presence or absence of Amphotericin B. The quadrupolar splitting in the presence of Amphotericin B is that of the "major" component (see text). The symbols give an estimate of the error.

temperature, whereas the other is not.

IV.2.2 Variation of the Delta 2 Parameter with Temperature

It has been shown that the Δ_2 parameter (see its definition in Materials and Methods) is sensitive to sample inhomogeneities such as the coexistence of phases (Davis, 1979; Davis, et al., 1980). It has been used for instance to determine the temperature of the gel-to-liquid crystalline phase transition of A. laidlawii membranes enriched in deuterated oleic acid (Rance, et al., 1980). This parameter gives the relative mean square width of the distribution of quadrupolar splittings. A plot of Δ_2 versus temperature is shown in Figure IV.2-3 for [4'-$^2H_2$]-DMPC with and without Amphotericin B. A system having only one $\Delta\nu_Q$, that is, one single order parameter gives $\Delta_2=0$, when the transverse relaxation time, T_2, is neglected and when the signal-to-noise ratio is close to infinity. Therefore, any non zero value of Δ_2 would be indicative of a distribution of order parameters. However, accounting for the natural broadening of the individual lines one can obtain an expression of a broadened delta-2, Δ_2^B, as (assuming Gaussian broadening, see Section I.3.5a):

$$\Delta_2^B = \frac{\sigma^2}{1.35M_1^2} + \Delta_2 \qquad \text{(IV.2.2)}$$

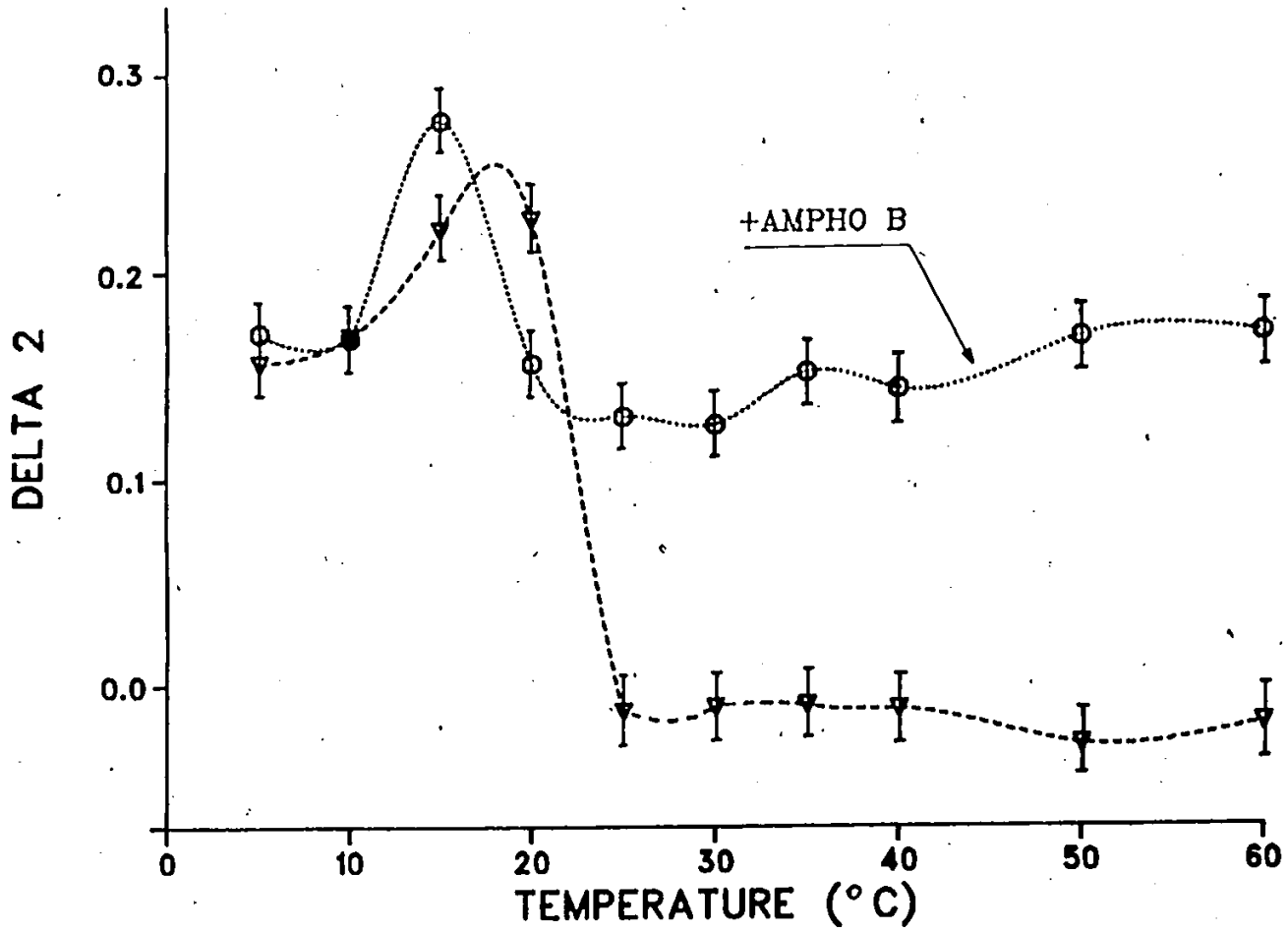

Fig. IV.2–3. Temperature variation of the delta 2 parameter of $[4'\text{--}^2H_2]$ DMPC powder spectra in the presence or absence of Ampho B. The bars give an estimate of the error.

where σ is the Gaussian linewidth, M_1 the first moment of the spectrum and Δ_2 the delta 2 parameter in absence of broadening. Therefore, in a situation where $\Delta_2=0$, $\Delta_2^B = \sigma^2/1.35M_1^2$, which leads to the fact that the measured delta 2 (which is really Δ_2^B) can be different from zero, even if there is no distribution of order parameters. Fortunately, one often deals with large quadrupolar splittings, for example, ca. 30 kHz for the pure [4'-$^2H_2$]-DMPC above 23°C and therefore even if σ = 3kHz in the liquid crystalline phase $\Delta_2^B \simeq 0.001$ which is clearly negligible. It is therefore not surprising that the delta 2 parameter of the pure DMPC is virtually 0 above 23°C. On cooling pure DMPC below 23°C, the delta 2 undergoes a marked increase due to the appearance of a gel phase whose ordering properties are different from those of the liquid crystalline phase. The presence of a maximum is due to the coexistence of both phases at the same temperature, hence the distribution of order parameters and hence the increase in delta 2. It should be mentioned that in the gel phase, around 20°C, the linewidth might play a role in the increase of the delta 2 value, but this contribution will be at least one order of magnitude lower than that of the distribution of quadrupolar splittings. One thus remarks that the Δ_2 is useful to detect phase transitions. The delta 2 profile of the labeled lipid in presence of Ampho B has a behaviour similar to that of

the pure lipid at low temperatures. This correlates well with the finding that at 5°C the gel phase spectra of DMPC with and without Ampho B were quasi-identical (Figure IV.2-2). The maximum in delta 2 of the system containing the antibiotic (Figure IV.2-3) appears shifted towards low temperatures, when compared to that of the pure lipid. However the discontinuity is less marked in the presence of Ampho B; indeed the delta 2 of the lipid antibiotic system never reaches zero when the temperature is increased above the maximum. This is mainly due to the fact that at high temperatures this system is not homogeneous, that is, it is composed by two domains in which the lipid sits in two different physical environments (whose ordering properties are very different see previous section). However, the presence of a maximum in the delta 2 profile, with Ampho B, indicates that the lipid not sequestered by the antibiotic still undergoes a phase transition some 5-10°C below the temperature of the gel-to-liquid crystalline phase transition of the pure lipid.

IV.2.3 Spectral Changes Induced by the Concentration of Ampho B

Figure IV.2-4 shows the change in the ^{2}H-NMR spectra of DMPC on addition of Amphotericin B, at 25°C. One notices that increasing the concentration of antibiotic leads to a

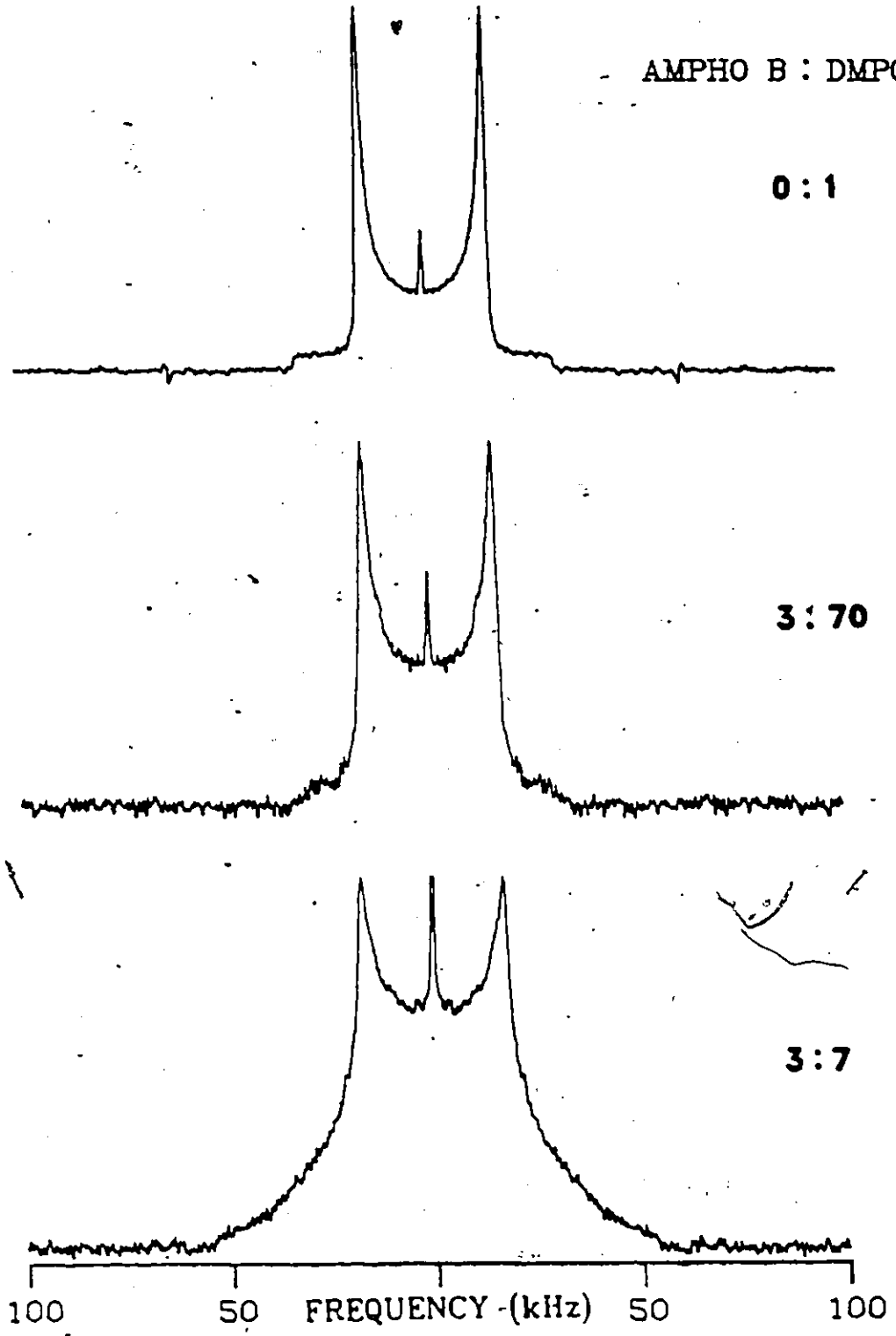

Fig. IV.2-4. Effect of Amphotericin B concentration on the ^{2}H-NMR spectral shapes of DMPC labeled at C4', at 25°C. Same experimental parameters as in Fig. IV.2-1.

progressive loss of the shape characteristic of the axially symmetric motions in the liquid crystalline phase of the pure lipid. When the Ampho B: DMPC ratio reaches 3:7 the axially symmetric shape is completely lost. Although the shape of the bottom spectrum of Figure IV.2-4 is not well understood, it seems reasonable to think that it might be the result of the two lipid domains already observed in higher temperature spectra with the restriction that these two regions in which the motions are different are not well separated here. The end result would thus be a "continuum" spectrum from the broad spectral component of maximum width of ca. 120 kHz to the possibly axially symmetric powder pattern of $\Delta\nu_Q$ = 36.3 kHz (Figure IV.2-4, bottom). The quadrupolar splitting of the spectrum originating from the sample where the Ampho B is present in low concentration (3:70) is equal to 33.4 kHz which represents an increase of ~5% compared to $\Delta\nu_Q$ of the pure lipid at 25°C. It is therefore interesting to notice that even used in weak doses, this polyene antibiotic orders markedly the membrane lipids. Unfortunately, the low S/N ratio of the central spectrum of Figure (IV.2-4) does not allow to observe whether at low antibiotic concentration, the "immobilized" lipid domain does really exist.

IV.2.2 Perturbation Throughout the Entire Bilayer Membrane

In order to monitor the ordering and sequestering action of the Amphotericin B at several bilayer depths, the system previously described (30% Ampho B in DMPC) has been reconstituted using a DMPC whose sn-2 fatty acyl chain was perdeuterated ([sn-2-$^2H_{27}$]-DMPC). Due to the non equivalence of the sn-1 and sn-2 chains (Seelig and Seelig, 1975) it was chosen to label only one acyl chain to simplify the analysis. Figure IV.2-5 shows the resulting spectra of [sn-2-$^2H_{27}$]-DMPC with and without Ampotericin B at 35°C. One notices the presence of the 120-125 kHz broad spectral feature on the bottom spectrum of Figure IV.2-5 which has already been attributed to the "immobilized" lipid. The spectra of Figure IV.2-5 have been dePaked (see Material and Methods) and are shown in figure IV.2-6. In that figure the numbers represent the value of the quadrupolar splitting, $\Delta\nu_Q$ (in kHz), and the primed numbers designate the labeled carbon position. The assignment was made on the basis of specifically deuterated DMPC (Oldfield, et al., 1978). To first order, it appears that the shape of the dePaked spectra are quasi identical (except for the splitting of the plateau region large peak in the bottom spectrum of Figure IV.2-6 which will not be discussed further due to the lack of additional information). It is interesting to notice that all the $\Delta\nu_Q$

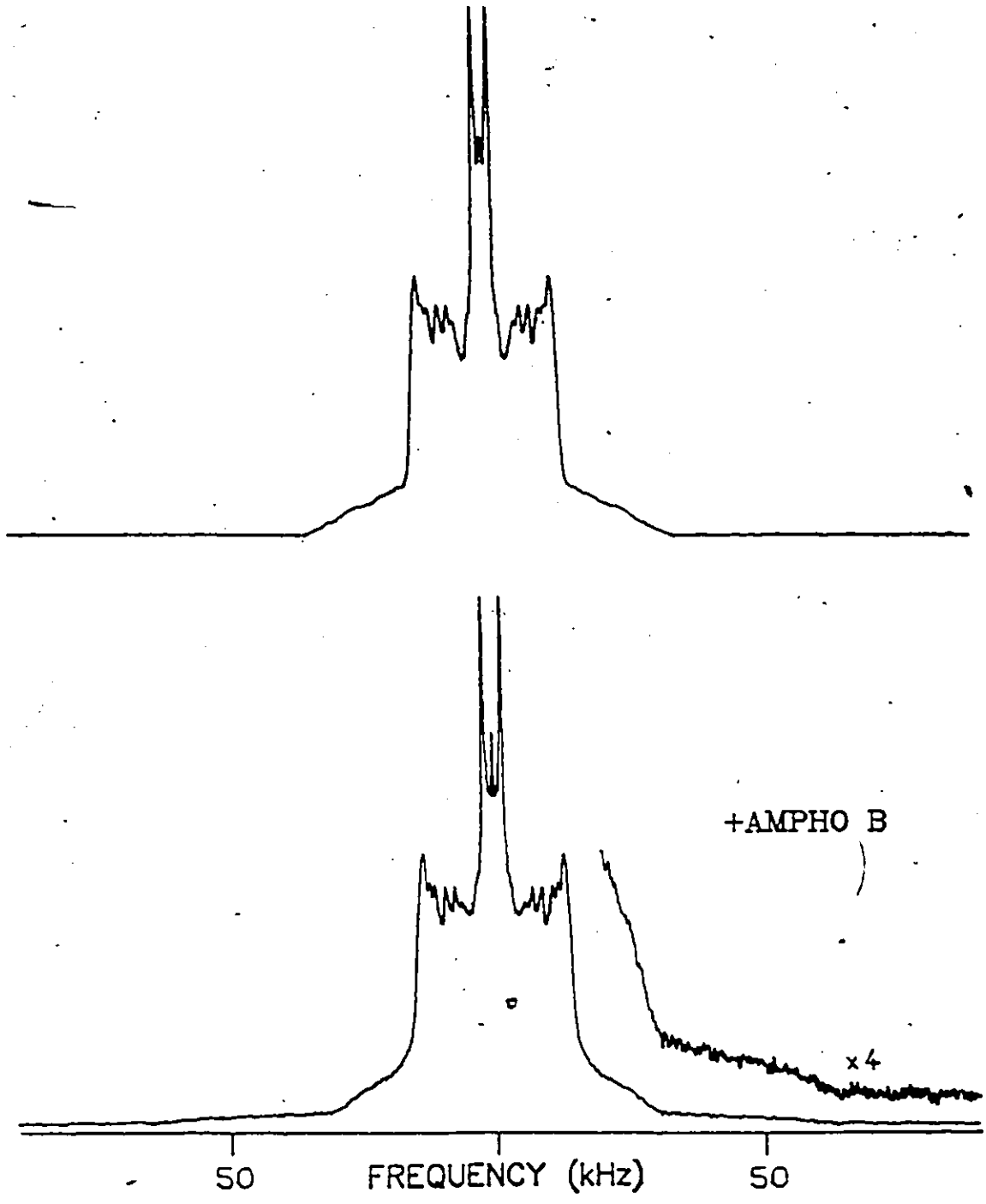

Fig. IV.2-5. ^2H-NMR spectra of $[sn\text{-}2\text{-}^2H_{27}]$ DMPC in the presence or absence of Amphotericin B (30 mole %) at 35 °C. Same experimental parameters as in Fig. IV.2-1 except recycle time of 1 s and spectral window of 500 kHz

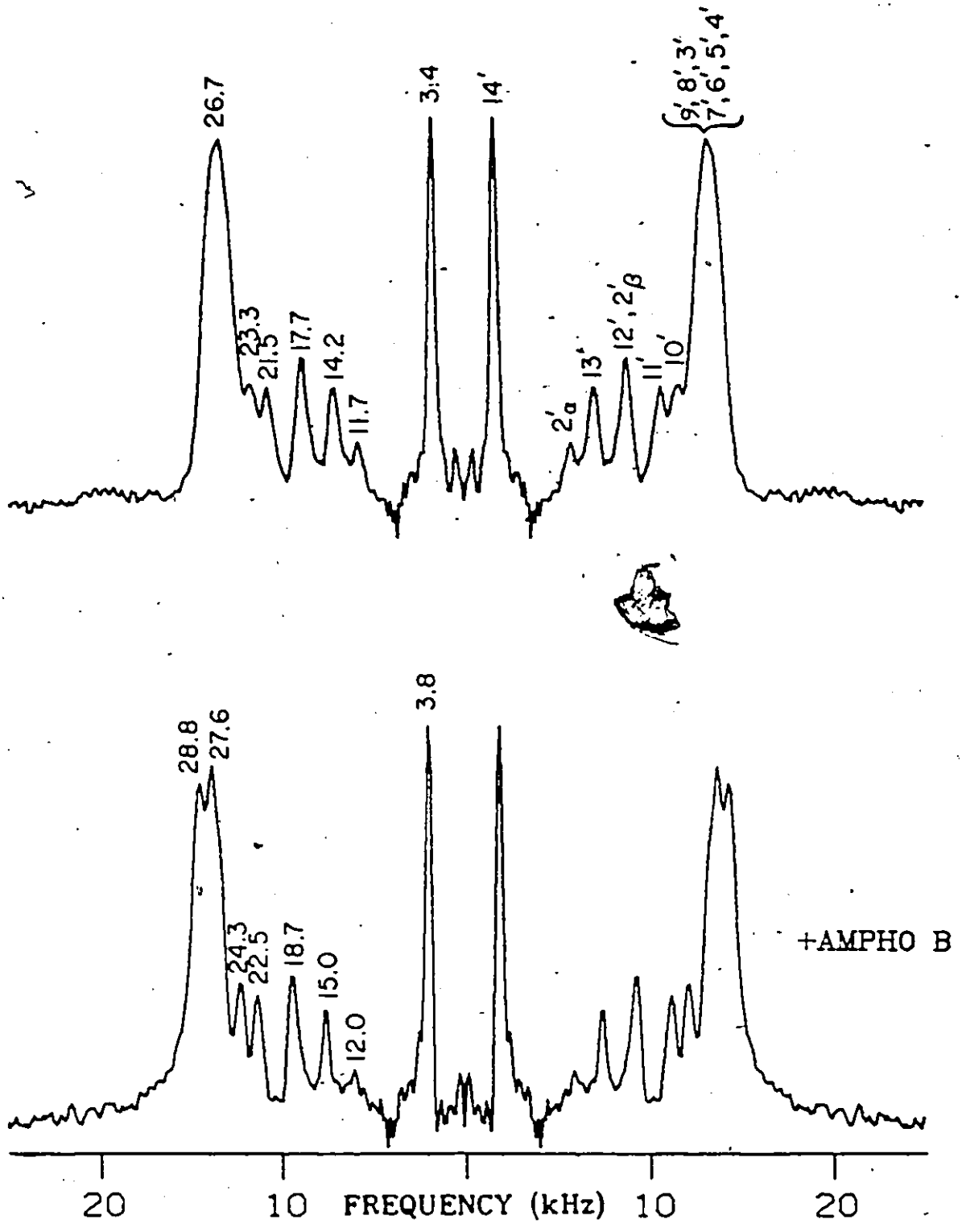

Fig. IV.2–6. Same as Fig. IV.2–5, but dePaked.
Processing parameters: spectral deconvolution on 600 points 3 iterations.
Numbers: quadrupolar splitting values in kHz.
Primed numbers: carbon atom assignments (see text).

are increased by 5-10%. Assuming that this increase is monotonic for all positions, that is, there is no inversion in the labeled carbon assignment, one can conclude that the entire S_{C-^2H} order parameter profile is shifted towards higher ordering by 5-10%. In other words, the perturbation induced by the antibiotic on the lipid chains which are not "immobilized" is perceived at the top as well as in the center of the bilayer. This finding proves that the Ampho B is well within the bilayer, possibly aggregated with 30% of the total lipid.

IV.2.5 Relaxation Time Measurements

Using the techniques described in Materials and Methods, spin-lattice, T_{1z}, and spin-spin, T_2, relaxation times have been measured for [4'-$^2H_2$]-DMPC with and without the antibiotic at 25°C. The pure lipid has a T_{1z} of 18.6 ± 0.5 ms whereas in presence of Amphotericin B (30% in DMPC) the T_{1z} is equal to 19.1 ± 1.0 ms. The T_{1z} were orientationally independent in both cases, that is, the reported relaxation times are constant across the powder pattern. The "mobile" and "immobilized" lipids had the same T_{1z}, within the experimental error; the spin-lattice relaxation time reported for the sample containing Ampho B stand therefore for the entire powder pattern. The spin-spin relaxation

time of the lipid has a value of 280 ± 30 μs in absence of the drug and 140 ± 20 μs in its presence. Although it is known that T_2 is orientationally dependent, the values given here stand for the entire powder pattern. Indeed it is hopeless trying to define 0° or 90° macroscopic orientations on the spectrum containing Amphotericin B at 25°C (Figure IV.2-4, bottom). The main remark that one can make from these relaxation measurements is that the T_2 of the lipid is altered by the presence of the antibiotic whereas T_{1z} is not. Since T_2 is much more sensitive to slow motions than T_{1z} (due to the presence of the $J(0)$ spectral density function in the spin-spin relaxation rate equation, see theoretical background) one may think that the main effect of Ampho B is to slow down the slow motions (lateral diffusion, director fluctuations, slow tumbling of the entire liposome ...). It would be interesting to separate the contribution from slow and fast motions, especially at high temperatures where the system containing the P.A. shows two distinct lipid domains. However, such an investigation would at least involve a field dependence study of the relaxation times T_{1z} and T_2 which is out of the scope of the present work.

IV.2.6 Concluding Remarks

When added to pure lipid membranes, Amphotericin B has a general ordering effect on the lipid fatty acyl chains.

The presence of a broad spectral component of ca. 120 kHz width, at high temperatures, indicates that 30% of the lipid C-^{2}H bonds (relative area of the broad component) no longer undergo angular fluctuations to time-average the quadrupolar interaction. On the other hand, the remaining 70% of the lipid still undergo a time averaging of the quadrupolar interaction between C-^{2}H bonds and the efg at temperatures higher than 25°C. The temperature variation of the delta 2 parameter indicates that the Ampho B-lipid system undergoes a phase transition some 5-10°C below that of the pure DMPC. Since increasing the temperature above 25°C affects neither the maximum spectral width nor the relative percentage of the broad spectral component, it seems reasonable to think that the observed phase transition is happening only on the 70% of the lipid, relatively free from the drug interaction. It appears therefore that at temperatures higher than 25°C the Amphotericin B is in aggregated form. The aggregate might be either composed of Ampho B molecules surrounded by a thin film of lipids strongly interacting with the antibiotic molecules or a mixture of Amphotericin B and lipids strongly coupled. In either forms, the drug:lipid ratio in the aggregate has to be approximately 1:1. At high temperatures, these aggregates would be entirely embedded in a lipid matrix whose properties are similar to those of the pure lipid system.

REFERENCES TO CHAPTER IV.2

Davis, J.H. (1979), Biophys. J., 27, 339.

Davis, J.H., Bloom, M., Butler, K.W. and Smith, I.C.P. (1980), Biochim. Biophys. Acta, 597, 477.

Jarrell, H.C., Byrd, R.A. and Smith, I.C.P. (1981), Biophys. J., 34, 341.

Oldfield, E., Meadows, M., Rice, D. and Jacobs, R. (1978), Biochemistry, 17, 2727.

Rance, M.A., Jeffrey, K.R., Tulloch, A.P., Butler, K.W. and Smith, I.C.P. (1980), Biochim. Biophys. Acta, 600, 245.

Seelig, A. and Seelig, J. (1975), Biochim. Biophys. Acta, 406, 1.

CHAPTER IV.3

AMPHOTERICIN B AND MODEL MEMBRANES

3. CHOLESTEROL-CONTAINING LIPID SYSTEMS- LIPID VIEWPONT

IV.3.1 Introduction

As it has been shown previously, both cholesterol and Amphotericin B have finite effects on the structure and dynamics of DMPC model membranes. Cholesterol acts as a regulatory agent with respect to the amplitude of the C-^{2}H angular fluctuations of the lipid fatty acyl chains: it orders the lipid above the transition temperature, T_c, of the pure lipid membrane and disorders it below T_c. The α-isomer of cholesterol possesses some of these regulatory properties and shows, in addition, a tilted configuration with respect to the director of motion (the bilayer normal) whereas β-cholesterol does not. On the other hand, the antibiotic "immobilizes" about 30% of the lipids when present at 30 moles per cent with respect to DMPC, at temperatures above T_c. The interaction between this immobilized portion of the lipids and the antibiotic is so strong that neither the width of the spectral feature representing these lipids nor its percentage with respect to the total lipid content change with temperature.

In what follows, polyene antibiotic-cholesterol-lipid interactions will be studied using the lipid as the reporter molecule, that is, this latter will be labeled with deuterium. In order to compare the results with those of the previous sections, the samples always contained 30 mole per cent of cholesterol with respect to the lipid; the antibiotic, when present, was in equimolar amounts with the sterol.

IV.3.2 Action of Amphotericin B on β-Cholesterol-Containing DMPC Membranes

IV.3.2a The Plateau Region

Deuterium spectra of β-cholesterol-[4'-$^2H_2$] DMPC model membranes with and without the antibiotic have been obtained for temperatures ranging from 0°C to 55°C. Figure IV.3-1 shows some of these spectra. The extreme similarity between the spectra in the absence or presence of the drug is remarkable. The quadrupolar splitting, $\Delta\nu_Q$, has been reported as a function of temperature for both systems in Figure IV.3-2. One notices that the behaviour of the lipid $\Delta\nu_Q$ with temperature is almost identical for both β-cholesterol: DMPC and β-cholesterol: DMPC: Ampho B systems. One may remark that the $\Delta\nu_Q$ in presence of Ampho B is always equal or slightly higher than the $\Delta\nu_Q$ in its absence

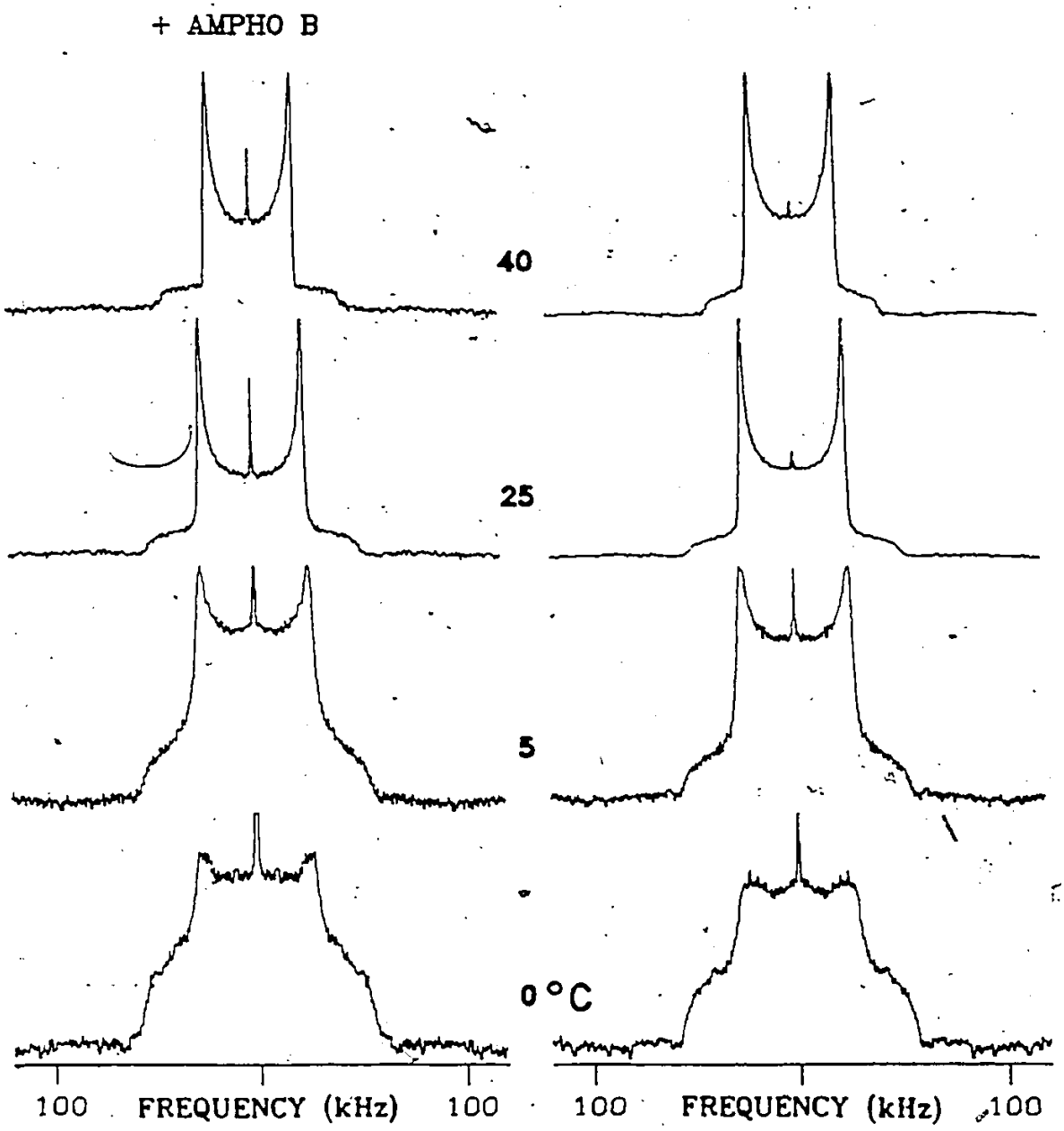

Fig. IV.3-1. ^{2}H-NMR spectra of the β-cholesterol: $[4'-^2H_2]$ - DMPC system in the presence or absence of Amphotericin B. Same experimental parameters as in Fig. IV.2-1.

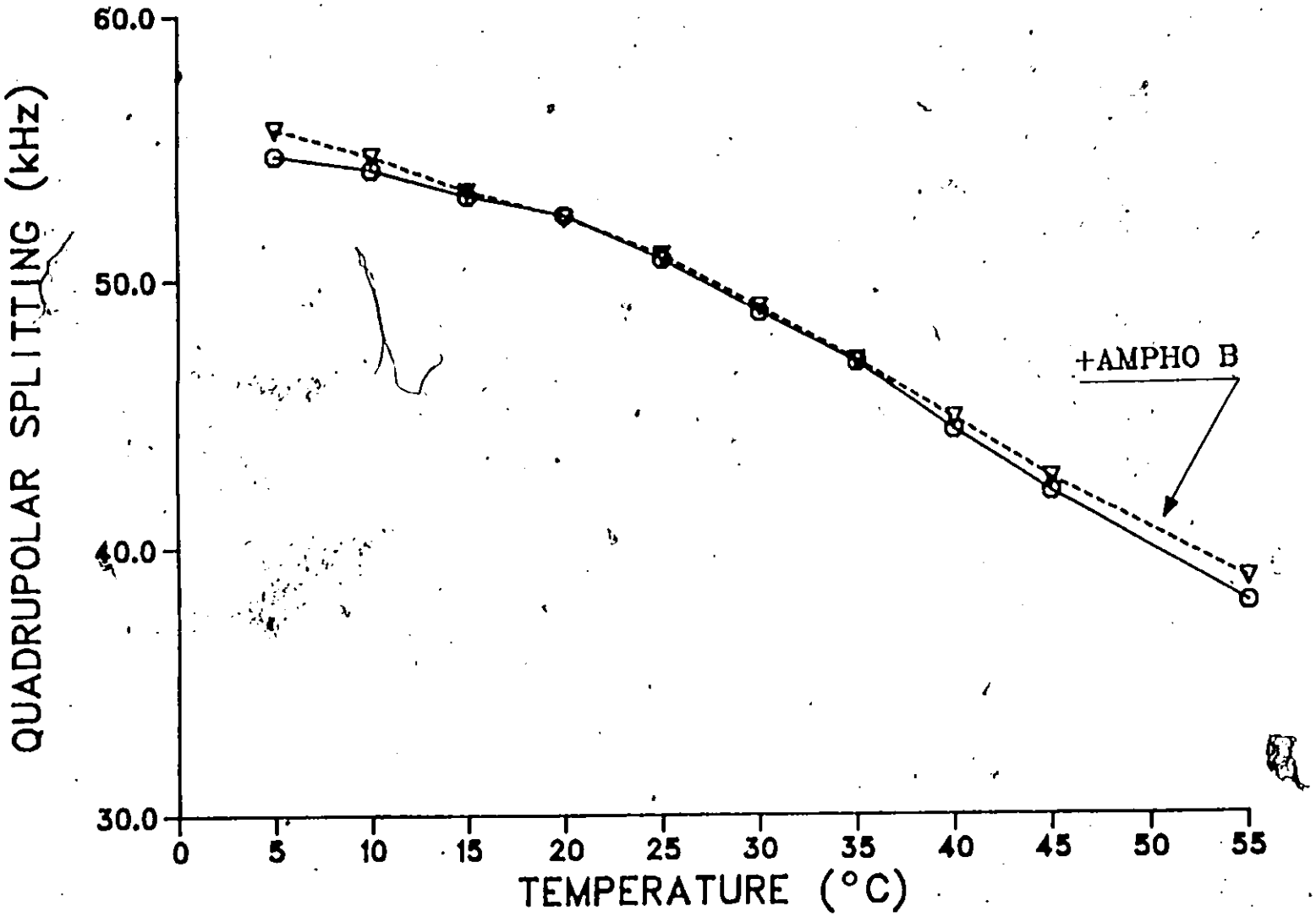

Fig. IV.3–2. Temperature variation of the quadrupolar splittings of DMPC labeled at C4' in DMPC:β-cholesterol with and without Amphotericin B. The symbols give an estimate of the error.

(especially at low (~5°C) and high (~55°C) temperatures). At low temperatures (0°, 5°C) the spectra begin to show axially asymmetric shapes as it has been mentioned in the earlier sections, but still, the spectral shapes are very similar for samples with and without the antibiotic. The spectral moments analysis led to little difference between both sets of spectra. The first and second moments of the sample containing the drug were however always greater than those of the sample without Ampho B, by 5-10% and 10-20%, respectively. The delta 2 parameter was nearly identical for both sets of spectra and close to 0 (Figure IV.3-3). Although these delta 2 values are very small and thereby subject to a great inaccuracy, one notices that both systems show the "memory" of the phase transition temperature of the pure lipid (T_c = 23°C) as already discussed in the section describing the effect of β-cholesterol on DMPC. One notices also that at high temperatures (above 40°C) the delta 2 of the system containing Ampho B is slightly greater than that of the system lacking the drug.

IV.3.2b The Tail Region

The above analysis has been repeated using [14,14,14-$^2H_3$] DMPC as reporter. The spectra are shown in Figure IV.3-4. One notices on this figure that the antibiotic has a marked

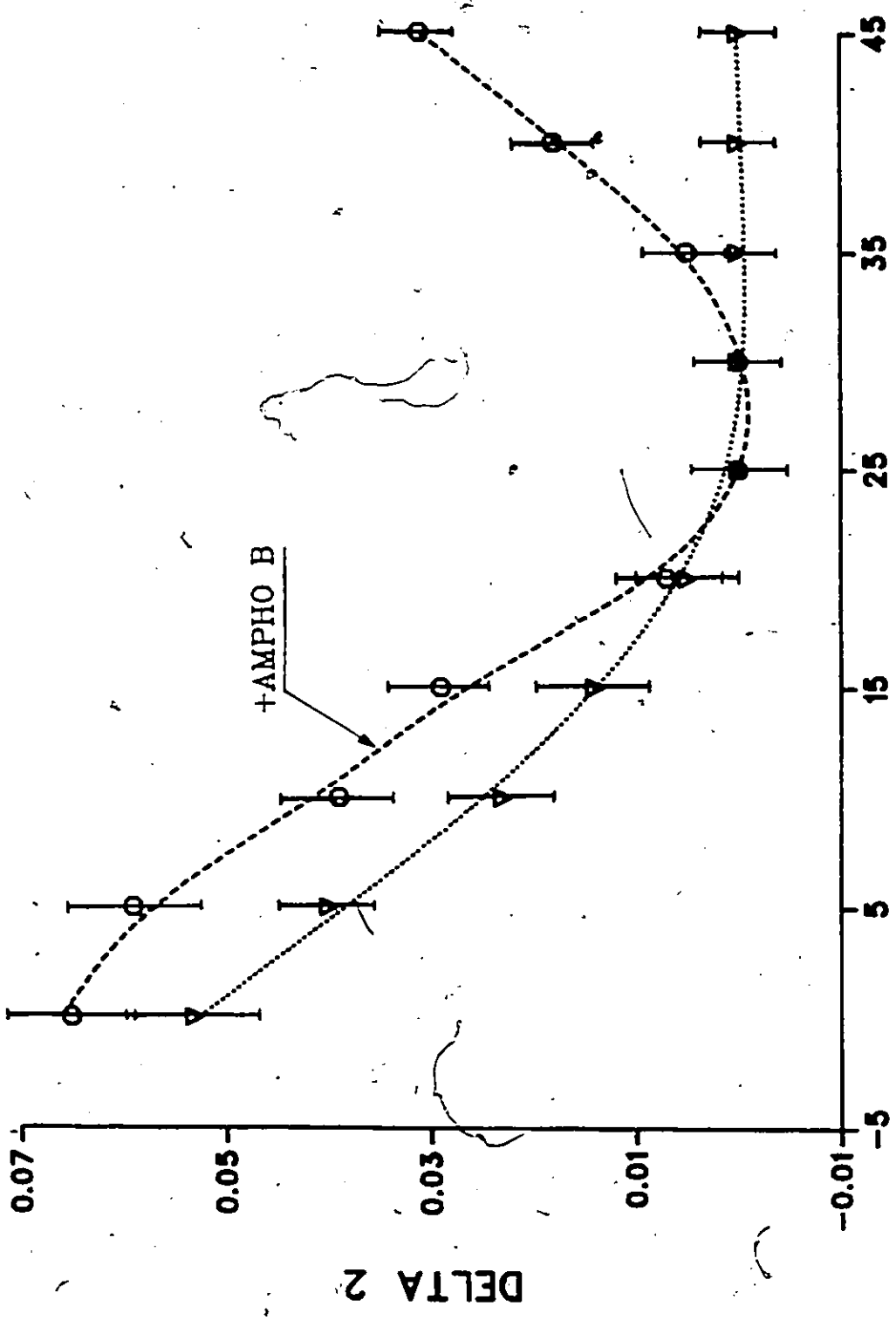

Fig. IV.3–3. Temperature variation of the delta 2 parameter. Spectral data from [4'-$^2H_2$] DMPC/β-cholesterol in the presence or absence of Amphotericin B.

effect on the lipid spectral shapes. A close look at Figure IV.3-4 reveals that a second spectral component appears below the shoulders of the major powder pattern in the spectral set whose sample contains Amphotericin B. The relative area of these two spectral components may be estimated by simulating the major powder pattern and substracting it from the experimental spectrum. The remaining spectral feature is thus that of the broad component whose area is integrated and scaled according to the total experimental spectrum area. An example of such an analysis is shown in Figure IV.3-5. Although the method is intrinsically inaccurate since it is model dependent, one can however rely in the relative integrated areas within ± 8%. The simplest model was chosen to simulate the major component of the Ampho B-containing spectra, that is, assuming a Lorenzian and angular independent linewidth. The broad component has 28% of the total area, at 5°C, and 10% at 55°C. Despite the inaccuracy involved in estimating the areas, one notices that the broad component is favoured at low temperatures. From the substracted spectrum of Figure IV.3-5 one can measure the maximum spectral width of the broad component. In order to be compared with either the $\Delta\nu_Q$ of the spectra without the antibiotic this measured maximum spectral width was divided by 2 and plotted in Figure IV.3-6 as a function of temperature. If this broad

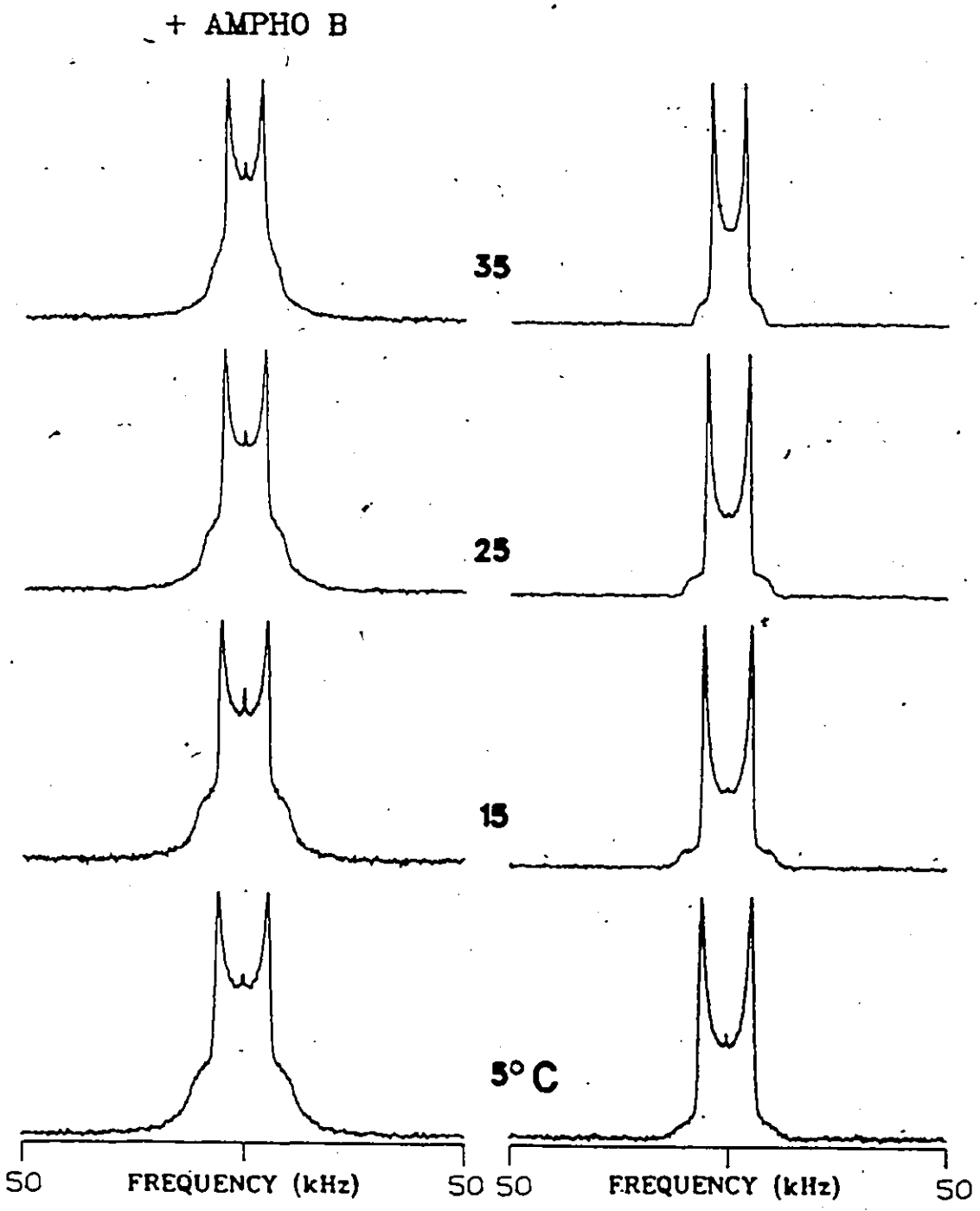

Fig. IV.3–4. ^{2}H–NMR spectra of the β–cholesterol:[14′–$^{2}H_{3}$] DMPC system in the presence or absence of Amphotericin B. Same experimental parameters as in Fig. IV.2–1 except recycle time of 1 s and 5,000 accumulations.

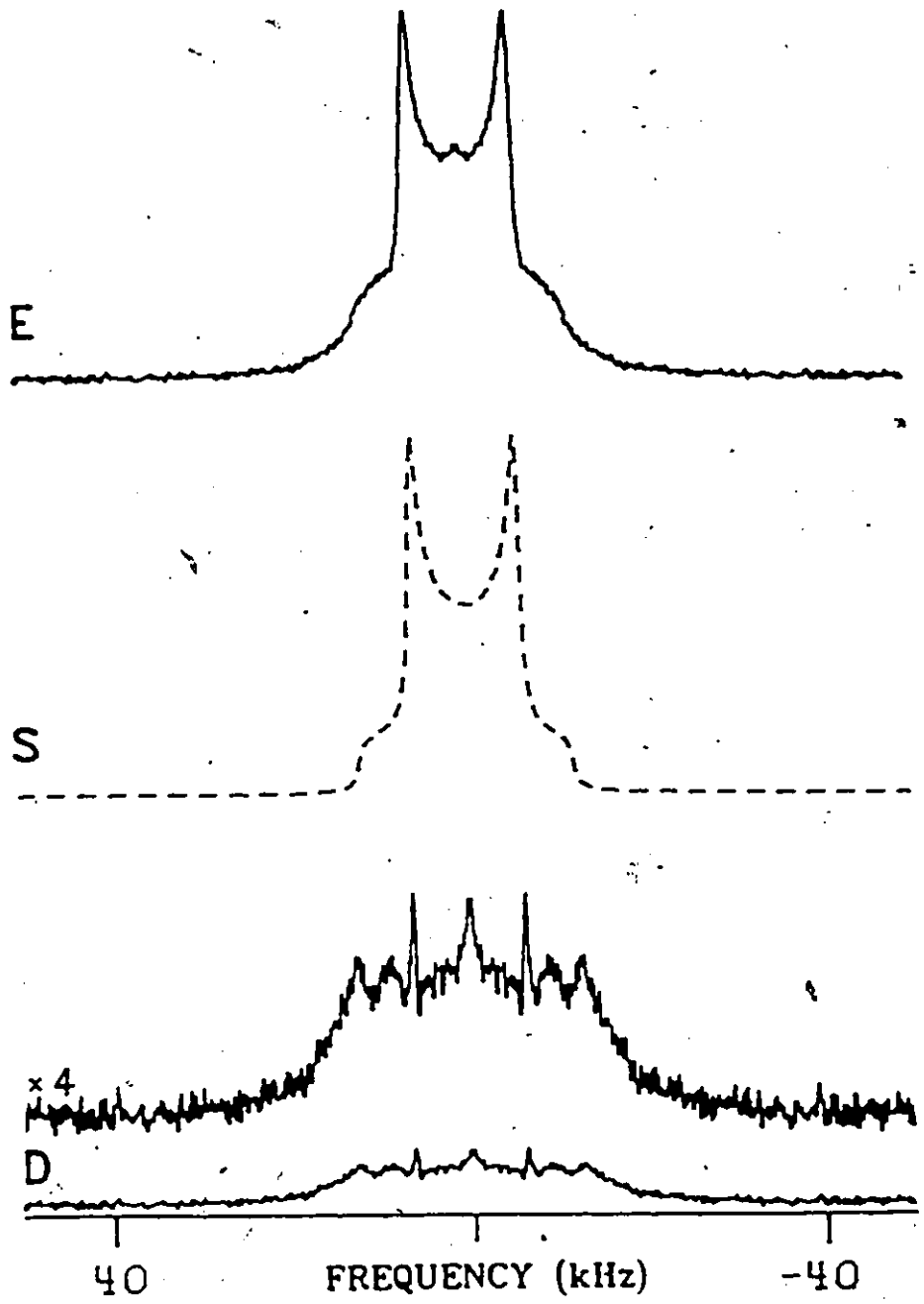

Fig. IV.3-5. Determination of the broad component area (see text).
E= Experimental spectrum.
S= Simulated spectrum of the "major" component (see text).
D= E-S = Broad component spectrum.

spectral feature represented an "immobilized" lipid, that is, if the acyl chains were all trans and only rotating around the axis of motion, the maximum observed splitting at that labeled position would be given by:

$$\Delta\nu = \frac{3}{2}A_Q\frac{1}{2}(3\cos^2\beta_b-1)\frac{1}{2}(3\cos^2\alpha-1)\frac{1}{2}(3\cos^2\gamma_1-1)\frac{1}{2}(3\cos^2\gamma_2-1) \qquad \text{(IV.3.1)}$$

with A_Q = 170 kHz, $\beta_b = 0^\circ$, $\alpha = 0^\circ$, $\gamma_1 = 35.25^\circ$ and $\gamma_2 = 109.5^\circ$, that is, $\Delta\nu_{max}$ = 42.5 kHz or $\Delta\nu_Q(\beta_b = 90^\circ)$ = 21.25 kHz. Equation (IV.3.1) is simply an extension of the equation derived by Stockton, et al. (1976) for methyl groups. From Figure IV.3-6 one can therefore conclude that the broad component is representative of a lipid in an environment such that there are no angular fluctuations of the C-^{2}H methyl bonds whereas above 25°C some angular fluctuations of these bonds take place. Figure IV.3-6 might summarize in some aspects the action of Ampho B on cholesterol-containing lipids, at the bilayer center level. When the drug is present, the lipid methyl group senses two environments: in one of them the C-^{2}H angular fluctuations are highly restricted whereas in the other the C-^{2}H bond fluctuations are identical to those of the sample without the drug. It is worthwhile to point out that the percentage as well as the motional restrictions of the so-called broad component decrease on raising the temperature.

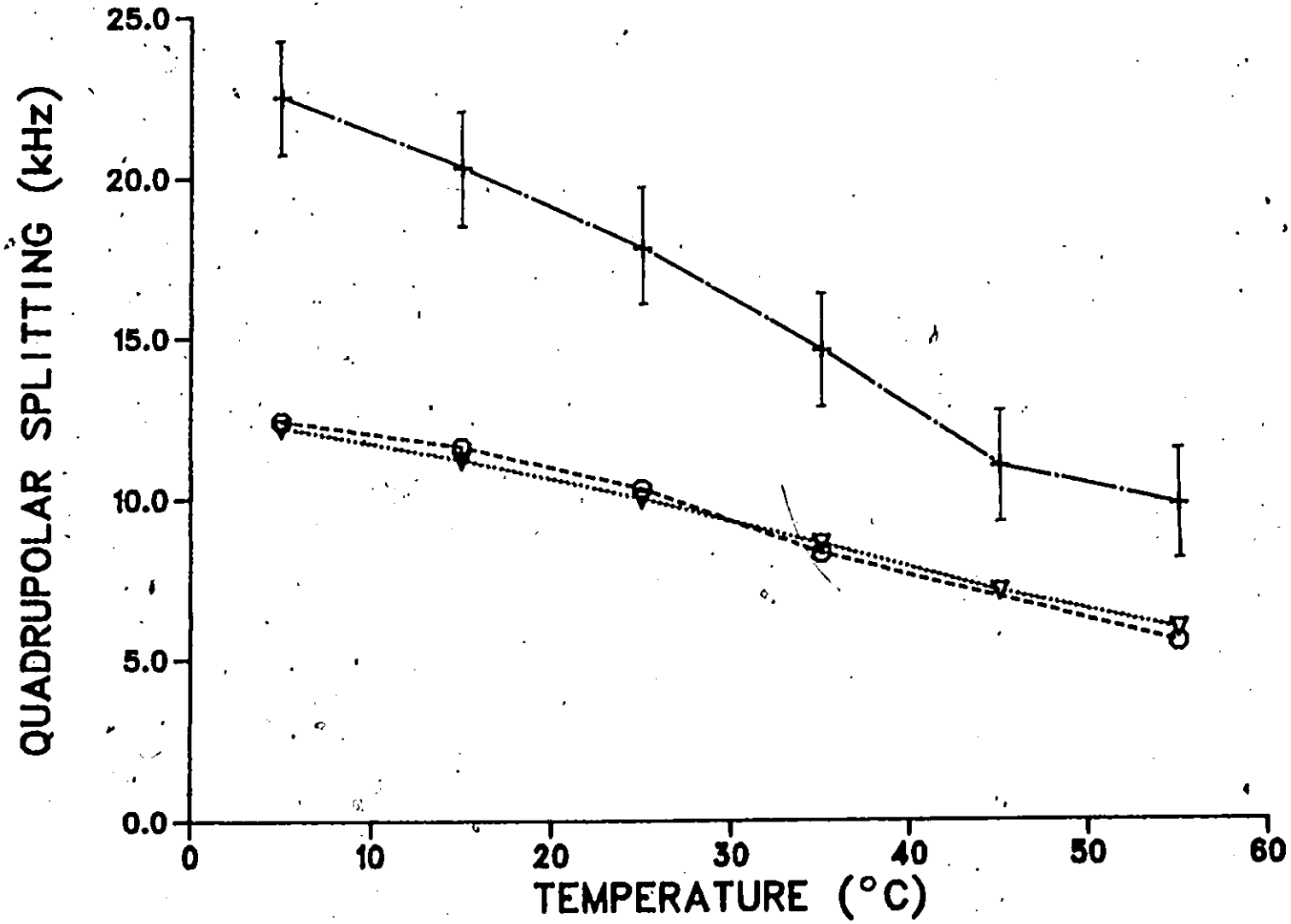

Fig. IV.3-6. Temperature variation of the quadrupolar splittings of DMPC labeled at C14'.
∇ – DMPC:β-cholesterol:Ampho B (major component).
+ – DMPC:β cholesterol:Ampho B (broad component).
O – DMPC:β-cholesterol.
The bars or symbols give an estimate of the error.

IV.3.2c Effect on the Entire Bilayer Thickness

In order to monitor the effect of Ampho B at several bilayer depths the above experiments have also been repeated using [sn-2-$^2H_{27}$] DMPC. Figure IV.3-7 shows the powder spectra with and without the antibiotic whereas Figure IV.3-8 shows the corresponding dePaked spectra, at 25°C. One notices in Figure IV.3-7, bottom, that the central methyl resonance exhibits a remarkable change in shape, as discussed above. The numbers on the dePaked spectra (Figure IV.3-8) represent $\Delta\nu_Q$ in kHz whereas the primed numbers stand for the labeled carbon position (the assignment has been accomplished based on previously published results, Oldfield, et al., 1978). At first sight, there are no changes between dePaked spectra arising from samples with and without Ampho B. However, a more detailed analysis shows that the resonances of C-^2H bonds at C14' and C13' decrease in intensity when the drug is present. This observation correlates well with the fact that a second broad component was observed at C14' but not at C4' (see previous section). The area at C14' is partitioned between the major and broad components; the major peak at C14', in presence of Ampho B, will be thereby less important relative to the plateau positions (C4' to C10') (the dePaked broad component cannot be reasonably detected in Figure IV.3-8). Since the plateau dePaked peaks for spectra with and without the

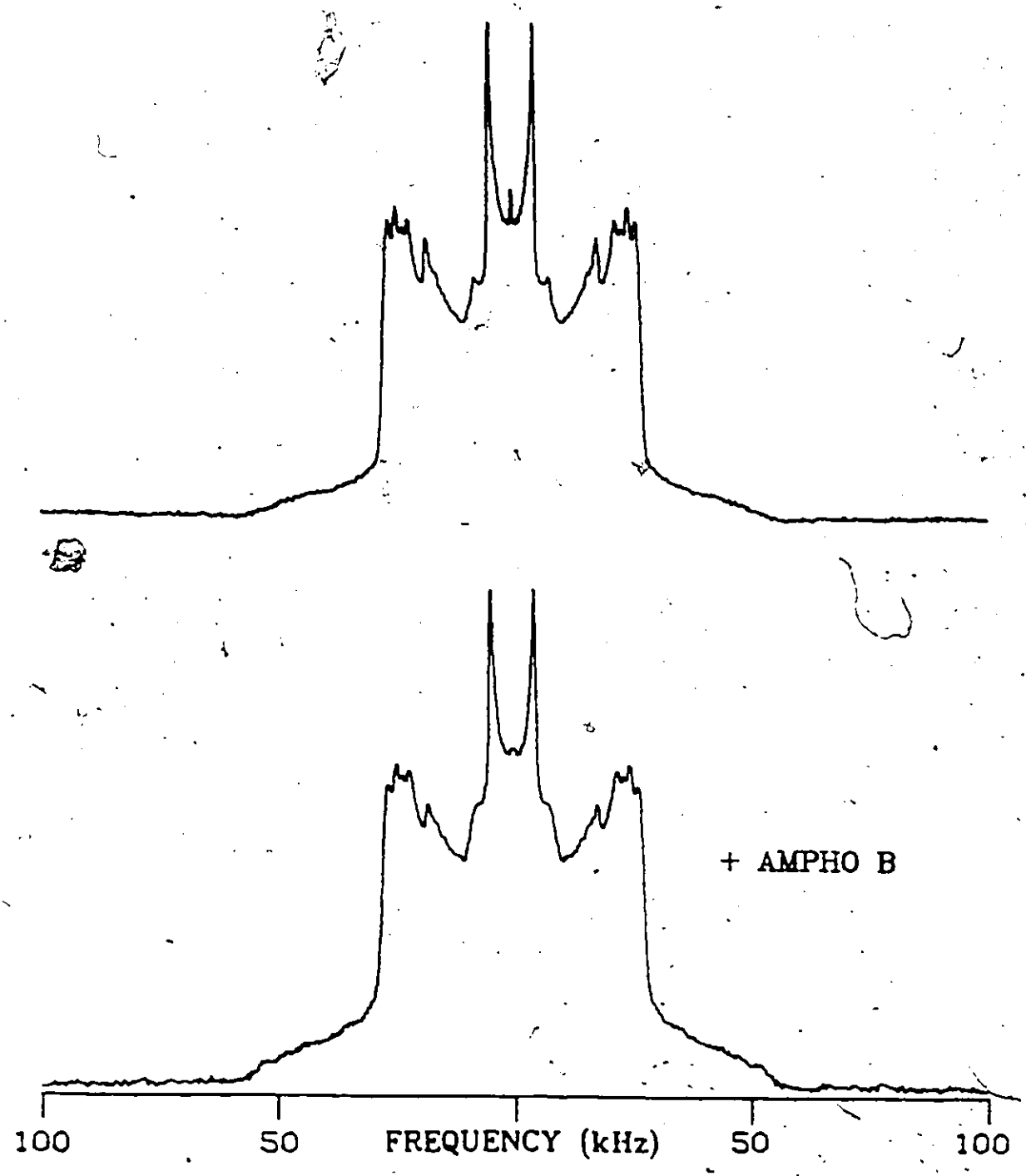

Fig. IV.3-7. ^2H-NMR spectra of the $[sn\text{-}2\text{-}^2H_{27}]$ DMPC:β-cholesterol system in the presence or absence of Ampho B, at 25 °C. Same experimental parameters as in Fig. IV.3-4 except spectral window of 500 kHz.

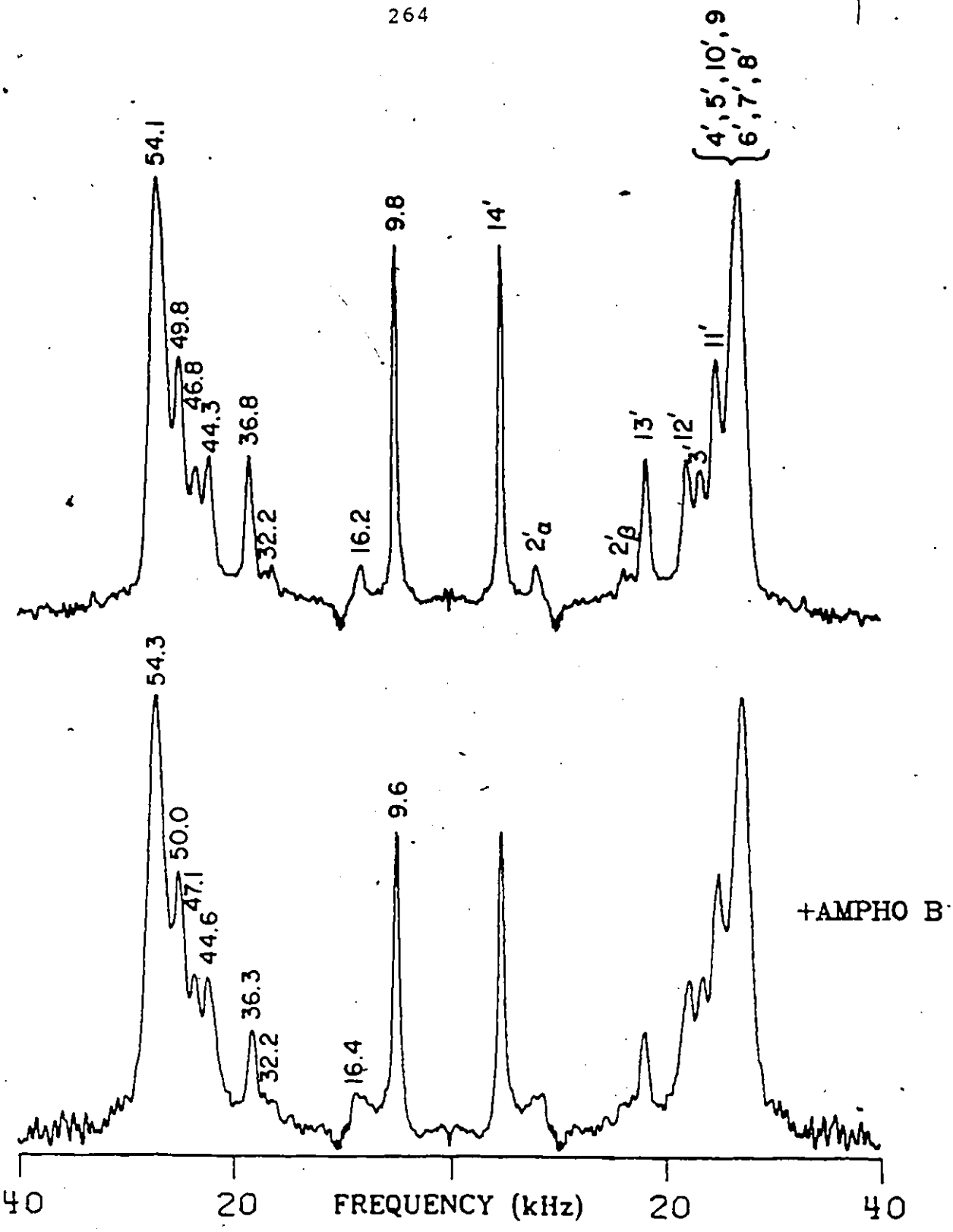

Fig. IV.3–8. Same as Fig. IV.3–7, but dePaked. Same processing parameters and notations as in Fig. IV.2–7.

antibiotic are scaled accordingly, the C14' peaks appear less intense in presence of the drug than in its absence. Similarly, the peaks at C13', on the bottom spectrum of Figure IV.3-8 appear less intense than their analogs on the top spectrum; this leads to the conclusion that a broad component appears also at C13', in addition to the detected major component. One should mention here that the line widths of the spectra with and without Ampho B are different (vide infra); however, the relative change is similar either at C4' or at C14' which leads to think that the comparison between relative intensities is reasonable.

It is also interesting to remark that the splittings at C14' and C13' are slightly smaller in the presence of the drug than in its absence, whereas for all other splittings, the converse is true. It appears therefore that although the Amphotericin B induces small spectral changes on the lipid deuterium powder spectra of cholesterol-containing membrane lipids, these changes are different at the plateau level than at the center of the bilayer. This will be discussed in Chapter IV.5.

IV.3.2d Relaxation Time Measurements

The spin-lattice, T_{1z}, and spin-spin, T_2, relaxation times were measured as described in Material and Methods.

T_{1z} and T_2 have been obtained at the lipid-labeled positions C4' and C14' for the DMPC:β-cholesterol system, in the presence or absence of Amphotericin B. The results are summarized in Table IV.3-1. T_{1z} and T_2 of the pure DMPC at C4' have also been reported in Table IV.3-1 for comparison. At 25°C, the spin lattice relaxation times at C4' are nearly identical for pure DMPC, DMPC:β-cholesterol or DMPC:β-cholesterol:Ampho B systems; the same is true for the lipid methyl group, C14'. The spin-spin relaxation time appears, however, to be more sensitive to the presence of Amphotericin B. Although the T_2 was found to vary across the powder pattern, the values reported in Table IV.3-1 were obtained from the total spectrum. The reason for doing so is that, up to now, there is no reliable theory, to our knowledge, to describe variation of T_2 across the powder pattern, in cases where this variation is not scaled as $P_2(\cos \beta_b)$. However, when there are marked changes in T_2 for different systems one can discuss in a general way the dynamics involved in the spin-spin relaxation mechanism. On comparing the T_2 at C4' and C14' for systems with and without Amphotericin B one notices (Table IV.3-1) that the spin-spin relaxation rates ($1/T_2$) are the greatest in presence of the drug. The broad component has a very high relaxation rate compared to that of C14' without the antibiotic. As a general comment, one can thus state that the presence of Ampho B in β-

Table IV.3-1

RELAXATION TIMES[a] OF THE β-CHOLESTEROL: AMPHO B:DMPC SYSTEM

System	Labeled Carbon Position	T_{1z} in ms	T_2[b] in μs
DMPC	[4'-$^2H_2$]	18.6	280
β-cholesterol:	[4'-$^2H_2$]	21.7	[illegible]
DMPC	[14'-$^2H_3$]	174	1180
β-cholesterol:	[4'-$^2H_2$]	20.2	264
Ampho B:DMPC	[14'-$^2H_3$][c]	183	632
	[14'-$^2H_3$][d]	158	282

[a] At 25°C and 46.1 MHz. Accuracy ± 5% on T_{1z} and ± 10% on T_2.
[b] Estimated from the entire powder pattern.
[c] Major component (see text).
[d] Broad component (see text), accuracy ~10% in T_{1z} and ~20% in T_2.

cholesterol:DMPC bilayers influences T_2 but not T_{1z}, that is, the antibiotic modulates the slow motions but has no effect on the fast motions. Since the ordering properties are nearly identical for both the DMPC:β-cholesterol and the DMPC:β-cholesterol:Ampho B model membrane systems one may conclude that the addition of Ampho B increases the amount of slow motions contributing to the lipid spin-spin relaxation time.

IV.3.3 Action of Amphotericin B on α-Cholesterol-Containing DMPC Membranes

The permeability studies mentioned in the introductory section concluded that the antibiotic was inducing more leakage when β-cholesterol rather than α-cholesterol was present in the membrane. This differential efficiency was attributed to the ability of the sterol OH group to make more hydrogen bonds with the Amphotericin B when located in β rather than in α position with respect to the steroid skeleton. In order to verify this hypothesis, the experiments described for β-cholesterol were repeated with the α-isomer. The lipid behaviour in systems containing only the sterol or the drug and the sterol, was monitored at both the plateau region and at the center of the bilayer by means of the [4', 14'-$^2H_5$] DMPC. Figure IV.3-9 shows the spectra of the lipid labeled at C4' and C14' either in presence of α-cholesterol

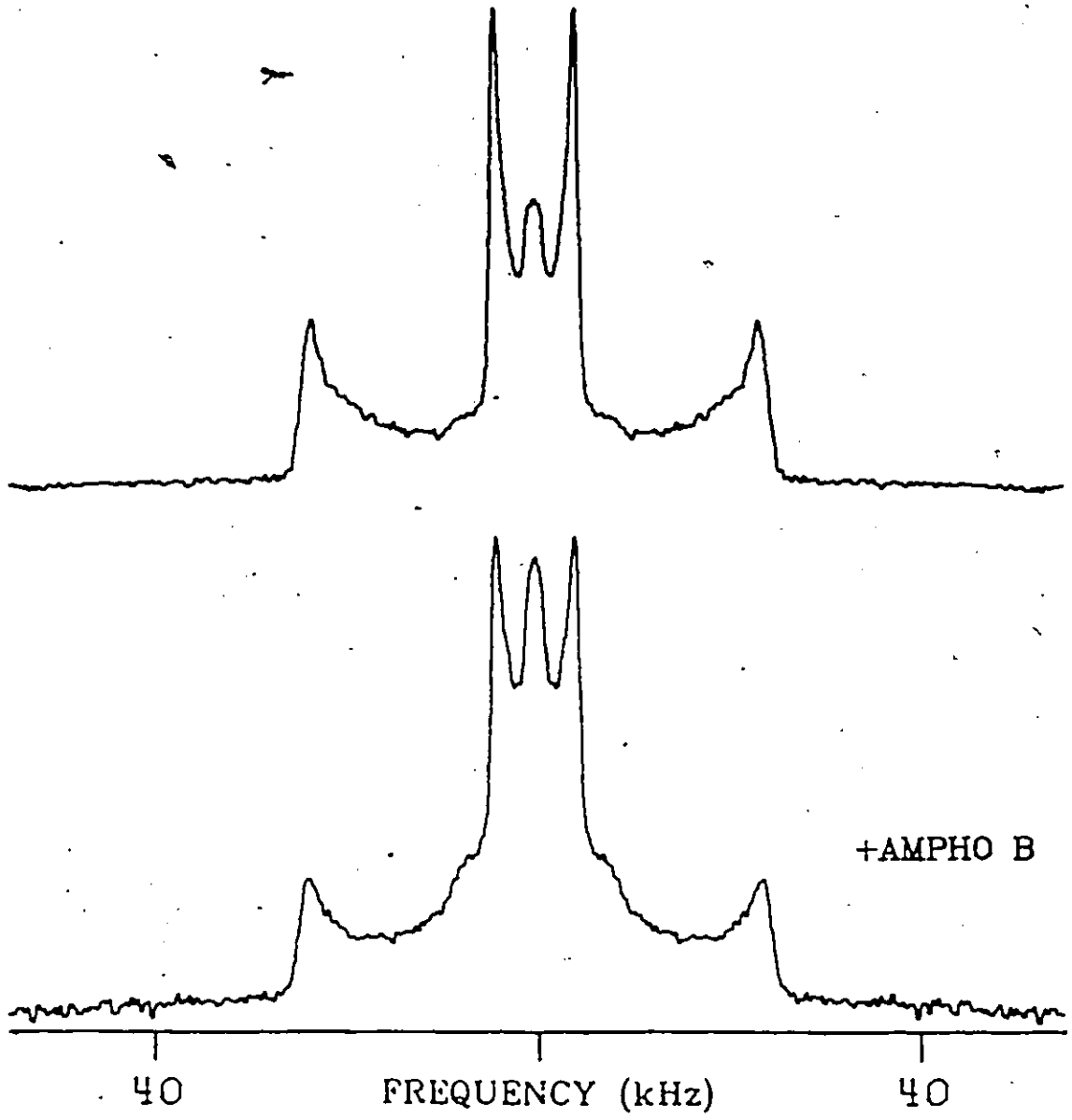

Fig. IV.3–9. ^{2}H–NMR spectra of the [4',14'–$^2H_5$] DMPC: α–cholesterol system in the presence or absence of Ampho B at 25°C. Same experimental parameters as in Fig. IV.3–7.

and α-cholesterol:Ampho B (1:1 molar ratio), at 25°C. The broad component found at C14' for the DMPC:β-cholesterol: Ampho B system is also present in the bottom spectrum of Figure IV.3-9, whereas no additional component is detected at C4'. The lipid quadrupolar splittings of these two systems (α-cholesterol with and without the antibiotic) have been measured at several temperatures and reported in Table IV.3-2. In this table, the $\Delta\nu_Q$ of the DMPC:β-cholesterol: Ampho B system have been also included for comparison.

It is interesting to notice in Table IV.3-2 that Amphotericin B acts so as to increase the lipid $\Delta\nu_Q$ of the DMPC:α-cholesterol system, especially at C4' and high temperatures. Assuming that the average orientation of the C-^{2}H reporter bonds is the same in samples with and without the Ampho B, one can say that the antibiotic induces ordering on the lipid of the DMPC:α-cholesterol system. It is also interesting to remark that this ordering effect is accomplished such that, at high temperatures, the lipid at C4' in the DPMC:α-cholesterol:Ampho B system almost reaches that of the lipid at C4' in the DMPC:β-cholesterol:Ampho B model membrane system. Since it has been shown already that α-cholesterol induces less ordering on the lipid than does β-cholesterol, at temperatures above 23°C (see Chapter III.1), it appears thus the Amphotericin B provides some of this "missing" ordering to the α-cholesterol-containing lipid

Table IV.3-2

LIPID QUADRUPOLAR SPLITTINGS[a] IN THE α-CHOLESTEROL: AMPHO B:DMPC SYSTEM

System	Labeled Carbon Position	Temperature (°C) 10	20	25	30	35	45	55
α-cholesterol	[4'-$^2H_2$]	53.7[b]	50.8	48.3	45.9	43.0	38.3	34.9
DMPC	[14'-$^2H_3$]	12.0[b]	10.3	9.3	8.3	7.3	5.9	5.1
α-cholesterol:	[4'-$^2H_2$]	54.0[b]	51.7	47.0		45.0	41.0	37.1
Ampho B:DMPC	[14'-$^2H_3$][c]	11.7[b]	10.3	9.3		7.5	6.4	5.4
β-cholesterol:	[4'-$^2H_2$]	54.7[b]	52.4	51.0	49.0	47.0	42.6	38.8
Ampho B:DMPC	[14'-$^2H_3$][c]			10.0		8.6	7.1	5.9

[a] From dePaked spectra, in kHz, accuracy 1-2%.
[b] Estimated on the powder spectra, accuracy ~5%.
[c] Quadrupolar splitting of the major component (see text).

system in order to mimic the ordering properties of the β-cholesterol-containing DMPC (with or without Ampho B). At C14', the situation is even more complex. Indeed Ampho B orders the major lipid component weakly and restricts highly the angular fluctuations of a certain percentage of the lipid, previously described as being the C14' "broad component". The percentage of that broad component as well as its spectral width were found to decrease when the temperature of the system was increased. It is thus interesting to remark that the antibiotic induces similar effects on lipid membranes containing either α- or β-isomers of cholesterol.

IV.3.4 Concluding Remarks

The ^{2}H-NMR changes induced by the polyene antibiotic Amphotericin B when it is added to lipid model membranes containing α- or β-cholesterol vary with the bilayer depth. At the plateau level, there are no detectable changes in the lipid ordering of the system containing β-cholesterol whereas the antibiotic induces order in lipid containing α-cholesterol. At the lipid tail (C14' and probably C13') two spectral components appear (either with α- or β-cholesterol) when the drug is present. One of these spectral components shows ordering properties nearly identical to those of the labeled tail positions when the antibiotic is absent whereas

the other broad component indicates that the lipid C-^{2}H bond fluctuations at C14' are highly restricted by the presence of Ampho B. The amount of the additional component as well as its ordering properties are a function of the temperature: both decrease when the temperature increases.

Amphotericin B was also found to affect T_2 rather than T_{1z} of the lipid containing β-cholesterol. The reduction in T_2 for both the plateau and the tail labeled positions led to the conclusion that the antibiotic increases the density of slow motions participating in the spin-spin relaxation phenomenon of the lipid, at 25°C.

CHAPTER IV.4

AMPHOTERICIN B AND MODEL MEMBRANES

4. CHOLESTEROL-CONTAINING LIPID SYSTEMS-CHOLESTEROL VIEWPOINT

IV.4.1 Introduction

Using a deuterium labeled lipid, it has been possible to follow the perturbations induced by Amphotericin B on a cholesterol-containing model membrane (see Chapter IV.3). The structural and dynamical information was obtained from the lipid ^{2}H-NMR response, that is, the properties of the matrix in which the antibiotic and the cholesterol are embedded are now better understood. However, one still needs to know in which way the cholesterol and the antibiotic interact, at the molecular level.

In the following section the cholesterol:Ampho B: DMPC interactions will be studied from the cholesterol molecule viewpoint, that is, using deuterated cholesterol as the reporter molecule. The model membrane of interest will be identical to that of the previous section, that is, DMPC:deuterated sterol (7:3 molar ratio) in which the antibiotic, when added will be at equimolar amounts with the cholesterol.

IV.4.2 Action of Ampho B on DMPC Model Membranes Containing β-Cholesterol

IV.4.2a The Plateau Region

In the previous sections, the structural and dynamical informations at the plateau level were recorded by means of the [4'-$^2H_2$] DMPC. In order to follow the sterol properties at the same bilayer level, cholesterol labeled in the two first rings ([2,2,3,4,4,6-$^2H_6$]β-cholesterol) was employed. Figure IV.4-1 shows the deuterium spectra of cholesterol in DMPC in the presence and absence of antibiotic, at several temperatures. The central peak of the powder patterns has been deliberately truncated in order to enhance details of the overall spectral shapes. One notices that the perturbations induced by Ampho B are of weak magnitude or undetectable. The only noticeable changes in spectral shape occur at low temperatures (0°, 5°C). It has been shown in the previous sections that at these temperatures the β-cholesterol spectral shape changes, in DMPC, could be explained by the appearance of axially-asymmetric motions. The same phenomenon also appears for β-cholesterol in presence of the antibiotic. However, the loss of axially-symmetric shapes seems to occur at higher temperatures in the presence of Ampho B than in its absence; one notices indeed that the spectral shape of β-cholesterol with Ampho B

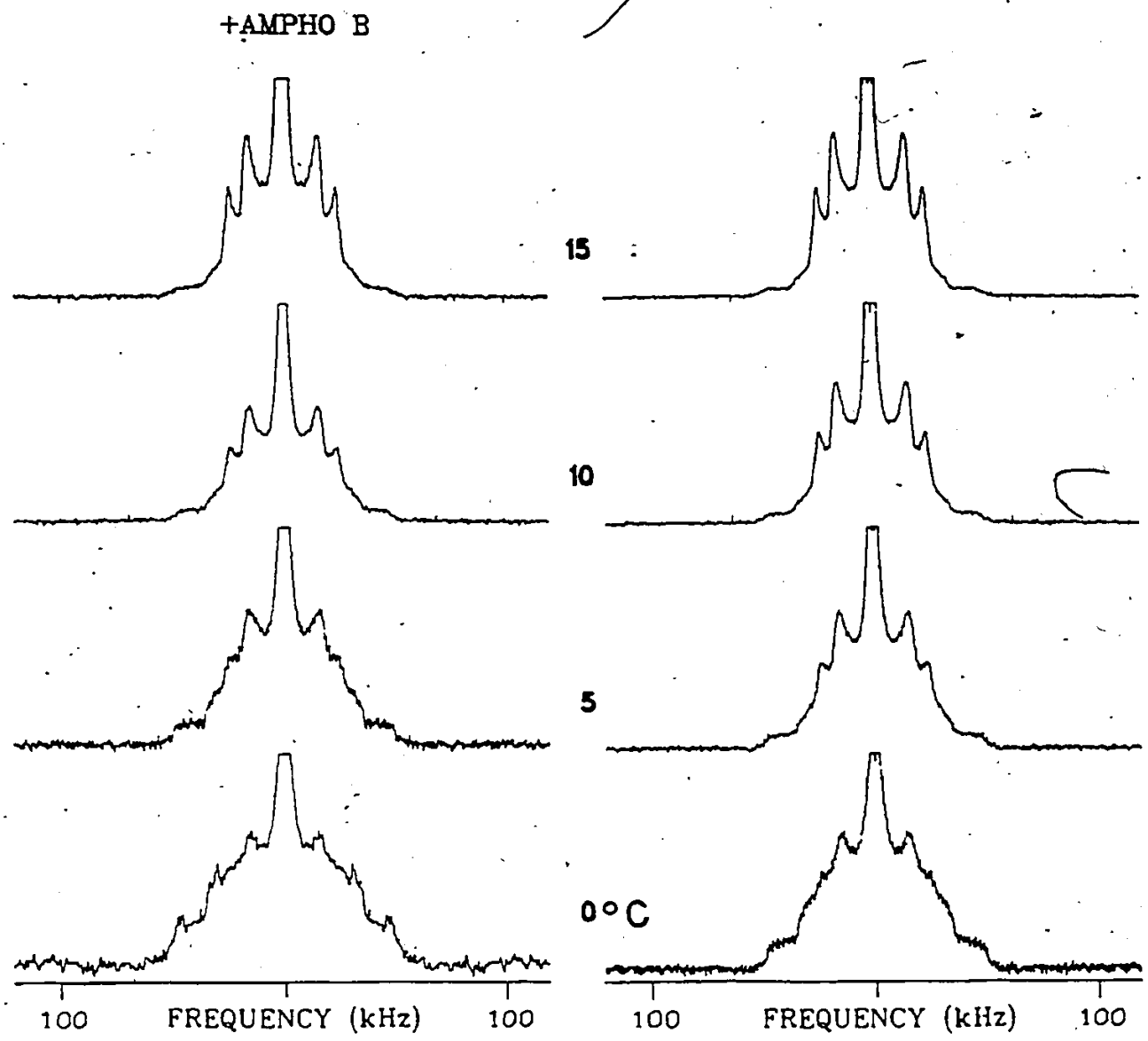

Fig. IV.4–1. Temperature dependence of the ^2H–NMR spectral shapes of [2,2,3,4,4,6–$^2H_6$] β–cholesterol in DMPC, in the presence or absence of Amphotericin B. Same experimental parameters as in Fig. III.1–3.

at 5°C is almost identical to that of the sterol without the P.A. at 0°C. It appears therefore that the presence of Amphotericin B in the model membrane could restrict the axial motions of cholesterol at low temperature.

At temperatures above 10°C, the spectra with and without the drug do not exhibit marked differences. The variation of the β-cholesterol quadrupolar splittings with temperature has been followed up to 65°C. Some representative values are reported in Table IV.4-1 for systems with and without Ampho B. One notices that the only significant differences in quadrupolar splitting occur at high temperatures, for example, at 65°C where the sample containing the drug exhibits higher cholesterol quadrupolar splittings than the system lacking the antibiotic. The segmental or molecular order parameter of β-cholesterol has been calculated for the sample containing Amphotericin B, as described in Section III.1.3b, and compared with that of β-cholesterol in DMPC, without the P.A. (Figure IV.4-2). It appears in Figure IV.4-2 that up to 40°C both order profiles are identical. The two profiles diverge at high temperatures; the β-cholesterol order parameter of the sample containing the drug is slightly higher than that of the system without it. This finding shows that Ampho B extends the temperature-independent "wobbling" of cholesterol by some 20°C, such that there is almost no change in the angular

Table IV.4-1

QUADRUPOLAR SPLITTINGS[a] OF α- AND β-CHOLESTEROL

System	Labeled Carbon[b] Position	Temperature 25°C	40°C	65°C
β-cholesterol:	[6-^{2}H]	3.4	3.2	2.2
DMPC	[3-^{2}H]	51.5	50.8	46.4
	[2-^{2}H]$_{eq}$[c]	34.2	33.6	30.3
	[4-^{2}H]$_{eq}$[c]	32.0	31.4	30.3
	[2,4-^{2}H$_2$]$_{ax}$	48.2	47.0	43.4
β-cholesterol:	[6-^{2}H]	3.6	3.3	3.0
DMPC:Ampho B	[3-^{2}H]	51.8	50.2	47.4
	[2-^{2}H]$_{eq}$[c]	34.4	33.8	31.2
	[4-^{2}H]$_{eq}$[c]	31.8	31.4	31.2
	[2,4-^{2}H$_2$]$_{ax}$	48.4	47.4	44.6
α-cholesterol:	[6-^{2}H]	5.8	7.8	10.2
DMPC	[2-^{2}H]$_{ax}$	54.7	52.2	46.6
	[2-^{2}H]$_{eq}$	24.9	20.5	13.1
	[4-^{2}H]$_{ax}$	54.7	52.2	46.6
	[4-^{2}H]$_{eq}$	24.9	23.0	18.6
α-cholesterol:	[6-^{2}H]	4.2	4.9	7.5
DMPC:Ampho B	[2-^{2}H]$_{ax}$	54.8	54.2	49.3
	[2-^{2}H]$_{eq}$	26.4	24.2	19.0
	[4-^{2}H]$_{ax}$	54.8	54.2	49.3
	[4-^{2}H]$_{eq}$	26.4	24.2	19.0

[a] In kHz, accuracy 1-2%.
[b] Assignment according to calculations described in Section III.1.3b.
[c] The assignment of these deuterons is arbitrary and could be reversed.

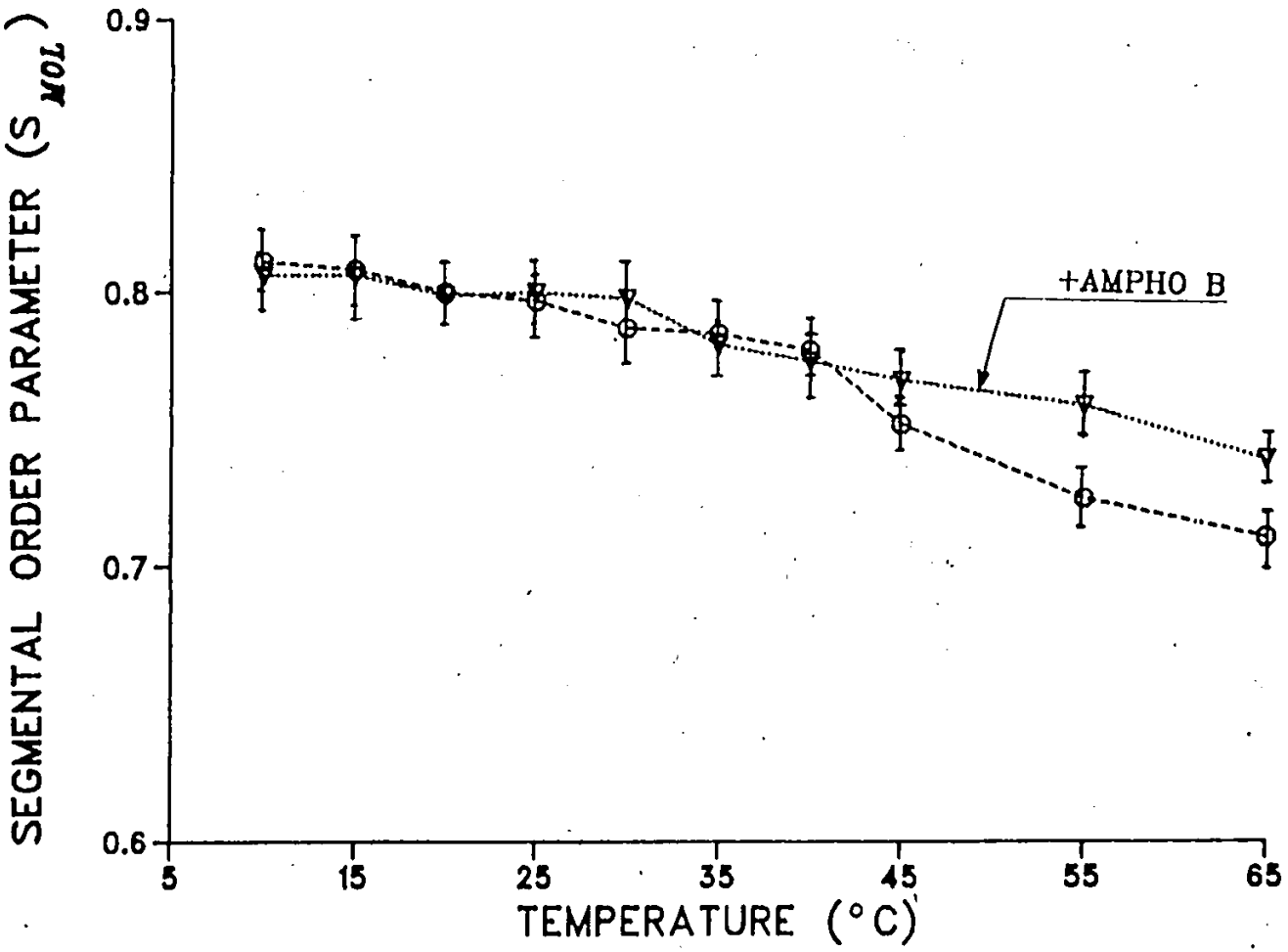

Fig. IV.4–2. Temperature dependence of the segmental order parameter, S_{MOL} , of the four rings of β–cholesterol, in DMPC, with and without Amphotericin B.

fluctuations of cholesterol from 10°C to ~60°C. The motional axis of the sterol and thereby the orientation of the β-cholesterol molecule with respect to the bilayer normal were calculated using the method already described in Section III.1.3b. It was found that the position of the β-cholesterol within the bilayer membrane is identical for systems with and without the antibiotic, that is, if the complex Amphotericin B:β-cholesterol exists it must be such that the sterol is normal to the membrane surface.

IV.4.2b The Tail Region

[24-$^2H_2$]-β-cholesterol and [26,27-$^2H_6$]-β-cholesterol were also used to monitor the spectral changes induced by Amphotericin B on cholesterol-containing model membranes. The spectra of both labeled sterols are shown in Figure IV.4-3 and IV.4-4, respectively, as a function of temperature. The two superimposed powder patterns of Figure IV.4-3 (without the Ampho B) are the result of two different average orientations, with respect to the axis of motion, of the two C-^2H bonds at C24 (see Section III.1.4). One notices in Figure IV.4-3 that the deuterium spectra, with and without the antibiotic, are very similar. Table IV.4-2 shows some representative quadrupolar splitting values for both sets of spectra. One remarks again that the presence of Ampho B induces very

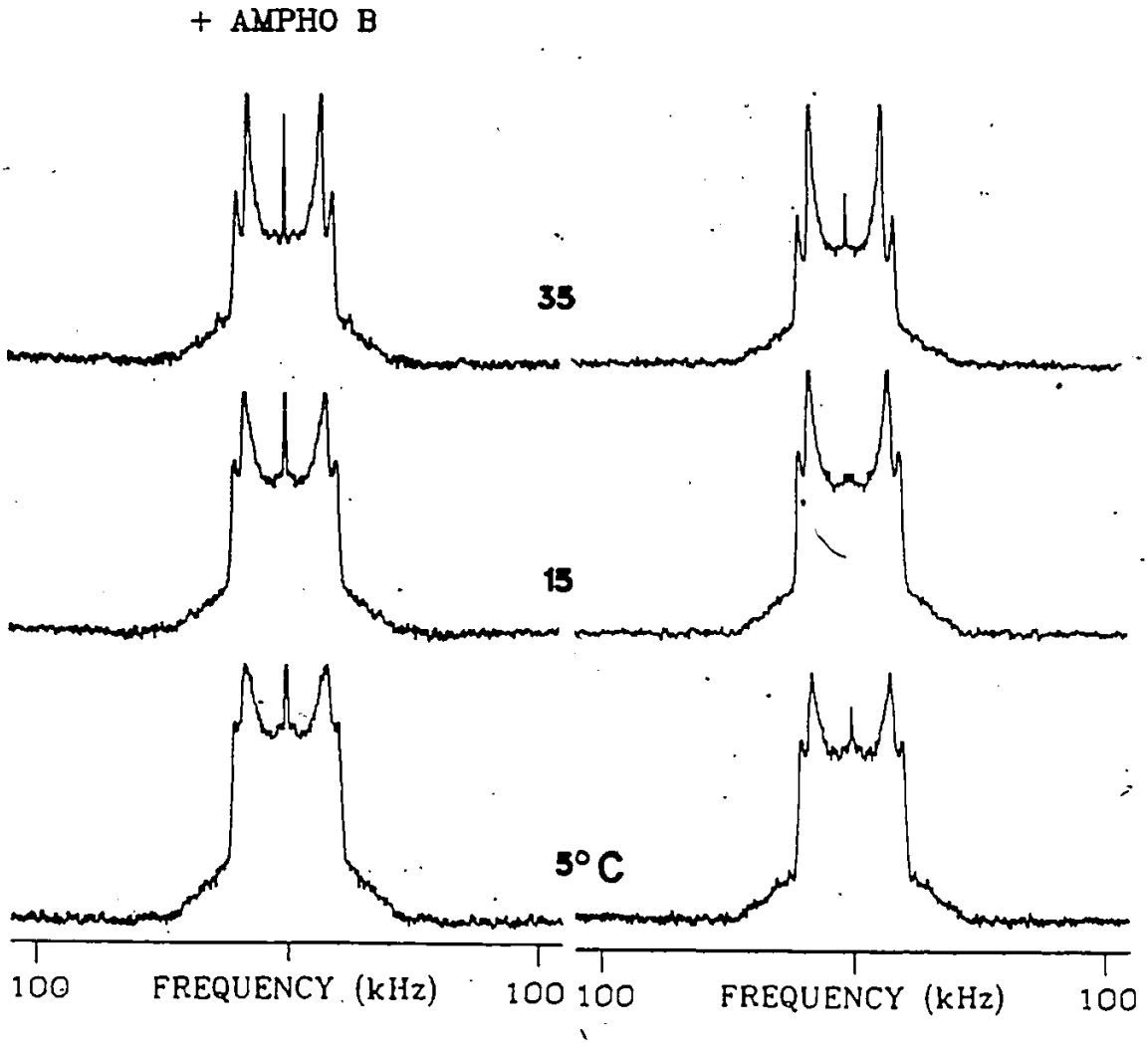

Fig. IV.4–3. ^{2}H–NMR spectra of $[24-^2H_2]\beta$–cholesterol, in DMPC, with and without Ampho B. Same experimental parameters as in Fig. IV.4–1 except recycle time of 100 ms.

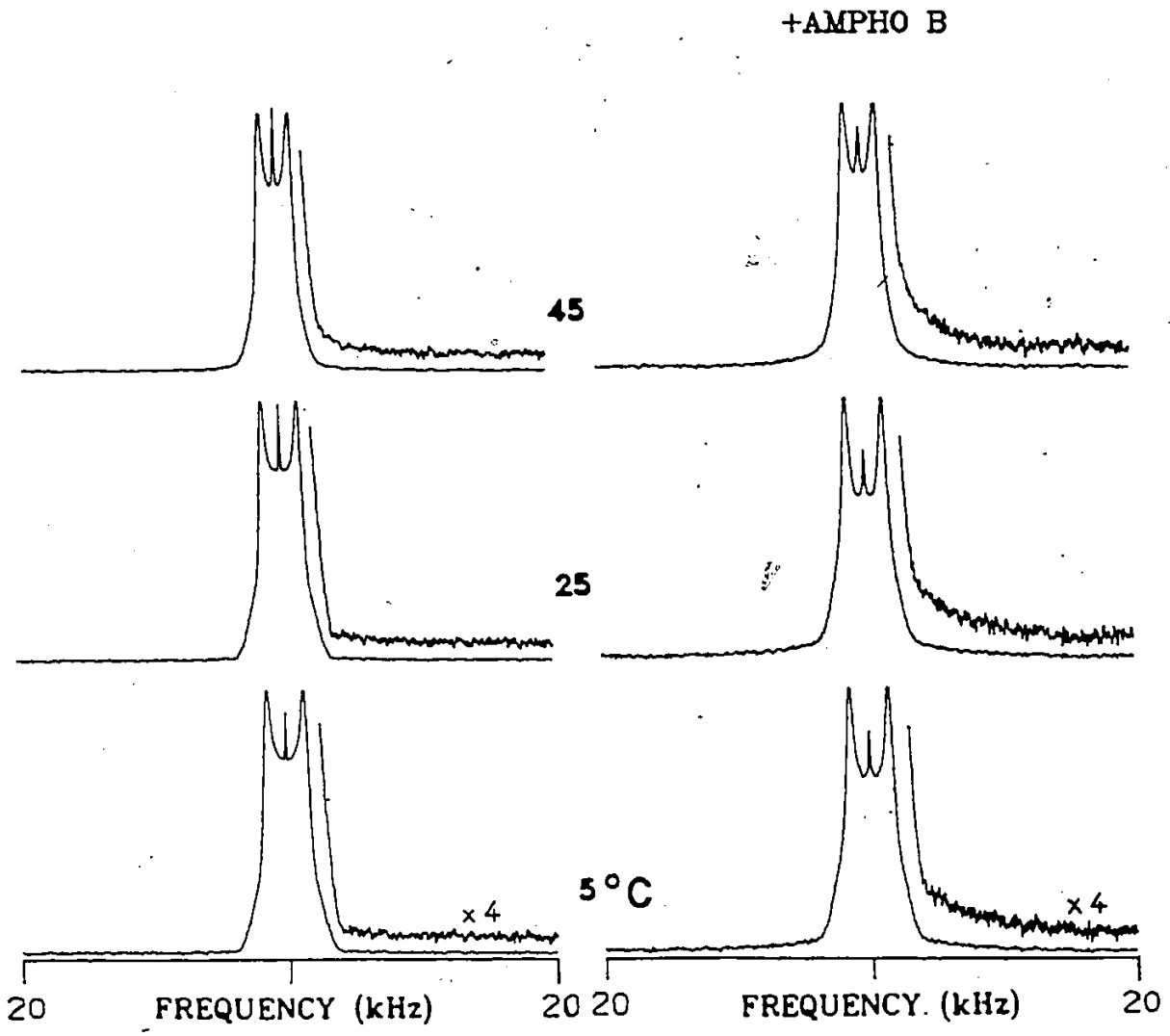

Fig. IV.4–4. ^{2}H–NMR spectra of $[26,27\text{-}^2H_6]$ β–cholesterol, in DMPC, with and without Amphotericin B.
Same experimental parameters as in Fig. IV.4–1 except recycle time of 300 ms; spectral window of 125 kHz; and 5,000 accumulations.

Table IV.4-2

QUADRUPOLAR SPLITTINGS[a] OF β-CHOLESTEROL WITH AND WITHOUT AMPHOTERICIN B

System	Labeled Carbon Position	Temperature 15°C	45°C	65°C
β-cholesterol:	[24-^{2}H]	33.2	27.8	23.7
DMPC	[24-^{2}H]	42.0	38.1	34.4
β-cholesterol:	[24-^{2}H]	33.4	28.3	23.4
DMPC:Ampho B	[24-^{2}H]	42.2	38.1	34.0

[a] In kHz, accuracy 1-2%.

weak changes in $\Delta\nu_Q$. Figure IV.4-4 exhibits the ^{2}H-NMR response of the two methyl groups (at C26 and C27) of cholesterol in DMPC, in the presence or absence of Amphotericin B. Although the shapes of both spectral sets are very similar one notices that the spectra of sample containing the antibiotic show a broad component in addition to the major powder spectrum. This may be compared with the occurrence of a similar spectral feature in the spectra of [14'-$^2H_3$] DMPC for the same model membrane system (see previous chapter). However, the relative amount of that broad component (≤5%), at C26 and C27, is very small in comparison to that found at C14' in DMPC. Therefore, the occurrence of such a small feature will not be discussed further. The major component in the spectral set with Ampho B has identical $\Delta\nu_Q$ to that found at C26 and C27 in absence of the antibiotic at corresponding temperatures. One can therefore conclude that the antibiotic has little effect on the ordering properties of the cholesterol tail, in the DMPC:β-cholesterol: Ampho B model membrane system.

IV.4.2c Relaxation Times, T_{1z}, T_2

The spin-spin, T_2, and spin-lattice, T_{1z}, relaxation times have been measured for cholesterol in DMPC containing Ampho B according to the techniques described in Materials

and Methods. Table IV.4-3 summarizes the results. It is interesting to compare the T_{1z} of cholesterol in DMPC (Chapter III.2) with those of Table IV.4-3. The spin-lattice relaxation times at position C6 have been plotted in Figure IV.4-5 for systems with and without the Ampho B. It is interesting to notice that both sets of data yield a minimum in T_{1z}, at which the effective correlation time, τ_{eff}, of the motion is equal to $p2\pi\nu_0$ (see Chapter III.2), that is, 1.73×10^{-9} s $\leq \tau_{eff} \leq 3.45\ 10^{-9}$ s. The presence of such a minimum has already been discussed in Chapter III.2 where an attempt was made to describe the cholesterol motions in terms of fast and slow motions using the theoretical model derived by Brown (1982). Although a similar analysis could also be carried out with the present data, we will only discuss the cholesterol motions in a general way by analogy with the results of Chapter III.2. The noticeable feature in Figure IV.4-5 is the shift in the minimum of T_{1z} towards high temperatures in the presence of Amphotericin B. The minimum occurs around 32-35°C when Ampho B is absent, and around 38-40°C when it is present. This indicates that the system containing Ampho B has to be warmed by ~5°C in order to relax with the same efficiency as the system without the drug. In other words, the motions of β-cholesterol in DMPC are slowed down when the Amphotericin B is added. Unfortunately, the two minima are not separated enough to allow

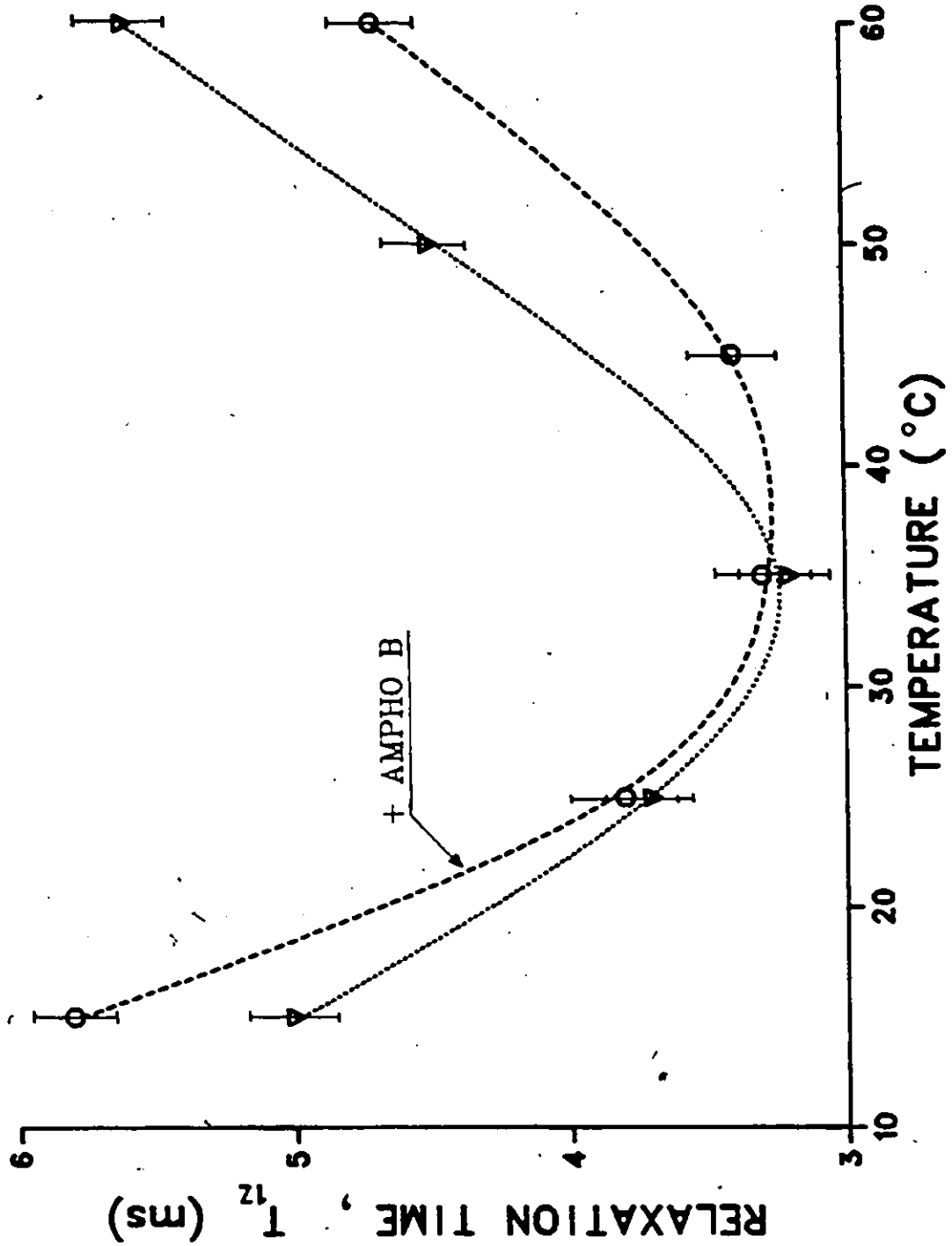

Fig. IV.4–5. Temperature dependence of the relaxation time, T_{12}, of $[\beta\text{-}^2H]\beta$-cholesterol in DMPC, in the presence or absence of Amphotericin B. The bars give an estimate of the error.

Table IV.4-3

RELAXATION TIMES OF β-CHOLESTEROL AT 46.1 MHz

System	Labeled Carbon Position	T_{1z} 15°C	T_{1z} 25°C	T_{1z} 35°C	T_{1z} 45°C	T_{1z} 60°C	T_2 25°C	T_2 25°C
β-cholesterol:	[6-^{2}H]	5.8	3.8	3.3	3.4	4.7	200	(260)[c]
DMPC:Ampho B	[3-^{2}H][d]	9.3	6.4	6.6	6.7	10.1	200	(260)[c]
	[2,4-$^2H_2$]$_{ax}$	9.2	6.0	5.6	6.2	8.3	200	(260)[c]
	[2-^{2}H]$_{eq}$	7.1	4.5	4.1	4.1	6.0	200	(260)[c]
	[4-^{2}H]$_{eq}$	7.1	4.6	4.0	4.4	6.0	200	(260)[c]
α-cholesterol:	[6-^{2}H]		4.4					
DMPC:Ampho B	[2,4-$^2H_2$]$_{ax}$		7.3					
	[2,4-$^2H_2$]$_{eq}$		5.4					

[a] T_{1z} in ms, accuracy ~5%; T_2 in μs, accuracy ~20%.
[b] The assignment of these positions is arbitrary and could be inverted.
[c] T_2 of β-cholesterol in DMPC, without Amphotericin B.
[d] Accuracy ~10%.

a quantitative characterization of the motional reduction induced by Amphotericin B.

The spin-spin relaxation time of β-cholesterol has also been measured with and without the antibiotic (Table IV.4-3). It has to be mentioned that it was impossible to measure T_2 for each deuteron (T_2 was found to vary across the powder patterns); the values reported in Table IV.4-3 stand for the entire spectrum of β-cholesterol. Unlike the results found for the deuterated lipids (see previous chapter) there is little change in the cholesterol T_2 on addition of Amphotericin B.

IV.4.3 Action of Ampho B on α-Cholesterol-Containing DMPC Model Membranes

The experiments carried out with β-cholesterol labeled in the two first rings (A, B) (previous section) were repeated with [2,2,3,4,4,6-$^2H_6$]-α-cholesterol for temperatures between 20 and 65°C. Some representative spectra are shown in Figure IV.4-6. One notices that the spectra of deuterated α-cholesterol in DMPC, with and without Ampho B are quite similar at 25°C whereas they differ markedly at higher temperatures. Some representative values of $\Delta\nu_Q$ have been reported in Table IV.4-1 for systems with and without the antibiotic. It has been shown in the preceding sections that the collapse

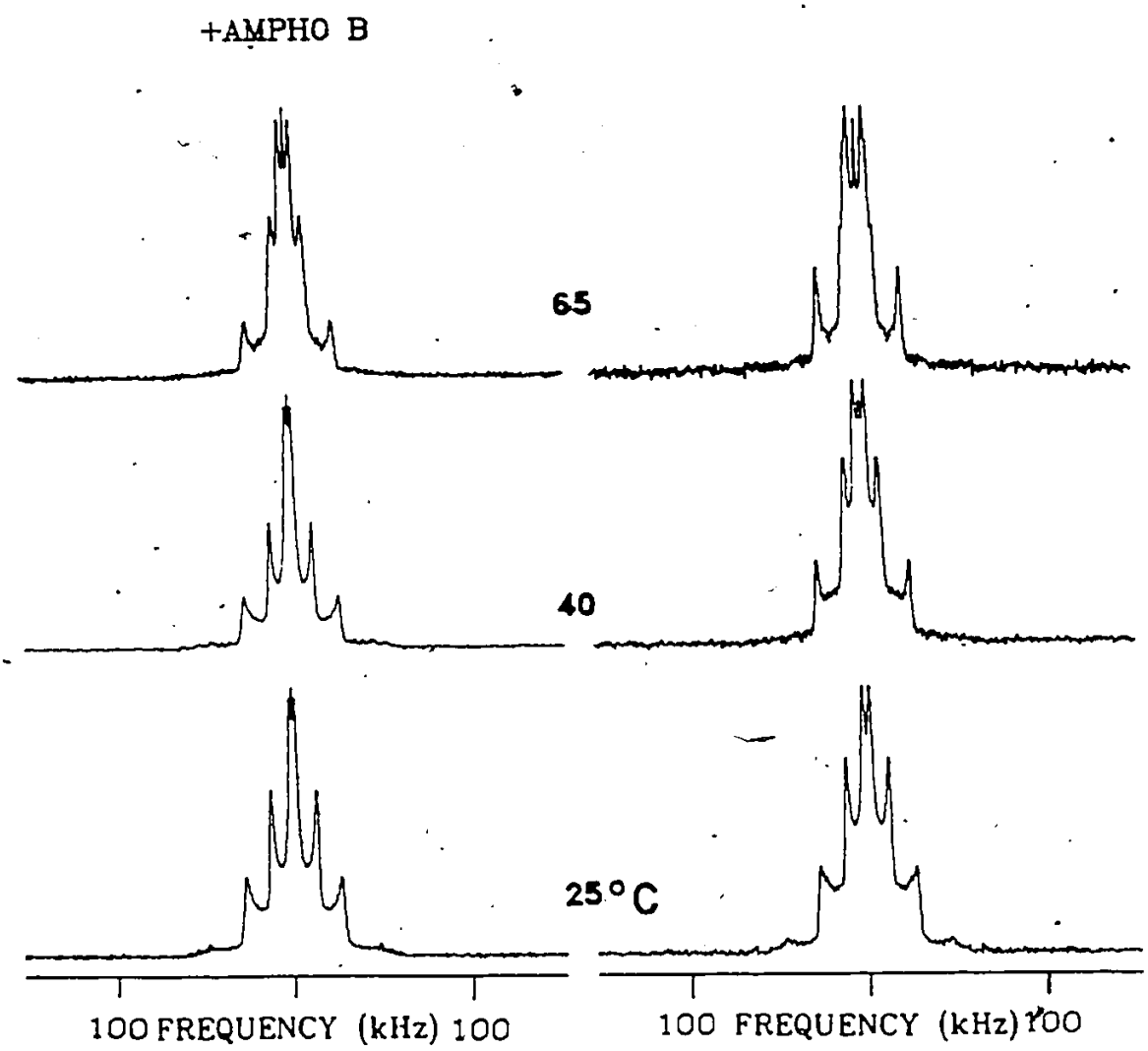

Fig. IV.4–6. ^{2}H–NMR spectra of [2,2,3,4,4,6–$^2H_6$]α–cholesterol in DMPC, with and without Amphotericin B. Same experimental parameters as in Fig. IV.4–1.

of the central part of the powder pattern of α-cholesterol in DMPC, at high temperatures, was due to the reorientation of α-cholesterol within the bilayer membrane. This reorientation is characterized by a marked decrease of the quadrupolar splittings at the equatorial positions C2 and C4 with a concomitant increase of $\Delta\nu_Q$ at C6. The spectra of the antibiotic-containing sample show a similar behaviour, that is, a reorientation of α-cholesterol on raising the temperature. However, it appears that the variation of splittings at C2, C4 and C6 is less pronounced when Ampho B is present in the system, over the same temperature range. It appears therefore that the antibiotic retards in some way the temperature-induced reorientation of α-cholesterol in DMPC. The reorientation of α-cholesterol can be characterized, as shown in Chapter III.1, by following the change in average orientation of a given C-^{2}H bond with respect to the axis of motion. Unfortunately, due to the inaccuracy involved in the measurement of $\Delta\nu_Q$ and due to the intrinsic inaccuracy of the calculation, the change in average orientation of this given C-^{2}H bond, in presence versus absence of Ampho B, was within the error domain ($\pm 2^o$). One cannot therefore describe quantitatively the retardation induced by Ampho B in the reorientation of α-cholesterol in DMPC, on raising the temperature.

The molecular order parameter of α-cholesterol in the DMPC: α-cholesterol: Amphotericin B system was calculated according to the procedure described in Chapter III.1. The results are plotted together with S_{mol} of α-cholesterol in DMPC (see Chapter III.1) as a function of temperature (Figure IV.4-7). It has to be remembered that the calculation described in Appendix F could not discriminate between two solutions for the axis of motion of α-cholesterol in DMPC and hence, between the two possible order parameters at a given temperature (Chapter III.1). Therefore, the calculation for the Ampho B-containing case was carried out for both solutions (1 and 2), leading to four curves in Figure IV.4-7. The filled symbols on that figure represent S_{mol} of α-cholesterol, in the presence of Amphotericin B, according to solutions 1 and 2. One notices that the Ampho B increases the molecular order parameter of the four-ring structure of α-cholesterol by ca. 10% and that this conclusion is independent of choice of solution. It is interesting to notice that this increase is quasi-constant over the temperature range 20°C to 65°C. This finding agrees well with the increase in the segmental order parameter of DMPC labeled at C4', induced by the addition of Ampho B to the DMPC: α-cholesterol model membrane system (vide supra).

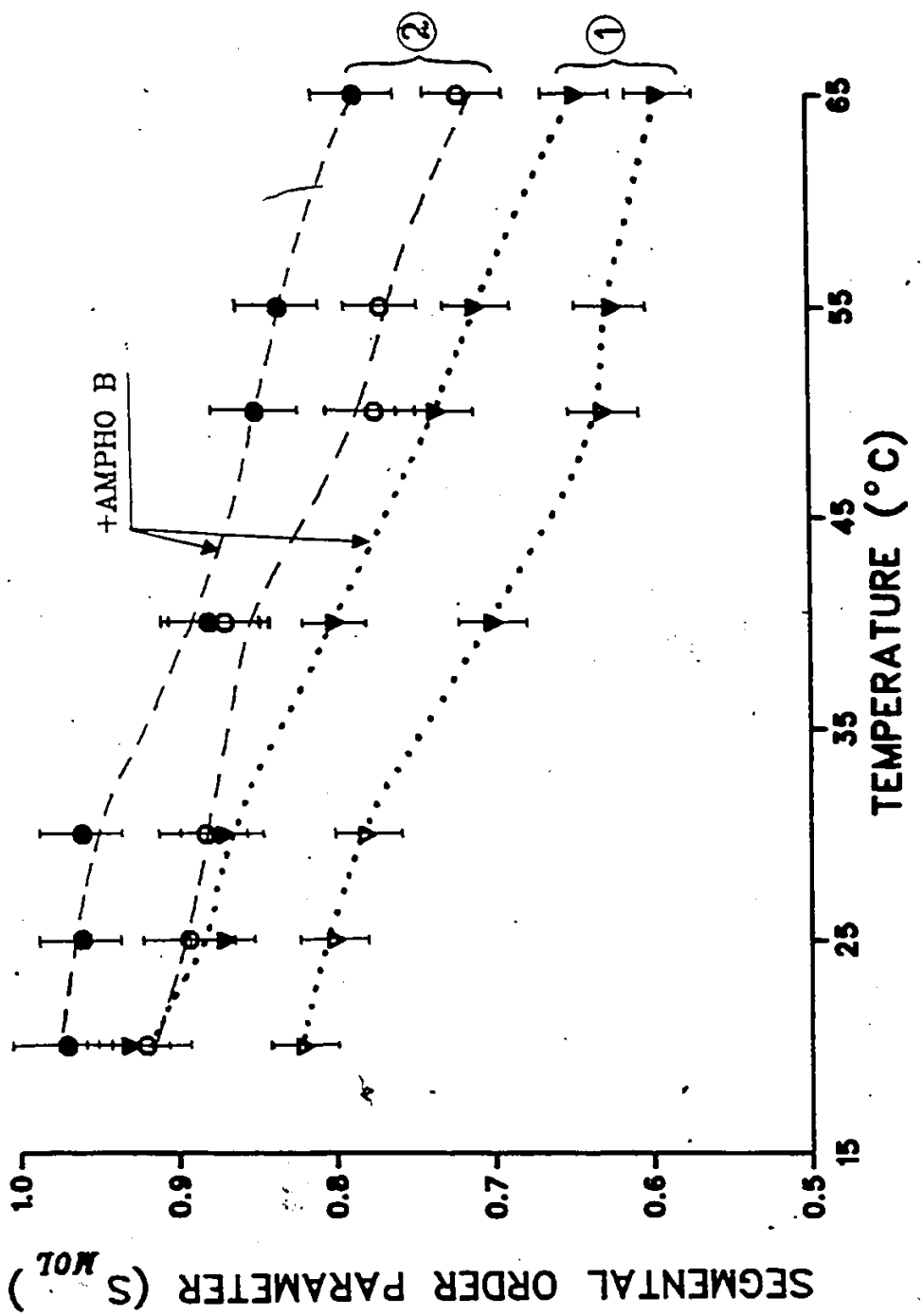

Fig. IV.4-7. Temperature dependence of the segmental order parameter, S_{MOL}, of the four rings of α-cholesterol in DMPC, in the presence (filled symbols) or absence (emptied symbols) of Ampholericin B, according to solutions ① and ② (see text).

IV.4.4 Concluding Remarks

As viewed by ^{2}H-NMR, the ordering properties of β-cholesterol in model membrane systems are weakly modified by the addition of Amphotericin B. The only noticeable changes were observed at low temperatures where it appeared that the antibiotic increased by 5°C the lower limit of the cessation of rapid, axially-symmetric motions of β-cholesterol in DMPC. At high temperatures, Ampho B extends by 20°C the temperature independent cholesterol "wobbling", that is, it acts on the system in a way such that the angular fluctuations of the four-ring structure of β-cholesterol vary by less than 10% between 10°C and 65°C. On the other hand, β-cholesterol labeled in its side chain at C24, showed that the antibiotic did not induce detectable ^{2}H-NMR spectral changes when present in the DMPC: β-cholesterol mixture. A small broad component (less than 5% of the total spectral intensity) appeared when Ampho B was added to DMPC containing β-cholesterol labeled at C26 and C27 (the terminal methyl groups); however, the major spectral component had quadrupolar splittings identical to those of spectra without the drug.

It was also observed that the addition of Ampho B increased the temperature of the minimum in T_{1z} of β-cholesterol by 5°C, which corroborates the increase by 5°C of the lower limit of the axially symmetric motions of β-cholesterol.

The addition of Amphotericin B to α-cholesterol containing DMPC membranes retarded the temperature-induced reorientation of α-cholesterol in the lipid bilayer. It was also shown that the order parameter of the four-ring structure of α-cholesterol was increased by ~10% when the antibiotic was present in the system. This finding is in good agreement with the ordering induced by Ampho B on the lipid labeled at C4' and containing α-cholesterol (see Chapter IV.3). At the light of these ordering effects induced by Ampho B on either the lipid or the α-cholesterol it is therefore difficult to decide whether the retardation observed of the reorientation of the α-isomer of cholesterol is due to a direct interaction between the α-cholesterol and the antibiotic or due to a general increase in ordering of that model membrane system.

REFERENCES TO CHAPTERS IV.3 AND IV.4

Brown, M.F. (1982), J. Chem. Phys., 77, 1576.

Oldfield, E., Meadows, M., Rice, D. and Jacobs, R. (1978), Biochemistry, 17, 2727.

Stockton, G.W., Polnaszek, C.F., Tulloch, A.P., Hasan, F. and Smith, I.C.P. (1976), Biochemistry, 15, 954.

CHAPTER IV.5

AMPHOTERICIN B AND MODEL MEMBRANES

5. CONCLUSION

In the previous sections, the action of the polyene antibiotic Amphotericin B on model membranes in the presence and absence of sterols was studied by ^{2}H-NMR. In the light of these data, the present section will discuss the hypotheses which have been put forward about the mode of action of Ampho B on biological membranes.

The permeability studies mentioned earlier led to the conclusion that when Ampho B was added to a sterol-free membrane there was no induced permeability. From the ^{2}H-NMR results of Chapter IV.2, it appears that besides inducing a general ordering effect on DMPC, the antibiotic segregates a certain amount of these lipids (such that the ratio Ampho B: lipid is 1:1) possibly to form macroscopic aggregates. It appears thus that Ampho B, at low concentrations, acts in the opposite way to that of inducing permeability in the lipid membrane: it decreases the C-^{2}H angular fluctuations of the lipids decreasing therefore the intrinsic possibility of in and out motions of solutes. In addition, the presence of such lipid-polyene antibiotic aggregates, spanning the bilayer membrane, leads one to think that very high concentrations of Ampho B could provoke disruption of

the membrane. However, up to now, there is no experimental evidence, to our knowledge, that very high doses of Ampho B on membranes lacking sterols lead to an increase in permeability or to the death of the cell.

The interpretation of the ^{2}H-NMR data of systems composed of lipids, sterols and Ampho B is not straightforward in terms of the existence of a cholesterol-polyene antibiotic complex. The authors postulating such a complex indicated that the antibiotic was segregating the sterol as shown in Figure IV.1-3. If such a situation occurred in the present model membrane system, two physical events would be detectable by ^{2}H-NMR: the first would be a decrease in the local order of the bulk lipid and the second would be the restoration of the lipid phase transition. It is easily understandable that if the antibiotic complexed the sterol tightly, the ordering effect of the latter on the lipid would be removed and the lipids would be free from the sterol interaction and thus capable of undergoing a gel to liquid crystalline phase transition. Chapter IV.3 shows clearly that none of these events occur with either α- or β-cholesterol in the presence of Amphotericin B in DMPC. Therefore, if the complex exists, it has to be dynamic with respect to the ^{2}H-NMR time scale, that is, the cholesterol has to be in exchange between a site in which it is associated with the antibiotic (site A) and a site in which it is not (site NA)

and thereby able to order the lipid. Prior to characterizing these sites, the existence of the cholesterol:Ampho B complex needs to be clarified. The lipid ^{2}H-NMR response indicates that the DMPC is sensing only one environment at C4' (the plateau level) and two different regions at C14' (the center of the bilayer). It has been shown in Chapter IV.2 that Ampho B was segregated ~30% of the total lipid in the absence of sterols and that the width as well as the amount of the spectral feature representing the "immobilized" lipid were temperature independent. When the sterol is present, this broad spectral component was not detected at C4' whereas at C14' either the width and the amount of the observed broad component were diminished on raising the temperature. These findings indicate clearly that there is no region in the bilayer membrane where the antibiotic interacts freely with the DMPC. This is therefore an argument in favour of a "complex" Ampho B:sterol. The ^{2}H-NMR results using labeled sterols showed that in the presence of Ampho B, the sterols were sensing only one environment at the four-ring structure level, and possibly two regions at the terminal methyl groups of the sterol side chain. These findings agree well with the results obtained from the labeled lipids and lead to the conclusion that an Ampho B:sterol "complex" would have different ordering properties depending upon the bilayer depth. As pointed out above and in order to satisfy to the experimental observations, the cholesterol molecule needs to

be in exchange between two sites, namely sites A and NA. At the light of Chapters IV.3 and IV.4, it appears therefore that site A and site NA possess the same ordering properties, at the plateau level, that is, the sites in which the cholesterol is associated with the antibiotic and freely interacting with the lipid are indistinguishable at the level of the rigid four-ring skeleton. Near the center of the bilayer, the situation appears different. The lipids sense clearly two environments at C14' (and probably C13') whereas the sterol does not perceive these different regions at C24 and shows an indication of a very small (≤5%) second spectral component at C26 and C27. It is therefore quite difficult to make a straightforward attribution of sites A and NA. At this stage of the discussion, it is worthwhile to recall the results of Chapter III.1. It was shown in this chapter that the β-cholesterol molecule could be considered as a "rigid" entity up to carbons 22-24. It is meant by rigid that the molecular or segmental order parameter of either the four-ring skeleton or the cholesterol tail (up to C24) was near 0.8 which indicates that little motional averaging of the quadrupolar interaction is taking place. Bearing this in mind, one can think of cholesterol as being a "rigid cylinder"; very insensitive to external ordering such as that possibly induced by Ampho B. With this peculiar property, the cholesterol molecule could act as a "screen", preventing the Amphotericin B from "seeing" the lipid, up to position

14' (and 13'). Such a situation would explain why cholesterol appears to sense only one environment at the plateau level and why DMPC does sense also a unique region at c4', the site in which cholesterol is not associated with the Ampho B (site NA). At the center of the bilayer, the two environments are differentiated and one can possibly describe the events in two ways: the terminal methyls of the cholesterol tail are less "rigid" than the rest of the molecule and therefore Ampho B can reduce their angular fluctuations as well as those of DMPC at C14', when the sterol is in site A or the methyl groups of the cholesterol tail are almost as "rigid" as the rest of the molecule but the length of cholesterol mismatches that of Ampho B, thus allowing the antibiotic to restrict the motions of DMPC at C14' when cholesterol is in site A. This latter possibility would explain why the second broad component is more important at C14', on the lipid, than at C24 and C27, on the cholesterol tail. However, a definite answer cannot be given based on the available data. A better understanding of the cholesterol:Ampho B: DMPC interactions at the center of the bilayer will certainly be obtained when the local ordering of the terminal methyls of the cholesterol tail is determined.

The interactions of α-cholesterol with Amphotericin B may be described as above since the spectral features of model membranes containing either the α- or the β-isomer of

cholesterol with the antibiotic were similar. The noticeable difference between systems containing α- or β-cholesterol resides in a ~10% increase in local order induced by Amphotericin B in the model membrane containing α-cholesterol, especially at the plateau level. It has to be remembered that there was no change in ordering, at the plateau level, of either the lipid or the β-cholesterol when the Ampho B was added to the system. The dependence of the Ampho B on whether the sterol OH group is α or β leads to the suggestion that the antibiotic may induce a reduction in the α-cholesterol "wobbling" through a direct interaction with the hydroxyl group. This fact might appear contradictory with what has been found in the permeability studies: Ampho B induced greater permeability when β-cholesterol, rather than α-cholesterol, was present in the membrane. However, it has to be kept in mind that the α-isomer of cholesterol does not sit vertically as does the β-isomer, but exhibits a tilted orientation with respect to the membrane surface. It is now easy to understand that even if Ampho B were interacting more with α- than β-cholesterol (which is not proven yet) it could not possibly go easily into the membrane and form a dynamic complex with α-cholesterol, when added externally, due to the peculiar orientation of the latter in the lipid bilayer.

It was shown in Chapter IV.4 that at 25°C the orientation of α-cholesterol in DMPC was not modified by the addition of Amphotericin B. The same conclusion was obtained for β-cholesterol. It appears therefore that the antibiotic molecule does not decide upon the orientation of the dynamic complex, but rather adopts the orientation that the sterol already possesses within the bilayer. This latter point is of interest and could explain why the sterols are essential to the Ampho B-induced permeability. Indeed, due to their character of "rigid cylinders" the sterols may provide the framework of the antibiotic: sterol complex and thereby the orientation of the complex. The antibiotic, on the other hand, may play the role of conducting cement. The words used here to describe the Ampho B-cholesterol complex must not be taken in their original sense; the complex being, from the ^{2}H-NMR viewpoint, essentially dynamic. The lifetime of this complex, which certainly depends on the strength of the sterol-polyene antibiotic interaction, cannot be estimated from the experiments presented herein; however, a measure of the rate of lateral diffusion of cholesterol in the bilayer would give an idea of its magnitude.

PART V

CONCLUSIONS AND SUGGESTIONS

CHAPTER V.1

1. CONCLUSIONS

The aim of this work was to show that deuterium solid state Nuclear Magnetic Resonance was a very suitable technique to study in detail the organization and the dynamics of model membrane systems.

For the major part of this thesis, the ^{2}H-NMR observables, namely the quadrupolar splittings, were analyzed in terms of segmental motions and geometrical orientation of the rigid subunit bearing the deuterium atom. Such a separation between order and geometry allowed the formulation of a model for the occurrence of cyclopropane groups in the lipid acyl chains of biological membranes. It was indeed proposed that due either to the peculiar average orientation of the cyclopropane group in the lipid bilayer, and to the decrease in both the amplitude and the rates of motions of the C-^{2}H bonds of the cyclopropane group, this latter was regulating the lipid chain motions within the bilayer membrane and thus providing a motionally stable membrane over a large range of temperatures.

Using the same separation between order and geometry, it was shown that due to its temperature independent "wobbling", β-cholesterol was able to provide motions to the acyl chains of DMPC below the gel-to-liquid crystalline phase

transition temperature, T_c, of the pure lipid and to reduce the amplitudes of these motions above T_c. The α-isomer of cholesterol was found to possess some of the regulatory properties of the β-isomer and, in addition, to exhibit a titled orientation with respect to the bilayer surface, unlike β-cholesterol which sits vertically in the membrane bilayer.

When studying the ordering properties of cholesterol in DMPC or of lipids containing cyclopropane functions, it was noticed that the deuterium probe senses only its direct environment, i.e., at the same bilayer depth different ordering answers may be obtained depending on the molecular subunit in which the C-^{2}H reporter bond is fixed, for example, sn-1 and sn-2 chains in PDSPC or S_{mol} of cholesterol versus S_{mol} of the lipid at C4' at high temperatures. These findings show that in mixed systems one may often measure the properties of the probe within the system and not necessarily the properties of the system.

The last part of this work showed that the polyene antibiotic, Amphotericin B, could segregate lipids, when present in a pure lipid system, in a ratio 1:1. When this antibiotic was added to a cholesterol-containing lipid model membrane, this segregating effect was not seen and it was postulated that due to the "rigid cylinder" character of cholesterol, this latter was providing a "screen" preventing

thus the Amphotericin B from "seeing" the lipid. The "rigidity" of cholesterol was thought to be a requirement for the formation of dynamic Ampho B: cholesterol complexes which induce permeability in membrane systems.

CHAPTER V.2

2. SUGGESTIONS FOR FUTURE WORK

Throughout this thesis it was found in some cases that the experiments which were conducted could not give a definite answer or even any answer at all.

For instance, the spin-spin relaxation time was found to vary across the powder pattern according to an angular function which was not $P_2(\cos\beta_b)$. It would be interesting to construct a model for the spin-spin relaxation mechanism to fit the actual experimental data. Such a study would be of great importance to characterize slow motions, especially when Ampho B is added to DMPC:cholesterol mixtures. As mentioned in Chapter IV.5 the lateral diffusion of cholesterol, which is thought to be a slow motion, could thus be measured and thereby the magnitude of the lifetime of the dynamic complex Ampho B:cholesterol could be estimated.

It was also found in the present work that one could not decide between two models to describe the spin-lattice relaxation of β-cholesterol in DMPC. Spin-lattice relaxation measurements at other magnetic fields should in principle allow this distinction.

Two solutions were found for the average orientation of α-cholesterol in DMPC. In order to choose the correct answer, a single experiment using [3-^{2}H]-α-cholesterol should in principle be necessary, as mentioned in Chapter III.1.

The ordering of the two terminal methyl groups of the β-cholesterol side chain is still not well understood. As suggested in Chapter III.1, the labeling at C25 of the cholesterol side chain should give additional information about the extreme apparent motional averaging of the quadrupolar interaction at C26 and C27.

Amphotericin B is only one among the 70 compounds found to belong to the class of polyene antibiotics. It would be interesting, for instance, to investigate the effect of Filipin on cholesterol-containing model membranes using cholesterol labeled in the two rings (A and B). The ability that one has to separate the ordering and the orientation within the membrane, of molecules possessing a rigid body (for example, the cyclopropane group, the four rings of cholesterol) should allow in principle verification that the Filipin:cholesterol complex is parallel to the bilayer surface as postulated by the Kruijff and Demel (1974).

REFERENCES TO CHAPTERS V.1 AND V.2

deKruifjj, B. and Demel, R.A. (1974), Biochim. Biophys. Acta, 339, 57.

APPENDICES

APPENDIX A

USE OF THE WIGNER-ECKART THEOREM

The interaction between the efg tensor and the electric quadrupolar moment of the deuterium nucleus may be written in tensor form as:

$$\mathcal{H}_Q = \frac{1}{6} \overline{\overline{V}} . \overline{\overline{Q}} \qquad (A.1)$$

The Wigner-Eckart theorem (Sclichter, 1980, p. 279) states that the effect of the operator $Q^{(OP)}$ on a set of wave functions $|m>$ is:

$$<m|Q^{(OP)}_{\alpha\beta}|m'> = C_Q <m|\frac{3}{2}(I_\alpha I_\beta + I_\beta I_\alpha) - I^2 \delta_{\alpha\beta}|m'>, \qquad (A.2)$$

for instance:

$$<m|Q^{(OP)}_{xx}|m'> = C_Q <m|3\ I_x^2 - I^2|m'> \qquad (A.3)$$

$$<m|Q^{(OP)}_{xy}|m'> = C_Q <m|\frac{3}{2}(I_x I_y + I_y I_x)|m'> \qquad (A.4)$$

$\mathcal{H}_Q$ thus transforms to:

$$\mathcal{H}_Q = \frac{C_Q}{6} \sum_{\alpha\beta} V_{\alpha\beta} \left(\frac{3}{2}(I_\alpha I_\beta + I_\beta I_\alpha) - \delta_{\alpha\beta} I^2\right) \qquad (A.5)$$

with $\alpha, \beta = x, y, z$.

Using the raising and lowering operators, H_Q becomes:

$$H_Q = \frac{C_Q}{4} [V_{zz}(3\ I_z^2 - I^2) + \frac{1}{2}(V_{xx} - V_{yy} \pm 2iV_{xy})(I_\pm)^2$$

$$+ (V_{xz} \pm iV_{yz})(I_\pm I_z + I_z I_\pm)], \qquad (A.6)$$

with the convention of Equations (I.2.10) and with $V_{\alpha\beta} = \frac{\partial^2 V}{\partial_\alpha \partial_\beta}$ it comes:

$$H_Q = \frac{C_Q}{4} \sum_{k=-2}^{+2} (-1)^k A_k V_{-k} \qquad (A.7)$$

Elements $D^{(2)}_{pm}(\alpha\beta\gamma)$ *of the rotation matrix* $D^{(2)}(\alpha\beta\gamma)$

p \ m				
$e^{+2i\alpha}\left(\frac{1+\cos\beta}{2}\right)^2 e^{+2i\gamma}$ $D_{-2,-2}$	$e^{+2i\alpha}\sin\beta\left(\frac{1+\cos\beta}{2}\right) e^{+i\gamma}$ $D_{-2,-1}$	$e^{+2i\alpha}\sqrt{\frac{3}{8}}\sin^2\beta$ $D_{-2,0}$	$-e^{+2i\alpha}\sin\beta\left(\frac{\cos\beta-1}{2}\right) e^{-i\gamma}$ $D_{-2,1}$	$e^{+2i\alpha}\left(\frac{\cos\beta-1}{2}\right)^2 e^{-2i\gamma}$ $D_{-2,2}$
$-e^{+i\alpha}\sin\beta\left(\frac{1+\cos\beta}{2}\right) e^{+2i\gamma}$ $D_{-1,-2}$	$e^{+i\alpha}(2\cos\beta-1)\left(\frac{\cos\beta+1}{2}\right) e^{+i\gamma}$ $D_{-1,-1}$	$e^{+i\alpha}\sqrt{\frac{3}{8}}\sin\beta\cos\beta$ $D_{-1,0}$	$e^{+i\alpha}(2\cos\beta+1)\left(\frac{1-\cos\beta}{2}\right) e^{-i\gamma}$ $D_{-1,1}$	$-e^{+i\alpha}\sin\beta\left(\frac{\cos\beta-1}{2}\right) e^{-2i\gamma}$ $D_{-1,2}$
$\sqrt{\frac{3}{8}}\sin^2\beta\, e^{+2i\gamma}$ $D_{0,-2}$	$-\sqrt{\frac{3}{8}}\sin\beta\cos\beta\, e^{+i\gamma}$ $D_{0,-1}$	$\frac{1}{2}(3\cos^2\beta-1)$ $D_{0,0}$	$\sqrt{\frac{3}{8}}\sin\beta\cos\beta\, e^{-i\gamma}$ $D_{0,1}$	$\sqrt{\frac{3}{8}}\sin^2\beta\, e^{-2i\gamma}$ $D_{0,2}$
$e^{-i\alpha}\sin\beta\left(\frac{\cos\beta-1}{2}\right) e^{+2i\gamma}$ $D_{1,-2}$	$e^{-i\alpha}(2\cos\beta+1)\left(\frac{1-\cos\beta}{2}\right) e^{+i\gamma}$ $D_{1,-1}$	$-e^{-i\alpha}\sqrt{\frac{3}{8}}\sin\beta\cos\beta$ $D_{1,0}$	$e^{-i\alpha}(2\cos\beta-1)\left(\frac{\cos\beta+1}{2}\right) e^{-i\gamma}$ $D_{1,1}$	$e^{-i\alpha}\sin\beta\left(\frac{1+\cos\beta}{2}\right) e^{-2i\gamma}$ $D_{1,2}$
$e^{-2i\alpha}\left(\frac{1-\cos\beta}{2}\right)^2 e^{+2i\gamma}$ $D_{2,-2}$	$e^{-2i\alpha}\sin\beta\left(\frac{\cos\beta-1}{2}\right) e^{+i\gamma}$ $D_{2,-1}$	$e^{-2i\alpha}\sqrt{\frac{3}{8}}\sin^2\beta$ $D_{2,0}$	$-e^{-2i\alpha}\sin\beta\left(\frac{1+\cos\beta}{2}\right) e^{-i\gamma}$ $D_{2,1}$	$e^{-2i\alpha}\left(\frac{1+\cos\beta}{2}\right)^2 e^{-2i\gamma}$ $D_{2,2}$

APPENDIX C

According to Mehring (1976) one can write the Free Induction Decay (FID) as:

$$G(t) = \sum_{n=0}^{\infty} (-\frac{it}{n!})^n M_n \qquad (C.1)$$

where M_n represents the nth moment of the spectrum. The nth moment can thus be defined as:

$$\frac{d^n G(t)}{dt^n}\Big|_{t=0} = (-i)^n M_n \qquad (C.2)$$

Assuming a Gaussian broadening of the individual lines of the powder pattern, one can write the broadened FID, $G^B(t)$, as:

$$G^B(t) = e^{-\frac{\sigma^2 t^2}{2}} G(t) \qquad (C.3)$$

where σ represents the Gaussian linewidth.

Using Equations (C.2) and (C.3) one can define the first and second moments of the broadened spectrum as:

$$M_1^B = M_1$$

$$M_2^B = \sigma^2 + M_2 \qquad (C.4)$$

where M_n^B and M_n represent the broadened and the non-broadened nth moment, respectively, and thus:

$$\Delta_2^B = \frac{\sigma^2}{1.35\ M_1^2} + \Delta_2 \qquad (C.5)$$

where Δ_2^B represent the delta 2 accounting for the Gaussian broadening and Δ_2 the delta 2 without broadening.

APPENDIX D

ORIENTATION OF THE CYCLOPROPANE RING IN THE LIPID BILAYER

A right-handed coordinate-system $\underline{C}$ (x,y,z) is defined for the cyclopropane ring, as shown in Figure D-1. The four deuterons are differentiated as a, b, c and d. The 9', 10' and 19' carbon atoms are taken to define an equilateral triangle, the values of the different angles indicated in Figure A-1 were derived geometrically for the free cyclopropane structure, with the HCH angle taken to be 119° (Büchi/Brinkman, 1982).

In the principal coordinate system $\underline{P}$ (x', y', z' with z' directed along the C-^{2}H bond vector) the electric field gradient tensor is axially symmetric ($\eta=(V_{xx}-V_{yy})/V_{zz}=0$) and can be written as:

$$\underline{\underline{V}}^{P} = eq \begin{pmatrix} -\frac{1}{2} & & \\ & -\frac{1}{2} & \\ & & 1 \end{pmatrix} \qquad (D.1)$$

This tensor can be rewritten in the system $\underline{C}$ (x,y,z) as:

$$\underline{\underline{V}}^{C}_{i} = \underline{\underline{M}}_{i} \; \underline{\underline{V}}^{P} \; \underline{\underline{M}}_{i}^{-1} \qquad (D.2)$$

where i=a,b,c,d; M_i being the orthogonal transformation matrix rotating the coordinate system $\underline{P}$ into the coordinate system $\underline{C}$.

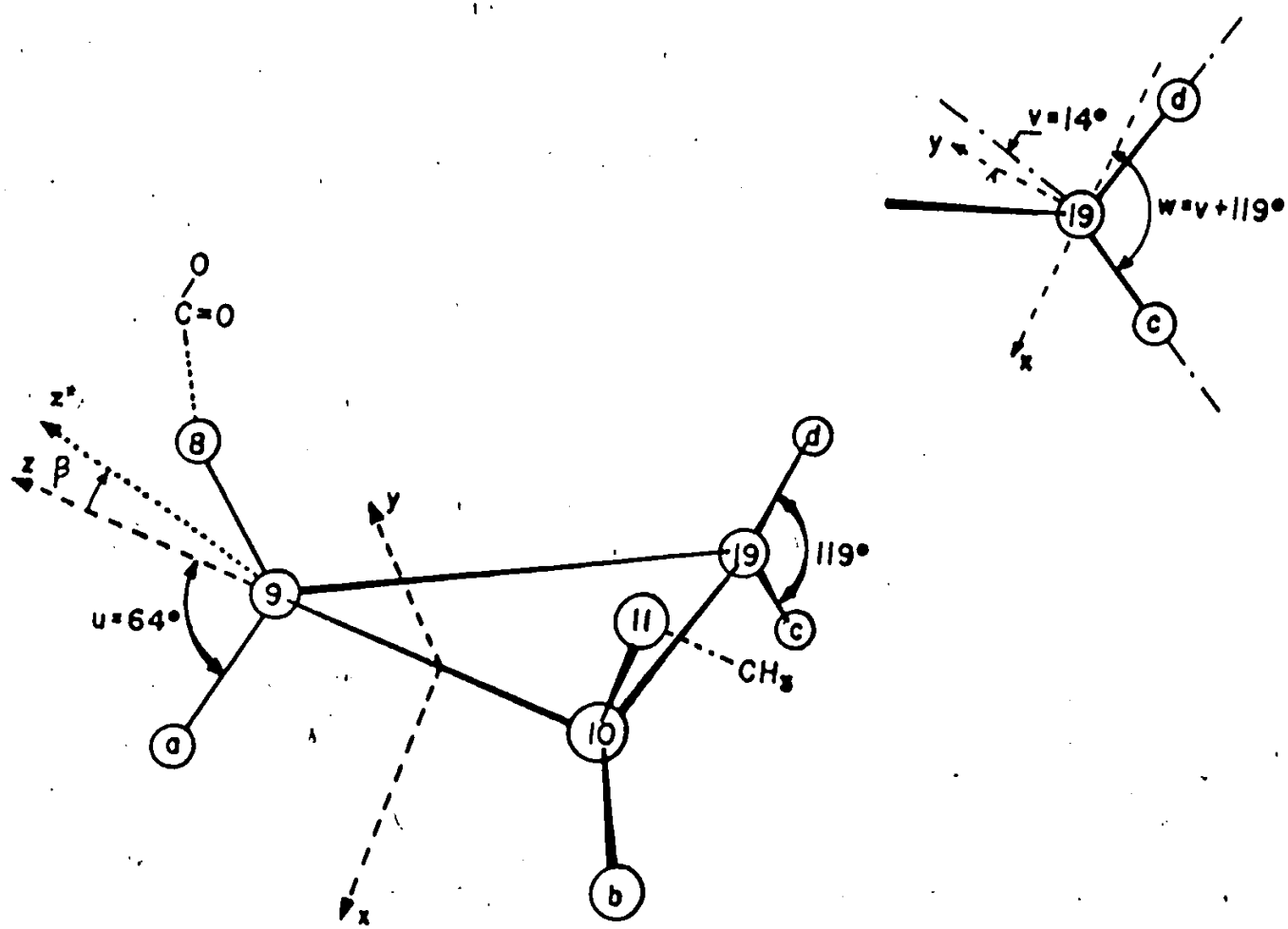

Fig. D–1. Cyclopropane–bound coordinate system C(X,Y,Z). Deuterium and carbon atoms are differentiated by letters and numbers, respectively. The X–axis lies in the (a,9,10,b) plane and in the (d,19,c) plane. The Z–axis is along the 9–10 carbon bond. Rotation angles u,v and w are identified in the text. The axis of motion is identified as Z* and makes the angle β with the Z–axis.

Thus

$$\underline{\underline{V}}^{C}_{a} = eq \begin{pmatrix} 1 - \frac{3}{2}\cos^2\underline{u} & 0 & \frac{3}{2}\cos\underline{u}.\sin\underline{u} \\ 0 & -\frac{1}{2} & 0 \\ \frac{3}{2}\cos\underline{u}.\sin\underline{u} & 0 & \frac{3}{2}\cos^2\underline{u} - \frac{1}{2} \end{pmatrix}$$

$$\underline{\underline{V}}^{C}_{b} = eq \begin{pmatrix} 1 - \frac{3}{2}\cos^2\underline{u} & 0 & -\frac{3}{2}\cos\underline{u}.\sin\underline{u} \\ 0 & -\frac{1}{2} & 0 \\ -\frac{3}{2}\cos\underline{u}.\sin\underline{u} & 0 & \frac{3}{2}\cos^2\underline{u} - \frac{1}{2} \end{pmatrix} \qquad (D.3)$$

$$\underline{\underline{V}}^{C}_{c} = eq \begin{pmatrix} \frac{3}{2}\cos^2\underline{w} - \frac{1}{2} & \frac{3}{2}\cos\underline{w}.\sin\underline{w} & 0 \\ \frac{3}{2}\cos\underline{w}.\sin\underline{w} & 1 - \frac{3}{2}\cos^2\underline{w} & 0 \\ 0 & 0 & -\frac{1}{2} \end{pmatrix} \quad *$$

$$\underline{\underline{V}}^{C}_{d} = eq \begin{pmatrix} \frac{3}{2}\cos^2\underline{v} - \frac{1}{2} & \frac{3}{2}\cos\underline{v}.\sin\underline{v} & 0 \\ \frac{3}{2}\cos\underline{v}.\sin\underline{v} & 1 - \frac{3}{2}\cos^2\underline{v} & 0 \\ 0 & 0 & -\frac{1}{2} \end{pmatrix} \quad *$$

The component of the average field gradient tensor parallel to the rotation axis, $\vec{n}$, is given by

$$\underline{V}^{C}_{i,\parallel} = \vec{n}.\underline{\underline{V}}^{C}_{i}.\vec{n} \qquad (D.4)$$

---

* M_c (M_d) was obtained from two rotations: the first around x' by angle $\underline{w}$ ($\underline{v}$). the second around y by 90°.

where $\vec{n} = (\gamma_1, \gamma_2, \gamma_3)$, and γ_i (i=1,2,3) are the direction cosines between the director of the motion $\vec{n}$ and the x,y,z axes of the system C. As an example,

$$V^{C}_{a,\parallel} = eq\,[(1 - \tfrac{3}{2}\cos^2\underline{u})\bar{\gamma}_1^2 - \tfrac{1}{2}\bar{\gamma}_2^2 + (\tfrac{3}{2}\cos^2\underline{u} - \tfrac{1}{2})\bar{\gamma}_3^2 + 2\bar{\gamma}_1\bar{\gamma}_3\,\tfrac{3}{2}\sin\underline{u}.\cos\underline{u}].$$

Using Equation (I.2.21) and expression $V^{C}_{i,\parallel}$ in terms of the experimentally available order parameters $S^{i}_{C-^2H}$, listed in Table D-1, of the individual C-^{2}H bonds (Seelig and Waespe-Šarčević, 1978):

$$V^{C}_{i,\parallel} = eq\; S^{i}_{C-^2H}\,, \tag{D.5}$$

we obtain the following set of equations:

$$\begin{aligned}
S^{a}_{C-^2H} &= S_{11}\sin^2\underline{u} + S_{33}\cos^2\underline{u} + 2S_{13}\cos\underline{u}.\sin\underline{u} \\
S^{b}_{C-^2H} &= S_{11}\sin^2\underline{u} + S_{33}\cos^2\underline{u} - 2S_{13}\cos\underline{u}.\sin\underline{u} \\
S^{c}_{C-^2H} &= S_{11}\cos^2\underline{w} + S_{22}\sin^2\underline{w} + 2S_{12}\cos\underline{w}.\sin\underline{w} \\
S^{d}_{C-^2H} &= S_{11}\cos^2\underline{v} + S_{22}\sin^2\underline{v} + 2S_{12}\cos\underline{v}.\sin\underline{v}\,.
\end{aligned} \tag{D.6}$$

In addition to this set of equations we have:

$$\sum_{j=1}^{3} S_{jj} = 0 \tag{D.7}$$

Table D-1

S_{C-^2H} ORDER PARAMETERS
OF THE CYCLOPROPANE RING

	Remarks
$S^a_{C-^2H} = 0.084$	^{2}H-NMR data at 25°C. Lipids dispersed in excess deuterium depleted water. The assignment of the quadrupolar splittings a and b, as well as c and d is arbitrary. The sign of the S_{C-^2H} cannot be determined from experimental spectra. The accuracy on the S_{C-^2H} is about 2-3%.
$S^b_{C-^2H} = 0.130$	
$S^c_{C-^2H} = 0.146_4$	
$S^d_{C-^2H} = 0.218_6$	

Therefore, using Equations (D.6) and (D.7), the order matrix $\underline{\underline{S}}^{C}$ expressed in the $\underline{C}(x,y,z)$ coordinate system is accessible from the ^{2}H-NMR observables.

However, since the signs of the deuterium order parameters are unknown, and since the quadrupolar splittings observed for the [9', 10'-$^{2}H_{2}$] and [19'-$^{2}H_{2}$] PDSPC positions cannot be assigned unambiguously to the a or b and c or d deuterons, respectively, there are 64 possible order matrices $\underline{\underline{S}}^{C}$.

For instance we have:

$$\underline{\underline{S}}^{C} = \begin{pmatrix} -0.060 & 0.387 & 0.029 \\ 0.387 & 0.365 & 0.000 \\ 0.029 & 0.000 & -0.305 \end{pmatrix} \qquad (D.8)$$

calculated with:

$$S^{a}_{C-^{2}H} = -0.084;\ S^{b}_{C-^{2}H} = -0.130;\ S^{c}_{C-^{2}H} = -0.218_{6};\ S^{d}_{C-^{2}H} = 0.146_{4}.$$

All the matrices were diagonalized using a computing process based on the estimation of the eigenvalues according to Smith, et al. (1974). As an example, the (D.8) matrix takes the form

$$\underline{\underline{S}}^{*} = \begin{pmatrix} -0.323 & & \\ & -0.271 & \\ & & 0.594 \end{pmatrix} \qquad (D.9)$$

The "*" standing for a coordinate system (x*,y*,z*) in which the matrix $\underline{\underline{S}}^C$ is diagonal. The choice of the correct solution can be done on the basis of an asymmetry parameter η^* (Seelig and Wasepe-Šarčevič, 1978):

$$\eta^* = \left| \frac{S^*_{11} - S^*_{22}}{S^*_{33}} \right| \qquad \text{(D.10)}$$

which has to be very small to reflect the apparent axially symmetric powder pattern lineshapes obtained with the PSDPC system (Figure II.1-3). Table D-2 shows some of the η^* values found to range between 0 and 0.5. In the most general case, the eigenvector matrix derived from the eigenvalues can be equated to a rotational matrix $\underline{\underline{E}}(\alpha,\beta,\gamma)$ obtained by doing three consecutive rotations of angles α,β,γ as described by Rose (1957).

Table D-2 shows the α,β, and γ angles obtained from the corresponding eigenvector matrix elements. The accuracy of the eigenvalues of Equation (D.9) is about 8-10%, and consequently values of η^* of about 0.10 are within the error bar. The minimum value of η^* in Table D-2 leads to the solutions:

$$S^a_{C-^2H} = -0.084 \text{ or } -0.130$$

$$S^b_{C-^2H} = -0.130 \text{ or } -0.084$$

$$S^{c}_{C-^{2}H} = -0.218_{6}$$

$$S^{d}_{C-^{2}H} = 0.146_{4}$$

The quadrupolar splittings of the 19' position on the cyclopropane ring can then be assigned, but there is still an ambiguity in the assignment of those due to positions 9' and 10'.

Table D-2

VALUES OF η^* RANGING BETWEEN 0 AND 0.5 WITH THE CORRESPONDING PARAMETERS DERIVED IN APPENDIX D, OF THE CYCLOPROPANE RING

$S^a_{C-^2H}$	$S^b_{C-^2H}$	$S^c_{C-^2H}$	$S^d_{C-^2H}$	S^*_{33}	η^*	β	γ	α
0.084	0.130	-0.146_4	0.218_6	0.247	0.41	85	-28	82
-0.084	-0.130	-0.146_4	0.218_6	0.756	0.36	-89	-61	175
-0.084	-0.130	-0.146_4	-0.218_6	0.343	0.29	- 3	3	-164
0.084	-0.130	-0.218_6	-0.146_4	0.470	0.30	-13	1	- 88
-0.084	-0.130	0.218_6	-0.146_4	0.286	0.20	91	70	- 53
-0.084	*-0.130*	*-0.218_6*	*0.146_4*	*0.594*	*0.09*	*-89*	*-59*	*144*
0.130	0.084	-0.146_4	0.218_6	0.247	0.41	-85	-28	- 98
-0.130	-0.084	-0.146_4	0.218_6	0.756	0.36	89	-61	- 5
-0.130	-0.084	-0.146_4	-0.218_6	0.343	0.29	3	3	16
-0.130	0.084	-0.218_6	-0.146_4	0.470	0.30	13	1	92
-0.130	-0.084	0.218_6	-0.146_4	0.286	0.20	-91	70	127
-0.130	*-0.084*	*-0.218_6*	*0.146_4*	*0.594*	*0.09*	*89*	*-59*	*- 36*

The accuracy on the angles is $\pm 1^o$. When the matrix S* is axially symmetric, the angle α is undetermined.

APPENDIX E

ORIENTATION OF THE CYCLOPROPANE RING IN THE LIPID BILAYER

The same right-handed system described in Appendix D is used herein. Since we defined $\underline{\underline{S}}^*$ as:

$$\underline{\underline{S}}^* = \underline{\underline{E}}(\alpha,\beta,\gamma)^{-1}.\underline{\underline{S}}^{C}.\underline{\underline{E}}(\alpha,\beta,\gamma), \qquad (E.1)$$

the rotation axis aligned along the z* axis and represented as a unit vector $\vec{n}$ having its origin at (0,0,0) can then be expressed in the $\underline{C}(x,y,z)$ system as:

$$\vec{n} = (-\sin\beta.\cos\gamma,\ \sin\beta.\sin\gamma,\ \cos\beta). \qquad (E.2)$$

The direction cosines (l_i, m_i, n_i) for a particular C-^{2}H bond can be calculated from its atomic carbon (x_c,y_c,z_c) and deuterium (x_d,y_d,z_d) coordinates (Taylor, et al., 1981). Any orientation of the rotation axis $\vec{n}$ with respect to the ith C-^{2}H bond vector can be defined by an angle θ_{in} such as

$$\cos\theta_{in} = \frac{\vec{i}.\vec{n}}{\|\vec{i}\|.\|\vec{n}\|} = -l_i.\sin\beta.\cos\gamma + m_i.\sin\beta.\sin\gamma + n_i.\cos\beta\ . \qquad (E.3)$$

where $\|\vec{i}\|$ represents the magnitude of the vector $\vec{i}$. The C-^{2}H bond lengths were normalized to 1 for convenience. Using Equation (E.3) ratios such as:

$$R^{c}_{i,j} = \frac{3\cos^2\theta_{in}-1}{3\cos^2\theta_{jn}-1} \qquad (E.4)$$

may be calculated for given values of β and γ.

From the ^{2}H-NMR results, experimental ratios can also be estimated by means of Equation (II.1.5):

$$R^{e}_{i,j} = \frac{\Delta\nu^{i}_{Q}}{\Delta\nu^{j}_{Q}} = \frac{3\cos^2\gamma_i-1}{3\cos^2\gamma_j-1} \qquad (E.5)$$

Equation (E.5) is valid as long as we assume that S_α is the same for all C-^{2}H bonds in the rigid body and the asymmetry parameter η equal to zero; γ_i can then be taken to be equal to θ_{in}.

In our case, the $R^{e}_{i,j}$ were calculated with respect to the C-9' position, and since both signs and magnitude of the splittings for the [9', 10'-$^2H_2$] and [19'-$^2H_2$] positions are unknown, 64 sets of ratios can be created *a priori*.

Our calculation proceeded as follows: the angles γ and β were varied from -90° to 90° by 1° intervals and the values of $R^{c}_{i,j}$ then obtained were compared to the experimental R^{e}_{k} by means of the deviation:

$$D = \sum_i \left[\frac{\left|R^{c}_{i,j}\right| - R^{e}_{i,j}}{R^{e}_{i,j}}\right]^2 \qquad (E.6)$$

By using the absolute value of $R^{c}_{i,j}$ in Equation (E.6) we can access the relative signs of the S_{C-2_H} order parameters. For D = 0.01, a set of answers was obtained, Table E-1. The S_{mol} indicated in Table E-1 were calculated from the values of β and γ using Equations (E.3) and (II.1.5). However, we do not have a criterion, such as the η^* used in Appendix D, to determine the correct value of S_{mol} from Table E-1. Nevertheless, looking at Tables D-2 and E-1, we note that they only intersect for falues of $\eta^* = 0.09$ and 0.20, on the basis of similarities in S_{C-2_H} and S^{*}_{33} (or S_{mol}). Comparisons of γ and β angles between Tables D-2 and E-1 show that the $\eta^* = 0.09$ solution is the only one which fits in Table E-1 within the error limits.

Orientation of the 8' and 11' Positions

Method of Appendix E was used for calculating the orientation of the [8'-$^2H_2$] and [11'-$^2H_2$] positions each of which exhibit two quadrupolar splittings. The right-handed system used here is shown in Figure E-1. In each case, only one ratio can be created, and the calculation was carried out until the same absolute value was obtained for R^{c}_{k} and R^{e}_{k}.

It turns out that the [8'-$^2H_2$] position gives an average value of S_{mol} in the range 0.32 to 0.40 and an orientation defined by $\beta = 19^{o} - 31^{o}$ and $\gamma = 70^{o} - 85^{o}$. The

Table E-1

β, γ ANGLES AND S_{mol} FOR THE CYCLOPROPANE RING DERIVED FROM APPENDIX E

$S^a_{C-^2H}$	$S^b_{C-^2H}$	$S^c_{C-^2H}$	$S^d_{C-^2H}$	S_{mol}	β	γ
± 0.130	± 0.084	$\pm 0.146_4$	$\pm 0.218_6$	0.425	23	83
± 0.130	± 0.084	$\mp 0.218_6$	$\pm 0.146_4$	0.293	78	71
± 0.130	∓ 0.084	$\pm 0.218_6$	$\mp 0.146_4$	0.442	69	-51
± 0.130	*± 0.084*	*$\pm 0.218_6$*	*$\mp 0.146_4$*	*0.587*	*86*	*-59*
± 0.084	± 0.130	$\mp 0.218_6$	$\pm 0.146_4$	0.302	-79	70
± 0.084	± 0.130	$\pm 0.146_4$	$\pm 0.218_6$	0.433	-23	82
± 0.084	∓ 0.130	$\mp 0.218_6$	$\pm 0.146_4$	0.464	-69	-52
± 0.084	*± 0.130*	*$\pm 0.218_6$*	*$\mp 0.146_4$*	*0.571*	*-87*	*-59*

The accuracy on the angles is $\pm 2^\circ$.

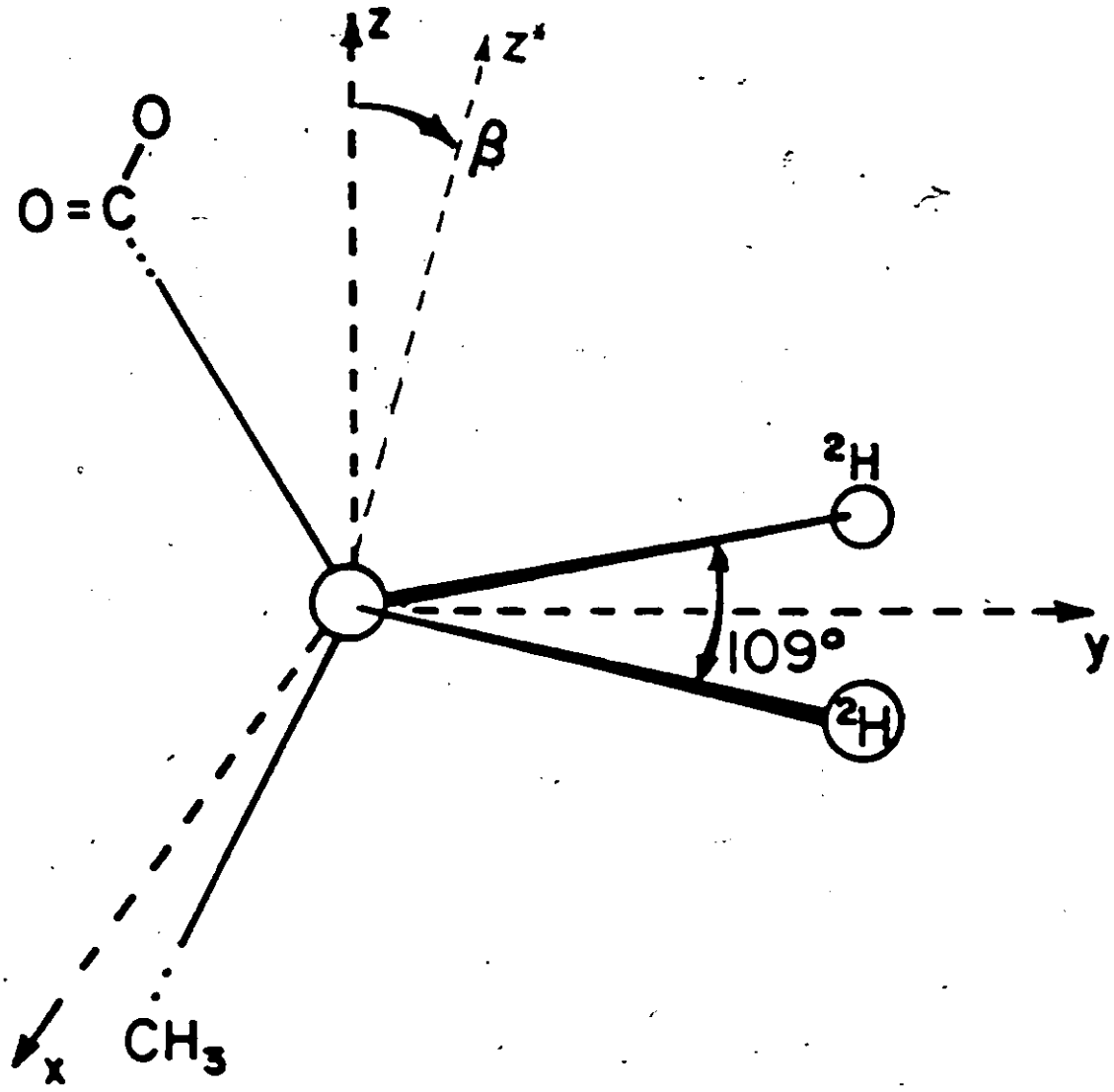

Fig. E–1. Methylene bound coordinate system used for the C8′ and C11′ positions of the PDSPC molecule. The Y–axis lies in the (^{2}H,C,^{2}H) plane and bisects the di–hedral angle; the Z–axis is perpendicular to that plane and makes the angle β with the axis of motion Z*.

angle β defines the tilt of the z axis perpendicular to the (^{2}H,C,^{2}H) plane) with respect to the axis of motion z* (see Figure E-1). The small amplitude of this tilt seems to be reasonably what one can expect at that position. In the case of the C-11' position, the decision is much more difficult. However, on the basis of stereochemical relationships between the cyclopropane group and the methylene unit at C-11' and although very inaccurate, a value of $\beta = 70^{\circ}$-86° and $S_{mol} = 0.20 \pm 0.06$ would depict the average orientation and ordering of the deuterons at this position. For C-11' the angle γ has a very large scatter, from 10° to 70°, and an average value cannot be given. The calculation gave positive and negative values of the angles β and γ; therefore, the assignment of quadrupolar splittings to individual deuterons at the C-8' and C-11' positions is not possible.

It must be emphasized that the accuracy involved in these latter calculations is much less than for the labeled cyclopropane ring positions.

APPENDIX F

AXIS OF MOTION AND ORDERING OF CHOLESTEROL

Since the method used herein has already been discussed elsewhere (Appendix E) we will only indicate the general idea and report the resulting calculation as used for α- and β-cholesterol.

A coordinate system $\underline{C}$ (x,y,z) is attached to the cholesterol molecule as shown in Figure F-1. In this figure the letters, a, b, c, c', d, e, f represent the deuterons and the numbers the carbon atoms. The $\underline{C}$ (x,y,z) axis system is defined such that the x-axis is colinear with the C_3c bond and the z-axis belongs to the $c'C_3c$ plane. The molecule sketched in Figure F-1 represents β-cholesterol when c = ^2H and c' = OH and α-cholesterol when c = OH and c' = ^2H. The atomic coordinates of both the carbon and hydrogen atoms have been extracted from the fractional atomic coordinates of cholesteryl palmitate (x-ray data, Sawsik and Craven, 1980).

The axis of motion $\vec{n}$ (aligned along the z* axis) is defined in the axis system $\underline{C}$ as:

$$\vec{n} = \begin{pmatrix} \cos\gamma \sin\beta \\ \sin\gamma \sin\beta \\ \cos\beta \end{pmatrix}$$

The angle $\theta_{i,n}$ that an individual C-i bond vector makes with the axis of motion can thus be defined by:

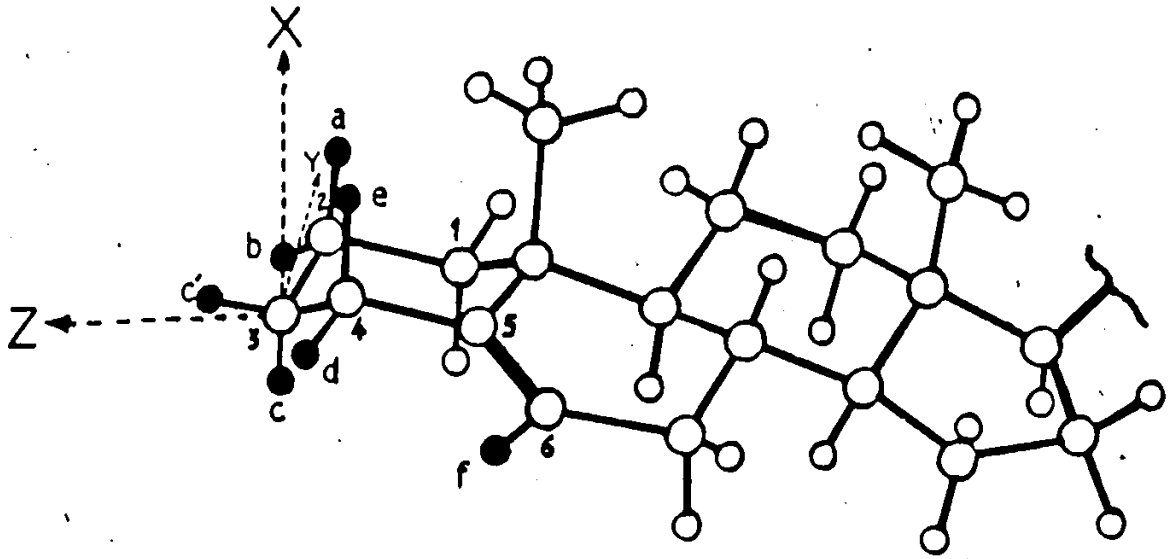

Fig. F–1. Sterol–bound axis system C(X,Y,Z,). The Z–axis belongs to the $c'C_3c$ plane and the X–axis is along the cC_3 bond. Numbers and letters represent carbon numbering and deuterium atoms, respectively.

$$\cos\theta_{i,n} = \frac{l_i \cos\gamma \cdot \sin\beta + m_i \sin\gamma \cdot \sin\beta + n_i \cos\beta}{\|C\text{-}i\| \cdot \|\vec{n}\|}$$

where l_i, m_i and n_i are the direction cosines of the C-i bond vector obtained from the atomic coordinates of carbon and deuterium atoms in the C axis system.

The position of the axis of motion is then "sought" by varying the angles β and γ. One sees that for given values of β and γ one can obtain $P_2(\cos\theta_{i,n})$ terms ($P_2(\cos\theta_{i,n}) \doteq \frac{1}{2}(3\cos^2\theta_{i,n}-1)$) and compare them with the experimental values. It has already been described in Appendix E how these terms were compared. Once the correct orientation of the axis of motion, $\vec{n}$, has been defined with respect to C (x,y,z) by a certain value of the angles β and γ, one knows therefore the geometrical orientation of a given C-i bond with respect to the axis of motion, that is, one knows S_γ (see theoretical background), it is therefore straightforward to obtain the segmental order parameter S_α (which is also called S_{mol}) by making use of Equation (II.1.5). We would like to emphasize that this analysis assumes that the angular fluctuations of cholesterol (α or β) can be defined, in the liquid-crystalline phase in which the motions have axial symmetry (spectral shapes axially symmetric), by an axially symmetric order matrix.

The Table F-1 summarizes the results for β- and α-cholesterol. Few comments need be made about this table.

Table F-1

ORDERING AND ORIENTATION OF α- AND β- CHOLESTEROL

β-cholesterol	10	15	20	25	30	35	40	45	50	55	65	
$S_{mol} \pm 0.03$	0.81	0.81	0.80	0.80	0.79	0.78_5	0.78	0.75		0.72_5	0.71	
$\beta \pm 1^o$	21	21	21	21	21.5	21	21	22		22	21.5	
$\gamma \pm 3^o$	108	107.5	106.5	106.5	106	106.5	105.5	106.5		104	106	
$\theta(C_3\text{-c}, \vec{n})^a \pm 2^o$	83.5	84	84	84	84	84	84.5	84		85	84	
$\theta(C_2\text{-b}, \vec{n})^b \pm 2^o$	44	44	44	44	43.5	44	44	43		43	43.5	
α-cholesterol[c]												
$S_{mol} \pm 0.03$			0.82	0.80	0.78		0.70		0.63	0.62_5	0.59_5	1
$\beta \pm 1^o$			30	27.5	26.5		23		19	19	17.5	1
$\gamma \pm 3^o$			150	148	147		141.5		134.5	134	130.5	1
$\theta(C_2\text{-b}, \vec{n}) \pm 2^o$			46	46.5	46.5		47.5		49	49	49.5	1
$\theta(C_3\text{-c}, \vec{n}) \pm 2^o$			64.5	67	68		72.5		77	77	79	1
$S_{mol} \pm 0.03$			0.92	0.89_5	0.88		0.87		0.77_5	0.77	0.72	2
$\beta \pm 1^o$			4	4	4		4		5	5.5	6	2
$\gamma \pm 3^o$			24.5	68	67		60.5		74.5	74.5	80.5	2
$\theta(C_2\text{-b}, \vec{n}) \pm 2^o$			64	61.5	61.5		62		60.5	60.5	59.5	2
$\theta(C_3\text{-c}, \vec{n}) \pm 2^o$			93.5	91.5	91.5		92		91.5	91.5	91	2

[a] Angle between the C_3-c bond vector and the axis of motion, $\vec{n}$.

[b] Angle between the C_2-b bond vector (equatorial deuteron at C_2) and $\vec{n}$.

[c] The two possible solutions 1 and 2 are listed.

During the calculation, all possible combinations of C-i direction cosines and quadrupolar splittings were performed, leading to one main solution for β-cholesterol and two main solutions for α-cholesterol. Exchanging the quadrupolar splitting of C_2-b with that of C_4-b gave the same results for β-cholesterol (Table F-1, top part) with, however, less accuracy.

Both solutions (1 and 2) in the case of α-cholesterol were obtained by only one combination of splittings and C-i bonds, for the lowest margin of error, leading therefore to the assignment shown in Figure III.1-9. Whereas one obtains a unique solution for β-cholesterol, it is difficult to choose between the two answers in the case of α-cholesterol. Solution 1 indicates that the hydroxyl group (in α) is pointing towards the hydrophobic medium, that is, the water surface, whereas solution 2 shows that the OH group points slightly towards the hydrophobic core. It is not possible to decide, based on the available data, on which solution is correct; however, from the calculated orientations one can predict that the quadrupolar splitting arising from the deuteron at the 3β-position (in α-cholesterol) will be about 40 kHz according to solution 1 and 100 kHz according to solution 2, at 25°C. A single experiment with [3-^{2}H]-α-cholesterol in DMPC (3:7) will thus give an unambiguous way of determining the correct answer.

In order to calculate the position of the axis of motion of a methylene subunit (for example, cholesterol tail) the fixed axis system $\underline{C}$ (x,y,z) was defined such that the y-axis bissects the $^{2}H\text{-}C\text{-}^{2}H$ plane and such that the z-axis is normal to that plane.

REFERENCES TO APPENDICES

Büchi/Brinkman (1982), Dreiding Stereomodels, Bulletin BR 297C.

Sawsik, P. and Craven, B.M. (1980), Acta Cryst., B36, 3027.

Mehring, M. (1976), High Resolution NMR Spectroscopy in Solids, Springer-Verlag, New York.

Sclichter, C.P. (1980), Principles of Magnetic Resonance, Springer-Verlag, New York.

Seelig, J. and Waespe-Šarčević, N. (1978), Biochemistry, 17, 3311.

Smith, B.T., Boyle, J.M., Garbow, B.S., Ikeke, Y., Kema, V.C., and Moler, C.B. (1974), Matrix Eigensystem Routines, Springer-Verlag, Berlin.

Rose, M.E. (1957), Elementary Theory of Angular Momentum, John Wiley and Sons Inc., New York.

Taylor, M.G., Akiyama, T. and Smith, I.C.P. (1981), Chem. Phys. Lipids, 29.